OpenAIR@RGU

The Open Access Institutional Repository
at Robert Gordon University

http://openair.rgu.ac.uk

Citation Details

Citation for the version of the work held in 'OpenAIR@RGU':

THE MOLECULAR MECHANISMS OF DIABETES MEDIATED IMPAIRED WOUND HEALING AND THE DEVELOPMENT OF THERAPEUTIC STRATEGIES

PRAMOD C GADAD

PhD   2011

THE MOLECULAR MECHANISMS OF DIABETES MEDIATED IMPAIRED WOUND HEALING AND THE DEVELOPMENT OF THERAPEUTIC STRATEGIES

PRAMOD C GADAD

A thesis submitted in partial fulfilment of the
requirements of the
Robert Gordon University
for the degree of Doctor of Philosophy

School of Pharmacy and Life Sciences
Robert Gordon Univeristy
Aberdeen
January 2011

DECLARATION

This thesis has been composed by myself and has not been submitted in any previous application for a higher degree. The work that is documented was carried out by myself. All verbatim extracts have been distinguished by quotation marks and the source of information specifically acknoweldged.

Pramod C Gadad

To my Grandma Sangamma

Figures

Tables

Contents

Acknowledgements

I owe my deepest gratitude to my principal supervisor Dr. Rachel M Knott for her advice, time and guidance. Her encouragement and knowledge made my PhD experience productive, stimulating and enjoyable. I highly appreciate her help through the thick and thin of this thesis, both at an academic and at a personal level. I am equally indebted to my second supervisor Dr. Kerr H Matthews for his support, advice and guidance on all formulation-related aspects of this thesis. I am equally grateful to the RDI of RGU and ORSAS for funding this study.

I would like to thank Dorothy Moir for her help with cell culture lab during the initial days and making the subsequent days so enjoyable. I would like to express my gratitude to the other technicians, Vivienne Hamilton, Margaret Brown, Moira Innes, Liz Hendrie and Laurie Mearns for their help. Special thanks are due to Raymond Reid, Moira Middleton and Maureen Byres for helping me with HPLC and Brain DeJonckheere for his excellent help with IT related issues.

I would like to express my gratitude to Dr. Stuart Cruickshank for his critical and useful feedback on my interim reports. I express my thanks to Dr. Alberto DiSalvo, Dr. Emma Hector, Dr. Andrew Lamb, Dr. Graeme Kay, Dr. Yash Kumarasamy, Dr. Bridgeen McCaughan, Dr. Morag McFadyen, Dr. Narinder Singh, Dr. Colin Thompson and Dr. Anita Weidmann for their helpful advice and help. I also would like to express my thanks to Dr. Cherry Wainwright for being inspirational. I thank Dr. Hector Williams for his wonderful and much needed help in statistics. I thank Mr. Martin Simpson, Research Support Officer for his immense help throughout the course.

I am thankful to all my past and present fellow PhD students in PC27 for making my days enjoyable. I thank Ray, Ben, Tim, Karen, Nicola, Cip, Vibhu, Maxwell, Barbara, Owen, Sarah, Scott, Liang, Claire and Lisa. Special thanks to Noelle, Olga and Ania for fun filled RSA days and being great friends. I express my sincere thanks to the Williams family including Hector, Albert, Esther and little James for making me one amongst them and for all the enjoyable days in Aberdeen.

Lastly, I would like to thank my previous employer Dr. B. M. Patil and KLE Society, India for granting me study leave. I would like to acknowledge the help of my uncles who have provided me fatherly guidance. I also thank my siblings and my mother for their love and affection. I thank my wife Shreya and our daughter Pramiti without whose sacrifice this thesis would have been an uphill task. I would like to thank all the rest of my family members and friends for their support and encouragement.

Abstract

Increased levels of blood glucose are associated with the vascular complications of diabetes. Microvascular complications lead to delayed wound healing in patients suffering from diabetes. Hypoxia and hyperglycaemia characterise a wound environment of a person with diabetes. Angiogenesis is central to restore the supply of oxygen and nutrients to the wounded tissue. Endothelial cell migration is central to angiogenesis which is aided by hypoxia and attenuated by hyperglycaemia. However, the molecular mechanisms underlying the disruption to angiogenesis of diabetic wounds are not completely understood. The effect of hypoxia and/or high glucose concentration on the endothelial cell migration *in vitro* was studied and an anti-oxidant, silymarin formulated as freeze dried wafer discs was tested for its beneficial effect.

A radial migration and a wound healing assay were developed, validated and used to assess the effect of hypoxia and/or high glucose concentration on the migration of human endothelial cells of dermal origin. Circular and semi-circular monolayers of endothelial cells were used for the measurement of the migration by radial migration and wound healing assay respectively. Net migration was calculated by subtracting the radii at a specified time point from that measured at time zero. The migration was studied under normal (20%) or below (5%) normal oxygen tension in combination with normal (5mM) or high (20mM) glucose concentration. Endothelial cells were treated with an anti-proliferative agent, intracellular signal inhibitors and silymarin.

Results demonstrated that hypoxia and high glucose concentration have opposing effects of increase ($p<0.001$) and decrease ($p<0.001$) respectively on the migration of endothelial cells. The results of the wound healing assay revealed that re-endothelialisation occurs faster ($p<0.001$) than endothelialisation. The effects of hypoxia and high glucose concentration appeared to be mediated via PI3K-Akt and PKC$_{\beta II}$ pathways respectively. Further investigations revealed the possibility of HIF-1α being involved in both the pathways. High glucose concentration-induced decrease in cell migration was successfully restored ($p<0.001$) by the use of an anti-oxidant silymarin. This could be due to anti-oxidant activity of silymarin on glucose-induced overproduction of reactive oxygen species. Silymarin formulated as freeze dried wafer discs, sterilised by gamma irradiation was successful in retaining its effect ($p<0.001$) against the high glucose impaired cell migration compared to control wafers.

In conclusion, delayed wound healing due to disrupted endothelial cell migration was reaffirmed to be due to elevated glucose concentration. Silymarin was successful in restoring glucose-induced attenuation of cell migration. Freeze dried wafers show promising potential as a topical application for the treatment of chronic wounds for people with diabetes.

Abbrevations

ADF	actin depolymerizing factor
AGE	advanced glycation end products
Akt	adenosine-triphosphate dependant tyrosine kinase
aLA	α-lipoic acid
ALP	Alkaline phosphatase
ALT	alanine amminotransferase
ANG	angiotensin
ANOVA	analysis of variance
AR	aldose reductase
ATM	ataxia telangiectasia, mututated
ATP	adenosine triphosphate
AST	aspartate amino transferase
AUC	area under the curve
bFGF	basic fibroblast growth factor
Ca^{2+}	calcium
CAK	CDK activating kinase
CAT	catalase
CBP	CREB binding protein
Cip-1	CDK inhibitor protein
CDK	cyclin dependant kinase
CKI	CDK inhibitor protein
CREB	cAMP response element-binding protein
CTGF	connective tissue growth factor
DAG	diacylglycerol
DCCT	Diabetes Control and Complications Trial
DMSO	dimethylsulfoxide
DNA	deoxyribonucleic acid
EC	endothelial cell
ECACC	European Collection of Cell Culture
ECAM	endothelial cell adhesion molecule
ECM	extracellular matrix
EDIC	Epidemology of Diabetes Intervention and Complications Study
EDTA	ethylenediaminetetraacetic acid
EGF	epidermal growth factor
eNOS	endothelial nitric oxide synthase

ERK	extracellular regulated kinase
ET	endothelin
FAK	focal adhesion kinase
FCS	foetal calf serum
FIH-1	factor inhibiting HIF-1
GLUT	facilitative glucose transporters
GMEM	Glasgow Minimum Essaential Medium
GSHP$_X$	glutathione peroxidase
GTP	guanosine-5'-triphosphate
GTPase	family of hydrolase enzymes that can bind and hydrolyze GTP
H$_2$O$_2$	hydrogen peroxide
HBSS	Hanks Balanced Salt Solution
HDL	high density lipoprotein
HIF	hypoxia inducible factor
HIV	human immunodeficiency virus
HPLC	high performance liquid choramatography
HRE	hypoxia responsive element
HUVEC	human umbilical vein endothelial cell
ICAM	intercellular adhesion molecule
IDF	International Diabetes Federation
IFN	interferon
IGF	insulin-like growth factor
IL	interleukin
INK	inhibitor of CDK
iNOS	inducible nitric oxide synthase
JAK/STAT	Janus kinase/signal transducer and activator protein
JNK	c-Jun NH$_2$ terminal kiase
Kip	kinase inhibitor protein
LDL	low density lipoprotein
Mg^{2+}	magnesium
MAPK	mitogen activated protein kinase
MMPs	matrix metaloproteinases
Mn-SOD	manganese-superoxide dismutase
MTOC	microtuble organising centre
NAD$^+$	nicotinamide adenine dinucleotide
NADH	reduced nicotinamide-adenine dinucleotide

NADP+	oxidized form of NADPH
NADPH	nicotinamide-adenine dinucleotide phosphate
NF-κβ	nuclear factor – kappa beta
NGF	nerve growth factor
NO	nitric oxide
PAI	plasminogen activator inhibitor
PAK	p21 activated motor kinase
PARP	poly (ADP-ribose) polymerase
PBS	phosphate buffered saline
PECAM	platelet endothelial cell adhesion molecule
PDGF	platelet dependant growth factor
PGI2	prostacyclin
PHD	prolyl hydroxylases
PI	phosphotidylinositides
PI3K	phosphatidylinoisitol 3-Kinase
PKC	protein kinase C
PLC	protein lipase C
PLGF	placental growth factor
PPAR	peroxisome proliferators-activated receptor
RAGE	receptors for AGE
RNA	ribonucleic acid
ROCK	Rho associated coiled coil kinase
ROS	reactive oxygen species
RTK	receptor for tyrosine kinase
SCF	stromal cell factor
SDF	stromal cell deriaved factor
SDH	sorbitol dehydrogenase
SEM	standard errors of the mean
SGOT	serum glutamate oxalate transaminase
SGPT	serum glutamate pyruvate transaminase
SM	silymarin
SOD	superoxide dismutase
TBS	tris buffered saline
TCA	tricaroboxylicacid cycle
TGF	transforming growth factor
TNF	tissue necrosis factor

t-PA	tissue plasminogen activator
UKPDS	UK Prospective Diabetes Study
VCAM	vascular cell adhesion molecule
VEGF	vascular endothelial growth factor
VEGFR	VEGF receptor
vHL	von Hippel-Lindau protein
VLDL	very low density lipoprotein
VSMC	vascular smooth muscle cells
vWF	von willebrand factor
WHO	world health organisation
XG	xanthan gum

Chapter 1 - Introduction

Diabetes is a debilitating disease and whose incidence has increased significantly in recent years. The associated vascular complications remain a major cause of morbidity and mortality within this patient group. Central to vascular complications are the endothelial cells that line or form the basis of a blood vessel as these cells are exposed to high and/or fluctuating concentration of glucose and reduced oxygen availability that are associated with diabetes. The focus of this study is to establish an *in vitro* model of wound healing in order to investigate the key parameters of endothelial cell growth, migration and/or proliferation that are affected by elevated glucose concentration and reduced oxygen availability. The role of silymarin in the amelioration of the condition and the development of a novel silymarin formulation for topical application are part of this study. In this first chapter the rationale and the context of the existing work is explored in order to demonstrate the integrity and feasibility of the study and the conclusions that have been made.

1.1 Diabetes Mellitus

The International diabetes federation (IDF) defines diabetes mellitus as ''a group of heterogeneous disorders with the common elements of hyperglycaemia and glucose intolerance, due to insulin deficiency, impaired effectiveness of insulin action, or both'' (International Diabetes Federation 2009). The current WHO criteria for diagnosis of diabetes include fasting plasma glucose level at ≥7.0mmol/L (120mg/dL) or 2-h after 75g oral glucose load challenge with plasma glucose at ≥11.1mmol/L (200mg/dL) (World Health Organisation Consultation 2006).

Diabetes currently affects approximately 285 million adults worldwide (i.e. 6.6% of world population), 70% of whom belong to the developing world. It is expected that diabetes will affect 439 million adults (7.8% of world population) by 2030. Presently, one million more women than men are estimated to suffer from diabetes and this difference is likely to go up to six million by 2030 (International Diabetes Federation 2009). Diabetes is the fourth or fifth leading cause of global death by disease in the developed world with approximately four million deaths, accounting for around 6.8% of global all-cause mortality each year. The high mortality is estimated to be from India, China, USA and Russia as there is a larger population size and thus relatively more people suffering from diabetes (International Diabetes Federation 2009).

Diabetes is one of the largest non-communicable diseases, imposing heavy economic burden on individuals, families, health systems and nations with an expected 11.6% of a total global healthcare expenditure spent on it. Today, the estimated global healthcare expenditure is 360 billion United States Dollars (USD). This is expected to increase to 490 billion USD by 2030. However, there is a huge disparity in the money

spent on diabetes by different countries, with USA spending the majority and countries like India, Burundi and Myanmar spending meagre amount of total global spending (International Diabetes Federation 2009). The economic implications of this are of greater significance if lost productivity and the consequent loss of national income are included in the finances.

Etiologically, diabetes mellitus is classified into type 1 diabetes mellitus (T1DM) and type 2 diabetes mellitus (T2DM) which were previously known as insulin dependent diabetes mellitus (IDDM) and non insulin dependent diabetes mellitus (NIDDM) respectively. Type 1 diabetes, primarily considered to be an autoimmune disorder, is a result of lack of insulin due to the destruction of beta cells from the islets of Langerhans in the pancreas, and type 2 diabetes is a result of insulin resistance and/or insulin insufficiency (Balkau and Eschwege 2003). Gestational diabetes and other specific types like genetic defects of β-cell function, genetic defects of insulin action, disease of exocrine pancreas, endocrinopathies, drug- or chemical- or infection-induced, uncommon forms of immune-mediated diabetes and other genetic syndromes associated with diabetes are also recognized (Balkau and Eschwege 2003).

Acute complications of T1DM include ketosis, ketoacidosis, hypoglycemic episodes, hyperglycemic crises and infections (Slama Gerard 2003). Later complications include retinopathy, cataract, nephropathy (renal insufficiency and hypertension), neuropathy (polyneuropathy, mononeuropathy, foot ulcers and impotence), cardiovascular complications (macro vascular disorders like coronary heart disease, cerebrovascular disease, and peripheral vascular disease), skin disorders (infections, mycosis, lipodystropy) and psychosocial disorders like depression (Slama Gerard 2003). The complications of T2DM are similar to those of T1DM although prevalence of respective complications does vary. Blindness due to proliferative retinopathy and risk of development of end stage renal disease are low in T2DM compared to T1DM patients. On the other hand, the rate of mortality due to cardiovascular diseases is high in T2DM compared to T1DM patients (Katsilambros and Tentolouris 2003).

The Diabetes Control and Complication Trial (DCCT) and the United Kingdom Prospective Diabetes Study (UKPDS) were two milestone studies conducted in the USA and UK respectively on diabetes and its complications. The DCCT was a multi-centre (29 centres) randomized clinical trial conducted during 1983 to 1993 and involved 1,441 patients suffering from type 1 diabetes for a minimum of a year to a maximum of 15 years. After 1993, the follow up study called Epidemiology of Diabetes Interventions and Complications (EDIC) was continued with more than 90% patients of DCCT. The EDIC trial continues to study the incidences of CVS and other diabetes related complications (National Institute of Diabetes and Digestive and Kidney Diseases (NIDDK) 2008). The

DCCT has shown that intense therapy of adjusted doses of insulin with diet and exercise reduced the risks of developing complications compared with conventional therapy of unadjusted doses of insulin with only education about diet and exercise. Intensive therapy reduced the development of proliferative or non severe retinopathy by 47% and clinical neuropathy by 60%. The risk of albuminurea and microalbumin urea was reduced by 54 and 39% respectively indicating dramatic risk reduction in nephropathy in patients receiving intensive insulin therapy compared with conventional therapy (DCCT Group 1993). The follow-up study, EDIC, showed that there was a reduction in cardiovascular events by 42% and nonfatal myocardial infraction, stroke or death from diabetes by 57% in the intensive insulin therapy group (DCCT/EDIC Study Research Group et al. 2005).

The UKPDS was designed and conducted between 1977 to 1997 by Professor Robert Turner and Rury Holman of diabetes trial unit of Oxford University. It was a multicentre (23 UK clinical sites) trial involving randomized glucose therapies in 5,102 newly diagnosed type 2 diabetes patients (Diabetes Trials Unit 2010a). The post trial monitoring ran for another ten years until 2007 with all the surviving patients of UKPDS trial (Diabetes Trials Unit 2010b). The UKPDS was conducted in T2DM patients over a period of 10 years with the patients assigned to either intense glucose control with sulphonylurea or with insulin or conventional glucose control through diet. Haemoglobin A1c (HbA1c), any diabetes related deaths and microvascular endpoints were lower by 11, 10 and 25% respectively in the group receiving intense therapy compared to their counterparts assigned to conventional glucose control treatment of dietary restrictions (UKPDS Group 1998). The UKPDS post trial monitoring study indicated that although the reduction in HbA1c was lost after a year, the reductions in the risk of diabetes related deaths and microvascular complications continued in the intensive glucose therapy group (Holman et al. 2008). These reports conclusively suggest that the prolonged exposure to hyperglycaemia is a primary causal factor in the development of vascular and other complications of diabetes.

1.2 Vascular complications of Diabetes

1.2.1 Macrovascular complications

Macrovascular complications of diabetes include coronary heart disease (CHD), stroke, myocardial infarction and peripheral vascular disorders. The CHD in patients suffering from diabetes may result due to a number of risk factors including hypertension, hyperglycaemia and effects of advanced glycation end (AGE) products, dyslipidemia, microvascular disease and autonomic neuropathy (Adler et al. 2002). Dyslipidemia is thought to be a major contributory risk factor for CHD. In T1DM increased lipolysis and overproduction of non esterified fatty acids, and decreased activity of lipoprotein lipase

results in hypertriglyceridemia which acts as a risk factor. In T2DM, dyslipidemia is a result of raised triglycerides, decreased high density lipoproteins (HDL), raised low density lipoproteins (LDL) and increased levels of apolipoprotein B (apoB), an integral part of very low density lipoprotein (VLDL) (Poirier and Despres 2003). Hypertension is another major risk factor which worsens both macro and microvascular complications in diabetes. Insulin resistance associated with T2DM contribute to hypertension by loss of insulin's normal vasodilator activity or through effects of accompanying hyperinsulinaemia (Kashyap and Defronzo 2007). Furthermore atheroma is known to develop earlier and faster in diabetes causing widespread lesions throughout the arterial walls (Renard et al. 2004).

1.2.2 Microvascular complications

1.2.2.1 Diabetic Retinopathy

Diabetic retinopathy results from damage to the microvasculature of the retina. Retinal vessels consist of an inner layer of endothelial cells covered by a protein-proteoglycan basement membrane and contractile pericytes. Hyperglycaemia is known to be the major causative factor for retinopathy causing damage to all the three parts of retinal vessels (Knott and Forrester 2003). Hyperglycaemia increases the auto-oxidation, polyol pathway flux and diacylglyerol (DAG) synthesis (reviewed in Knott and Forrester 2003). The auto-oxidation and polyol pathway lead to the formation of free radicals due to depletion of two major non-enzymatic anti-oxidants glutathione and ascorbate, and this deleterious effect of glucose on the retina could be overcome by treatment of antioxidants (Knott and Forrester 2003, Obrosova et al. 2005). Higher glucose levels also cause *de-novo* synthesis of DAG leading to activation of the protein kinase C (PKC) pathway which may lead to an increase in the expression of vascular endothelial growth factor (VEGF) and increased production of endothelin-1 causing increased vascular permeability, vasoconstriction and ischemia respectively (Idris and Donnelly 2006, Matsuo et al. 2009, Park et al. 2000). Studies have suggested that endothelial cells (EC) and pericytes undergo apoptosis in hyperglycaemic conditions leading to the structural and functional alterations of retinal blood vessels (Kowluru 2005). Interestingly, when co-cultured, retinal endothelial cells proliferated and pericytes underwent apoptosis in the presence of elevated glucose level and this was attenuated by fidarestat, an antioxidant (Takamura et al. 2008). Apoptosis of retinal endothelial cells in hyperglycaemia has been linked to mitochondrial fragmentation with decreased oxygen consumption (Trudeau et al. 2010). Hyperglycaemia leading to the formation of advanced glycation end products (AGEs) is also known to cause the thickening of the basement membrane altering its barrier functions (Gardiner, Anderson and Stitt 2003).

1.2.2.2 Diabetic Nephropathy

In diabetic nephropathy both the glomerulus and the tubular interstitium are affected. The glomerulus consists of a tuft of around 20 to 30 capillary loops supported by mesengium made up of cells and matrix. The lumen of the capillary loop consists of fenestrated endothelial cells lying on basement membrane and podocytes on the extraluminal side. Hyperglycaemia causes expansion of the mesengium and basement membrane thickening due to synthesis and accumulation of extracellular matrix (Wolf, Chen and Ziyadeh 2005). The hypertrophy of renal and glomerular cells and podocytes, hyaline deposits, glomerular sclerosis and tubulointerstitial fibrosis are also associated with diabetic nephropathy (Herbach et al. 2009). The expansion of glomerular mesengium leads to a decrease in the glomerular filtration rate and development of protienuria (Gnudi, Gruden and Viberti 2003, Wolf 2002). Some patients with diabetes do not develop nephropathy even though the hyperglycaemia is a known factor in the development of renal damage (Gnudi, Gruden and Viberti 2003). Other factors like increased glomerular capillary pressure, proteinuria on its own and hypertension are known to contribute towards the development of diabetic nepropathy (Gnudi, Gruden and Viberti 2003).

The mediators of hyperglycaemia induced nephropathy are thought to result from a change in the expression of growth factors such as transforming growth factor–β1 (TGF-β1), connective tissue growth factor (CTGF), insulin like growth factor (IGF), VEGF and angiotensin -2 (Gnudi, Gruden and Viberti 2003). The intracellular signalling pathways that have been associated with diabetic nephropathy include the activation of PKC and mitogen activated protein kinase (MAPK) pathways along with transcription factors such as nuclear factor–kβ (NF–kβ) and activator protein–1 (Toyoda et al. 2004). The enhanced expression of janus kinase/signal transducer and activator of transcription (JAK/STAT) has also been implicated in the progression of diabetic nephropathy (Berthier et al. 2009, Marrero et al. 2006). The biochemical mechanisms of glucose toxicity are discussed further in section 1.5.

1.2.2.3 Diabetic Neuropathy

Diabetes mellitus causes peripheral neuronal degeneration leading to diabetic neuropathies. Distal symmetrical polyneuropathies (DSPs) and focal and multifocal neuropathies are two main categories of diabetic neuropathies. The third category, entrapment neuropathies are highly prevalent in patients suffering from diabetes although they are seen also in non-diabetic patients. The DSPs are nerve length dependant, hence severely affect the nerves of feet and contribute towards the development of foot ulcers. Focal neuropathies are acute and cause damage to single nerves or bundles of single nerves, usually in isolation and independent of other complications of diabetes. The early

manifestations of DSPs include abnormal sensations followed by sensory loss, anaesthesia, paraesthesia, allodynia and hyperalgesia. The loss of thermal sensation is due to damage to the small fibres and loss of sensation of touch, pressure, joint position and vibration are due to damage to the longer fibres (Tomlinson 2003). Hyperglycaemia causes the loss of proliferation and migration of Schwann cells and regeneration of axons contributing towards diabetic neuropathy (Gumy, Bampton and Tolkovsky 2008). The biochemical pathways, due to oxidative stress, responsible for diabetic complications including neuropathy involve advanced glycation endproducts/receptor for advanced glycation endproducts (AGE/RAGE), polyol pathway, hexosamine pathway, PKC pathway, poly-ADP ribose polymerase pathway (PARP) and inflammation (Figueroa-Romero, Sadidi and Feldman 2008) are detailed in section 1.5.

1.3 Impaired wound healing of diabetes

The chronic wounds of diabetes are another set of daunting challenges of microvascular complications. The wound healing process involves four continuous and overlapping phases of coagulation, inflammation, migration-proliferation (including matrix deposition) and remodelling (Falanga 2005, Guo and Dipietro 2010). Initial phases of coagulation and inflammation set in early after injury. The formation of the fibrin plug helps in recruiting the inflammatory cells to the site of injury. The aggregated platelets at the site of injury release a range of growth factors such as platelet-derived growth factor (PDGF), TGF-β1, epidermal growth factor (EGF) and proinflammatory cytokines like interlukin – 1 (IL – 1) (reviewed in Barrientos 2008). The release of growth factors help in the recruitment of neutrophils and macrophages to the wound site. The neutrophils decontaminate the wound site by phagocytosising the bacteria and with help of macrophages, augment the inflammatory response and tissue debridement. Further, neutrophils and macrophages release various growth factors like EGF, TGF – β, PDGF, fibroblast growth factor (FGF) and cytokines like IL – 1α and β, IL – 6, IL – 8 and tissue necrosis factor - 1α (TNF-1α) (Christian et al. 2006, Hubner et al. 1996). These secretions activate fibroblasts and keratinocytes which help in the development of tissue granulation (reviewed in Barrientos et al. 2008, Martin 1997). The newly recruited monocytes differentiate into macrophages and degrade extracellular matrix by producing enzymes such as hyaluronidase, elastase and collagenase which degrade hyaluronic acid, elastin and collagen in connective tissue (Christian et al. 2006). This process helps in the migration of keratinocytes, fibroblasts and endothelial cells to the site of wound.

Decreased oxygen tension (hypoxia) at the site of wound, due to injury to the blood vessels immediately after wounding, is essential for the progression of wound healing process. Hypoxia activates the migration of keratinocytes in order to re-epithelise

the epidermal tissue by secretion of extracellular matrix proteins (Fitsialos et al. 2008, Woodley et al. 2009). Hypoxia also enhances the migration and proliferation of fibroblasts through the expression of hypoxia inducible factor - 1α (HIF-1α) and the consequent secretion of growth factors like VEGF and matrix metalloproteinases (MMPs) (Lerman et al. 2003, Mace et al. 2007). The fibroblasts play a crucial role during the wound healing process of extracellular matrix deposition and remodelling. Hypoxia is also essential for the migration of endothelial cells in order to form new blood vessels out of the pre-existing ones at the site of injury (Im et al. 2009, Wang et al. 2009). However, exposure of endothelial cells to hypoxia and hyperglycaemia is known to cause endothelial cell DNA damage which was attenuated by treating with the antioxidant, Silymarin (Weidmann et al. 2005). The positive effect of the antioxidant illustrates the key role that oxidative damage has in this process. The migration and proliferation of these cells and the presence of the cocktail of growth factors and cytokines at the site of injury help the wound healing process to progress to the next stage.

The events of migration and proliferation during wound healing are important as the migration of keratinocytes and fibroblasts to the wound site is due to the secretions of pro-migratory cocktail of growth factors and cytokines. The restoration of supply of oxygen and nutrients due to angiogenesis play an important preparatory role for the wound closure. The collagen, fibronectin and growth factors such as CTGF secreted by fibroblasts aid the formation of the extracellular matrix (Qiu, Kwon and Kamiyama 2007, Thomson et al. 2010). Myofibroblasts, a specialised form of fibroblasts which express α-smooth muscle actin, facilitate the wound closure with help of focal adhesion proteins by contracting the extracellular matrix (Leask et al. 2008). Finally, the formation of extra cellular matrix at the beginning and later its degradation by serine proteases and MMPs assist in the remodelling of the wound healing process (Christiansen et al. 2007, Thomson et al. 2010).

The presence of diabetes is reported to impair all of the phases of wound healing outlined above. These phases are shown in the following table (Table 1), which also summarises the main events during each phase with key cells (Falanga 2005). The functional changes responsible for the vascular complications of recalcitrant wounds of diabetes are known to be due to three main factors - endothelial dysfunction, smooth muscle cell dysfunction and impairment of the nerve-axon reflex (Dinh and Veves 2005). The endothelial function/dysfunction is dealt in detail in the following section.

Table 1.1: Phases of wound healing Major types of cells involved in each phase with selected specific events of wound healing (Adapted from Falanga 2005).

Time	Phases	Main cell types	Specific events
Hours	**Coagulation** Fibrin plug formation, release of growth factors, cytokines, hypoxia ↓ **Inflammation** Cell recruitment and chemotaxis, wound debriment ↓	Platelets Neutrophils, monocytes Macrophages	Platelet aggregation, release of fibrinogen fragments and other proinflammatory mediators Selectins slow down blood cells and binding to integrins - diapedesis
Days	**Migration/proliferation** Epidermal resurfacing, fibroplasia, angiogenesis, ECM deposition, contraction ↓	Keratinocytes, fibroblasts, endothelial cells	Hemidesmosome breakdown- Keratinocyte migration Cross talk between MMPs, integrins, cells, cytokines - Cell migration, ECM production
Weeks to months	**Remodelling** Scar formation and revision, ECM degradation, further contraction and tensile strength	Myofibroblasts	Phenotypic switch to myofibroblasts from fibroblasts

1.4 Diabetes and the endothelium

The endothelium is an active inner monolayer of the blood vessels and participates in many homeostatic mechanisms. Different responses of the endothelium to intrinsic and extrinsic factors are observed due to the phenotypic variations observed in endothelial cells (ECs) at different vascular sites. The lining of ECs from the liver, spleen and bone marrow sinusoids is discontinuous so that nutrients and other macro molecules can pass through the intercellular gaps. The retina and brain are lined with continuous ECs to maintain the blood retinal and brain barrier respectively, while the endocrine glands and kidneys are lined with fenestrated ECs that facilitate selective permeability (Cines et al. 1998). ECs also differ with respect to the genes expressed that may be classified depending on whether they are constitutively or inducibly expressed. Many extracellular signals like hypoxia, hemodynamic forces, chemokines and cytokines, growth factors, hormones, glucose, lipoproteins, and drugs alter transcription of specific genes and bring about various functional changes (Minami and Aird 2005).

Endothelial dysfunction has increasingly been implicated in the vascular diseases as it is known to play a central role in both micro and macro vascular complications of diabetes (Rask-Madsen and King 2007, Tesfamariam and DeFelice 2007). Endothelium regulates the vascular tone by secreting vasodilators and vasoconstrictors. The presence of diabetes impairs the vascular tone by upsetting the balance between vasodilators and vasoconstrictors (Schalkwijk and Stehouwer 2005). The vasodilator agents such as nitric oxide (Victor et al. 2009), endothelium derived hyperpolarisation factor (EDHF) (Hosoya et al. 2010) and prostacyclins (Wotherspoon et al. 2005) and vasoconstrictor agents such as endothelin I and angiotensin II (Kobayashi et al. 2008) secreted by endothelium help in maintaining the vascular tone.

Platelet adhesion and aggregation is regulated by the balance between pro and anti-aggregants. Prostacyclin (PGI_2) and nitric oxide (NO) prevent platelet adherence to endothelium and platelet adhesion and aggregation involve phosphorylation by cAMP and cGMP dependant protein kinases respectively (Dunn and Grant 2005). The balance between coagulation and fibrinolysis is impaired by diabetes, otherwise well regulated by endothelium with the help of thrombomodulin/protein C, heparan sulphate/antithrombin, tissue factor/tissue factor inhibitor interactions, tissue-type plasminogen activator (t-PA) and plasminogen activator inhibitor-1 (PAI-1) (Schalkwijk and Stehouwer 2005, Stegenga et al. 2006, Stegenga et al. 2008). The level of cellular fibronectin was elevated in patients with diabetes indicating the disruption to the subendothelial matrix due to the damage to the endothelium by glucotoxicity (Kanters et al. 2001).

The endothelium plays a vital role in the inflammatory process by recruiting neutrophils, monocytes/macrophages and lymphocytes to the site of inflammation. The neutrophils initiate inflammation reaction by secreting a variety of destructive enzymes like myeloperoxidase, elastase, matrix metalloproteases and cathespins (Kaneider, Leger and Kuliopulos 2006). The exposure of endothelium to inflammatory agents increases the production of selectins, cell adhesion molecules (CAMs) and other cytokines which help in the rolling, tethering, adhesion and transmigration of leukocytes (Kubes, Suzuki and Granger 1991, Ulbrich, Eriksson and Lindbom 2003). Normal endothelial function is summarized in the following figure (Figure 1.1).
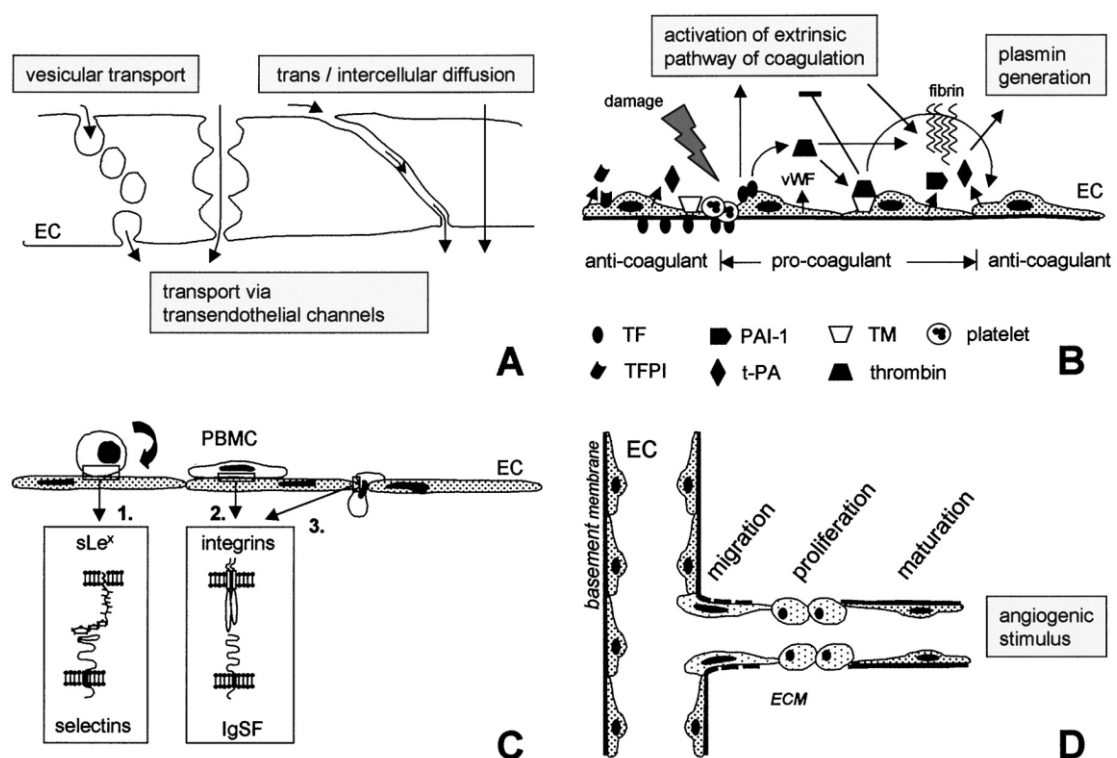
Figure 1.1: Physiological functions of endothelium Endothelial cells perform important functions in the body. Endothelium A) acts as a semi permeable barrier for the transport of various proteins and other soluble molecules; B) maintains the haemostatic balance and regulates the coagulation; C) facilitates leukocyte extravasation during inflammation; D) actively participates in angiogenesis.

EC, endothelial cells; IgSF, Ig superfamily; PAI-1, plasminogen activator inhibitor; PBMC, peripheral blood mononuclear cells; sLex, sialyl Lewis X; TFPI, Tissue Factor pathway inhibitor; TM, thrombomodulin

(Reproduced with permission from Griffioen and Molema 2000).

Endothelial cells exposed to high concentration of glucose *in vitro* increase the production of extra cellular matrix components such as collagen and fibronectin, and of procoagulant proteins such as vWF and tissue factor. Due to the increase in the production of these factors, hyperglycaemia decreased the proliferation, migration and fibrinolytic potential of cells and has been reported to increase apoptosis (Baumgartner-Parzer et al. 1995b, Boeri et al. 1989, Cagliero et al. 1988, Graier et al. 1995, Maiello et al. 1992, McGinn et al. 2003b). During diabetes, hyperaggregability of platelets coupled with activation of leukocytes and increased expression of adhesion molecules on endothelial cells (Ouedraogo et al. 2007) disrupts the homeostasis and may lead to protracted inflammation resulting in a chronic wound. In patients with diabetic retinopathy, lymphocytes were activated with reduced expression of surface L-selectin but increased circulation of L-selectin resulting in an increase in the adhesion of leukocytes (MacKinnon, Knott and Forrester 2004). Incubation of HUVECs with 25mM glucose induced the expression of P-selectin and intercellular adhesion molecule – 1 (ICAM-1), which was reversed by the addition of 1nM insulin and anti-P-selectin monoclonal antibody implying that the activation of ECs leads to the adhesion of monocytes in high glucose concentration (Puente Navazo et al. 2001). *In vitro* exposure of ECs to hyperglycaemia resulted in the induction of E-selectin, vascular cell adhesion molecule – 1 (VCAM-1), ICAM-1 and endothelial leukocyte adhesion molecule-1 (ECAM-1) mediated by a cytokine tissue necrosis factor – α (TNF-α), NF-kB and PKC (Altannavch et al. 2004, Morigi et al. 1998).

A large number of studies show that high glucose concentration causes adverse changes indirectly in endothelial cell function by impairing the synthesis of growth factors and vasoactive agents in other cells. Various growth factors like VEGF, PDGF, TGF-β, IGF, bFGF, NGF, EGF and others have been reported to play a role in vascular complications of diabetes (Kofler, Nickel and Weis 2005). In human retinal endothelial cells (HREC) glucose up-regulated the production of TGF-β1 at 15mM concentration, and TGF-β1 mRNA and TGF-β receptors expression showed glucose dependant and time dependant changes (Pascal, Forrester and Knott 1999) suggesting a role for growth factors in advancing diabetic retinopathy. The expression of growth factors by leukocytes may also be altered by diabetes. In leukocytes of patients with diabetic retinopathy, the expression of VEGF$_{121}$ and VEGF$_{165-189}$ mRNA was found to be lower at the early stage of the disease compared to increased levels at later stage (Knott et al. 1999). This increase in the level of transcription of the mRNA could result in a higher level of VEGF expression leading to neovascularisation aggravating the complications of retinopathy. Increased expression of VEGF protein has also been shown to be associated with retinal disease by aggravating the fibrosis by inducing the expression of CTGF genes via PI3K-Akt pathway

(Suzuma et al. 2000). Furthermore insulin resistance, hyperinsulinemia, dyslipidemia or hyperlipidemia, hypertension, impaired fibrinolysis and abdominal obesity are implicated in the development of T2DM and cause endothelial dysfunction either directly or indirectly (Cacicedo et al. 2004, Schalkwijk and Stehouwer 2005).

1.5 Mechanisms of diabetic complications

Chronic hyperglycaemia in persons with diabetes increases the intracellular concentration of glucose in certain cells such as endothelial cells, mesangial cells and neurons and Schwann cells of peripheral nerves (Berthier et al. 2009, Gumy, Bampton and Tolkovsky 2008). The rate of glucose transport is similar in all the above mentioned cells. Glucose transport into endothelial and vascular smooth muscle cells occurs by GLUT-1 mediated facilitated diffusion and is thus insulin-independent. Glucose transport is auto regulated in smooth muscle cells, but not in endothelial cells, in which an increase in blood glucose concentration will increase the intracellular accumulation of glucose and its metabolites. The increased levels of glucose inside these cells produces deleterious effects leading to the diabetic complication through the following four pathways

a. Increased flux of glucose through the *polyol pathway*
b. Increased intracellular production of *advanced glycation end products (AGEs)*
c. *Protein kinase C (PKC)* activation
d. The *hexosamine pathway*

The *polyol pathway* is regulated by aldose reductase (AR) enzyme which converts the glucose to sorbitol. Under normal circumstances, AR converts the toxic aldehydes into non-toxic alcohols. During hyperglycaemia, the increased concentration of glucose in the cells is reduced to sorbitol by AR and this is later oxidised to fructose by sorbitol dehydrogenase (SDH). NADPH is increasingly oxidised to $NADP^+$ and NAD^+ is increasingly reduced to NADH during this process. The decrease in NADPH adversely affects the production of reduced glutathione, an important intracellular antioxidant. The decreased amount of reduced glutathione increases the oxidative stress of the cells, leading to diabetic complications (Brownlee 2001, Nakamura et al. 2000, Srivastava, Ramana and Bhatnagar 2005).

Advanced glycation end products (AGEs) are a group of hetergenous compounds resulting from non-enzymatic glycation of proteins and other molecules such as nucleic acids by glucose and other glycating dicarbonyl compounds such as 3-deoxyglucosone, methylglycoxal and glyoxal (Taguchi and Brownlee 2003). The AGEs are formed through a reaction pathway known as the Maillard pathway, in which the carbonyl group of reducing sugars are converted to reversible Schiff bases and amadori products, but eventually leading to the formation of irreversible AGEs. The fructose-3-phosphate and 3-

deoxyglucosone produced as a result of metabolism of fructose by the polyol pathway also contribute to the formation of AGEs (Schalkwijk, Stehouwer and van Hinsbergh 2004). The accumulation of excessive triosphosphates within the cells converts the intracellular proteins and lipids into oxoaldehyde and AGEs (Thornalley 2005). These AGEs cause cell damage by modifying the functioning of intracellular and extracellular proteins, alteration of the 3D configuration of the extracellular matrix molecules and by up-regulation of receptor for AGEs (RAGEs) (Brownlee 2001, Brownlee 2005).

The different isoforms of *protein kinase-C (PKC)*, mainly α, β, δ, ε and ζ are activated by hyperglycaemia via *de novo* synthesis of diacylglycerol (DAG) (Das Evcimen and King 2007). Activated PKC_β produces many effects including impairment of blood flow and contractility by altering the production of eNOS and ET-1 (Kuboki et al. 2000, Matsuo et al. 2009) and increased vascular permeability and angiogenesis by increasing the expression of VEGF (Rask-Madsen and King 2008). It is also reported to cause an increase in basement membrane thickness and capillary occlusion by increasing the production of collagen and fibronectin via CTGF and TGF- β (Koya et al. 2000). The activation of PKC is also reported to cause vascular occlusion by decreasing fibrinolysis via increasing PAI-1 (Ahn et al. 2001), activation of adhesion by increasing ICAMs (Ramana et al. 2004) and various other effects by increasing the expression of NF-κB and ROS (Brownlee 2005, Das Evcimen and King 2007).

Glucose is mainly metabolised through glycolysis inside the cells. It is first converted to glucose-6-phosphate, next to fructose-6-phosphate and later to the remaining steps of glycolysis to yield pyruvate and lactate. However, during normal conditions two to three percent of fructose-6-phosphate undergoes metabolism via the *hexosamine pathway*, in which it is converted to glucosamine-6 phosphate with the help of the enzyme glutamine:fructose-6 phosphate amidotransferase (GFAT) and finally uridine phosphate N-acetyl glucosamine (UDP-GlcNAc). UDP-GlcNAc and other nucleotide hexosamines are substrates for glycosylation of many cytoplasmic and nuclear proteins. These proteins are glycosylated by the addition of a single molecule of O-linked β-GlcNAc on their serine and/or threonine residues (Bouche et al. 2004). During diabetes, glucose metabolism through hexosamine pathway is increased resulting in an increase in the level of expression of TGF- β1 and PAI-1 (Du et al. 2000), cardiomyopathy (Clark et al. 2003, Kohda et al. 2009) and impaired gene expression in endothelial cells (El-Osta et al. 2008, Xue et al. 2008).

Michael Brownlee (2005) and his co-workers have proposed a unifying mechanism linking the four pathways outlined above to a common upstream event (Brownlee 2005, Nishikawa et al. 2000). The common link is the overproduction of superoxide (reactive oxygen species) (ROS) by the mitochondria as a result of excessive glucose metabolism.

In support of their hypothesis, Brownlee and his team demonstrated that three pathways of glucotoxicity were blocked by preventing the over production of mitochondrial superoxides (Nishikawa et al. 2000). Hyperglycaemia is known to over produce the mitochondrial superoxides by inhibiting the glycolytic enzyme glyceraldehyde 3-phosphate dehydrogenase (GAPDH). The inhibition of GAPDH activates the upstream intermediates of the glycolytic pathway, which in turn lead to the metabolism of glucose through the four above-mentioned pathways mainly by activating poly (ADP-ribose) polymerase (PARP) (Du et al. 2003). The following figure 1.2 summarises the unifying mechanism of complications of hyperglycaemia that has been proposed.
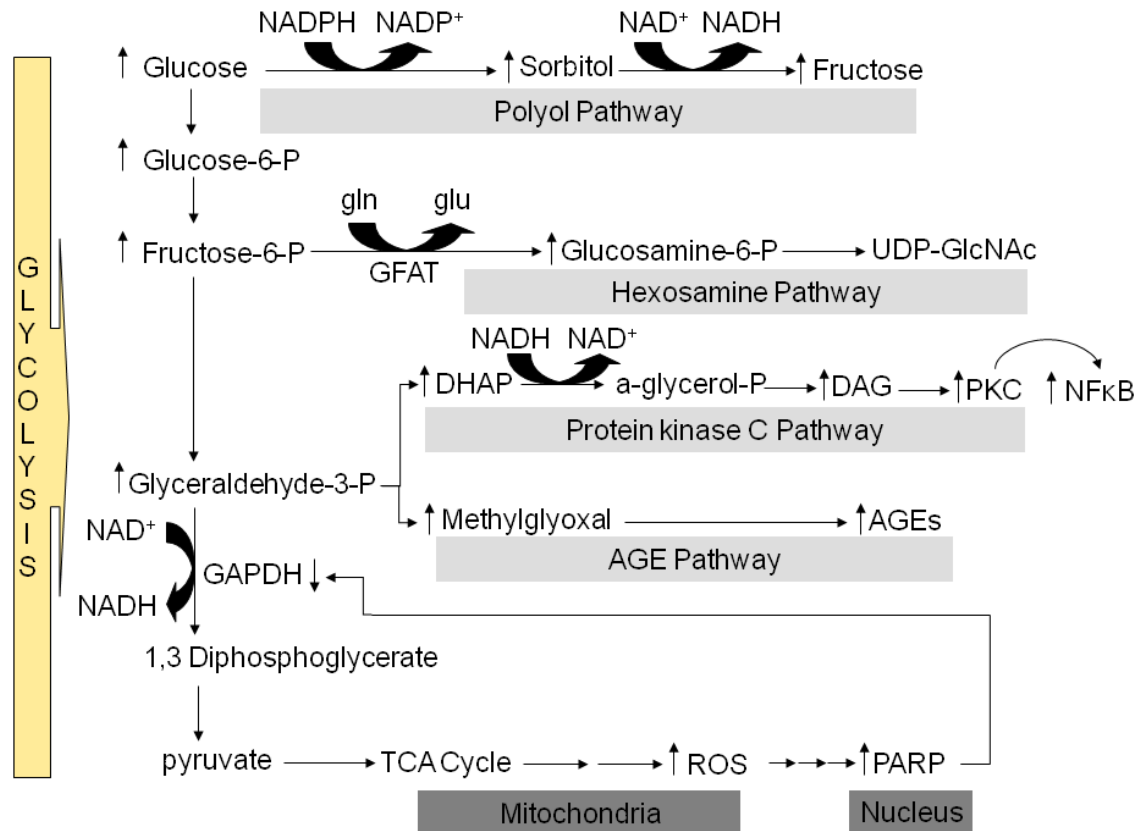
Fig. 1.2 The main four biochemical pathways of diabetes complications with unifying mechanism. In normal physiology, glucose is metabolised to pyruvate by glycolytic pathway, which later enters into TCA cycle to produce ATP. In hyperglycaemic condition cells become unable to metabolise the glucose sufficiently and lead to the overproduction of ROS, which in turn activates PARP and inhibit GAPDH. As the inhibition of GAPDH slows down the glycolytic pathway and increases the upstream substrates of glycolysis, more of accumulating intracellular glucose passes through four deleterious pathways: polyol, hexosamine, protein kinase C and AGE pathway (Adapted from Brownlee 2001, Brownlee 2005).

1.6 Hypoxia and Angiogenesis

Blood vessels of the microvasculature are formed by two different mechanisms namely vasculogenesis and angiogenesis. Vasculogenesis, like in embryonic development, is the *de novo* formation of endothelial cells from angioblasts. Angiogenesis in adult life is the formation of new capillary blood vessels from existent micro vessels. It is a complex and regulated process which involves multiple gene products expressed by different cell types, all contributing to an integrated sequence of events. (Carmeliet 2005, Griffioen and Molema 2000, Nussenbaum and Herman 2010). Angiogenesis has gained importance since Folkman published his pioneering hypothesis in 1971 about the need of angiogenesis in order for tumours to grow and metastasize (Folkman 1971). Angiogenesis is crucial in cancer therapy and diabetic retinopathy from the perspectives of anti-angiogenic strategies and in different ischemic conditions like cardiovascular diseases and impaired wound healing of diabetes for therapeutic angiogenesis (Cook and Figg 2010, Ferrara and Kerbel 2005). In the physiological condition, the activity of inducers and inhibitors of angiogenesis maintains it in balance (Conway, Collen and Carmeliet 2001). Table 1.2 lists the stimulatory and inhibitory regulators of the angiogenesis.

Hypoxia stimulates angiogenesis by regulating the expression of growth factors such as VEGF, VEGFR, bFGF, PDGF and other cytokines via expression of the transcription factor HIF-1 and other transcription factors (Pugh and Ratcliffe 2003). Table 1.3 summarizes the action of hypoxia on some molecules involved in different steps in angiogenesis.

Angiogenesis involves different stages. The initial vasodilation acts as a prelude leading to the increased permeability and matrix degradation of pre-existing vessels. The endothelial cells proliferate and migrate as shown in Fig. 1.1D which later lead to the formation of cords and lumen. Once the endothelial cells along with others mature into a vessel, they remodel according to the local environment forming a complex functional network (Conway, Collen and Carmeliet 2001). Out of these different stages of vessel development, endothelial proliferation and migration are pertinent to this project and are detailed in the following sections as general cell proliferation and migration.

Table 1.2: Selected list of regulators of angiogenesis (Adapted from Pandya, Dhalla and Santani 2006)

Stimulators	Inhibitors
HIF-1α, VEGF, VEGFR	Angiostatin
Angiopoietin-1 and Tie2 receptors	Anti-angiogenic anti-thrombin III
β-Estradiol	Canstatin
FGF, HGF, MCP-1	Endostatin (collagen XIII fragment)
IL-8	Fibronectin fragment
Leptin	Heparinases
PAI-1	IFN-α, β, γ; IP-10
MMPs	IL4, IL12, IL18
NOS and COX-2	TIMPs
PDGF-BB and receptors	PEDF
TNF-α	Prolactin 16 kDa fragment
Angiogenin	TSP-1
TGF-β1, endoglin, TGF-β receptors	Retinoids
Integrins $\alpha_v\beta_3$, $\alpha_v\beta_5$	Meth-1, Meth-2
VE-cadherin, PECAM-1	Platelet factor-4

Abbreviations: HIF-1α – hypoxia inducible factor - 1α; VEGF—vascular endothelial growth factor; VEGFR – VEGF receptors; FGF—fibroblast growth factor; HGF – hepatocyte growth factor; MCP-1 -macrophage chemoattractant protein; IL - interleukin; PAI-1 - platelet activator inhibitor-1; MMPs - matrix metalloproteases; NOS - nitric oxide synthase; COX-2 – cyclooxygenase – 2; PDGF-BB - platelet derived growth factor-BB; TGF - transforming growth factor; VE-cadherin – vascular endothelial cadherin; PECAM-1 – platelet endothelial cell adhesion molecule-1; TNF - tumour necrosis factor; IFN - interferon; TIMPs – tissue localised inhibitors of metalloproteinases; PEDF - pigment epithelium derived growth factor; TSP-1 - thrombospondin-1.

Table 1.3: Action of hypoxia on angiogenesis Some of the molecules involved in different steps in angiogenesis (Adapted from Pugh and Ratcliffe 2003).

Steps in angiogenesis	Stimulatory factors	Inhibitory factors
Vasodilation	NOS	
Increased vascular permeability	VEGF, Flt-1, Kdr	ANGPT-1, Tie-2
Extravasation of plasma proteins	VEGF	ANGPT-1, Tie-2
Endothelial sprouting	ANGPT-2, Tie-2	
Degradation of extra cellular matrix	Balance between MMPs (MMP-2) and TIMPs (TIMP-1), Collagen prolyl-4-hydroxylase	PAI-1
Liberation of growth factors(including VEGF, IGF-1 and bFGF)	uPA receptors	Thrombospondin-1 PAI-1
Endothelial cell proliferation & migration	Interplay between VEGFs, angiopoietins and FGFs. MCP-1, PDGF	
Pericyte and smooth muscle recruitment	PDGF	
Endothelial assembly & lumen acquisition	VEGF$_{121/165}$, ANGPT-1, Tie-2, Integrins	VEGF$_{189}$ Thrombospondin-1
Stabilization of nascent vessels	PAI-1	
Maintenance, differentiation and remodelling	ANGPT-1, Tie-2	ANGPT-2; Tie-2

Blue, direct transcriptional targets of HIF;

Red hypoxia regulated genes which are indirectly connected via cobalt, iron chelators or von Hippel–Lindau (VHL) inactivation to HIF or related pathways;

Green responses unconnected to HIF pathway.

IGF, insulin like growth factor; bFGF, basic fibroblast growth factor; MMP, matrix metalloproteinase; TIMP, tissue inhibitor of metalloprotienase; uPA, urokinase plasminogen activator; MCP, monocyte chemoattractant protein; PDGF, platelet-derived growth factor; PAI, plasminogen activator inhibitor; ANGPT, angiopoietin

1.7 Cell proliferation

All eukaryotic cells undergo proliferation through cell division. The events of the cell cycle include duplicating all the cell contents and a subsequent division into two daughter cells. The cell cycle involves four phases: gap phase 1 (G_1), DNA synthesis (S), gap phase 2 (G_2) and mitosis (M). Interphase constitutes G_1, S and G_2 phases and the M phase consists of mitosis and cytokinesis. In a typical proliferating human cell in culture, interphase is around 23 h and M phase is around 1 h. The chromosomes are duplicated during S phase (around 10 to 12 h) and segregated before the cell division during M phase. Two DNA molecules are disentangled and condensed into pairs known as sister chromatids during prophase of mitosis. Sister chromatids attached to the opposite poles of the spindle are aligned at the equator in metaphase stage. The sister chromatids are separated after the destruction of their cohesion and pulled to the opposite poles of the spindle in anaphase stage. The spindle is disassembled and separated chromosomes are packed into separate nuclei at telophase, which is followed by separation of daughter cells by cytokinesis. The two gap phases – G_1 between M and S phase and G_2 between S and M phase are utilised by the cells to increase their mass of proteins and organelles and to monitor external and internal conditions. If the extracellular conditions are unfavourable during early G_1, after M phase, the cells may under go an additional gap phase known as G_0. If the conditions are favourable, cells in early G_1 or G_0 progress through a commitment point known as restriction point (R). Once the cells pass through the irreversible restriction point, the DNA duplication begins taking the cell into S phase (Alberts et al. 2008). Increase in the glucose level prevented the progression of HUVECs from G_1 to S phase by increasing the cells in G_0/G_1 phase and reducing the cell count in S phase. This effect was reported to be mediated through PI3K/Akt/eNOS/NO pathway (Zhong et al. 2010). In porcine aortic endothelial cells, high glucose caused the cell cycle progression into S phase and increased expression of FGF-2 failed to protect TNF-α induced cell death (Clyne, Zhu and Edelman 2008).

The complex, orderly and unidirectional cell cycle is regulated by cell cycle control system which involves cyclins, cyclin dependant protein kinases (CDKs) and CDK inhibitors. The cell cycle progresses through three biochemical switches which are known as check points. The first one is restriction point (R) or G_1/S check point where the cell is committed to enter into S phase and duplicates the chromosomes. The second is the G_2/M checkpoint where the cell enters into M phase leading to the alignment of chromosomes on the spindle. The third is the metaphase to anaphase transition, where the sister chromatids are separated followed by the completion of mitosis and chemokinesis (Alberts et al. 2008).

Central to the cell cycle regulation are the activities of CDKs, which are in turn regulated by cyclins. The CDK subunit, a serine/threonine protein kinase alone is inactive as its catalytical activity is produced only upon the tight binding with cyclins and phosphorylation of their T loops by CDK activating kinase (CAK) (Lorincz and Reed 1984, Russo et al. 1996). Four types of CDKs i.e. CDK 1, 2, 4 and 6, are known to have active role in the regulation of cell cycle (Morgan 1997). Two types of cyclins are known, ones involved in cell cycle (cyclin A, B, D and E) and others which are not (cyclin H and C) (Meeran and Katiyar 2008). Cyclins involved with cell cycle are G_1/S cyclins (E), S cyclins (A), M cyclins (B) and G_1 cyclins (D). Cyclin E and D by pairing with CDK2 and CDK4/6 respectively are known to play a vital role in the progression of cell cycle from G1 to S phase. Others involved at different stages are cyclin A with CDK2 then with CDK1 at S phase, cyclin B with CDK1 at M phase and cyclin D with CDK4/6 at G_1 phase (Sherr 1994, Sherr 1996). The levels of cyclins change, as shown by the semi-circular shapes in Fig. 1.3, during the cell cycle resulting in the activation of cyclin-CDK complexes. Cyclin D synthesized during early G_1 gets degraded at the end of G_1 as the cell enters S phase. Cyclin E synthesized at late G_1 is degraded in S, cyclin A synthesized in S gets degraded at the exit of G_2 and cyclin B synthesized in late G_2 gets degraded at late M phase. However, unlike cyclins the levels of CDKs remain constant throughout the cell cycle (Alberts et al. 2008). Increased glucose concentration has been proved to lead to cycle arrest of endothelial progenitor cell (EPC) at G_0/G_1 phase by decreasing the expression of cyclin A and E, CDK2 and proliferating cell nuclear antigen (PCNA) (a marker of S phase) (Zhang et al. 2008).

Several mechanisms control the activities of CDKs at specific stages of cell cycle. A protein kinase known as Wee 1 inhibits CDK activity by phospohrylation and a phosphatase known as Cdc25 increases CDK activity by dephosphorylation (Enders 2010, Gutierrez et al. 2010). Along with these, CDK inhibitor proteins (CKIs) also regulate the cyclin-CDK complexes by acting as checkpoint effectors. There are two families of CKIs with multiple members in each family. The first family known as Cip/Kip (CDK inhibitor protein/Kinase inhibitor protein) consists of p21[Cip1], p27[Kip1] and p57[Kip2] (Lee, Reynisdottir and Massague 1995, Toyoshima and Hunter 1994). The CKIs bind with the cyclin-CDK complex and render it inactive. CKIs undergo ubiquitination and protesomal degradation by an ubiquitin ligase called Skp1-Cul1-F box (SCF) protein complex and allow the progression of cell cycle to next phase (Kitagawa, Kotake and Kitagawa 2009). The coexistence of hypertension with diabetes has been reported to decrease the proliferation of retinal cells by increasing the expression of p27[Kip1], a negative regulator of cell cycle (Lopes de Faria et al. 2008). A second family of CKIs, known as the INK4 (inhibitors of CDK4) family of p15[INK4b], p16[INK4a], p18[INK4c] and p19[INK4d] bind to cyclin D -

CDK4/6 complex causing the arrest of cell cycle at G_1 phase (Dai and Grant 2003, Hannon and Beach 1994, Hirai et al. 1995, Kim and Sharpless 2006, Serrano, Hannon and Beach 1993).

The following figure 1.3 is a simple summary of the events of cell cycle.
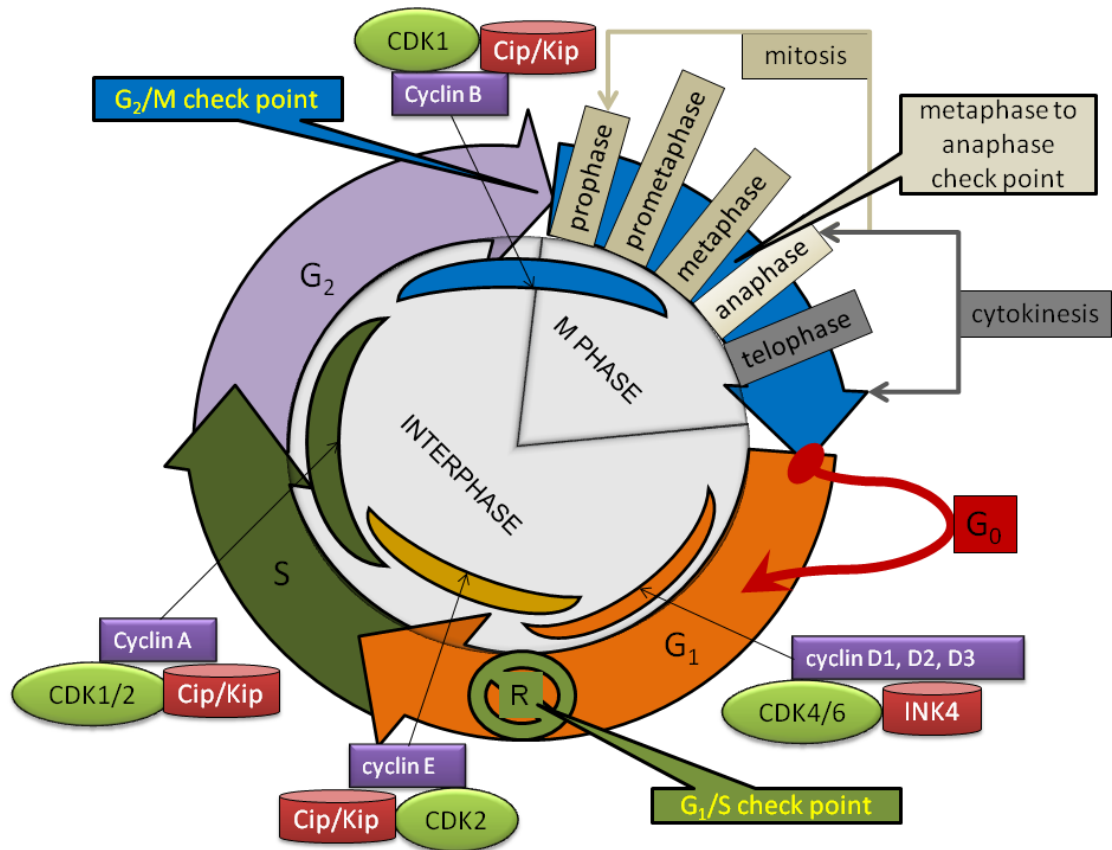
Fig.1.3 Cell cycle events G_1 and G_2 are the gap phases between mitosis (M) and DNA synthesis (S) phase. Cells go into a special gap phase (G_0) or into quiescence to avoid aberrant proliferation taking the cues from the internal and external cellular environment. The level of individual cyclin (indicated by inner shapes) varies as the cell progresses through the cell cycle assuring the uni-directionality of the cycle, whereas the levels of cyclin dependent kinases (CDKs) remain same. The complexes of cyclins-CDKs with CDK inhibitors (CKIs) play a central role in the progression of cell cycle. The CDK inhibitors (CKIs) need to be deactivated to allow the progression of cell cycle; otherwise activated CKIs play an inhibitory role by acting at different check points.

1.8 Cell migration

Cell migration is a crucial step for the wound healing process including endothelial cell migration during the angiogenesis (Lauffenburger and Horwitz 1996). Cells migrate randomly (chemokinesis) when their sense of intrinsic directionality is low and external cues are not present (Petrie, Doyle and Yamada 2009, Seppa et al. 1982). On the other hand, directional migration is driven by the intrinsic directionality and external regulation (Petrie, Doyle and Yamada 2009). Chemotaxis in response to soluble cues (Liu et al. 2009), haptotaxis in response to surface gradient like adhesion molecule or ECM (Hsu, Thakar and Li 2007), electrotaxis or galvanotaxis in response to electric fields (Lin et al. 2008) and durotaxis or mechanotaxis in response to mechanical signals (Li et al. 2002) follow directional migration. The following figure 1.4 schematically represents the cytoskeletal arrangement of a migrating cell (Le Clainche and Carlier 2008).

The cell motility cycle is also a highly organised event which includes polarization, protrusion, traction and retraction of a cell (Cell Migration Gateway 2010). The process of reorganisation of the cell into a leading front edge and trailing rear edge is known as polarization. Polarization initiates on the application of chemoattractants like VEGF leading to the next steps of migration (Shamloo et al. 2008). The cell's polarity signalling network consists of the Par (partitioning defective) protein complex, PKCε and PKCζ as atypical protein kinase C (aPKC) and RhoGTPase signalling molecule cdc42 (Cell Migration Gateway 2010, Joberty et al. 2000). The par3 and par6 are part of Par protein complex and participate in the formation of rear-front axis in a moving cell and apical-basal polarity with help of VE-cadherins and adherence junctions (Lampugnani et al. 2010). Cdc42 and Rac1 by recruiting the par3/6 complex activates aPKC in order to reorient the microtubule-organising centre (MTOC) from which the microtubule network radiates and Golgi apparatus towards the leading edge of a moving cell (Koh, Mahan and Davis 2008, Tzima et al. 2003). The nucleus of the cell moves rearward rather than MTOC moving between the nucleus and leading edge and reorientation is known also to involve dynactin and dyanein along with cdc42 (Etienne-Manneville and Hall 2001, Palazzo et al. 2001). Cdc42 acting through myotonic dystrophy kinase related cdc42 binding kinase (MRCK) was sufficient to make the nucleus move rearwards while others held the MTOC at the cell centroid with help of myosin dependant actin flow finally leading to the front-rear axis (Gomes, Jani and Gundersen 2005). Cdc42 and Rac1 phosphorylate p21 activated protein kinase 1 (Pak1), Pak2 and Pak4 which act as a downstream target for PKCε to initiate protrusion and stimulate the lumen and tube formation (Koh, Mahan and Davis 2008, Kupfer, Louvard and Singer 1982).
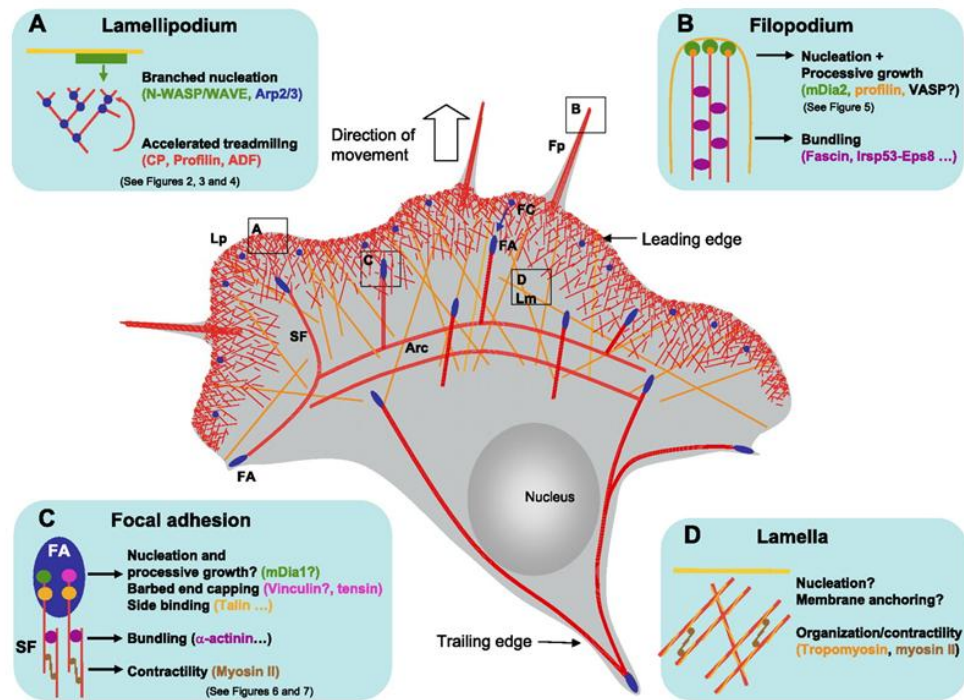
Fig. 1.4 "Schematic illustration of the actin cytoskeleton in a migrating cell. This schematic cell contains the major structures found in migrating cells common to different cells. Migrating cells have A) lamellipodia, where branched actin filaments are generated at the plasma membrane by the signal responsive WASP-Arp2/3 machinery and maintained in fast treadmilling by a set of regulatory proteins (ADF, capping proteins, profilin), B) fingerlike protrusions called filopodia to sense the environment at the tip of which, formins like mDia2 catalyze the processive assembly of profilin-actin. The processive assembly of profilin-actin is catalyzed by formins. C) Focal adhesions formed in response to RhoA signaling, connect the extracellular matrix to contractile bundles made of actin filaments, myosin II, and bundling proteins including α-actinin. Focal adhesions contain a variety of actin binding proteins including side binding proteins, capping proteins, and nucleators. D) Lamella contains the signature proteins tropomyosin and myosin II".

Lp, lamellipodium; Fp, filopodium; Lm, lamella; SF, stress fiber; FA, focal adhesion; FC, focal complex.

(Reproduced with permission from Le Clainche and Carlier 2008)

The actin filament polarization leads to the polymerization or formation of barbed ends and de-polymerization of pointed ends at the leading edge of a cell (Pollard and Borisy 2003). Polymerization of actin assembly at the leading edge extends the flat membrane (lamella) protrusions known as lamellopodia and finger like protrusions known as filopodia (Le Clainche and Carlier 2008, Pollard and Borisy 2003). The protrusions develop and initiate cell motility by a process known as 'treadmilling' which is accelerated by many actin binding proteins (Kueh and Mitchison 2009). These proteins are actin depolymerising factor (ADF) or cofilin, capping protein, Arp2/3 complex, an activator of Arp2/3 complex - profilin and many others and are involved in monomer sequestration, nucleation, capping, depolymerisation and termination of actin filament (Pollard and Borisy 2003).

The growth of the actin filament depends on the availability of un-polymerised actin monomers which are present in abundance bound to profilin and sequestering proteins such as thymosin-β4 and which are reported to increase the directional migration of cells (Ding et al. 2006, Malinda, Goldstein and Kleinman 1997, Malinda et al. 1999). Assembly or elongation of actin filament at the leading edge begins by the activation of nucleating promoting factors such as Wiscott-Aldrich Syndrome protein (WASp), neuronal WASp (N-WASp) and suppressor of cAMP receptor (Scar)/WASp-family Verprolin homologous (WAVE) proteins (Kang et al. 2010, Vicente-Manzanares, Webb and Horwitz 2005). WASp, N-WASp and Scar/Wave proteins are activated by signalling molecules such as the Rho-family GTPase (cdc42), phosphotidylionsitol-4,5-biphsophate (PIP2) and Src homology 3 (SH3) domain containing proteins like Grb2, Nck, or Abil (Carlier et al. 2000, Innocenti et al. 2005, Rohatgi, Ho and Kirschner 2000, Rohatgi et al. 2001). The WASp/WAVE proteins regulate actin polymerization by their ability to initiate the nucleation by Arp2/3 complex at the barbed end of actins (Kang et al. 2010, Hufner et al. 2001). Cotractin, an F-actin binding protein is also known to promote nucleation of actin filament by binding with Arp2/3 complex (Kinley et al. 2003)

The Arp2/3 complex localized at the lamellopodia, upon the activation by nucleating proteins caps the attachment of actin monomers at the pointed ends (Mullins, Heuser and Pollard 1998, Svitkina and Borisy 1999). Additionally, the Arp2/3 complex nucleates the barbed ends and extends the pre-existing actin filament at an angle of 70^0 leading to the formation of dendritic networks of actin filament branches (Mullins, Heuser and Pollard 1998, Fletcher and Mullins 2010). The elongation of actin filament is aided by another set of actin binding proteins, mDia1 and mDia2 – mammalian Diaphanous of Formin family. RhoA regulated mDia1 and cdc42 regulated mDia2 bind to the barbed ends and recruit profilin bound G actins in order to polymerize the actin filament and aid in the formation of the stress fibres (Vicente-Manzanares, Webb and Horwitz 2005,

Watanabe and Higashida 2004). The elongation of actin filaments at the barbed ends is stopped by capping by proteins known as Cap Z and gelsolin (Cooper and Schafer 2000). The activities of elongation, branching and capping of the actin filament lead to the formation of protrusive lamellopodia (Fletcher and Mullins 2010). The finger-like protrusions, filopodia sense the external environment in which the actin polymerization is carried out by mDia2 and vasodilator stimulated phoshoprotein (VASP). The polymerized actin filaments in filopodia are arranged as bundles with the help of fascin and Irsp53-Eps8 complex (Le Clainche and Carlier 2008, Mattila and Lappalainen 2008).

The de-branching of actin filament begins with the hydrolysis of ATP to ADP with the release of a phosphate group or due to the loss of ATP (Blanchoin, Pollard and Mullins 2000, Hinshaw et al. 1993). Loss of phosphate causes the detachment of Arp2/3 complex from the side of the actin filament and the free Arp2/3 complex caps the pointed ends and accelerates the de-branching (Blanchoin, Pollard and Mullins 2000). The de-branching of the actin filament and loss of ATP are mediated by the activation or dephosphorylation of ADF/cofilin (Suurna et al. 2006). ADF/cofilins sever the actin filaments and thus increase the availability of actin monomers. This activity of ADF/cofilin is regulated by phosphorylation of its upstream regulator LIM kinase (LIMK). LIMKs are in turn regulated by RhoA-ROCK or PI3-K, Ca^{2+}, phospholipid dependant PKC, Rac activated PAK1. PAK1 is in turn regulated by small G proteins or the DAG pathway (Campos et al. 2009, Gong, Stoletov and Terman 2004, Maciver and Hussey 2002). Profilin acting as a nucleotide exchange factor binds competitively to ADP actin and increases the disassociation of ADP from actin. This allows the actin to bind to abundantly available ATP leading to the formation of ATP-actin monomers ready to re-enter the cycle of actin polymerization (Pollard and Borisy 2003, Ding et al. 2006).

In cultured cells, the network of actin and myosin produce the retrograde flow, where the actin filaments of lamellopodia move rearward with respect to the substratum. Hence, the rate of forward protrusion of a cultured cell is a result of the difference between the retrograde flow and actin polymerization (Ridley 2004). The process of the protrusion is detailed in the following figure 1.5.
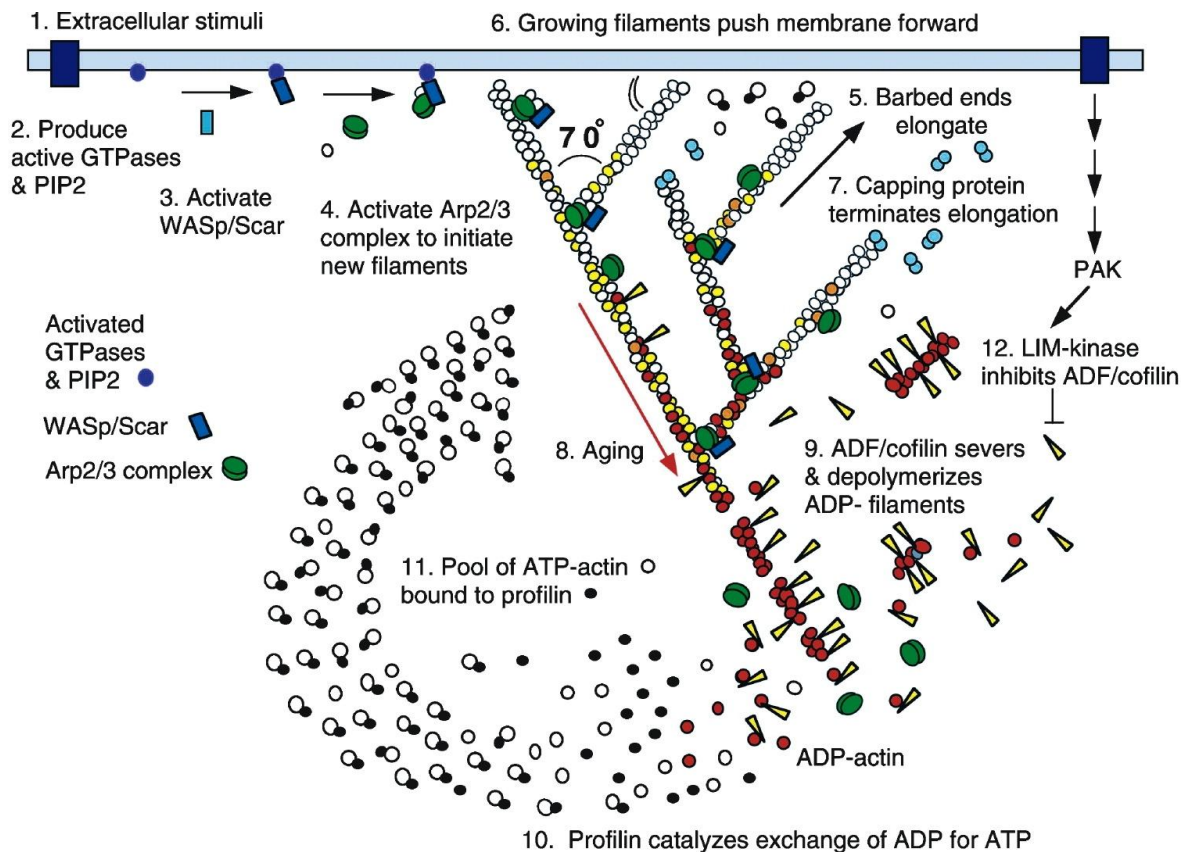
Fig. 1.5 "Dendritic nucleation/Array treadmilling model for protrusion of the leading edge. (1) Extracellular signals activate receptors. (2) The associated signal transduction pathways produce active Rho-family GTPases and PIP2 that (3) activate WASp/Scar proteins. (4) WASp/Scar proteins bring together Arp2/3 complex and an actin monomer on the side of a pre-existing filament to form a branch. (5) Rapid growth at the barbed end of the new branch (6) pushes the membrane forward. (7) Capping protein terminates growth within a second or two. (8) Filaments age by hydrolysis of ATP bound to each actin subunit (white subunits turn yellow) followed by dissociation of the γ phosphate (subunits turn red). (9) ADF/cofilin promotes phosphate dissociation, severs ADP-actin filaments and promotes dissociation of ADP-actin from filament ends. (10) Profilin catalyzes the exchange of ADP for ATP (turning the subunits white), returning subunits to (11) the pool of ATP-actin bound to profilin, ready to elongate barbed ends as they become available. (12) Rho-family GTPases also activate PAK and LIM kinase, which phosphorylates ADF/cofilin. This tends to slow down the turnover of the filaments."
(Reproduced with permission from Pollard and Borisy 2003).

The adhesions, points of interaction between the cell and the substratum, form at the leading edge and disassemble at the trailing edge of a cell in order to facilitate the traction and retraction of cells leading to rapid migration (Le Clainche and Carlier 2008, Vicente-Manzanares, Webb and Horwitz 2005). Along with the actin cytoskeleton, components of adhesions such as integrins, adaptor and signalling proteins and microfilament structures play a vital role in the assembly, maturation and turnover of adhesions (Lock, Wehrle-Haller and Stromblad 2008, Vicente-Manzanares, Choi and Horwitz 2009). Focal complexes, focal adhesions, fibrillar adhesions and 3D-matrix adhesions are different types of adhesions observed in cells such as fibroblasts (Berrier and Yamada 2007, Le Clainche and Carlier 2008). Nascent adhesions of focal complexes are assembled and disassembled during the adhesion turnover at the leading edge of a cell. The focal complex which is not disassembled mature into focal adhesions and contain integrins, vinculin, talin, α-actinin, paxillin, zyxin, VASP, focal adhesion kinase (FAK), actopaxin and phosphotyrosine proteins (Le Clainche and Carlier 2008).

Integrins are transmembrane glycoproteins expressed as alpha-beta heterodimers and 24 of them composed of eighteen alpha and eight beta subunits have been identified to constitute the receptors for ECM proteins (Hynes 2002). The outer domain of integrin binds to extracellular ligand and cytoplasmic domain binds the various signalling molecules and actin in order to produce the effect of protrusion and traction (Huveneers and Danen 2009). The cytoplasmic domain of integrin binds directly or indirectly to talin, vinculin, α actinin, FAK, Arp2/3 complex and actin filaments (Vicente-Manzanares, Choi and Horwitz 2009). The linkage between the actin and integrin acts as a molecular clutch integrating adhesion, retrograde flow and actin polymerization in order to produce the traction at the leading edge and retraction at the trailing edge (Le Clainche and Carlier 2008, Vicente-Manzanares, Choi and Horwitz 2009). The activation of integrin-actin linkage regulates Rho family GTPases such as RhoA, Rac1 and Cdc42. Activation of Rho GTPases is initiated by the recruitment of upstream molecules such as FAK, Src family of tyrosine kinases (SFKs) and paxillin. The SFKs regulate guanine exchange factors (GEFs) and GTPase activating factors (GAPs), which in turn control Rho GTPases (Huveneers and Danen 2009).

The disassembly of adhesions and retraction at the trailing end of a cell aided by the myosin-II induced contractility completes the cell motility cycle. Apart from creation of tension and retraction, myosin II plays role during polarization, protrusion and the traction as well (Vicente-Manzanares et al. 2009).

1.9.1 Hypoxia inducible factor-1 (HIF-1)

Hypoxia produces its effect by activating different transcriptional pathways including HIF, fos, jun, NF-κB and p53 (Pugh and Ratcliffe 2003). Out of these, the pathway for the hypoxia controlled regulation of the growth factors through hypoxia inducible factor -1 (HIF-1) is come to be known as the master regulator of oxygen homeostasis (Semenza 2002). Wang and Semenza first identified and purified HIF-1α as a nuclear factor induced by the hypoxia. Later it was characterised as a heterodimeric transcription factor composed of hypoxia inducible HIF-1α subunit and a constitutively expressed HIF-1β subunit, also known as aryl hydrocarbon nuclear translocator (ARNT) (Fig. 1.6) (Semenza et al. 1991, Semenza and Wang 1992, Wang and Semenza 1993). In addition to HIF-1α and HIF-1β, other isoforms of HIF-α such as HIF-2α and HIF-3α with its splice variant inhibitory PAS (IPAS) have been described (Ema et al. 1997, Gu et al. 1998, Makino et al. 2001).
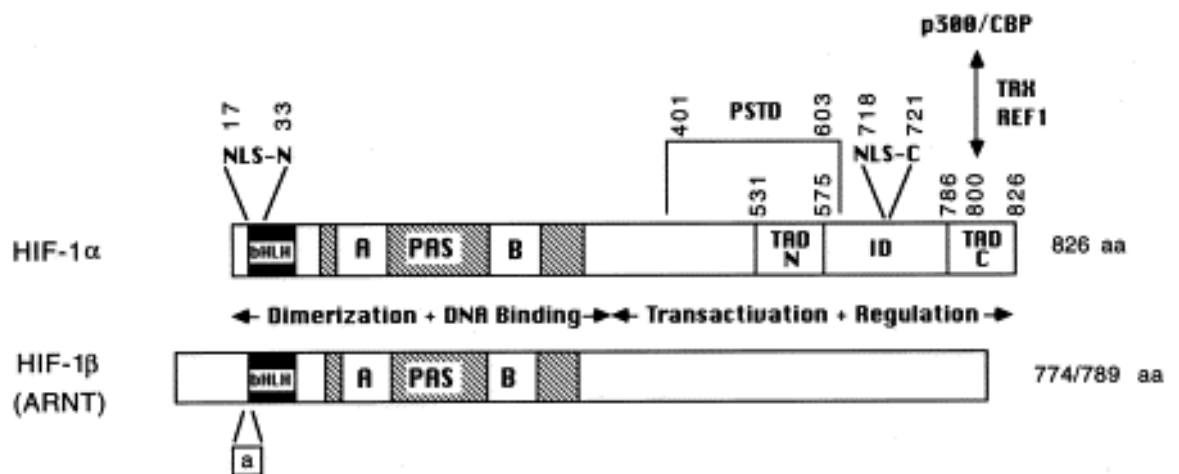
Fig. 1.6: ''Domain structure of HIF-1 Important functional domains of the HIF-1α and HIF-1β subunits are indicated as follows: a, alternate exon encoding 15 amino acids (aa) in HIF-1β; bHLH, basic-helix-loop-helix domain; ID, inhibitory domain; NLS-N and NLS-C, amino- and carboxyl-terminal nuclear localization signal; PAS, Per-ARNT-Sim homology domain with internal A and B repeats; PSTD, proline-serine-threonine-rich protein stability domain; TAD-N and TAD-C, amino- and carboxyl-terminal transactivation domain; REF-1, redox factor 1; TRX, thioredoxin''

(Reproduced with permission from Semenza 2000).

The human HIF-1α gene is located on chromosome 14 (14q21-q24) and the HIF-1β gene on chromosome 1 (1q21). HIF-1α and HIF-1β are large proteins consisting of 826 and 789 amino acids respectively. Both subunits contain nuclear localization signals and a basic helix–loop–helix motif (bHLH). The HLH and basic domain are responsible for dimerization and DNA binding respectively (Jiang et al. 1996, Wang et al. 1995). Per-ARNT-Sim (PAS) domain is common to both HIF-1α and HIF-1β. This sequence identifies a protein super family which was found in *Drosophilia* proteins period (Per) and single minded (Sim) and the vertebrate protein aryl hydrocarbon nuclear translocator (ARNT) (Wang et al. 1995). The dimerization of HIF-1α and HIF-1β is mediated by both HLH and PAS domain, which in turn is necessary for DNA binding by the basic domains (Jiang et al. 1996). In addition, the HIF-1α subunit contains two transactivating domains (TAD), the N- and C-terminal transactivating domains NTAD and CTAD, between residues 531–575 and 813–826 respectively (Ruas, Poellinger and Pereira 2002). The NTAD overlaps with a larger domain denoted as O_2-dependent degradation (ODD) domain, which confers regulation of HIF-1α protein levels as a function of O_2 concentration (Huang et al. 1998). The main function of CTAD is to recruit and interact with transcriptional co-activator proteins including CBP/p300, SRC-1 and TIF-2 (Kung et al. 2000, Hirota and Semenza 2006).

Under hypoxia HIF-1α and HIF-1β dimerize and bind to hypoxia response elements (HREs) within target genes. This HIF-HRE complex activates the transcription of target genes by recruiting the co activators p300 and CBP (Ruas, Poellinger and Pereira 2005). HIF-1α in non-hypoxic conditions is synthesized, ubiquinated and degraded whereas in hypoxic conditions HIF-1α stabilizes to dimerize with HIF-1β and transactivates the target genes (Webb, Coleman and Pugh 2009). Regulation of HIF-1α involves pVHL dependant as well as pVHL independent pathways (Yee Koh, Spivak-Kroizman and Powis 2008).

1.9.1.1 pVHL dependant degradation

In the presence of oxygen, HIF-1α is hydroxylated by prolyl hydroxylase domain-containing proteins (PHDs) 1, 2 and 3 at two proline residues Pro402 and Pro564 situated in the ODD domain (Masson et al. 2001). These modifications are mediated by Fe^{2+}, ascorbate and 2-oxoglutarate (Huang et al. 2002, Jaakkola et al. 2001). Hydroxylation of Pro402 and Pro564 promotes interaction between HIF-1α and the tumour supressor protein von Hippel–Lindau (pVHL) (Min et al. 2002). The VHL protein functions as a substrate recognition component of an E3 ubiquitin ligase complex that mediates ubiquitination of HIF-1α, leading to its rapid degradation by proteasomes (Kamura et al. 2000). The E3 ubiquitin ligase includes at least four other proteins: elongin B, elongin C,

cullin-2 and ring-box 1 (also called ROC1 or Hrt1) (Clifford et al. 2001, Maxwell et al. 1999). Acetyl transferase arrest defective-1 (ARD-1) mediated acetylation of lysine residue (Lys) 532, located in ODD domain of HIF-1α, increases the interaction of HIF-1α and pVHL leading to the destabilisation of HIF-1α (Jeong et al. 2002). Apart from pVHL, tumour suppressor protein p53 promoted murine double minute 2 (MDM2) also regulates proteasomal degradation of HIF-1α (Ravi et al. 2000). On the contrary, the pVHL interacting deubiquitanting enzyme 2 (VDU2) stabilises the HIF-1α by binding to it and deubiquitylating it and thus preventing its proteasomal degradation (Li et al. 2005).

A second type of modification, β-hydroxylation of an asparaginyl residue, Asn803, in the CTAD allows for direct O_2-dependent regulation of HIF-1 activity (Lando et al. 2002b). This modification which is mediated by factor inhibiting HIF-1 (FIH-1) blocks interaction of CTAD with the transcriptional co-activators CBP/p300 in the presence of oxygen, thereby inhibiting HIF-dependent transactivation (Lando et al. 2002a). Similar to PHDs, the asparaginyl hydroxylation of FIH-1 requires 2-oxoglutarate dependant dioxygenase, Fe^{2+} and ascorbate as coactivators (Lando et al. 2002a).

However during hypoxia, the activities of PHDs are inhibited leading to the stabilisation of HIF-1α. Reactive oxygen species (ROS) acting as an oxygen sensing mechanism increases during hypoxia. Further, ROS convert the oxidative status of Fe^{2+} to Fe^{3+} which leads to an inhibition of PHDs activity and stabilisation of HIF-1α (Simon 2006). Hypoxia is also known to stabilise the HIF-1α by inducing the expression of small ubiquitin like modifiers (SUMO)-1 through a process known as SUMOlyation (Bae et al. 2004). However, newer reports suggest that the SUMOlyation lead to the HIF-1α degradation which could be reversed by a nuclear SUMO protease known as sentrin/SUMO-1 specific peptidase (SENP) 1 (Xu et al. 2010b).

The stability and affinity of pVHL towards HIF-1α is regulated by E2 endemic pemphigus foliaceus (EPF) ubiquitin carrier protein (UCP). The UCP degrades pVHL by ubiquitylation and causes accumulation of HIF-1α during normoxia (Jung et al. 2006). Apart from UCP, osteosarcoma-9 (OS-9) and spermidine/spermine-N[1]-acetyltransferase (SSAT) 2 have been recognised as novel regulatory molecules (Yee Koh, Spivak-Kroizman and Powis 2008).

1.9.1.2 pVHL independent degradation

pVHL and oxygen independent degradation of HIF-1α is mediated through heat shock protein 90 (HSP90) and receptor of activated protein kinase C (RACK1). RACK1 competes with HSP90 for binding to HIF-1α at PAS domain leading to its binding with HIF-1α and subsequent homodimerization and recruitment of components of elongin E3 ligase complex and finally the degradation of HIF-1α (Liu et al. 2007a). RACK1 pathway is

regulated by SSAT1 which is essential for the stability of HIF-1α RACK1 interaction (Baek et al. 2007). RACK1 pathway is regulated also by calcineurin, a calcium and calmodulin dependent serine/threonine specific protein phosphatase which inhibits RACK1 mediated degradation of HIF-1α by blocking the dimerization due to dephosphorylation of the RACK1 (Liu et al. 2007b).

Phosphotidylinositol 3-kinase-Akt (PI3K-Akt) pathway not only regulates the transcriptional activity of HIF-1α, but also regulates its degradation via glycogen synthase kinase (GSK) 3β and forkhead transcription factors (FOXO) 4 or 3a (Yee Koh, Spivak-Kroizman and Powis 2008). The overexpression of GSK3β, which could be phosphorylated and degraded by protein kinase B, results in the ubiquitylation and proteasomal degradation of HIF-1α whereas inhibition of GSK3β resulted in the induction of HIF-1α (Flugel et al. 2007). The expression of FOXO4, which is negatively regulated by PI3K-Akt, leads to the down regulation of HIF-1α due to the induction of pVHL independent ubiquitylation and degradation of HIF-1α (Tang and Lasky 2003). Similarly, PTEN mediates FOXO3a over expression which is negatively regulated by PI3K-Akt, leads to the p300 dependant inactivation of transcriptional activity of HIF-1α (Emerling et al. 2008). The following figure 1.7 (Yee Koh, Spivak-Kroizman and Powis 2008) summarizes the regulation of HIF-1α degradation by various pathways.

1.9.1.3 Translational regulation of HIF-1α

Many mechanisms have been proposed to control the translational activity including HIF-1α induction by activation of PI3K-Akt mammalian target of rapamycin (mTOR) and mitogen activated protein kinase (MAPK) pathways (Yee Koh, Spivak-Kroizman and Powis 2008). In human microvascular endothelial cells (HMEC-1), hypoxia was able to induce the phosphorylation of both ERK1 and ERK2 MAPKs (Minet et al. 2000). In hypoxia, ERK1/2 was shown to be involved in the activation of HIF-1 transcriptional activity by directly phosphorylating the HIF-1α confirming the involvement of MAPKs (Minet et al. 2000, Richard et al. 1999). Along with ERK1/2 inhibitor, the p38 kinase inhibitor has also been known to cause the inactivation of HIF-1α (Sodhi et al. 2000). Further, the hypoxia induced DAG accumulation and HIF-1α stabilization was through the action of phosphatidylcholine phospholipase C (PC-PLC)/sphingomyelin synthase (SMS) activity and not through DAG-dependent protein kinase C (PKC) activity (Aragones et al. 2001, Temes et al. 2004). However, there are other reports suggesting the involvement of PKC in the regulation of HIF-1α activation (Kruger et al. 1998, Lee et al. 2007, Yun et al. 2009). The transcriptional activity of HIF-1α has also been shown to be regulated by other signalling pathways such as phosphatidylinositol-3 kinase/protein kinase B (PI3K/Akt) and p53 (Fang et al. 2005, Lin et al. 2010, Zhong et al. 2000).
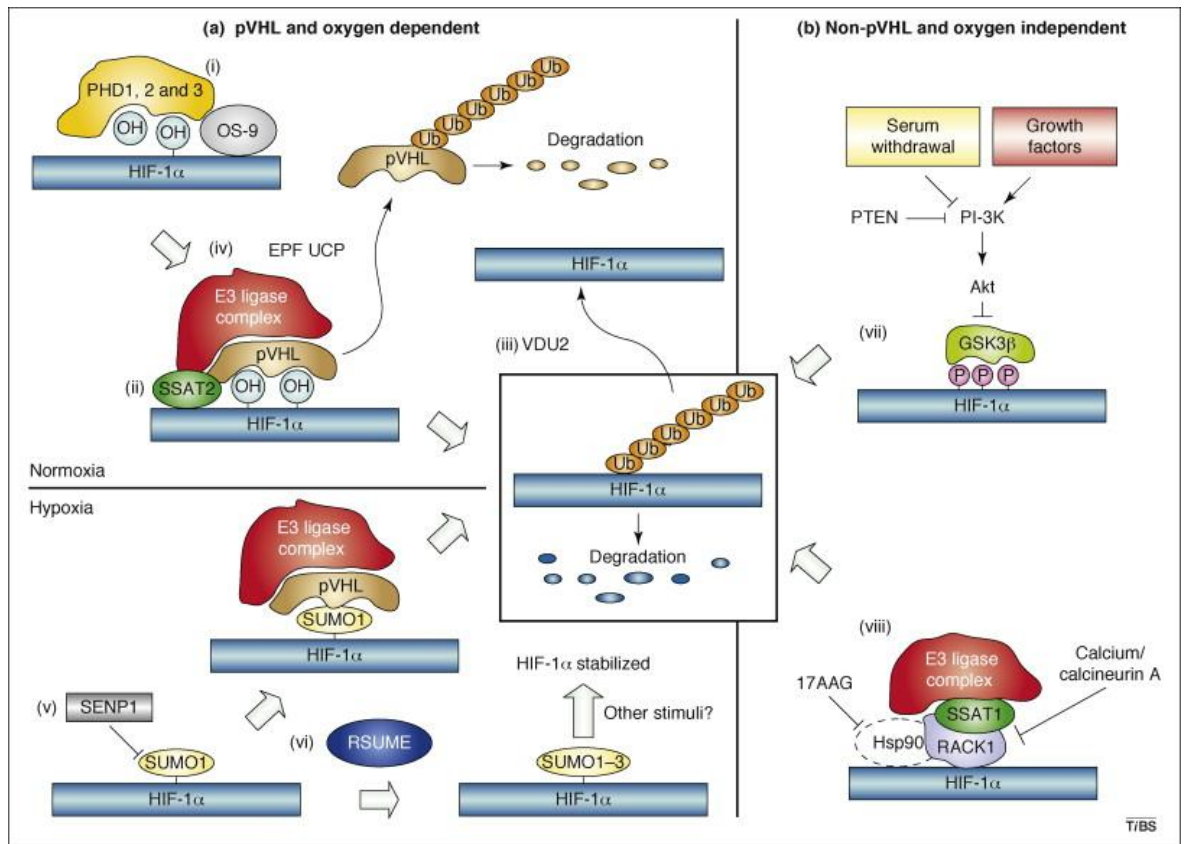
Fig 1.7 ''Important pathways regulating HIF-1α degradation HIF-1α degradation is regulated by multiple pathways that are either dependent (a) or independent (b) of oxygen and pVHL. (a) Under normoxic conditions, HIF-1α is hydroxylated by prolyl hydroxylases (PHDs) leading to the recruitment of the pVHL E3 ligase complex to HIF-1α. SSAT2 binds to HIF-1α, pVHL and elongin C and the pVHL E3 ligase complex ubiquitylates HIF-1α leading to its degradation. Alternatively, pVHL can be ubiquitylated and degraded by EPF UCP. Hypoxia results in HIF-1α SUMOylation, which can facilitate the recognition of HIF-1α by the pVHL E3 ligase complex and lead to HIF-1α degradation. HIF-1α SUMOylation can be reversed by SENP1 resulting in stabilization. However, hypoxia-induced RSUME-mediated SUMOylation (RSUME) can increase HIF-1α stability indicating that the role of SUMOylation in HIF-1α regulation is still unclear. (b) Oxygen-independent regulators of HIF-1 include GSK3β and RACK1.''

(Reproduced with permission from Yee Koh, Spivak-Kroizman and Powis 2008).

In addition to hypoxia, a variety of growth factors including EGF, FGF2, insulin, IGF1 and 2, IL-1 and NO are know to regulate the transactivational ability of HIF-1 (Natarajan, Fisher and Fowler 2003, Semenza 2002). Other than these, ROS are also known to regulate the HIF-1α activity (Chandel et al. 1998, Klimova and Chandel 2008). In streptozotocin induced diabetic rats under ischemic conditions, mRNA expression of HIF-1α was found to be reduced, which was restored by normoglycaemia or glutathione, a free radical scavenger indicating the role of ROS in regulating the expression of HIF-1α (Marfella et al. 2002). In another study HIF-1α protein was reported to be expressed in sciatic nerves of mice within three months of streptozotocin induced diabetes and anti-oxidant alpha lipoic acid attenuated the expression of HIF-1α suggesting the role of ROS in expression of HIF-1α (Knott et al. 2002, Knott et al. 2003).

1.9.2 Physiological and pathophysiological role of HIF-1

HIF-1 regulates most of the genes involved in oxygen homoestasis, including genes known to be responsible for angiogenic factors, erythropoiesis, cell proliferation and survival, apoptosis, glucose metabolism, pH regulation and protein metabolism (Brahimi-Horn and Pouyssegur 2009, Ke and Costa 2006). The following table 1.4 gives the list of some of the genes activated by HIF-1.

Many reports confirm VEGF as a potent angiogenic mitogen and a major target gene of HIF-1 (Rey and Semenza 2010). Apart from tumour angiogenesis HIF-1 is also involved in other hypoxic conditions like ischemic conditions of diabetes and delayed wound healing of diabetes. In diabetic patients with unstable angina, after myocardial ischemia low levels of HIF-1α and VEGF levels led to impaired angiogenesis in comparison with non diabetic patients (Marfella et al. 2004). Gene therapy of HIF-1α activated many angiogenic cytokines such as VEGF, Ang-1, Ang-2, PDGF, PLGF, HO-1 and iNOS correcting the impaired wound healing of diabetes (Mace et al. 2007, Liu et al. 2008). Ferulic acid, an anti-oxidant produced angiogenic effects by increasing HIF-1α mRNA and protein along with VEGF and PDGF through PI3K/MAPK activation (Lin et al. 2010). The 2-oxoglutarate analogue dimethyloxalylglycine (DMOG) and iron chelator deferoxamine (DFX) stabilised and activated HIF-1α by inhibiting HIF hydroxylases leading to the improvement in the wound healing of diabetic mice (Botusan et al. 2008).

Table 1.4: HIF-1 mediated transcriptional activation of genes (Adapted from Lee et al. 2004)

Function	Genes
Cell proliferation	Cyclin G2, IGF2, IGF-BP1,2,3, WAF-1,TGF-α, TGF-β3
Cell survival	ADM, EPO, IGF2, IGF-BP1,2,3, NOS2, TGF-α , VEGF
Apoptosis	NIP3, NIX, RTR801
Motility	ANF/GPI, c-MET, LRP1, TGF-α
Cytoskeletal structure	KRT14, KRT18, KRT19, VIM
Cell adhesion	MIC2
Erythropoiesis	EPO
Angiogenesis	EG-VEGF, ENG, LEP, LRP1, TGF-β3, VEGF
Vascular tone	AR$\alpha_{1\beta}$, ADM, ET1, Haem oxygenase-1, NOS2
Transcriptional regulation	DEC1, DEC2, ETS-1, NUR77
pH regulation	Carbonic anhydrase 9
Regulation of HIF-1 activity	P35srj
Epithelial homeostasis	Intestinal trefoil factor
Drug resistance	MDR1
Nucleotide metabolism	Adenylate kinase 3, Ecto-5'-nucleotidase
Iron metabolism	Ceruloplasmin, Transferrin, Transeferrin receptor
Glucose metabolism	HK1, HK2, AMF/GPI, ENO1, GLUT1, GAPDH, LDHA, PFKBF3, PFKL, PGK1, PKM, TPI, ALD-A, ALD-C
Extracellular-matrix metabolism	CATHD, Collagen type V (α1), FN1, MMP2, PAI1, Prolyl-4-hydroxylase α (1), UPAR
Energy metabolism	LEP
Amino-Acid metabolism	Transglutaminase 2

ADM, adrenomedullin; ALD, aldolase; AMF, autocrine motility factor; AR, adrenergic receptor CATHD, cathepsin D; DEC, differentiated embryo chondrocyte; EG-VEGF, endocrinegland-derived VEGF; ENG, endoglin; ET1, endothelin-1; ENO1, enolase 1; EPO, erythropoietin; FN1, fibronectin 1; GLUT, glucose transporter; GAPDH, glyceraldehyde-3-P-dehydrogenase; HK, hexokinase; IGF2, insulin-like growth-factor 2; IGF-BP, IGF-factor-binding-protein; KRT, keratin; LDHA, lactate dehydrogenase A; LEP, leptin; LRP1, LDL-receptor-related protein 1; MDR1, multidrug resistance 1; MMP2, matrix metalloproteinase 2; NOS2, nitric oxide synthase 2; PFKBF3, 6-phosphofructo-2-kinase/fructose-2,6-biphosphatase-3; PFKL, phosphofructokinase L; PGK 1, phosphoglycerate kinase 1; PAI1, plasminogen-activator inhibitor 1; PKM, pyruvate kinase M; TGF-α, transforming growth factor-α; TGF-β3, transforming growth factor-β3; TPI, triosephosphate isomerase; VEGF, vascular endothelial growth factor; UPAR, urokinase plasminogen activator receptor; VEGFR2, VEGF receptor-2; VIM, vimentin.

HIF-1α is also reported to play a key role in apoptosis and cell survival. At the cellular and molecular level, cell survival is controlled by a balance between pro-apoptotic and anti-apoptotic signals. These signals are mediated by a large number of gene families. Pro-apoptotic signalling gene families include Bcl-2 family members like bcl-2, A1 and bcl-X, whereas anti-apoptotic signalling gene families include Bax, Bad and Bid. HIF-1α transfected HUVEC and HDMEC were observed to show an inhibition of proliferation by increasing the levels of tumour suppressor protein p53 induced p21^{Cip1}, a cyclin dependant kinase inhibitor (CKI) and decreasing the levels of Bcl-2, a pro-apoptotic gene. Further reduction in the kinase activity of CDK4/6 was also observed in HIF-1α transfected HMEC. Hence Iida et. al. propose that by up regulating p21 and reducing the activity of CDK4/6, HIF-1α plays a pivotal role in the cell cycle arrest at the G_0/G_1 phase (Iida et al. 2002). In murine embryonic fibroblasts and splenic B lymphocytes HIF-1α causes the arrest of cell cycle by inducing p21^{Cip1} and p27^{Kip1} independent of p53 (Goda et al. 2003).

Few studies have investigated the role of diabetes/hyperglycaemia in the regulation of HIF-1α. Increased level of glucose in isolated fibroblasts of diabetic and non-diabetic patients and ischemic tissues of wild type and diabetic mice caused decrease in the transactivation ability of HIF-1α leading to reduction in the expression of VEGF in response to hypoxia (Thangarajah et al. 2009). In human dermal fibroblasts and microvascular endothelial cells, hyperglycaemia in the presence of hypoxia dose dependently interfered with the stability and activity of HIF-1α. Inhibition of pVHL and p53 independent proteosomal degradation of HIF-1α rectified the destabilising effect of hyperglycaemia (Catrina et al. 2004). High glucose concentrations and chronic hypoxia increased proliferation of bovine aortic smooth muscle cells (BASMC) via a HIF-1α mediated pathway. Higher glucose concentration attenuated the hypoxia-induced BASMC apoptosis by decreasing the levels of activity and expression of pro-apoptotic caspase-3 and BNIP3L, with a concurrent increase in the expression of the anti-apoptotic protein Bcl-xL (Gao et al. 2007). At an early stage of diabetic nephropathy, HIF-1α mRNA was found to be up regulated and remained elevated in isolated glomeruli of diabetic mice (Makino et al. 2006). In diabetic retinopathy, Alb-AGE activated the HIF-1 DNA binding activity mediated by an increase in the accumulation of the HIF-1α protein through an ERK-dependent pathway. Thus, stimulation of VEGF expression by Alb-AGE, through the activation of HIF-1α, could play an important role in the development of diabetic retinopathy (Treins et al. 2001). Genetic polymorphisms associated with HIF-1α have also been demonstrated. A report suggests that HIF-1α is associated with the occurrence of T2DM by identifying a susceptibility coding SNP (cSNP) (P582S) and haplotype in the HIF-1α gene for T2DM (Yamada et al. 2005).

1.10 Silymarin

Hypoxia and hyperglycaemia are known to produce reactive oxygen species which have been implicated as a causative factor for the damage of tissues in diabetes. An anti-oxidant such as silymarin has the potential to overcome the adverse effects of high glucose concentration and/or hypoxia on cell migration. Silymarin is an extract of the seeds of the milk thistle plant [*Silybum marianum* (L.) Gaertn. (Asteraceae); synonym *Carduus marianus* L.] native to the Mediterranean region (Kroll, Shaw and Oberlies 2007, Ramasamy and Agarwal 2008). It is a mixture containing 65-80% of silyamarin complex (made up of at least seven flavonlignans and a flavnoid) and 20-35% of fatty acids such as linoleic acid and other polyphelonic compounds (Kroll, Shaw and Oberlies 2007). Silyamrin mixture constitutes of seven flavanolignans namely silybin A, silybin B, isosilybin A, isosilybin B, silychristin, isosilychristin, silydianin and a flavanoid – toxifolin (Fig. 1.8) (Kim et al. 2003).

The majority of therapeutic activity of silymarin is attributed to silybin, also spelt as silibin or called silibinin, as it is the most abundant constituent of silymarin. Silybin and isosilybin (also known as isosilibinin) are roughly 1:1 mixtures of two diastreoisomeric compounds of Silybin A and B and isosilybin A and B respectively and isosilybins are regioisomers of silybin (Lee and Liu 2003). Tincture prepared from milk thistle fruit has been reported to contain newer flavonolignan, silymandin (MacKinnon et al. 2007). The white flowering variety of *Silybum marianum* is known to contain silandrin, silymonin, silyhermin and neosilyhermin A and B in addition to the above mentioned regular flavonolignans (Szilagi et al. 1981). Along with the above mentioned compounds, the impurities present in the silymarin extracts could also be responsible for producing the anti-oxidant effects (Kvasnicka et al. 2003).

1.10.1 Uses of silymarin

Silymarin has been in the use for the past 2000 years for the treatment of liver and biliary diseases (Post-White, Ladas and Kelly 2007). In the United States silymarin is sold under the different brand names such as Legalon, Silipide and Siliphos as dietary supplement, hence regulated as a food and so far not approved by US Food and Drug Administration for the treatment of any disorders (Post-White, Ladas and Kelly 2007).

Silymarin produces its hepatoprotective activity by a unified mechanism through its anti-inflammatory, anti-oxidant and immunomodulatory effects involving scavenging and anti-oxidant effects on ROS induced oxidative stress and sustained inflammation in tissues (Comelli et al. 2007). Oxidative stress increases the production of ROS leading to the damage of cells and tissues. Many anti-oxidant enzymes such as superoxide dismutase (SOD), glutathione peroxidase (GSHPx), glutathione reductase (GR) and

catalase (CAT) help in the elimination of the ROS (Comelli et al. 2007). Silymarin is reported to produce its hepatoprotective actions by decreasing the levels of serum alanine aminotransferase (ALT), aspartate amino transferase (AST) and alkaline phosphatase (ALP) as well as total bilirubin against isoniazid, refampicin and pyrazinamide induced hepatotoxicity (Eminzade, Uraz and Izzettin 2008).
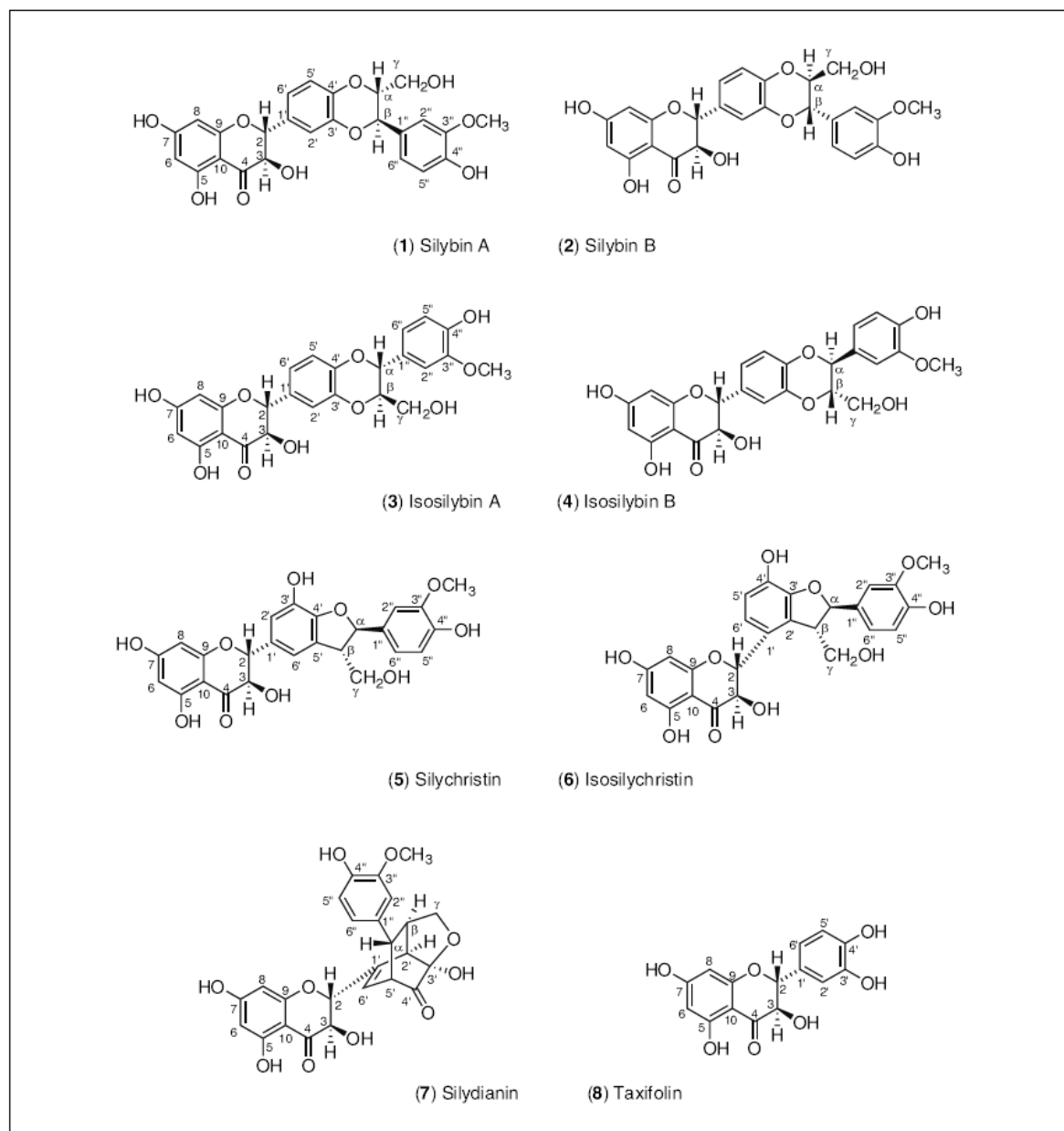
Fig. 1.8 Chemical structures of main flavanolignans and a falvanoid (Reproduced with permission from Kim et al. 2003).

Pretreatment of animals with silymarin prevented the hepatotoxicity caused by Cisplatin, an anti-cancer drug by decreasing the levels of ALT, AST, ALP and NO and by increasing the levels of GSHPx, SOD and GSH (Mansour, Hafez and Fahmy 2006). Similarly silymarin has been shown to produce hepatoprotective activities against many other hepato-toxins such as acetaminophen, methotrexate, diethylnitrosamine, ethanol and ionizing radiations (Comelli et al. 2007, Pradeep et al. 2007). Silymarin produces its hepatoprotective effect against hepatitis C virus by inhibiting the NF-κβ which in turn control the secretion of many cytokines such as TNF-α, interferon (IFN)-γ and IL-1 to 6 from T-cells (Morishima et al. 2010). Silymarin and its components protect the liver tissue against hepatitis C infection through their anti-viral, anti-oxidant, anti-proliferative effects and by inhibition of TNF-α induced NF-κβ dependant transcription with a varying degree (Polyak et al. 2010).

The results of clinical trails of silymarin use for hepatoprotective activity have not been uniform. In a study involving 170 patients, the treatment with silymarin proved to be effective against alcoholic cirrhosis compared to placebo treatment (Ferenci et al. 1989). In another trail involving 97 patients of acute and subacute liver disorder induced by alcohol received silymarin for the duration of four weeks. At the end of four weeks treatment, the silymarin group showed significantly lower levels of ALT and AST whereas the levels of total and conjugated bilirubin remained unchanged compared to the placebo group (Salmi and Sarna 1982). However, in a study involving 200 patients of liver injury due to alcohol the silymarin, after treating for two years, had no positive effect either on survival rate or on the prevention of liver injury (Pares et al. 1998). In a meta-analysis of the eighteen randomised trials conducted about the efficacy of silymarin, Rambaldi A et al. (2007) express their scepticism about the efficacy of silymarin as a hepatoprotectant against alcohol and/or hepatitis B or C induced liver damage (Rambaldi, Jacobs and Gluud 2007).

In recent years silymarin has received attention for its ability to affect the outcome of cancer and its usefulness as an adjuvant therapy for cancer (Ramasamy and Agarwal 2008). Silymarin is not only used as hepatoprotecatant but also to protect kidneys and heart during cancer treatment (Greenlee et al. 2007). Silymarin is proposed to produce its anti-cancer activity as a result of a combination of effects such as anti-inflammation, cell cycle regulation, induction of apoptosis, inhibition of invasion and metastasis, inhibition of proliferation and inhibition of angiogenesis (Ramasamy and Agarwal 2008). Silibinin produces its anti-cancerous activity by causing the arrest of progression of G_1 phase of the cell cycle by inducing CKIs such as $p21^{Cip1}$ and $p27^{Kip1}$ in prostate cancer cell lines (Roy et al. 2007). Further, silibinin is also to known to inhibit cell proliferation by arresting the G_2/M phase progression and by interfering with cell cycle regulators by decreasing the

levels of cyclin D1, D3, A and B1 and CDK 1, 2, 4 and 6 along with increasing the levels of p21^{Cip1} and p27^{Kip1} in advanced colorectal cancer and other tumour cell lines (Agarwal et al. 2006, Kaur et al. 2009). Apart from interfering with cell cycle regulators silibinin caused cell cycle arrest by down regulating the Rb-phosphorylation and E2F1/DP1 transcription complex and promotes apoptosis by down regulating survivin and up regulating the activated caspase-3 and 9 in hepatocarcinoma cells (Lah, Cui and Hu 2007).

Silibinin is reported to produce antiangiogenic effect by decreasing the size of microvessels and the tumour expression of angiogenic cytokines such as IL-13 and TNF-α in lung adenocarcinoma of A/J mice (Tyagi et al. 2009). The expression of TIMP-1 and 2 which are inhibitors of MMPs and ANG-2 and Tie-2 was increased by silibinin which produce an anti-angiogenic effect (Tyagi et al. 2009). Further, silibinin decreased the expression and nuclear localisation of HIF-1α and phosphorylation of NF-κβ and STAT-3 which act as stimulants in angiogenesis in tumour cells (Tyagi et al. 2009). Silibinin inhibited angiogenesis by decreasing the expression of angiogenic stimulants such HIF-1α, iNOS, PECAM-1, VEGF and down regulated VEGFR1 in trangenic adenocarcinoma of the mouse prostate model (Raina et al. 2008). In colorectal carcinoma, silibinin produced antiangiogenic effects by inhibiting not only HIF-1α, iNOS and VEGF but also by inhibition of COX1 and 3 (Singh, Gu and Agarwal 2008). Silymarin reduced the number of HUVECs and inhibited tube formation by decreasing the secretion of MMP-2 and VEGF (Jiang, Agarwal and Lu 2000). In HUVECs and HMVECs, silymarin caused the arrest of cell cycle progression by increasing the expression of p21, p27 and p53 and induce apoptosis by the increase of Bax and the decrease of Mcl-1 and survivin proteins (Singh et al. 2005).

Topical application as well as oral feeding of silibinin decreased the ultraviolet B irradiation induced proliferation and apoptosis in SKH1 hairless mouse skin by inhibiting the phosphorylation of MAPK/p38, ERK1/2, JNK1/2 and Akt (Gu et al. 2005). Silibinin produces its anti-proliferative and pro-apoptotic activity by inhibiting the phosphorylation of MAPK/ERK pathways in gastric and renal cancer cells (Kim et al. 2009, Li et al. 2008). Further, Zi and Agarwal (1999) suggested that silibinin produced anti-proliferative and pro-apoptotic effects in skin cancer cells by MAPK/ERK inactivation at a lower dose and MAPK/JNK1 activation at higher dose (Zi and Agarwal 1999). Silibinin reduced the invasiveness of lung cancer cells by inhibiting ERK1/2 and Akt activation along with inactivation of NF-κβ and JNK pathways. Further, PI3K and MEK inhibitors reduced the expression of MMP-2 and u-PA which were in turn inhibited by silibinin, suggesting that the silibinin effects involve MAPK and PI3K pathway (Chen et al. 2005). Silibinin produce anticancer effects in cervical and hepatoma cancer cells by reducing the accumulation and transcriptional activity of HIF-1α and decreasing the expression of VEGF which was potentiated by PI3K inhibitor (Garcia-Maceira and Mateo 2009). In other cells such as glial

cells, cardiac myocytes and neutrophils beneficial effects of silibinin are regulated by PKC activity along with other pathways (Tsai et al. 2010, Varga et al. 2004, Zhou et al. 2007).

1.10.2 Silymarin and diabetes

In spite of established anti-oxidant effect of silymarin being exploited in hepatic and cancer disorders, very few reports exist about the effect of silymarin in diabetes. In clinical trails involving type 2 diabetes patients, silymarin reduced the levels of fasting glucose level, glycated haemoglobin, total cholesterol, LDL, triglyceride, SGOT and SGPT when administered along with conventional or glibenclamide (Huseini et al. 2006, Hussain 2007). In another study involving patients of diabetes with liver cirrhosis, the blood glucose levels and fasting insulin levels decrease due to the administration of silymarin leading to reduced lipid peroxidation and insulin resistance (Velussi et al. 1997). These results were further confirmed in patients of T2DM with concomitant liver disorder when silybin-beta-cyclodextrin, a silibinin formulation reduced the blood glucose and triglycerides levels (Lirussi et al. 2002).

Silymarin prevented the alloxan from producing its deleterious effects on renal tissues and restored the level of SOD, GSPHx and CAT to their normal levels in rats (Soto et al. 2010). Earlier Soto et al. (2004) argued that silymarin reduced alloxan induced pancreatic tissue damage and was able to bring the level of glucose and expression of insulin and glucagon close to the level of control animals (Soto et al. 2004). In addition to improving the above mentioned glutothione enzymes levels, silymarin prevented alloxan induced pancreatic destruction by preventing the lipid peroxidation as well (Soto et al. 2003). Silibinin has been reported to produce its anti-hyperglyceamic effects by inhibiting the gluconeogenesis and glycogenolysis in hepatic cells of rats by inhibiting glucose-6-phosphatase activity and decreasing the phosphorylation of glucose-6-phospahate which is essential for production of glucose (Guigas et al. 2007). This decrease in hepatic glycolysis is accompanied by a reduction in the formation of ROS from the mitochondrial electron transfer chain (Detaille et al. 2008). Pretreatment of RINm5F insulinoma cells and human islet cells with silymarin protected them against IL-1β and/or IFN-γ induced cell damage by partial decrease of the production of NO and expression of iNOS in a dose dependent manner. Further, silymarin protected RINm5F insulinoma cells from IL-1β induced NO production and cell destruction via partial inactivation of c-Jun NH2 terminal kinase (JNK) and human islets from IFN-γ induced iNOS expression and cell destruction via inactivation of Janus kinase/stress transducer and activator of transcription (JAK/STAT) proteins (Matsuda et al. 2005). Taken together, the anti-hyperglycaemic effect of silibinin is a result of directly decreasing glycolysis, cytoprotective effects on

pancreatic cells, augmentation of anti-oxidant enzymes as well as free radical scavenging activity.

1.11 Topical Applications

One of the aims of this project was to develop a freeze dried wafers containing silymarin for topical application. Developments in the topical applications field has witnessed a rapid growth from simple bandages to modern topical applications for sustained release of therapeutic agents (reviewed in detail by Boateng et al. 2008). As with any other wound treatment, recalcitrant diabetic wounds require a suitable drug delivery system which releases the drug at the wound site with minimum systemic effects, while maintaining the stability of therapeutic agent intended to be released and also to show considerable therapeutic effect. One such drug delivery system is lyophilized or freeze dried wafers for the delivery of drugs as a topical applicant. Many reports suggest that lyophilized wafers could be prepared for the delivery of various therapeutic agents such as anti-bacterials, growth factors and other supplements such as vitamins and anti-oxidants using a variety of vehicles (Boateng et al. 2008).

Various polymers are used as vehicles to deliver the drugs in preparation of topical applications. Matthews and co-workers report the preparation of lyophilized wafers using sodium alginate and xanthan gum containing methyl cellulose. They tested these wafers on cut water melon serving as a suppurating wound surface model for qualitatative measurement (Matthews et al. 2005). The water insoluble drugs such as UK370106, a MMP-3 inhibitor could be formulated as lyophilized preparations using non ionic surfactant and xanthan gum as a vehicle (Matthews et al. 2008).

PDGF and other growth factors have been proved to be beneficial in normal wound healing and some of their formulation as topical application has led to their regulatory approval (Falanga 2005). Attempts have been made to test the effect of growth factors on fibroblast cells of diabetic wounds by the incorporation of EGF, IGF-1, PDGF-AB, and bFGF in various formulations (Loots et al. 2002). A chitosan film, prepared by freeze-drying hydroxypropylchitosan acetate buffer solution incorporated with bFGF solution applied on full-thickness wounds created on the backs of genetically diabetic mice reduced the wound size (Mizuno et al. 2003). In another study the chitosan hydrogels prepared by UV irradiation containing bFGF are reported to enhance the HUVECs growth and also induce the faster contraction of wounds in diabetic mice (Obara et al. 2003). TGF-β1 incorporated into various formulations was successfully tested for wound healing activity in diabetic rats (Puolakkainen et al. 1995).

There are very few reports about the lyophilisation of anti-oxidants with an intention of using them as topical applications for diabetic wounds. The wound dressings

prepared by lyophilising chlorhexidine diacetate with 5-methylpyrrolidinone chitosan as a vehicle produced not only anti-bacterial but also anti-oxidant activity (Rossi et al. 2007). Topical application of silymarin successfully prevented the photo-carcinogenesis of UV radiation on skins of mice and different components of silymarin permeate through skin with varying degree (Gu et al. 2005, Hung et al. 2010). However, there are no reports about the lyophilized preparations of silymarin as a topical application for wounds except for a report which uses lyophilized silymarin nano particles to characterise a development of a new polymer (Guhagarkar, Malshe and Devarajan 2009).

Sterile formulations are desirable in the treatment of chronic wounds of diabetes in order to avoid the possibility of increasing the microbial load at the wound site. Lyophilised wafers cannot be heat sterilised or autoclaved as the wafer structure would collapse due to heat and/or pressure risking the stability of the therapeutic agent. Therefore, gamma irradiation was employed to sterilise the lyophilised wafers (Matthews et al. 2006). Further detail about the freeze dried wafers is provided in chapter 7.

Taken together, there is a need to understand the effect of high glucose and hypoxia on the migration of endothelial cells at molecular level in order to understand angiogenesis during the wound healing process. As the production of ROS is proven to be a precursor in the development of vascular complications of diabetes, the therapeutic potential of anti-oxidants such as silymarin at least as an adjuvant therapy should be explored.

1.12.1 Aim and objectives of the study

This study aims to develop a suitable *in vitro* method of measuring the migration of endothelial cells simulating the angiogenesis stage of the wound healing process in diabetes and determine if there are any beneficial effects of silymarin on cell migration.

1.12.2 Objectives of the study

1. Develop a migration and wound healing method by validating and optimising a pre-existing model.
2. Determine the effects of hypoxia and hyperglycaemia on the migration of dermal microvascular endothelial cells and underlying molecular mechanisms.
3. Develop a freeze dried formulation containing silymarin and test the beneficial effects of silymarin on the changes in the migration owing to varying concentration of glucose and oxygen tension.

Chapter 2 - Materials and Methods

2.1.1 Materials

All chemicals used in the study were purchased from Sigma-Aldrich (Poole, UK) unless otherwise stated. Cell culture materials were purchased from Invitrogen (Paisley, UK) and all cell culture plastics and glassware from Fisher Scientific UK Ltd (Loughborough, UK), unless otherwise stated. Microvascular cell reagents were purchased from Cascade biologics (Invitrogen Ltd. Paisley, UK). All the materials were used as supplied as described in the text.

2.1.2 Endothelial Cells (ECs)

Human umbilical vein endothelial cells (HUVECs) and human microvascular endothelial cells (adult dermis) (HMVECad) were used at different stages during the study. The majority of the preliminary work was carried out with HUVEC before moving onto the primary HMVECad cell line.

HUVECs were cultured from an immortalised cell line purchased from the European Collection of Cell Cultures (ECACC). HUVECs were propagated from a cryopreserved primary culture isolated from normal human umbilical vein. The cells used during the study were of passages between 60 and 70.

The primary human microvascular endothelial cells were cryopreserved from adult dermis at the end of tertiary culture (i.e passage 2) were purchased from Cascade Biologics (Invitrogen Ltd. Paisley, UK). The cells were tested by the company for the presence of von Willebrand factor (vWF), CD31 antigen, and CD36 antigen and for the absence of α-actin. The uptake of DiI-Ac-LDL (Acetylated Low Density Lipoprotein, labelled with 1,1'-dioctadecyl-3,3,3',3'-tetramethyl-indocarbocyanine perchlorate) was confirmed. The absence of Hepatitis B, Hepatitis C, and HIV-1 viruses, mycoplasma, yeast and fungi was also confirmed. The HMVECad of passage number of 7 to 16 were used for all experiments carried out in this study.

2.2 Methods

2.2.1.1 Cell count by Trypan blue dye exclusion method

Viable cell number was determined by means of trypan blue dye exclusion. The cells were counted in order to seed experimental six well culture plates or for further sub culturing or for cryopreservation with the appropriate number of cells. An aliquot of 20µl of cell suspension was mixed by a gentle swirl (finger vortex) with 0.4% v/v of trypan blue dye at a 1:1 ratio and left to stand for 2 min to allow the dye to penetrate any non-viable cells. Trypan blue dye stains any dead or dying cells dark blue by permeating through their damaged cell membrane. Using a Pasteur pipette, a small volume ~10µl of the cell suspension was applied to the edge of cover slip placed on a Neubeur haemocytometer

and allowed to fill the area under the cover slip by means of capillary action. The cells were viewed under a microscope at 100x magnification. Viable cells were counted in the 25 squares contained within the large square (of 1mm^2 area) edged by double lines on both grids. The mean value of the two sides of the slide was noted before calculating total viable cell number as follows;

$$\text{Number of cells/ml} = \text{cell count per large square x dilution factor x } 10^4$$

The 10^4 in the above equation is a conversion factor used to convert 10^{-4}ml to 1ml. This conversion factor is based on volume of the cell suspension present in one large square (of 1mm^2 area) of the haemocytometer.

(Volume of 1 large square = 1mm x 1mm x 0.1mm = 0.1cm x 0.1cm x 0.01cm = 10^{-4} cm^3 = 10^{-4} ml)

2.2.1.2 Cell resuscitation

Aseptic procedures were used when working with cultured cells or any procedures linked to their use. A dedicated cell culture lab with a laminar flow air hood (Aura 2000, Bioair Instruments) was used. All solutions were filter or autoclave sterilised, plastics were autoclave sterilised and glassware was heat (180 ^{0}C for 2.5 h) sterilised prior to their use.

The HUVECs and HMVECad were supplied as a cryopreserved vial of ≥ 3.75 x 10^5 and 5 x 10^5 viable cells per ml respectively. The cell lines of HUVECs were initiated into 75cm^2 flasks (T-75) and HMVECad into 25 cm^2 flasks (T-25). The T-75 flasks for HUVECs were non-coated, whereas the T-25 flasks used for HMVECad were coated prior to use with sterile attachment factor (AF) (1x) solution made up of 0.1% gelatine (Cascade Biologics, UK). Two ml of AF solution was added to each of T-25 flasks. The flasks were gently agitated to allow the AF to cover the flask surface and incubated at 37 ^{0}C for 30 min or at room temperature for 2 h. The AF solution was completely removed by aspiration prior to the addition of cell suspension or medium. The coated flasks were used either immediately or capped tightly and stored at room temperature for using within 24 h.

A cryopreserved vial of HUVECs or HMVECad was thawed by dipping the lower half of the vial in 37 ^{0}C water bath. The cell count was determined using Trypan blue as explained in previous section 2.2.1.1. A cryopreserved vial containing HUVEC suspension (1ml) was pipetted into a T-75 flask containing 10ml of culture media at the rate of 5x10^3 to 1x10^4 cells per cm^2 area of a flask. The culture media for HUVECs was prepared by diluting glucose free Glasgow's Minimal Essential Medium (G-MEM) (10x) (40ml) with 15ml of 7.5% NaHCO$_3$, 5ml of 4-(2-hydroxyethyl)-1-piperazineethanesulfonic acid (HEPES) buffer and 50ml of tryptose phosphate broth to make 432ml of 1x G-MEM

(Macpherson and Stoker 1962). The diluted G-MEM was prepared into 87ml aliquots and stored at 4 ^{0}C until required. When used for HUVEC, the diluted G-MEM was combined with 10% (v/v) foetal calf serum (FCS), 2mM L-glutamine, 5mM D-glucose and 1 unit/ml penicillin, 1μg/ml streptomycin. All media for HUVEC was warmed to 37 ^{0}C before use.

The contents of the vial (1ml) containing HMVECad was diluted to a concentration of 2.5 x 10^4 viable cells/ml using microvascular growth supplement (MVGS) supplemented M-131. Each of an AF-coated T-25 flask was added with 5ml of the resulting cell suspension. M-131 is a basal medium containing essential and non essential amino acids, vitamins, other organic compounds, trace minerals, inorganic salts and 5.6mM D-glucose. MVGS is supplied as a concentrated (20x) solution containing foetal bovine serum (5% v/v final concentration), hydrocortisone, recombinant human fibroblast growth factor, heparin, recombinant human epidermal growth factor, and dibutyryl cyclic AMP.

Following initial cell seeding, the flasks were left undisturbed for 24 h in humidified atmosphere of 5% CO_2/95% air in an incubator (Galaxy S, Wolf Laboratories) at 37 ^{0}C. The media was replaced after 24 h to remove the traces of dimethylsulfoxide (DMSO) and any dead cells/debris. The media was changed every alternative day until the cells reached 60 % confluence. Once the cells reached 80% confluence, they were trypsinised for either sub-culturing as explained in section 2.2.1.4 or frozen for long term storage as explained below.

2.2.1.3 Cell storage

The supernatant obtained after centrifugation of trypsinised cell suspension was removed and the cell pellet was re-suspended in cryopreservation medium. The HUVECs were frozen in G-MEM containing 10% v/v of DMSO at a concentration of 3.75x10^5 to 7.5x10^5 cells per ml. The HMVECad were re-suspended in cold Synth-a-Freeze solution at a concentration of 5x10^5 to 3x10^6 cells per ml. Synth-a-Freeze solution is a sterile liquid cryopreservation medium containing 10% DMSO. It does not contain any antibiotics, antimycotics, hormones, growth factors, serum, or proteins and is HEPES and bicarbonate buffered. The cell suspension was aliquoted into an appropriate number of cryopreservation vials. The vials containing 1ml of cell suspension were cooled to 4 ^{0}C as quickly as possible and were transferred overnight to -80 ^{0}C. The following day the vials were transferred to the vapour phase of a liquid nitrogen refrigerator (LS3000, Taylor and Wharton, USA, liquid nitrogen capacity – 81l).

2.2.1.4 Routine sub-culture

To harvest HUVECs for subculture, growth medium was poured off and the monolayer was rinsed three times with 10ml calcium and magnesium free Hank's balanced salt solution (HBSS). The final wash was allowed to incubate for 10 min to remove all trace of serum containing medium. The cells were removed from the flask by incubating for 10 min with 5ml of 0.25% (v/v) trypsin solution. The flask was gently agitated for no longer than 2 min to detach the cells. An equal volume of medium containing FCS was then added to the flask to neutralize the enzymatic activity of the trypsin. The cell suspension of the flask was removed to a sterile universal tube. The cells in the suspension were pelleted by centrifugation (Biofuge PrimoR, Heraeus, Germany) at 220g force for 5 min. The supernatant was removed and the cell pellet was re-suspended in 1ml of fresh medium. The cell count was then determined using the Neubeur haemocytometer as explained earlier in section 2.2.1.1. For routine subculture, a sterile T-75 flask was used and 5x10^3 cells per cm^2 were supplemented with 10ml of fresh medium.

To harvest HMVECad for subculture, growth medium was poured off into a sterile empty beaker. Following the addition of 3ml of Trypsin/EDTA solution (Trypsin/EDTA solution (1x) is a phosphate buffered, sterile solution containing 0.025% trypsin and 0.01% ethylenediaminetetraacetic acid (EDTA), Cascade Biologics, UK) the flask was gently rocked to ensure that the entire surface was covered. The flask was immediately emptied and 1ml of fresh Trypsin/EDTA solution was added. The cells were incubated at room temperature (RT) for approximately 4 to 6 min until they were completely round. The flask was agitated gently, without exposing the cells for an excessive length of time to the Trypsin/EDTA solution, to dislodge the cells from the surface of the flask. Trypsin Neutraliser (3ml) solution (a sterile, phosphate buffered, calcium and magnesium free solution (1x) containing 0.5% newborn bovine serum) (Cascade Biologics, UK) was added to the flask and detached cells were transferred to a sterile universal tube. An additional 3ml of Trypsin Neutraliser solution was added to the flask and the solution was pipetted over the flask surface several times to dislodge any remaining cells. This solution was aspirated into a universal tube and centrifuged at 180g for 7 minutes. The supernatant was removed from the tube. The cell pellet was re-suspended in 5ml of MVGS supplemented M-131 and gently pipetted up and down several times to ensure a homogenous cell suspension. The cell count was determined using the Neubauer haemocytometer as explained earlier in section 2.2.1.1. The cell suspension was diluted in MVGS supplemented M-131 to give 5000 cells per cm^2 and added to the new culture flasks freshly coated with AF.

The flasks containing newly sub-cultured cells were transferred to an incubator and left undisturbed overnight to allow the cells to adhere and begin to grow. The growth

of cells was checked daily under the microscope and by observation of any change in the colour of medium, indicative of pH changes.

2.2.1.5 Cell growth conditions

The effect of normoxia (ambient O_2 tension) (N) or hypoxia (5% O_2 tension) (H) and normal (5mM) or elevated (20mM) glucose level was assessed by exposing the cells to these conditions for a specified period of time. The N5mM or N20mM conditions were achieved by growing the cells in media containing 5 or 20mM of D-glucose concentration in humidified atmosphere of 5% CO_2/95% air in an incubator (Galaxy S, Wolf Laboratories) (subsequently referred to as normoxia) at 37 ^{0}C. Similarly, the H5mM or H20mM conditions were achieved by growing the cells in media containing 5 or 20mM D-glucose in a humidified atmosphere of 5% O_2/ 5% CO_2/ 90% air in a Galaxy R CO_2 incubator (Wolf Laboratories) (subsequently referred to as hypoxia) at 37 ^{0}C. The hypoxic condition was created and maintained by purging oxygen from the incubator with nitrogen.

Different levels of glucose concentration (either 5mM or 20mM) in the media were achieved by adding the required quantities of previously prepared 1M D-glucose stock solution. Ten ml of 1M D-glucose stock solution was prepared by filter sterilisation (0.22μm syringe filter, Millipore) and stored at 4 ^{0}C until further use. It was prepared using glucose free/serum free (GF/SF) G-MEM to supplement the media of HUVEC and M-131 to supplement the media of HMVECad.

All the experiments involving the endothelial cells were carried out using 6 well plates. Where appropriate, the cells were supplemented with hydroxyurea 5mM, D-Mannitol 5 or 20mM, silymarin (SM) 50μM, α-lipoic acid (aLA) 100μM, PKC$_{βII}$/EGFR Inhibitor [4,5-bis(4-Fluoroanilino)-phthalimide] 1μM (Calbiochem, Merck Chemicals, Nottingham), p42/p44 MAPK Inhibitor (2′-Amino-3′-methoxyflavone) (PD98059) 2μM (Calbiochem, Merck Chemicals, Nottingham) and PI3K Inhibitor   [2-(4-Morpholinyl)-8-phenyl-4H-1-benzopyran-4-one] (LY294002) 10μM (Invitrogen, UK). DMSO and ethanol of molecular biology grade were used as a solvent wherever appropriate at a final concentration of ≤ 0.7% v/v.

The methods described below are the final methods used following the validation of radial migration and wound healing assay. The process by which the methods were validated is dealt with, in detail in chapter 3.

2.2.2 Formation of circular monolayers

Heat sterilised (180 ^{0}C for 2.5 h) glass cloning rings (Corning, UK) of 6 x 8mm (outer diameter x height) were placed centrally within each well of a non-coated 6 well tissue culture plates (Nunc, Denmark) having an area of 10.17 cm^2 per well (Fig. 2.1). The HUVECs were grown on non-coated surface without any coating. The culture plates were coated with 1.5ml of AF as described in section 2.2.1.2 before placing the glass rings in them, if HMVECad were to be grown onto them. The HUVEC and HMVECad were seeded into each glass ring at a density of 2 x 10^5 viable cells per ml, in a volume of 40µl. The 6 well plates were returned to the normoxic incubator for either overnight (in case of HUVECs) or 4 h (in case of HMVECad) to allow the cells to adhere to the plastic surface. The HMVECad successfully adhered to the treated surface within 4 h, but HUVEC took around 12 h to attach to the non-treated surface of the plates. The optimal incubation required for the cell adhesion of different cell types was determined experimentally. The shorter time period required for HMVECad may be due to the presence of AF and/or the other cell surface properties. This was not investigated further. After cell adhesion, the rings were taken off and the wells were supplemented with 2.5ml of appropriate growth media. The plates with circular cell monolayers were returned to the appropriate incubation conditions for further 24 and/or 48 h.

a) Cross sectional view with rings
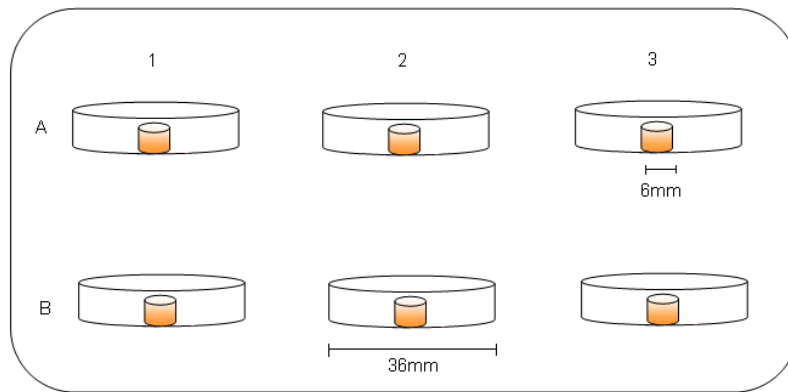
b) Cross sectional view after the removal of rings
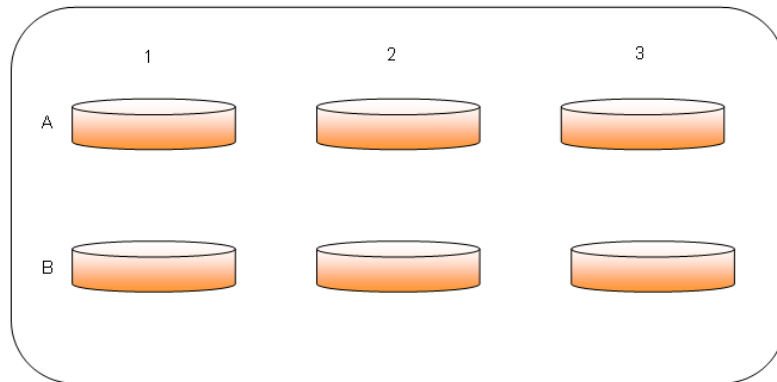
c) Aerial view of cell monolayers
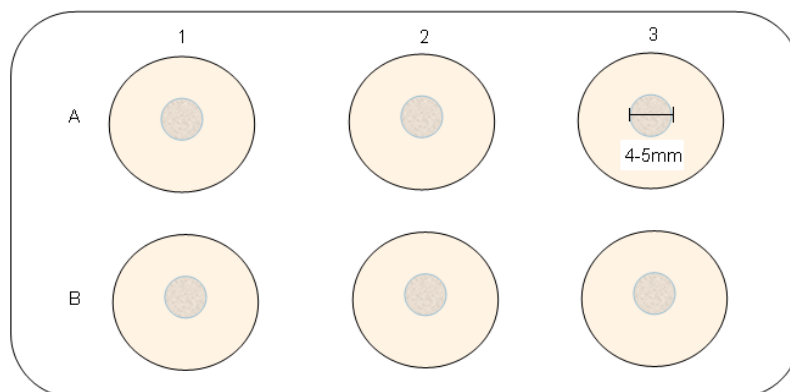
Fig. 2.1 Formation of circular cell monolayers The HMVECad or HUVEC were seeded in to glass rings (6mm outer diameter) at the centre of the wells of a 6 well plate (a). After initial incubation, the rings were taken off and the plates were returned to an incubator with wells filled with 2.5ml of media (b). Aerial view of the plates would reveal the formation of circular monolayer (4-5mm) of cells (c).

2.2.3 Radial migration assay

The images of the circular monolayers were acquired digitally at 0 h, before incubating in different conditions, and at 24 and 48 h using an inverted microscope (DMI 4000B, Leica Microsystems, Germany) at 25x magnification. The photomicrographs were analyzed by measuring the radii of the circular cell monolayers to determine the migration of cells with the help of Leica (QWin Standard v 2.8, Image Processing and Analysing System) software.

An image acquired at 0 h was opened (Fig. 2.2a) using *File Menu >Open* tool.
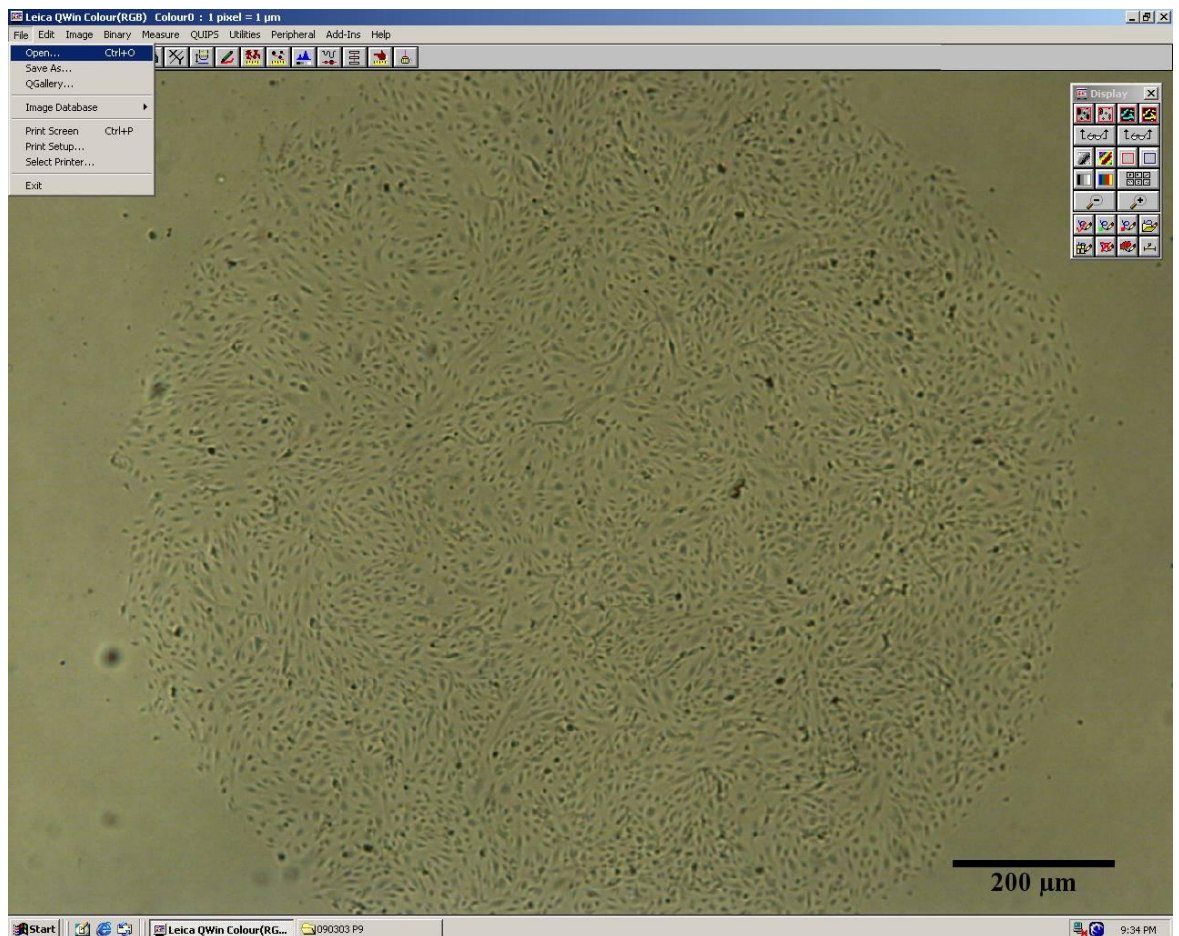
Fig. 2.2a Radial migration assay Image of a cell monolayer photographed at 0 h used to illustrate image analysis.

The annotation toolbox was opened using *Image Menu > Annotate Applet > Start* tool. A circle was drawn by selecting three points on the circumference of the monolayer with help of a *Circle calibrated measurement* button on the annotation toolbox. A circle with its diameter at the centre was displayed. The annotation was stopped by pressing *Image Menu > Annotate Applet > Stop* tool.
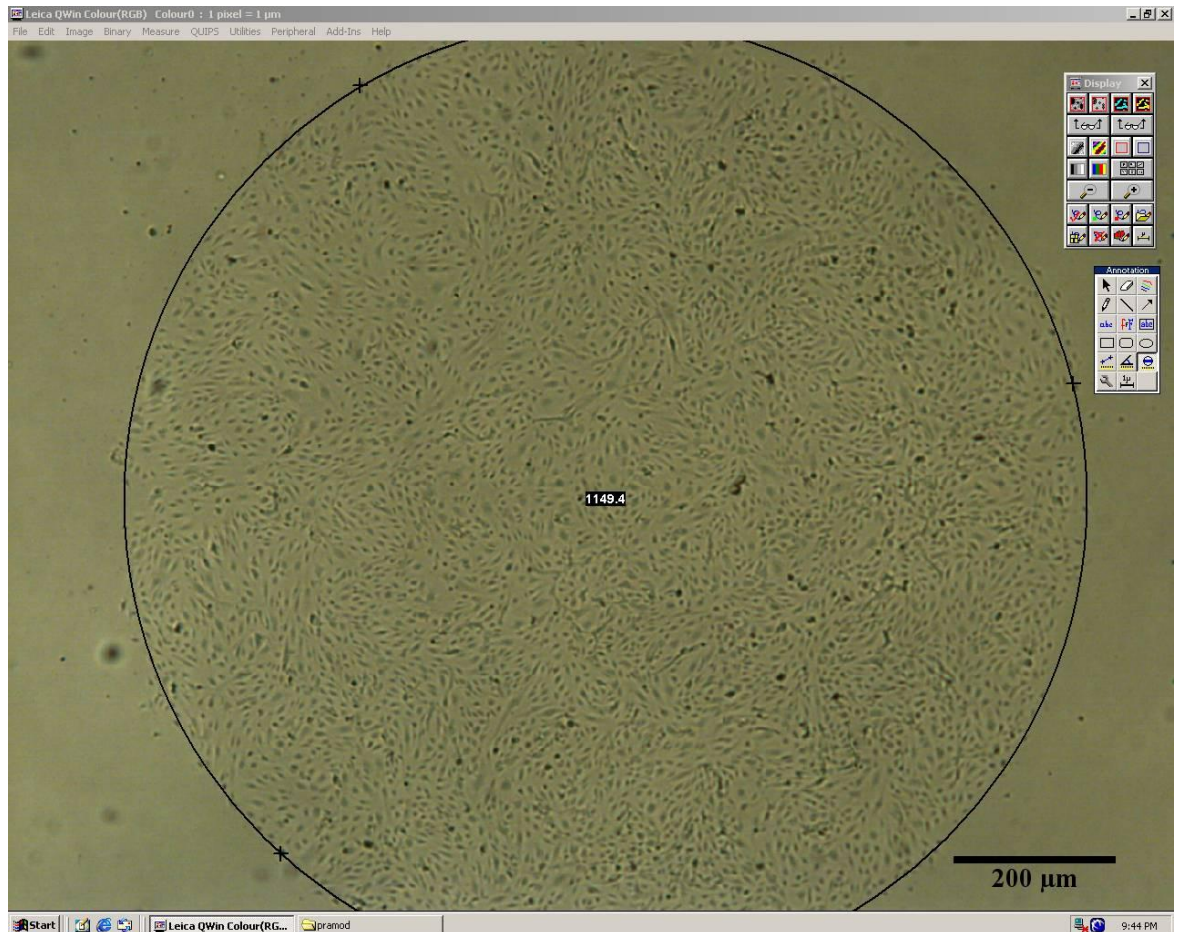
Fig. 2.2b Radial migration assay The annotated circle was overlaid on the cell monolayer, with the diameter of the circle displayed at the centre.

Next *Binary Menu > Binary graphics* tool was used to open the binary graphics dialog box. The radial blue lines were drawn within a binary plane of an image by selecting *Spokes* type of graphics (Fig. 2.2c). The settings for spokes were defined by *Spacing* at an angular spacing of 9^0 between two spokes. The *position* of the spokes was adjusted so that the blue radial lines were originating from the centre of a circle. The *size* of the spokes was also adjusted, so that the blue radial lines nearly touched the circumference of the annotated circle.
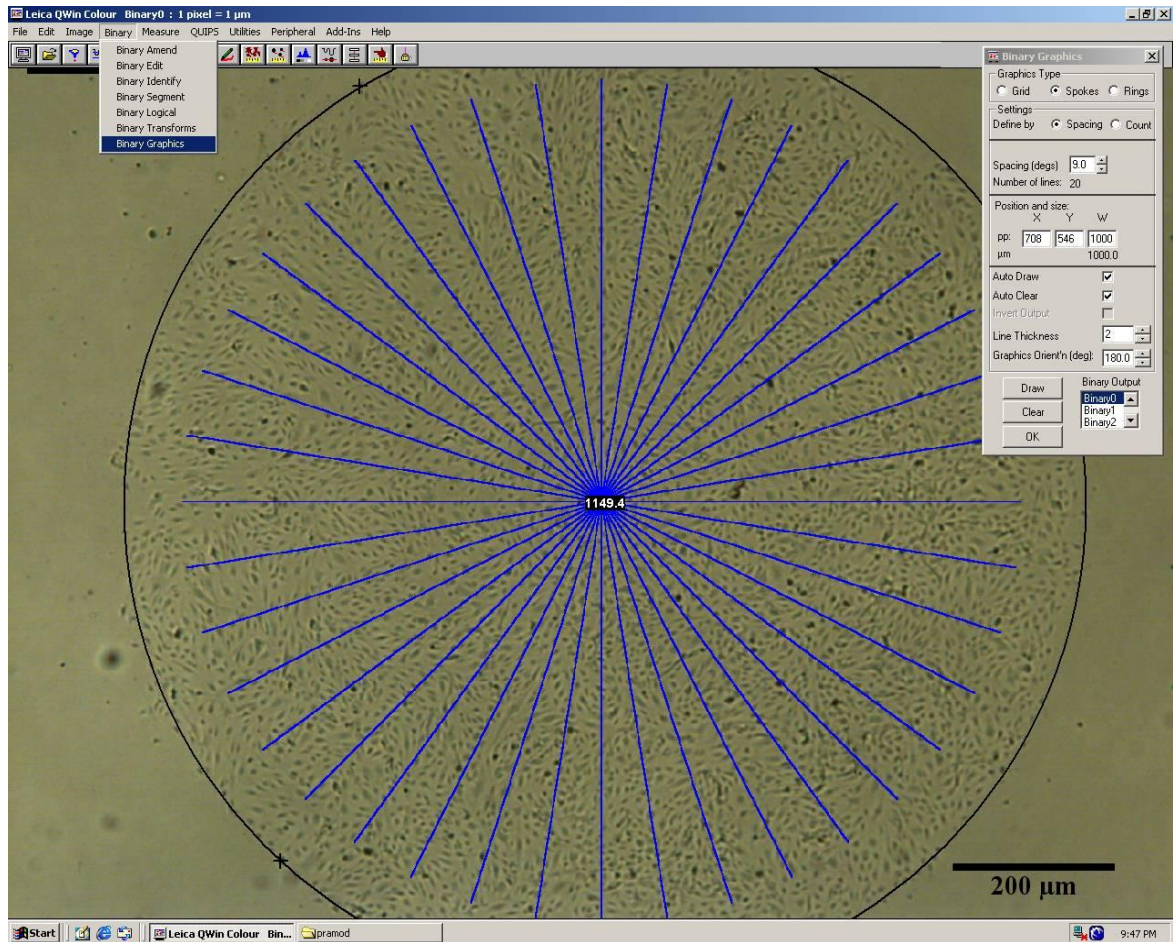
Fig. 2.2c Radial migration assay The blue coloured radial spokes with the angular spacing at 9^0 was overlaid at the centre of the annotated circle. The lengths of spokes were adjusted to not to touch the circumference of the monolayer as they could obscure the visibility of the cells at the edge.

Annotation toolbox was displayed again by using *Image Menu > Annotate Applet > Start* tool. The circle was selected with help of *Select object* button and deleted using *Remove selected objects* button on the annotation toolbox. Ten black lines were manually drawn on either side of the monolayer using a *Point-Point calibrated measurement* button. These black lines were drawn on the blue spokes from centre to the circumference of a circular monolayer. The distance (in μm) of black lines was displayed at their centre (Fig. 2.2d).
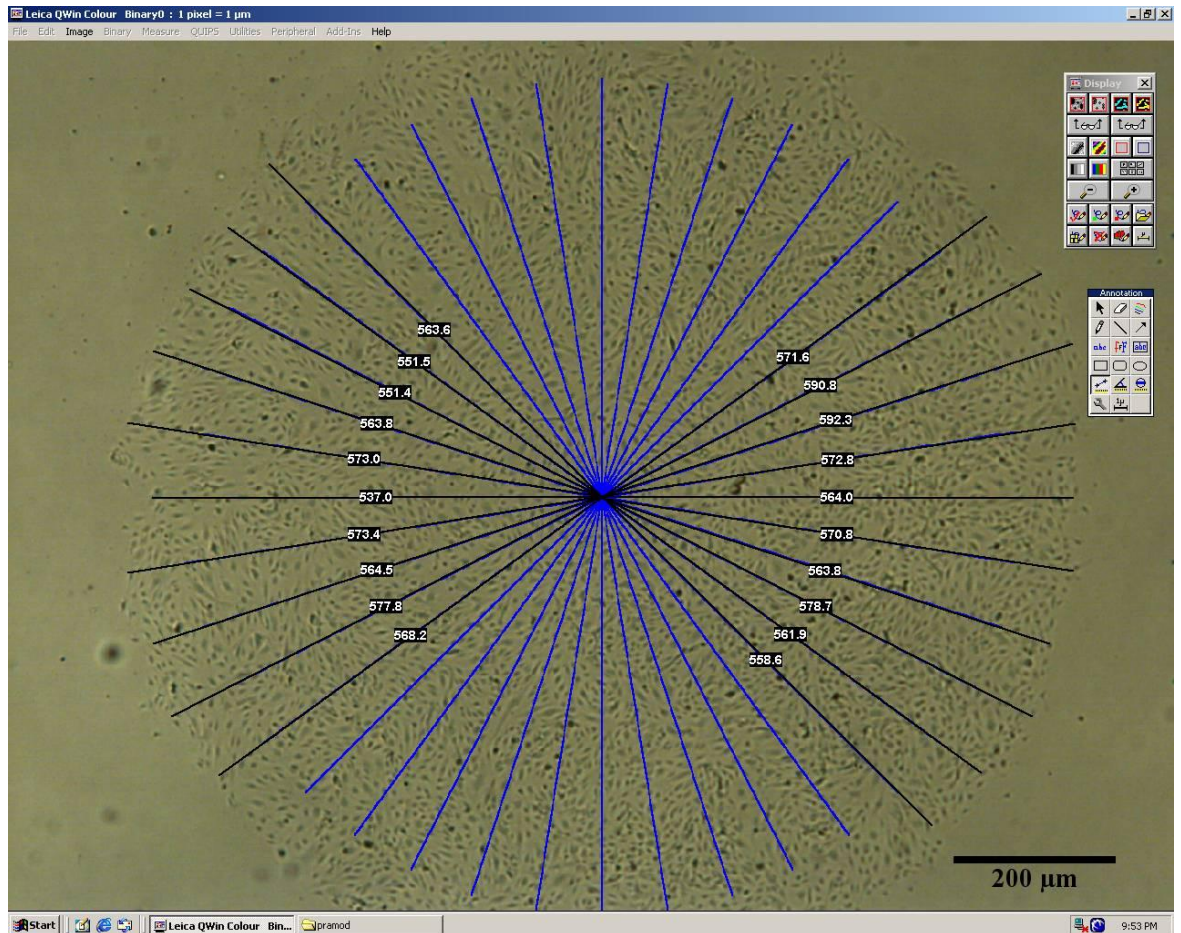
Fig. 2.2d Radial migration assay The manually drawn black lines on the blue spokes display the radius of each line. The radial distances on either side of the monolayer were regarded as the radial migration.

In total, lengths of twenty radial lines per image were noted down on a excel spread sheet. The same procedure was repeated for the images of 24 and 48 h. Net migration was defined as the difference between the length of radial lines at 24 or 48 h with that 0 h. Net migration as mean ± SEM of twenty radii, unless otherwise stated, is presented in the results section.

2.2.4 Wound healing assay

The HMVECad were grown in a circular monolayer in 6 well plates as explained in section 2.2.2. Once the glass rings were removed, the centre of a circular monolayer was approximately marked on the underside of the plastic to provide a reference point for subsequent measurements. Approximately half of the circular monolayer was removed using a cell scraper (Cell scraper, 23, Nunc, Denmark) and the well was then washed with phosphate buffered saline (PBS) to remove the detached cells and cell debris. This resulted in a semi-circular monolayer with both an intact edge and a wounded edge (Fig. 2.3a). The plates were returned to the appropriate incubation conditions for 48 h with 2.5ml of medium in each well.

Images of a semi-circular monolayer were acquired digitally at 0 h, before incubating in different conditions, and at 24 and 48 h using an inverted microscope (DMI 4000B, Leica Microsystems, Germany) at 25x magnification. The photomicrographs were analyzed by measuring ten radial distances from the intact edge and ten parallel distances from the wounded edge of the semi-circular cell monolayers (Fig. 2.3g). The migration distance of cells was measured with the help of Leica (QWin Standard v 2.8, Image Processing and Analysing System) software.

The image of the monolayer at 0 h was opened by *File Menu > Open* tool. The annotation toolbox was opened with help of *Image Menu > Annotate Applet > Start* tool. The shape of a semi-circular monolayer with a pre-marked reference point was drawn using *Draw free hand* button of annotation toolbox. The pre-marked reference point was helpful in identifying the original edges of monolayer when the annotated shape at 0 h would be superimposed over the images of either 24 or 48 h.
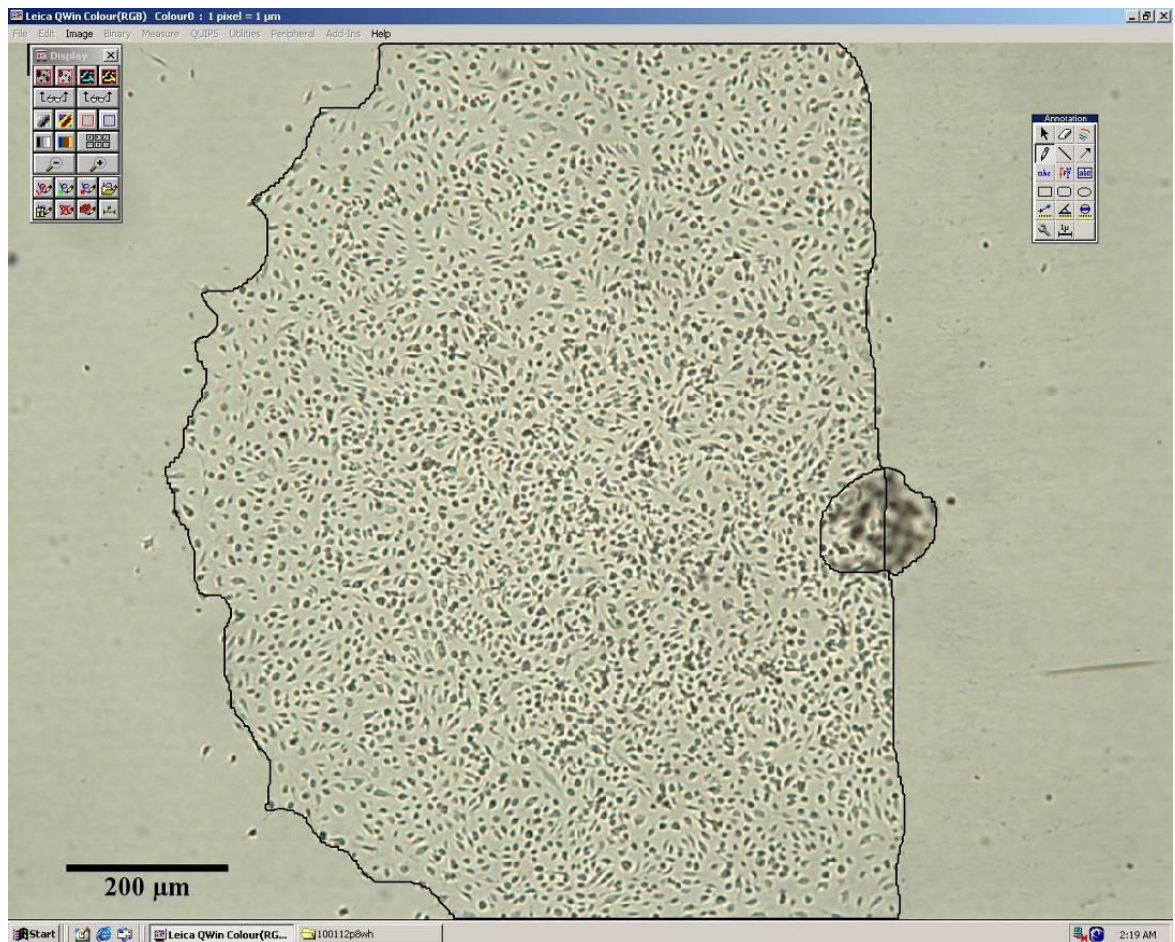
Fig. 2.3a Wound healing assay The shape of the semi-circular monolayer and the pre-made point mark on underside of the plate as a reference point was annotated on the image of a monolayer.

An image of a same monolayer acquired at 24 h was opened by *File Menu > Open* tool. The annotated shape of semi-circular monolayer of 0 h was superimposed on an image taken at 24 h as shown in Fig. 2.3b. A circle was drawn by selecting three points on the circumference of the intact edge of monolayer with help of a *Circle calibrated measurement* button on the annotation toolbox. A circle with its diameter was displayed at the centre. After drawing the circle, the annotation was stopped by pressing *Image Menu > Annotate Applet > Stop* tool.
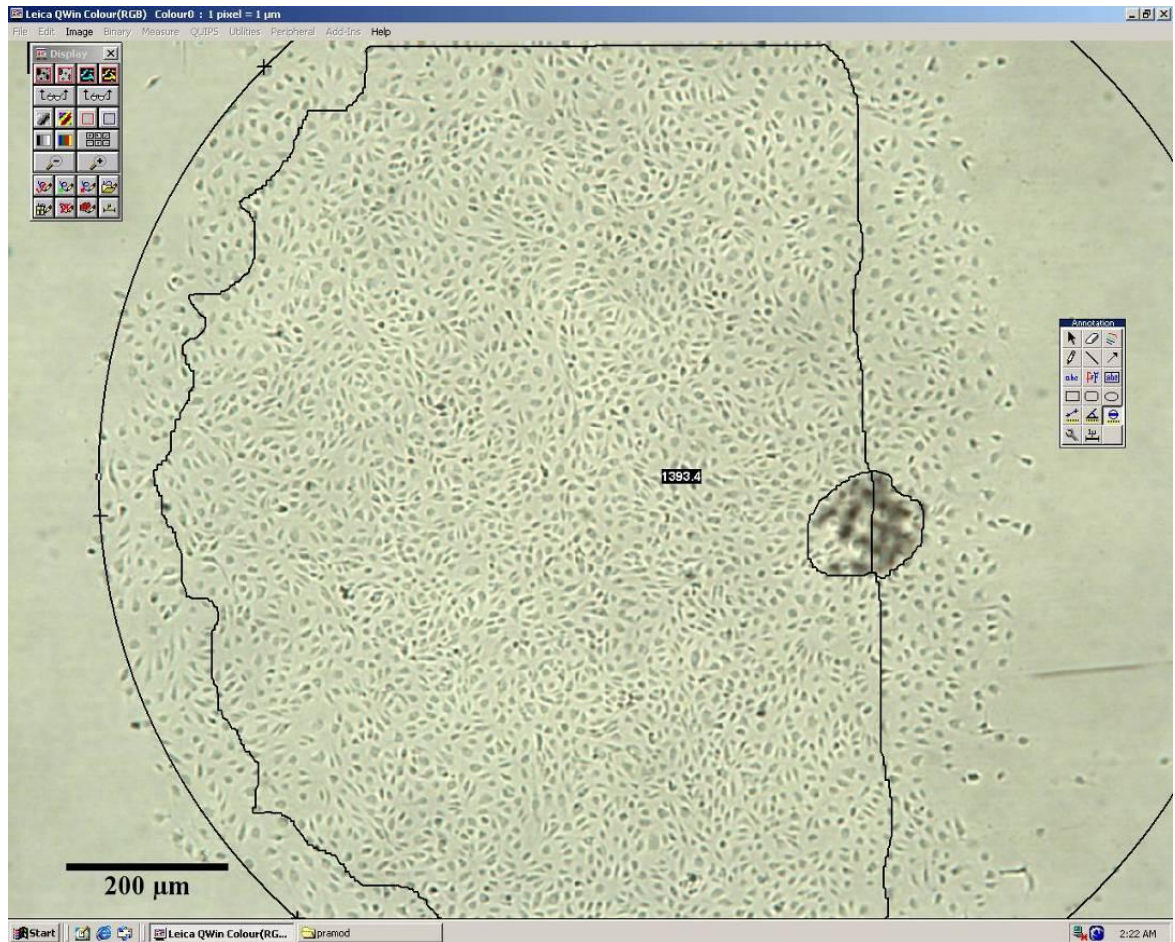
Fig. 2.3b Wound healing assay Annotated shape of 0 h was superimposed on the image of 24 h and its position is adjusted using the pre-drawn underside reference point.

Next *Binary Menu > Binary graphics* tool was used to open the binary graphics dialog box. The blue radial lines were drawn within a binary plane of an image by selecting *Spokes* type of graphics. The settings for spokes were defined by *Spacing* at an angular spacing of 9^0 between two spokes. The *position* of the spokes was adjusted so that the blue radial lines were originating from the centre of a circle. The *size* of the spokes was also adjusted, so that the blue radial lines nearly touched the circumference of the annotated circle (Fig. 2.3c).
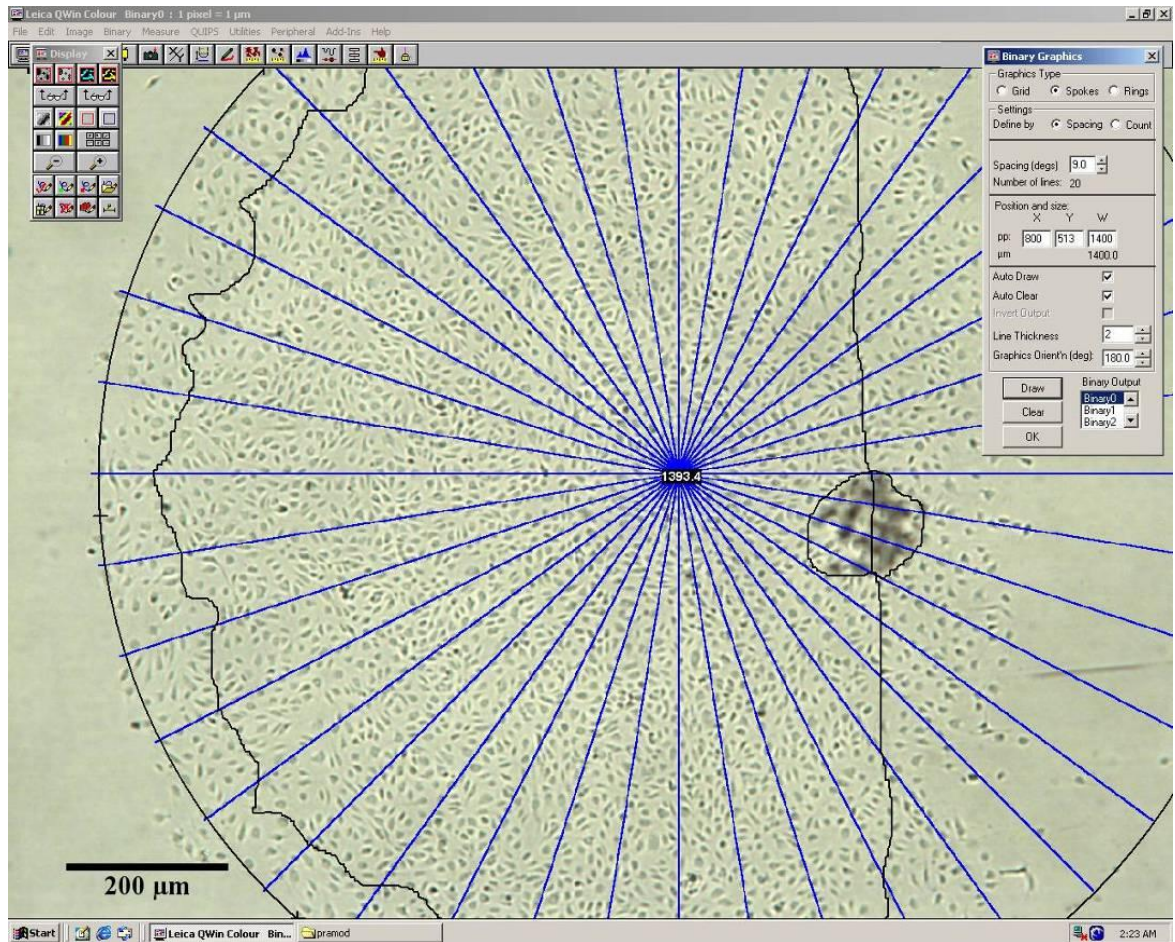
Fig. 2.3c Wound healing assay The blue coloured radial spokes with the angular spacing at 9^0 was overlaid at the centre of the annotated circle. The lengths of spokes were adjusted to lie between the circumference of the annotated image of 0 h and the circumference of the monolayer at 24 h.

Annotation toolbox was displayed again by using *Image Menu > Annotate Applet > Start* tool. The annotated circle was selected with the help of *Select object* button and deleted using *Remove selected objects* button on the annotation toolbox. Ten black lines were manually drawn on intact edge of the monolayer using the *Point-Point calibrated measurement* button. These black lines were drawn on the blue spokes from the circumference of annotated image taken at 0 h to the circumference of semi-circular monolayer of 24 h. The length (in µm) of black lines was displayed at their centre. The length of these lines was considered as the net migration of cells from intact edge of monolayer. The lengths of ten radial lines per image were noted down on a excel spread sheet.
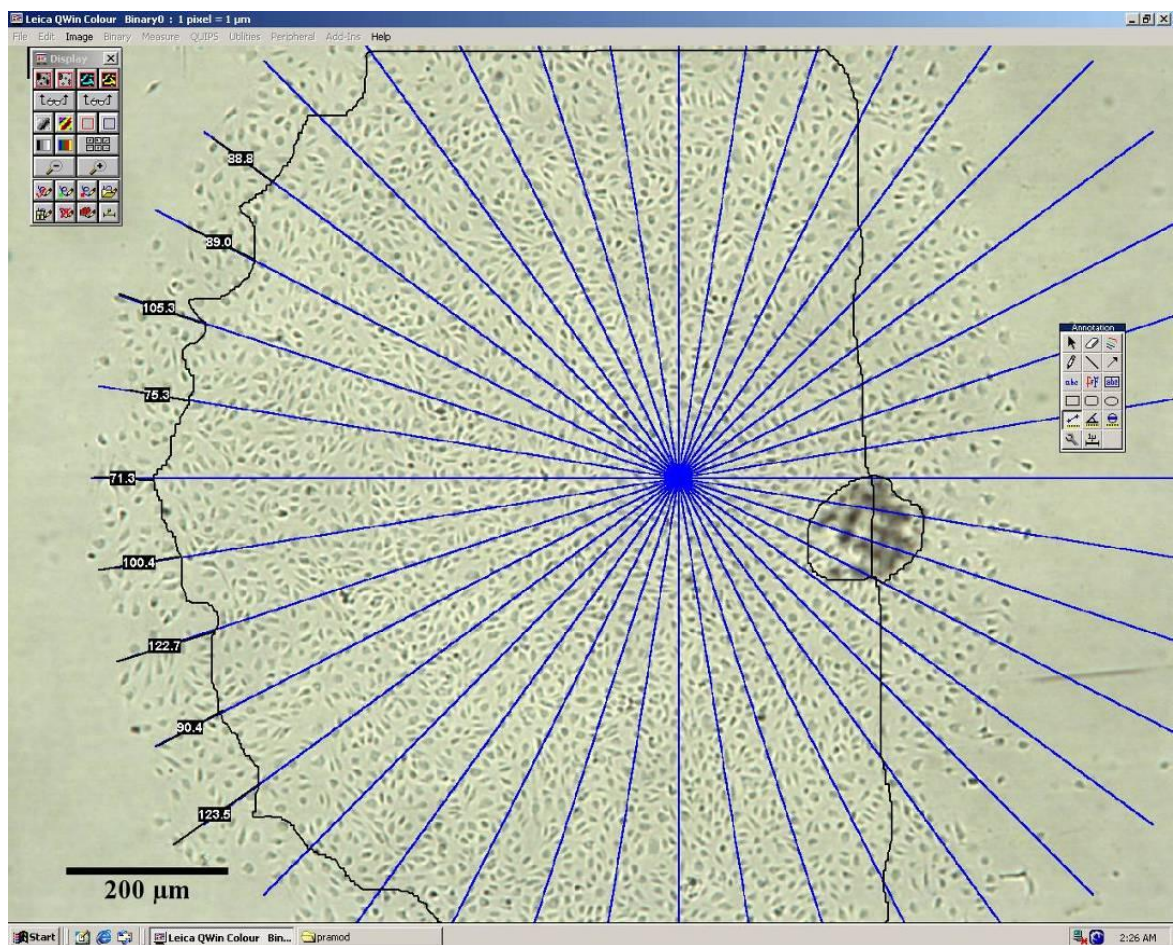
Fig. 2.3d Wound healing assay The black lines were drawn on the blue spokes from the circumference of the annotated image of 0 h to the circumference at 24 h.

Annotation was stopped and the binary graphics dialog box was opened. The dialog box was used to draw the parallel lines by selecting *Grid* type of graphics within a binary plane of the image. It produces a rectangular grid consisting of a number of horizontal and vertical lines. The settings for the grid were defined by *Spacing (µm)* resulting in lines of 200µm x 80µm (width x height). The *position* of the grid was adjusted so that the left arm of the grid was near to the wounded edge of monolayer. The *size (µm)* of the grid was 200 x 1040 (width x height). The *graphic's orientation* was used to rotate the grid so that it was in line with the wounded edge.
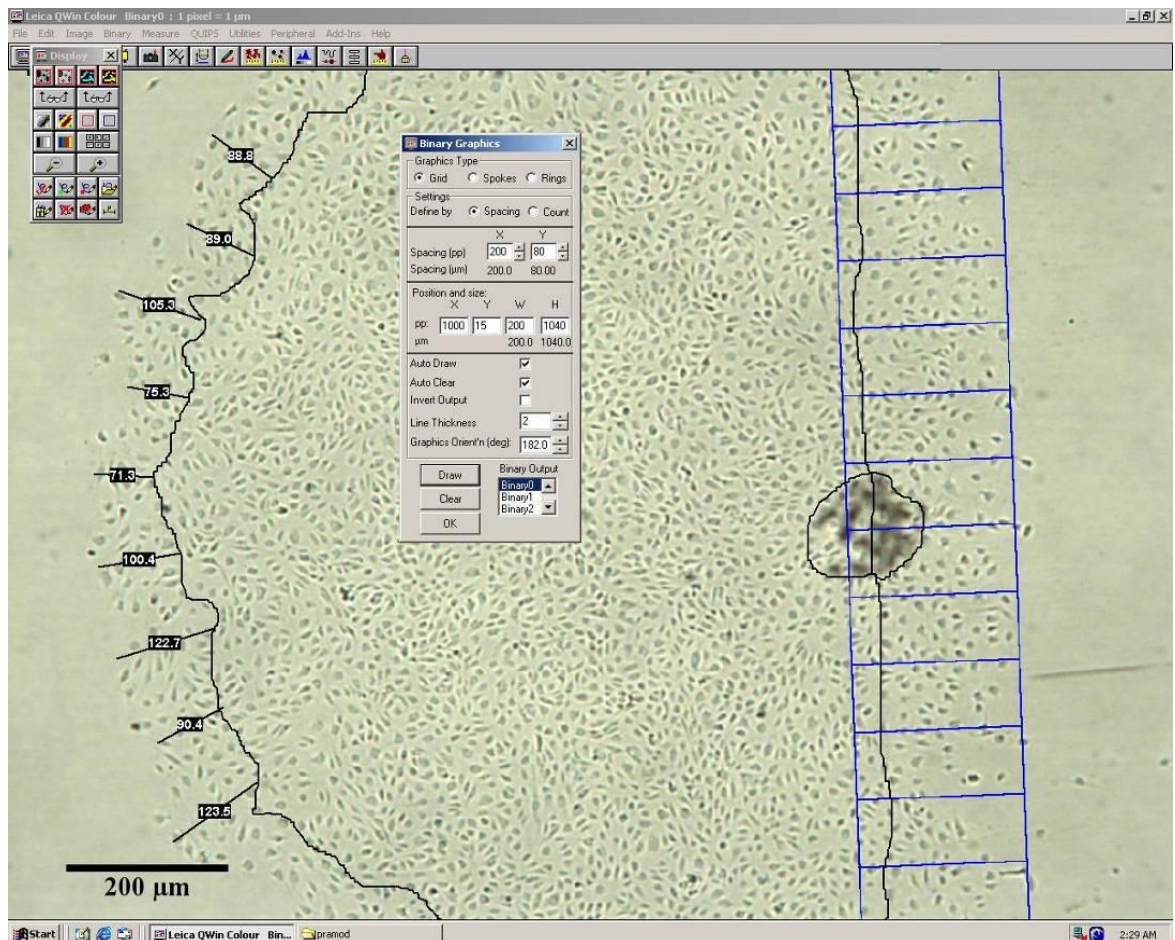
Fig. 2.3e Wound healing assay The blue coloured rectangular grid with the lines of length 200µm wide and spacing of 80µm between them was overlaid at the wounded edge of the monolayer. The blue rectangular grid was adjusted so that one arm of it is within the black line representing the wounded edge of 0 h and the other arm near to the edge of the monolayer of 24 h.

Annotation toolbox was displayed again by using the *Image Menu > Annotate Applet > Start* tool. Ten lines were manually drawn from the wounded edge of the monolayer using *Point-Point calibrated measurement* button. These lines were drawn on the lines of grid from wounded edge of 0 h to the new edge at 24 h. The lengths (in μm) of these lines were displayed at their centre. The length of these lines was considered as the net migration of cells from the wounded edge of a monolayer. The lengths of ten parallel lines per image were noted down on a excel spread sheet.
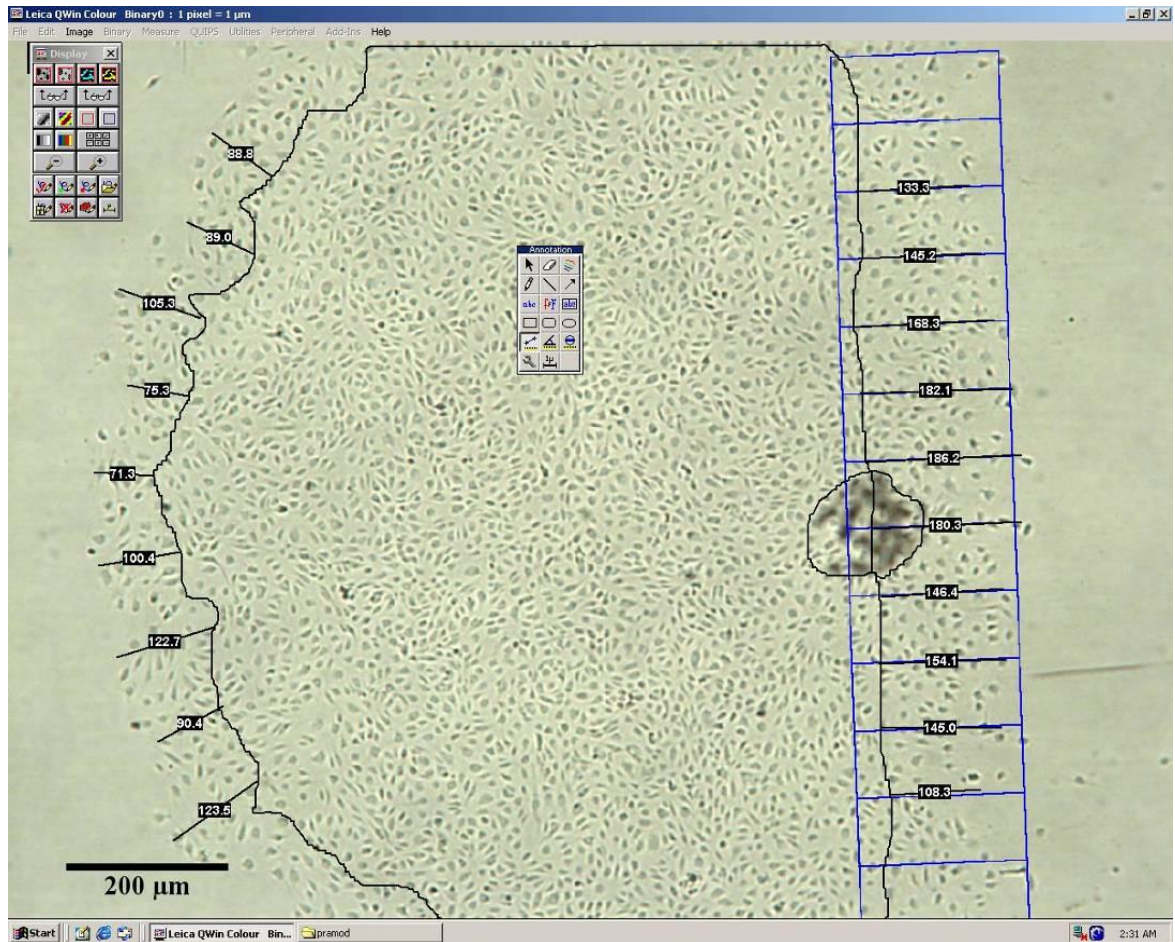
Fig. 2.3f Wound healing assay The black lines were drawn on the blue lines from the wounded edge of the annotated image of 0 h to the edge at 24 h.

The whole procedure was repeated for an image of 48 h or alternatively the graphics on an image of 24 h were superimposed on an image of 48 h. The net migration was recorded by extending the lines to the new edge on the either side of the monolayer.
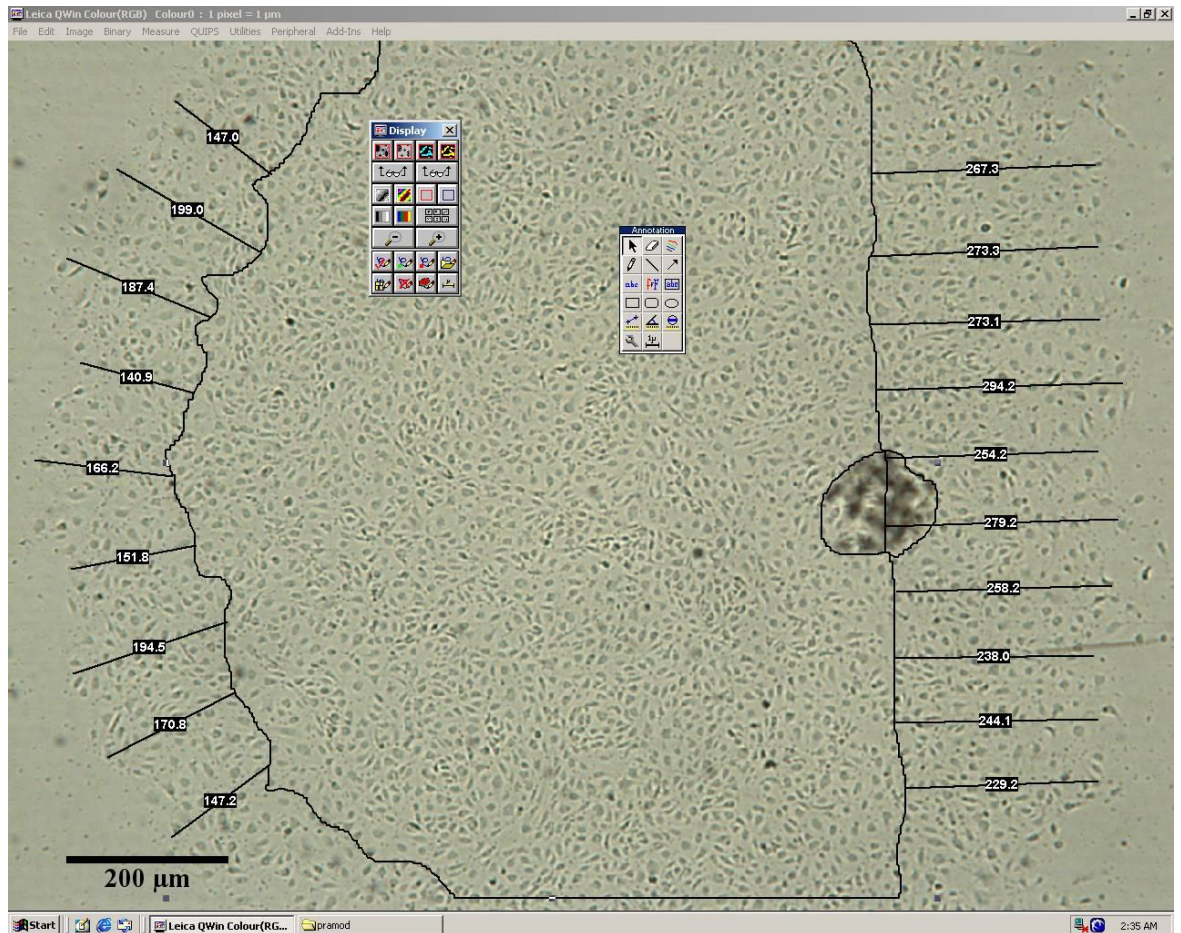
Fig. 2.3g Wound healing assay The lengths of black radial and parallel lines were noted as net migration from the intact and the wounded edge of the monolayer respectively.

Net migration presented in the results section, is given as the mean value of ten lines from each image, unless otherwise stated, each from the intact and wounded edge.

2.4 Immunocytochemical staining

2.4.1 Background

Immunocytochemical staining was employed to visualise specific proteins viz. hypoxia inducible factor -1α (HIF-1α), p27^{Kip1}, platelet endothelial cell adhesion molecule (PECAM) -1 and actin in endothelial cells. The method employed is known as streptavidin-biotin complex/alkaline phosphatase method (Fig. 2.4). This method was used for the detection of an antigen by light microscopy. The high affinity non-covalent bonding of biotin (vitamin H) with avidin and streptavidin is exploited in immunocytochemical detection (Molecular probes, handbook, Invitrogen). Avidin, an egg white protein and streptavidin, obtained from bacteria possess four binding sites for biotin. Avidin, being a glycoprotein with isoelectric point of 10, binds non-specifically to lectin like and negatively charged cell components at physiological pH. On the other hand, streptavidin with its more neutral iso-electric point and lack of oligosaccharide residues results in less non-specific binding. The biotin molecule conjugates easily with antibodies and enzymes. Up to 150 biotin molecules can be attached to one antibody molecule. The secondary antibodies are conjugated to biotin and function as a link between antigens on the tissue or cell bound primary antibodies. The labelled streptavidin-biotin method utilizes a biotinylated secondary antibody that links primary antibody to a streptavidin-alkaline phospatase conjugate. Streptavidin-alkaline phosphate conjugate is a highly sensitive detector conjugate. This conjugate binds to biotin labelled secondary antibody. A single primary antibody subsequently is associated with multiple enzyme molecules, and because of the large enzyme-to-antibody ratio, a considerable increase in sensitivity is achieved.

Endogenous alkaline phosphatase activity can be inhibited by addition of levamisol to the substrate solution. Napthol AS-MX phosphate is used as substrate. The alkaline phosphatase hydrolyses napthol phosphate esters (substrate) to phenolic compounds and phosphates. Insoluble coloured azo dyes are produced when the phenols couple with colourless diazonium salts (chromogen). The chromogen FastRed TR produces bright red end product. Aqueous mounting media must be used as FastRed TR is soluble in alcoholic and other organic solvents.
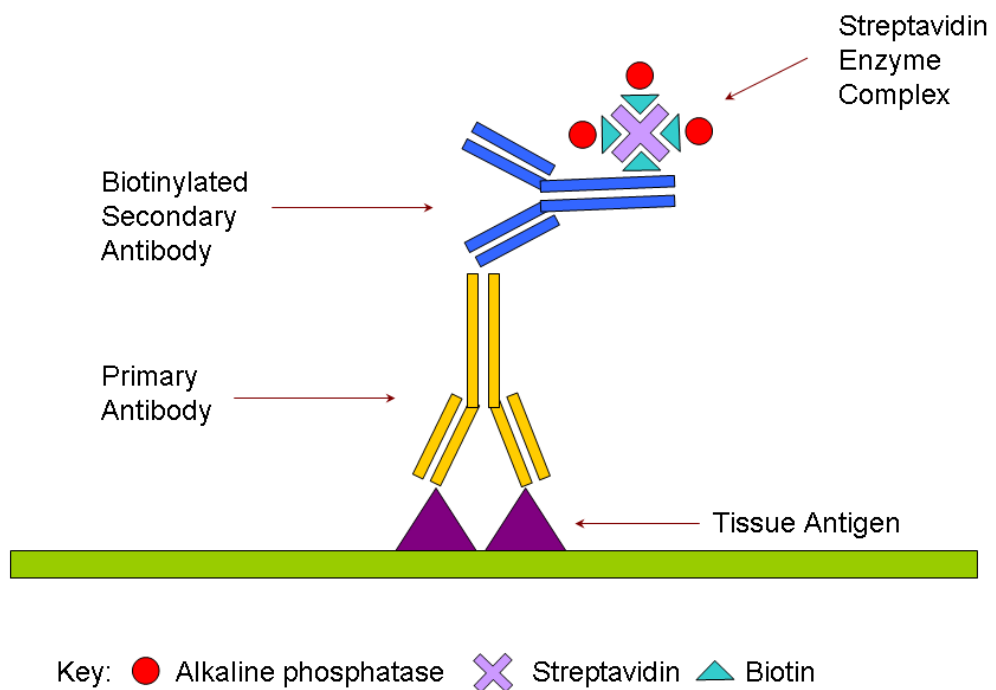
Fig. 2.4 Alkaline phosphatase labelled Streptavidin-Biotin method Alkaline phosphatase labelled streptavidin conjugates with biotinylated secondary antibody. The primary antibody is attached to multiple enzymes. The amplification of antigen signal is considerable due to the large enzyme to antibody ratio. (As adapted from 'Immunohistochemical Staining Methods', Fourth Edition, Dako Corporation, 2006)

2.4.2 Method

The circular or semi-circular endothelial cell monolayers were washed three times in ice cold PBS (0.01M phosphate buffer, 0.0027M potassium chloride and 0.137M sodium chloride, pH 7.4) at 48 h and fixed for 10 min in 4% paraformaldehyde (PFA) prepared in PBS solution. Preparation and fixation using PFA was carried out in a fume cupboard. After fixation, the cells were air dried and were either used immediately or stored at -20 ^{0}C for later use. The cells which were frozen were removed from the -20 ^{0}C freezer, and allowed 90 min to come up to room temperature prior to immunocytochemical detection.

The region to be stained was delineated either using a wax pen (Mini Pap Pen, Zymed, Invitrogen) or in situ frames of 25µl capacity (Eppendorf AG, Germany). The cells in 6 well plates were equilibrated in tris buffered saline (TBS) (0.05M Tris, 0.15M NaCl, pH 7.6) for 5 min before removal of excess liquid. Two more washes with TBS were given for 5min each. In order to reduce non specific binding of the secondary antibodies and background staining, the plates were incubated for 30min with 10% normal goat serum. Excess serum was aspirated and the plates were washed with TBS three times for 5min each. The plates were incubated with primary antibody diluted in TBS in a humid chamber overnight at 4 ^{0}C. The different primary antibodies and their dilutions used are listed in table 2.1 and are also mentioned in the relevant text. Mouse or rabbit isotype control depending on the primary antibody, was used as a negative control. After washing the plates with TBS three times for 5 min each, they were incubated for 60 min with biotinylated secondary antibody. The relevant secondary antibody is mentioned in table 2.1 and also in relevant text. The plates were washed in TBS three times for 5 min each and were incubated with streptavidin-alkaline phosphatase conjugate for 30 min. After removal of the conjugate, the plates were washed three times with TBS for 5min each. The substrate (1.2mM Napthol AS-MX phosphate disodium salt, 1mM Levamisol, 1.9mM Fast Red TR salt) was prepared in veronal acetate buffer (0.029M sodium acetate (tri-hydrate), 0.028M sodium diethyl barbiturate, pH 9.2) and the cells were incubated at room temperature for 10min until a bright red colour developed. The plates were washed with distilled water and allowed to dry and then aqueous mounting media (Vectamount, Vector Lab) was added and cover slip applied prior to visualisation.

Table 2.1 Various antibodies and ancillary materials used in ICC

Description of antibodies with their host and isotype	Type	Dilution used (in TBS)	Manufacturer
Anti-HIF-1α Monoclonal (Host /Isotype – Mouse/IgG1)	Primary	1:50	MA1-516, Affinity Bioreagents
Anti - HIF-1α Unconjugated Polyclonal (Host /Isotype – Mouse/IgG1)	Primary	1:50	38-9800, Zymed
Anti-phospho-p27 (Ser10) Unconjugated Polyclonal (Host – Rabbit)	Primary	1:100	34-6300, Invitrogen
Monoclonal anti human CD31 (PECAM-1) (Host /Isotype – Mouse/IgG1)	Primary	1:100	P8590, Sigma
Anti – Actin, N – terminal Polyclonal (Host – Rabbit)	Primary	1:100	A2103, Sigma
Isotype Control (Host – Mouse, Isotype - IgG and IgM)	Primary control	0.5µg/ml	08-6599, Invitrogen
Isotype Control Polyclonal (Host – Rabbit, Isotype - IgG and IgM)	Primary control	0.5µg/ml	08-6199, Invitrogen
DSB-X biotin anti-mouse (Host/Isotype – Goat/IgG(H+L))	Secondary	1:300	D20691, Invitrogen
F(ab')2 Anti Rabbit Ig's biotin (Host /Isotype – Goat/Ig's)	Secondary	1:300	ALI 4409, Biosource
AP-Streptavidin Conjugate	-	1:300	43-8322, Zymed
Normal goat serum	-	10%	PCN5000, Biosource

2.5 Statistical analysis

The data obtained from the radial migration (n=180) and the wound healing (n=90) assay of cells are shown as mean ± SEM The sample size is arrived at by multiplying the number of observation (i.e. 20 radii for radial migration assay or 10 distances for each edge of the wound healing assay) multiplied by number of samples (i.e. 3) and number of times the experiments were repeated (i.e. 3). The images for the measurement of migration by both radial migration and wound healing assay were acquired with pixel:distance ratio of 1:3.69. However, it should be noted that the images were analysed using pixel:distance ratio of 1:1. The differences among different conditions and/or treatments were evaluated, wherever appropriate using either one way analysis of variance (ANOVA) followed by Bonferroni post hoc test or independent t test. The level of significance was conveyed using the general notations *p<0.05, **p<0.01 and ***p<0.001 or as mentioned in the relevant legends of data figures. In addition, coefficients of variation were calculated to determine the reproducibility of the data.

Chapter 3 - Validation of methods used to assess the migration of endothelial cells

3.1 Introduction

Endothelial cell migration is an essential aspect of angiogenesis during the wound healing process. A range of *in vitro* methods have been developed to simulate *in vivo* conditions in order to understand the mechanism of cell migration and wound healing (Auerbach et al. 2003, Eccles, Box and Court 2005). These methods are helpful in providing an insight into the cellular and molecular mechanisms of impaired wound healing of diabetes. This chapter deals with development, validation and optimisation of cell migration and wound healing methods.

A commonly employed method to measure the migration *in vitro* includes scratching the cell monolayer and measuring the distance covered by the endothelial cells into the scratched region (Li et al. 2006). Some studies include the use of Boyden chambers (transwell migration) to study the cellular migration (Hervé et al. 2005, Lee et al. 2005), while other studies include wounding cell monolayer and counting the migrated cells into the wounded region (Hamuro et al. 2002).

The method employed in carrying out the cell migration assay in this study is an adaptation of the omni-directional migration method described by Dolle et al. (Dolle et al. 2005). The development of radial migration was carried out using HUVECs in the beginning and later made use of HMVECad. Endothelial cells were seeded as circular monolayers as explained in section 2.2.2 of previous chapter while developing and validating the migration assay. The measurements of area, length and radii of circular cell monolayer were carried out to validate the assay.

The development of a method to measure the migration of endothelial cells in the milieu of a wound environment was another objective of this project. In connection with this, a scratch wound and a radial wound method were developed. The wounds were made on a monolayer of cells either by using a sterile pipette tip or by removing half of the monolayer and the migration of cells was measured.

Unlike other chapters, this chapter is structured slightly differently. The section dealing with the development of the radial migration assay (section 3.2) has one general materials and methods section (section 3.2.1) and few subsections in the combined results and discussion section (section 3.2.2) where results of each method followed by a brief discussion explaining changes made to the method are presented. The rationale for this is that the outcomes of each experiment inform the next stage. The last subsection 3.2.3 summarises the method development process.

The development of the wound healing method (section 3.3) also has two subsections, one explaining the scratch wound assay (3.3.1) and another explains the wound healing assay (section 3.3.2). These subsections, in turn are divided into materials

and methods followed by the combined results and discussion. Similar to radial migration assay, wound assays are summarised in section 3.3.3.

The last two sections (section 3.4 and 3.5) dealing with Haematoxylin & Eosin staining and the expression of PECAM-1 and actin expression in microvascular endothelial cells respectively have three subsections each of introduction, materials and methods and finally combined results and discussion.

3.2 Radial migration assay

3.2.1 Materials and methods

HUVECs or HMVECad were seeded as a circular monolayer (Fig. 3.1a) as explained in the section 2.2.2.
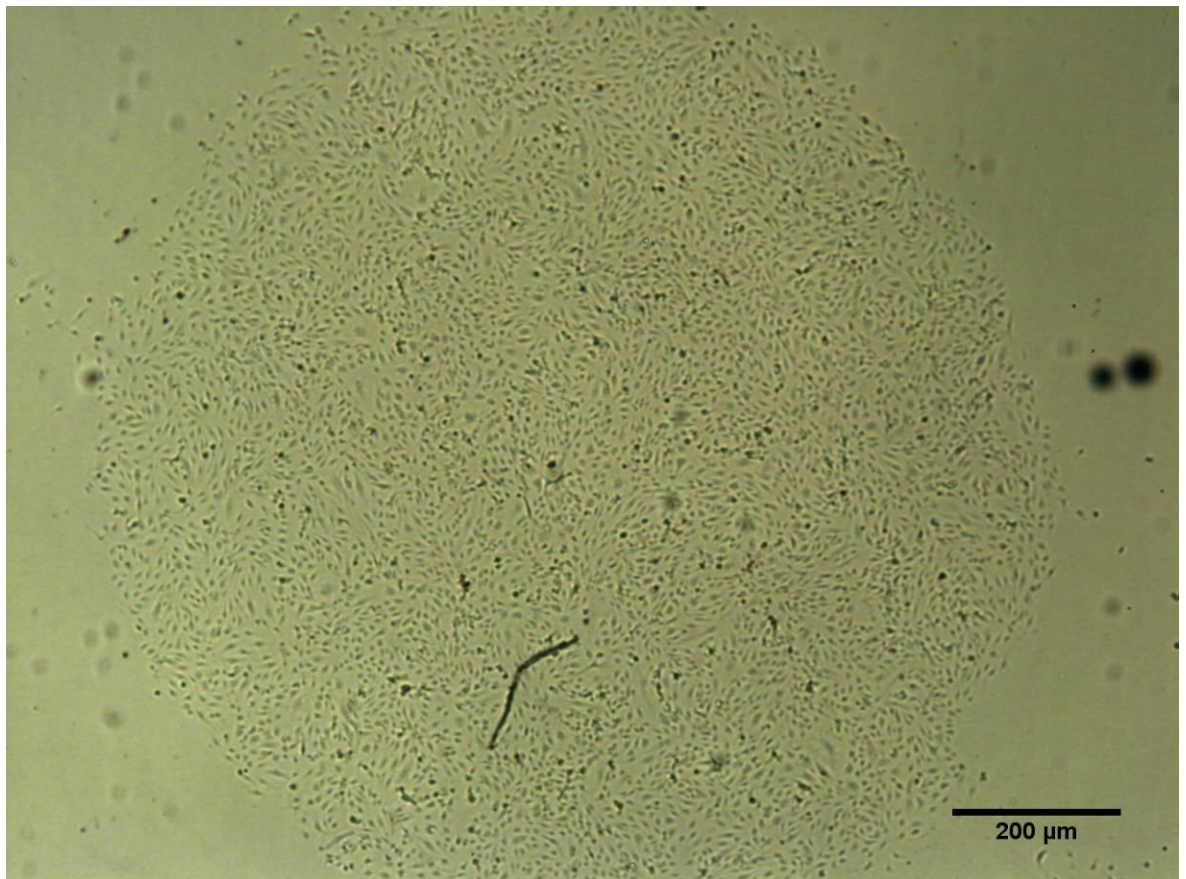
Fig. 3.1a Pictorial presentation of migration assay The HUVECs or HMVECad were grown into circular cell monolayers. The scale bar of photomicrographs represents 200µm (Magnification: 25 x).

Photomicrographs of cell monolayers were acquired before incubation and recorded as 0 h samples. Images were subsequently taken at 24 and 48 h after incubation and are recorded as 24 and 48 h samples. The images were analyzed by measuring the area (Fig.3.1b), length (Fig. 3.1b) and radii (Fig. 3.1b, 2.2a-d) of circular cell monolayers to determine the migration of cells. All three parameters viz. area, length and radii were measured to find out which of them best represents the migration of endothelial cells. The measurement of area and length was recorded by masking the circular monolayers with a hand drawn loop using Leica (QWin Standard v 2.8, Image Processing and Analysing System) software. The measurement of radii was carried out as explained in section 2.2.3. A minimum of 10 or 20 (as specified in the relevant sections) radii were drawn on the radial spokes and the measurements were noted down.
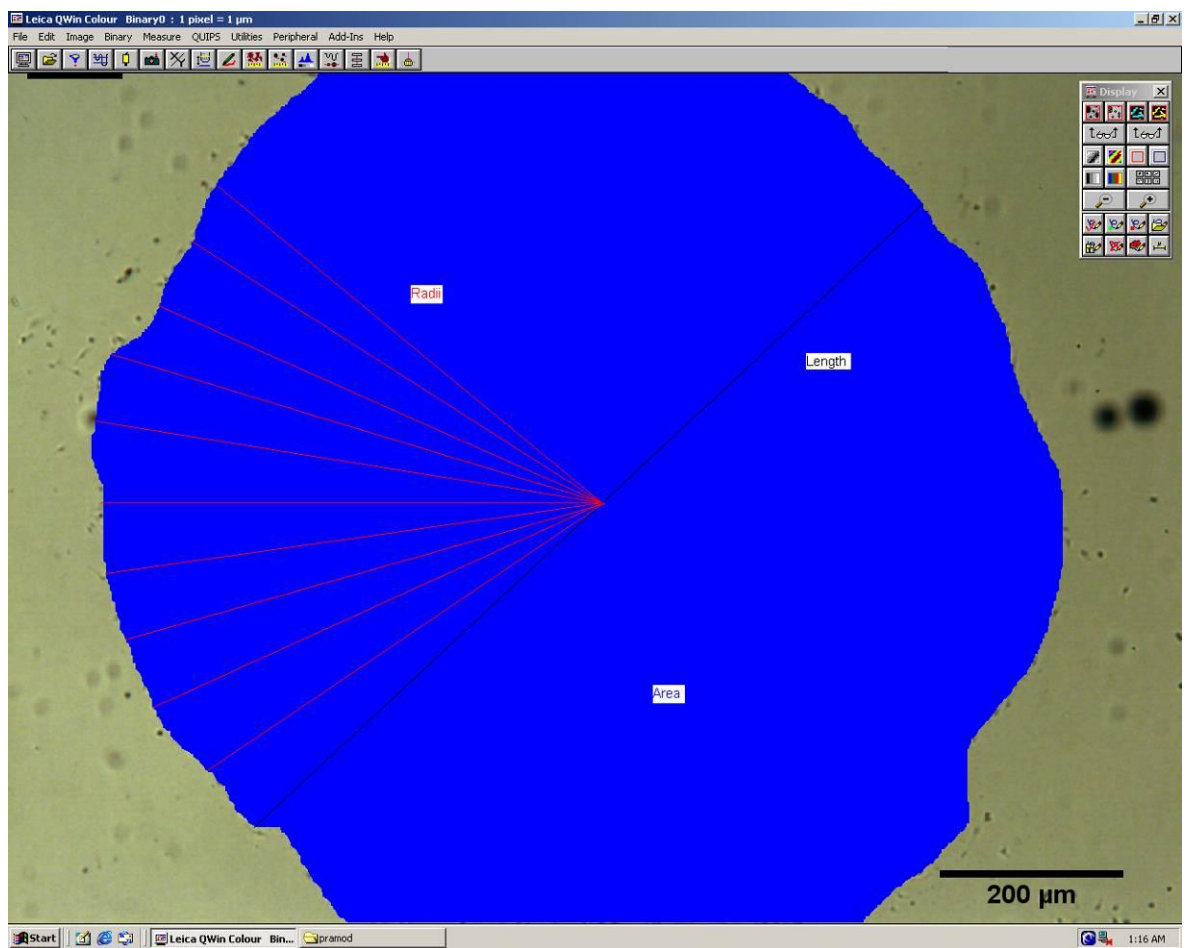
Fig. 3.1b Pictorial presentation of migration assay The migration was measured in terms of area and length by superimposing a manual drawn blue loop on a circular monolayer. The area (blue coloured loop) and length (black line) were recorded from the same loop, whereas radii (red lines) were measured by superimposing the radial spokes as explained in Fig 2.2a-d of previous chapter. The scale bar of photomicrographs represents 200µm (Magnification: 25x).

Three time points were used to record the migration viz. t_0 = 0 h, t_{24} = 24 h and t_{48} = 48 h. Images of cell monolayers were recorded prior to their incubation in test conditions as samples of t_0, after 24 h incubation as samples of t_{24} and after 48 h incubation as samples of t_{48}. Different samples were used while developing the methodology. The following table 3.1 serves as a guiding point to understand the sampling methods. The migration (section 3.2.2.1) was defined as area or length or radii measured at 0, 24 and 48 h. The analysis of net migration was more accurate and less time consuming compared to the measurement of migration; hence it was adopted from section 3.2.2.2 onwards and for the results of other chapter. The net migration was defined as the difference between the measurements of 24 or 48 h with those of 0 h. The migration measurements depending on the sample size are presented as median for area (μm^2) and length (μm) and as mean ± SEM (μm) for radii.

Table 3.1 Sampling methods Different samples (S) were used while developing the method for migration assay, while having three time points (t) during all the experiments. Recording of the net migration involved subtracting values of t_0 from either t_{24} or t_{48}.

Section	Time point (t) (h)	Sample used to capture images	Samples used to record the migration	Sample size
3.2.2.1	0 (t_0)	S1+S2+S3	S1+S2+S3	03
	24 (t_{24})	S4+S5+S6	S4+S5+S6	03
	48 (t_{48})	S7+S8+S9	S7+S8+S9	03
3.2.2.2 and 3.2.2.4	0 (t_0)	S1+S2+S3 +S4+S5+S6	-	06
	24 (t_{24})	S1+S2+S3	$(S1+S2+S3)t_{24}$ - $(S1+S2+S3)t_0$	03
	48 (t_{48})	S4+S5+S6	$(S4+S5+S6)t_{48}$ - $(S4+S5+S6)t_0$	03
3.2.2.3	The first time point (t_0) is 24 h after the formation of circular monolayer			
	0 (t_0)	S1+S2+S3 +S4+S5+S6	-	06
	24 (t_{24})	S1+S2+S3	$(S1+S2+S3)t_{24}$ - $(S1+S2+S3)t_0$	03
	48 (t_{48})	S4+S5+S6	$(S4+S5+S6)t_{48}$ - $(S4+S5+S6)t_0$	03
3.2.2.5 and 3.2.2.6	0 (t_0)	S1+S2+S3	-	03
	24 (t_{24})	S1+S2+S3	$(S1+S2+S3)t_{24}$ - $(S1+S2+S3)t_0$	03
	48 (t_{48})	S1+S2+S3	$(S1+S2+S3)t_{48}$ - $(S1+S2+S3)t_0$	03

3.2.2 Results and discussion

3.2.2.1 Migration assay using different samples at different time points

The results for the migration of HUVECs in N5mM condition were obtained by using three separate samples (n=3) at one single time point, S1 to S3 at 0 h, S4 to S6 at 24 h and S7 to S9 at 48 h, as mentioned in table 3.1. Thus, each time point contained separate samples of monolayers and did not represent the longitudinal results from an individual monolayer at the specified time point. The images were used to record the measurements as explained in section 3.2.1. Ten radii measurements were recorded for each sample and results are presented in figure 3.2.

No significant difference between 0 and 24 h was observed in area (μm^2) (0 h: 100884.1 vs. 24 h: 96095.8) and length (μm) (0 h: 375.5 vs. 24 h: 388.6). However, the radii (μm) were significantly less ($p<0.05$) at 24 h (179.8 ± 1.3) compared to 0 h (186.6 ± 1.1) (Fig. 3.2). The measurement of area, length and radii was 148461.5, 495.3 and 241.7 ± 2.3 respectively at 48 h. The migration was significantly higher ($p<0.001$) at 48 h compared to 0 and 24 h only in case of radii and no significant difference was detected in either area or length.

The migration assay using different samples at different time points (Fig. 3.2) failed to confirm any changes happening in the migration of cells over the period of time. On the contrary, the radii of 24 h samples were found to be of lesser size than those of 0 h. This clearly suggests that, the monolayers of cells were not of uniform size at the time of seeding (i.e. at 0 h). Although the cells might have migrated from their original position, this method failed to detect it because a different set of monolayers were used to measure the area, length and radii at 24 and 48 h. Hence it was decided that the use of different sets of monolayers at different time points was not suitable to record the migration of cells. As a result, in the next set of experiments the photographs of same monolayers of 0 and 24 h and 0 and 48 h were used for image analysis.

Fig 3.2 The migration assay using different samples at different time points The circular HUVEC monolayers were exposed to N5mM condition for 48 h. The migration was measured in terms of area (a), length (b) and radii (c) at 0, 24 and 48 h. The median of area and length were analysed by nonparametric (Mann-Whitney) analysis and means of radii were analysed by ANOVA followed by post hoc (Bonferroni) test.

(Area and length: n = 3, Radii: n = 30 (10 radii from each sample),

* $p<0.05$, *** and ††† $p<0.001$ when compared to 0 and 24 h respectively)

a)
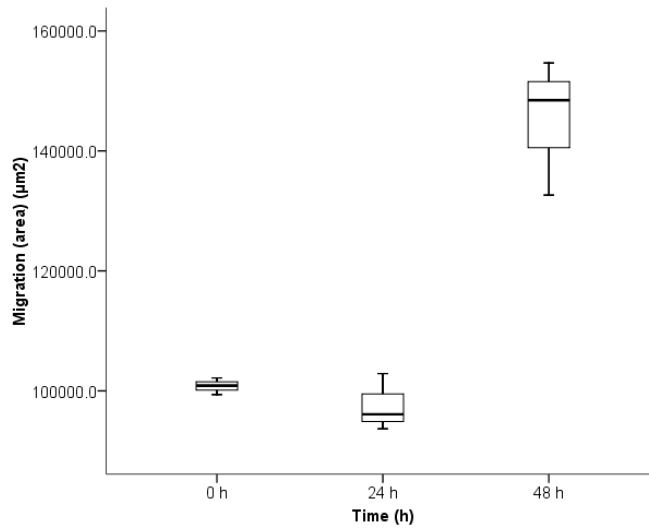
b)
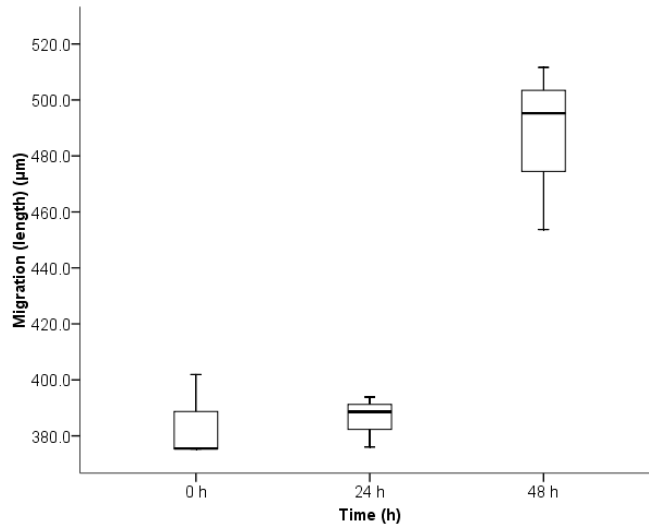
c)
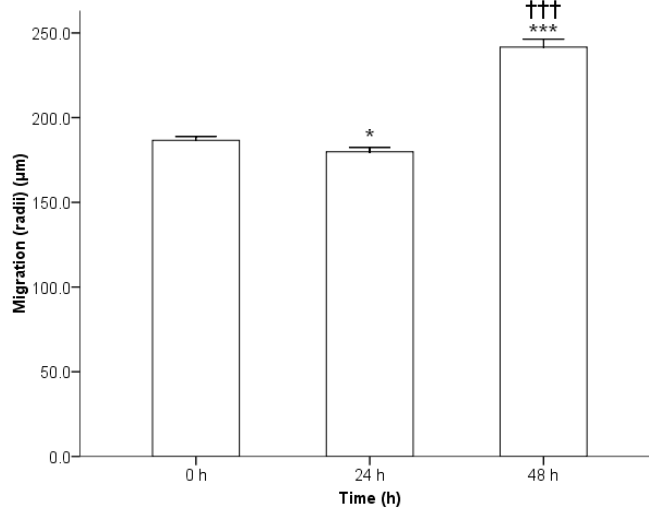
3.2.2.2 Migration assay using same samples at two different time points

A few changes were then made from the previous set of experiments. They were as follows

a) Validation of the migration assay was continued by using HMVECad rather than HUVECs in N5mM condition. HMVECad were used, as the larger aim of the project was to assess the migration of dermal microvascular endothelial cells.

b) Net migration rather than migration was assessed, as the migration at 0 h (t_0) of previous set of experiments (section 3.2.2.1) was actually not *per se* the migration but a mere dimension of the monolayers.

c) The sampling technique was altered in order to improve the accuracy of the measurements obtained.

The results presented here were obtained by using the same three samples at two different time points i.e. S1 to S3 at 0 and 24 h and S4 to S6 at 0 and 48 h as explained in table 3.1. The photomicrographs of all the six samples i.e. S1 to S6 were captured at 0 h. The samples were returned to the incubator and subsequently three samples i.e. S1 to S3 were photographed again at 24 h and other three i.e. S4 to S6 again at 48 h. That effectively meant that there were six samples at 0 h, three to be photographed again at 24 h and another three to be photographed again at 48 h. The images were later used to record the net migration as explained in 3.2.1 by subtracting the distance of cell migration at either 24 or 48 h with their respective images taken at 0 h.

No significant difference in the net migration in N5mM condition (Fig. 3.3) between 24 and 48 h was observed for area (μm^2) (24 h: 157296.0 vs. 48 h: 262240.0) and length (μm) (24 h: 163.0 vs. 48 h: 205.0). However, the net migration in terms of radii (μm) was significantly higher ($p<0.001$) at 48 h (116.3 ± 1.5) compared to 24 h (72.0 ± 1.2).

The results (Fig. 3.3) show that the area and length did not change significantly between different time points unlike radii which increased significantly at 48 h compared to 24 h. This was partly due to the limitation in the dimensions of the image frame. The dimension of the images captured at a magnification of 25x was 1392 x 1040 (width x height) pixels. The calibrated image size was 5136.5 x 3837.6 (width x height) in μm (1 pixel = 3.69μm). The circular cell monolayers seeded into a glass ring of 6mm of outer diameter could not be captured in its entirety within the image frame. The height of the image that could be captured as the frame height was smaller than the size of the circular monolayer, particularly at 24 and 48 h. As a result, the measurement of area and length at 24 and 48 h did not reflect an accurate migration of cells. Thus, the measurement of area and length at different time points were not sufficiently accurate at determining any changes in the migration of cells in specific conditions.

Fig 3.3 The migration assay using same samples at two different time points The circular HMVECad monolayers were exposed to N5mM condition for 48 h. The net migration was measured in terms of area (a), length (b) and radii (c) at 24 and 48 h. The data of area and length were analysed by nonparametric (Mann-Whitney) analysis and data of radii was analysed by independent *t* test.

(Area and length: n = 3, Radii: n = 60 (20 radii from each of 3 samples),

*** *p*<0.001 when compared to 24 h)

a)
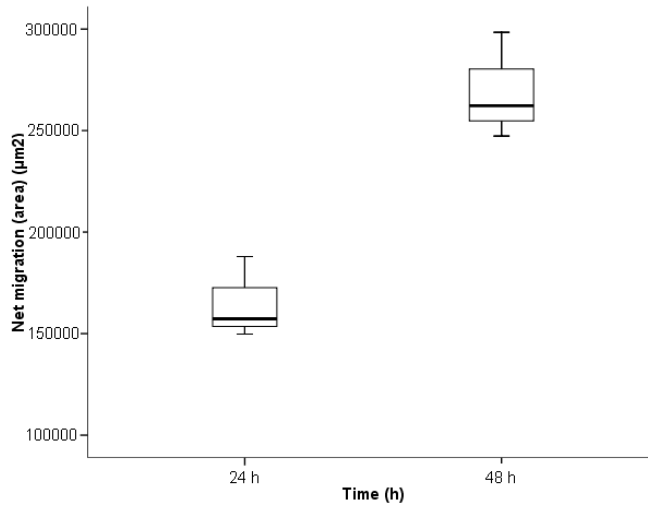
b)
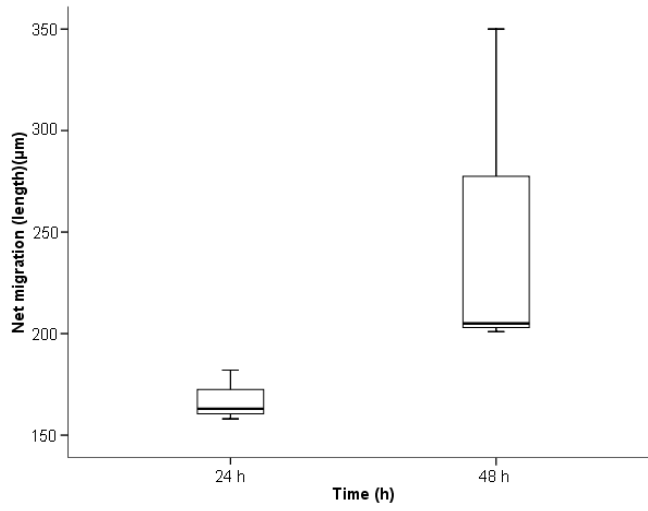
c)
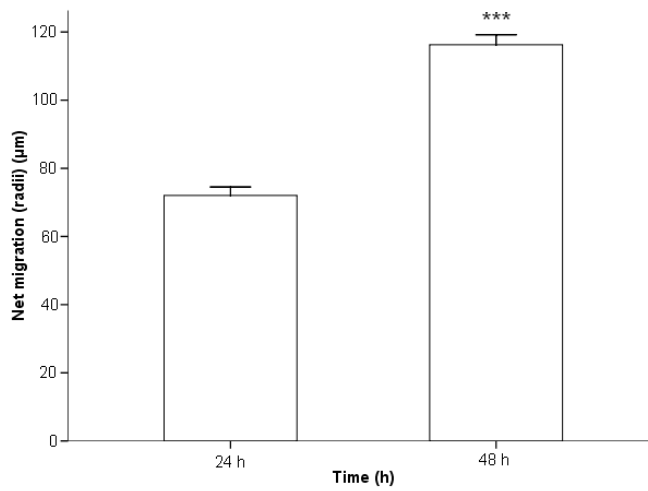
3.2.2.3 Migration assay using the same samples at two different time points with an extended incubation time

The results for the migration of HMVECad in N5mM condition were obtained very similarly as in the last section with the following exception. In the previous section 3.2.2.2, 0 h is when the glass rings were removed and the resulting circular monolayers were photographed before returning them to the incubator. However, to obtain the results of this sub-section the circular monolayers supplemented with media were allowed to remain in the incubator overnight after removal of the glass rings. Next day, the images of monolayers i.e. S1 to S6 were captured and these images were considered as samples at 0 h. The samples were returned to the incubator until the three samples i.e. S1 to S3 were photographed again at 24 h and the remaining three i.e. S4 to S6 at 48 h. The images were used to record the net migration as explained in section 3.2.1.

No significant difference in the net migration in N5mM condition (Fig. 3.4) between 24 and 48 h was observed for area (μm^2) (24 h: 83559.0 vs. 48 h: 146692.0) and length (μm) (24 h: 98.0 vs. 48 h: 141.0). However, like previously, in these set of experiments also the net migration in terms of radii (μm) was significantly higher ($p < 0.001$) at 48 h (77.7 ± 1.4) compared to 24 h (35.6 ± 0.7).

The results presented (Fig. 3.4) confirm that the area and length failed to change significantly at different time points unlike radii which increased significantly at 48 h compared to 24 h. The earlier explanation of image frame provided in section 3.2.2.2 holds true for this section also. As a result, the measurement of area and length was not subsequently used to record the migration of cells. The extra incubation for 24 h after the removal of rings produced the results similar to section 3.2.2.2. Hence, in the next set of experiments only radii was measured in order to assess the net migration in different conditions and further to understand the intra and inter-experimental variabilities.

Fig 3.4 The migration assay using the same samples at two different time points with an extended incubation time The circular HMVECad monolayers were exposed to N5mM condition for 48 h. The net migration was measured in terms of area (a), length (b) and radii (c) at 24 and 48 h. The median of area and length were analysed by nonparametric (Mann-Whitney) analysis and means of radii were analysed by independent *t* test.

(Area and length: n = 3, Radii: n = 60 (20 radii from each of 3 samples),

*** $p < 0.001$ when compared to 24 h)

a)
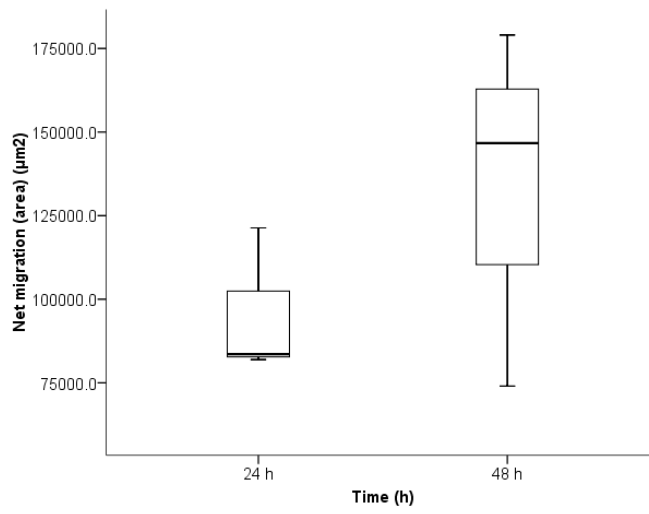
b)
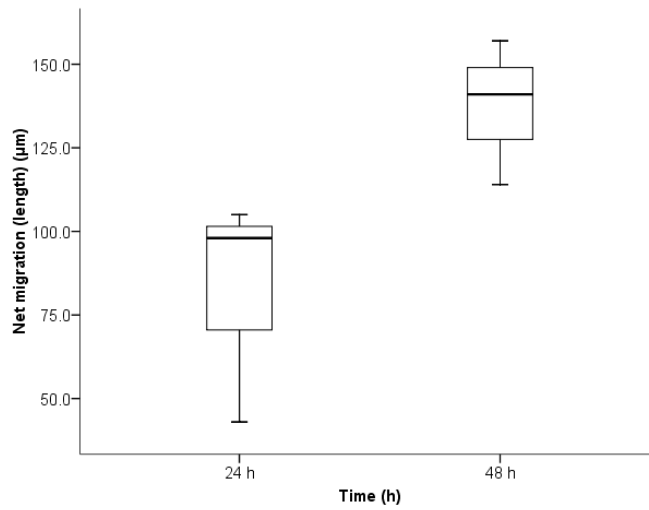
c)
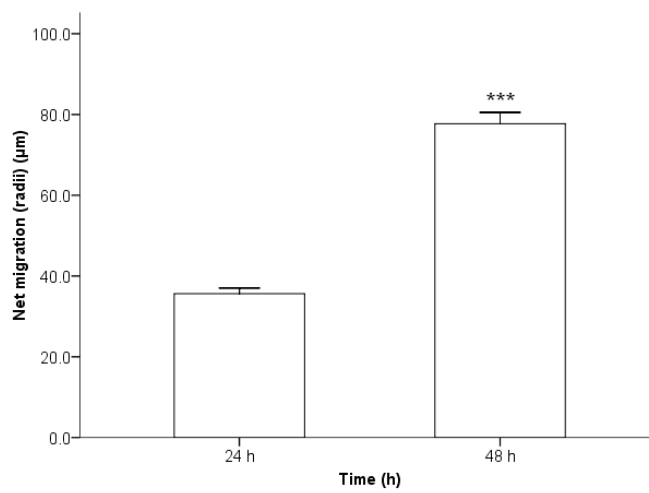
3.2.2.4 The radial migration assay in different conditions using the same samples at two different time points

The method of selecting the samples was similar to that presented in section 3.2.2.2 with following changes

a) Only radii, not the area and length, were used to assess the migration of endothelial cells.

b) The radii of the circular monolayer of HMVECad were recorded not only in N5mM condition but additionally in three other conditions viz. N20mM, H5mM and H20mM.

c) The migration assay was carried out on three different occasions to verify the reproducibility of the results.

The results obtained on the first occasion (Fig. 3.5a) show that the net migration (µm) in N20mM (24 h: 39.5 ± 1.5; 48 h: 91.3 ± 2.3) condition was significantly less ($p<0.001$) than in N5mM (24 h: 48.3 ± 1.5; 48 h: 132.5 ± 5.3) condition at 48 h, but not at 24 h ($p>0.05$). The migration significantly increased in H5mM (24 h: 64.7 ± 6.4; 48 h: 133.8 ± 2.7) at 24 h ($p<0.01$), but not at 48 h ($p>0.05$) compared to N5mM condition. The migration in H20mM (24 h: 60.8 ± 1.2; 48 h: 113.4 ± 2.0) condition was significantly less ($p<0.001$) at 48 h, but not at 24 h ($p>0.05$) when compared to H5mM condition.

In the next experiment (Fig. 3.5b), the net migration (µm) in N20mM (24 h: 68.6 ± 2.0; 48 h: 139.0 ± 3.1) condition was not significantly different ($p>0.05$) from that in N5mM (24 h: 65.0 ± 0.9; 48 h: 143.9 ± 4.0) condition at both time points. The migration in H5mM (24 h: 73.7 ± 0.7; 48 h: 153.5 ± 1.6) condition was significantly higher at 24 h ($p<0.01$), but not at 48 h ($p>0.05$) compared to N5mM condition. The migration in H20mM (24 h: 63.8 ± 2.5; 48 h: 141.4 ± 1.4) condition was significantly lower at 24 h ($p<0.001$) and 48 h ($p<0.05$) compared to H5mM condition.

On another occasion (Fig. 3.5c), the net migration (µm) in N20mM (24 h: 92.2 ± 1.8; 48 h: 139.2 ± 1.9) condition was not significantly different ($p>0.05$) than in N5mM (24 h: 92.6 ± 1.7; 48 h: 139.2 ± 1.9) condition at both time points. The migration in H5mM (24 h: 97.2 ± 0.7; 48 h: 149.3 ± 1.3) condition did not significantly alter at 24 h ($p>0.05$), but was higher at 48 h ($p<0.001$) compared to N5mM condition. The migration in H20mM (24 h: 83.0 ± 2.1; 48 h: 127.8 ± 1.3) condition was significantly less ($p<0.001$) than in H5mM condition at both time points.

The changes in the net migration (Fig. 3.5a-c) happening in response to different conditions were not reproducible over different occasions. This could be because of using different samples at 24 and 48 h. To overcome this inter- and intra-experimental variability, it was decided that the same circular monolayer will be photographed for all the time points as explained in next set of experiments.

Fig. 3.5 Radial migration assay in different conditions using the same samples at two different time points The circular HMVECad monolayers were exposed to either 5mM glucose or 20mM glucose under normoxic (20% O_2 tension) or hypoxic (5% O_2 tension) condition for 48 h. The migration in all the conditions was significantly higher at 48 h compared to 24 h on all three different occasions represented by figure a, b and c. The comparison between the conditions was analysed by ANOVA followed by Bonferroni post-hoc test. The comparison between the days of the same condition was analysed by independent *t* test.

(n=60 for all, except for H20mM at 24 h when n=40 in figure c;

NS = not significant ($p>0.05$), * $p<0.05$, **$p<0.01$, ***$p<0.001$ when compared as indicated)

a)
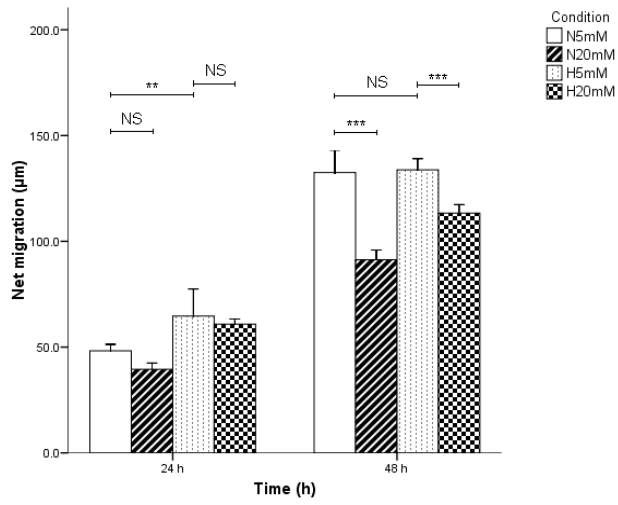
b)
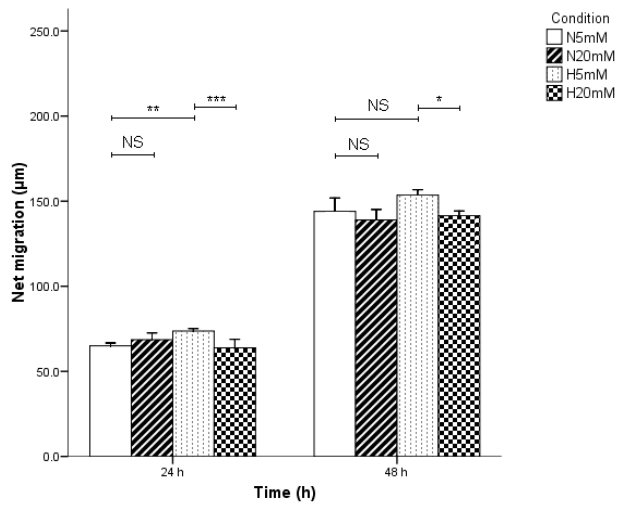
c)
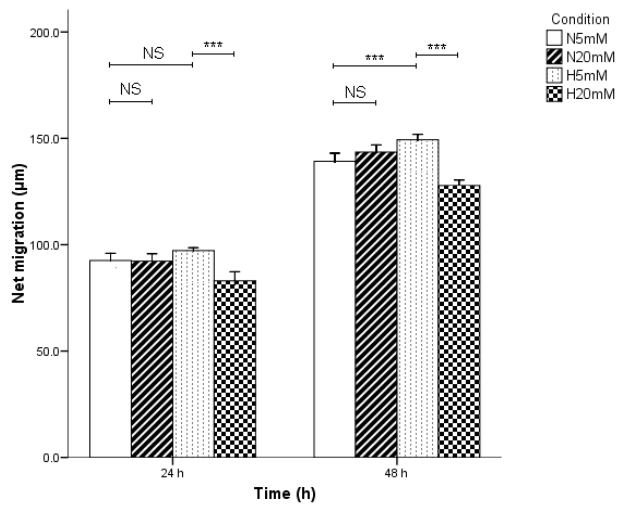
3.2.2.5 Migration assay using same samples for all the time points

In this set of experiments, the same monolayers of HMVECad in N5mM condition were photographed and analysed at three different time points of 0, 24 and 48 h as explained in table 3.1. The photomicrographs of all the three samples (S1 to S3) at 0 h were captured. The samples were returned to the incubator and were photographed at 24 h. The samples were returned to the incubator again for another day and finally photographed at 48 h. The images were used to record the net migration as explained in 3.2.1.

Area and length along with radii were measured in order to confirm the effect of the new sampling technique on the net migration. Similar to the previous set of experiments, no significant difference in the net migration in N5mM condition between 24 and 48 h was observed for area (μm^2) (24 h: 160128.0 vs. 48 h: 249116.0) and length (μm) (24 h: 162.0 vs. 48 h: 263.0) (Fig. 3.6). However, the net migration in terms of radii (μm) was significantly higher ($p<0.001$) at 48 h (111.0 ± 2.3) compared to 24 h (70.5 ± 1.4).

The results suggest that this sampling technique was reproducible over different occasions. Hence this method was followed to present the net migration in the all other chapters. The effects of different conditions on the migration of cells, using this method are presented in the next chapter. However, to overrule the user induced bias a single blind study of migration using this method was carried out and is presented in next section.

Fig 3.6 The migration assay using same samples for all the time points The circular HMVECad monolayers were exposed to N5mM condition for 48 h. The net migration was measured in terms of area (a), length (b) and radii (c) at 24 and 48 h. The data of area and length were analysed by nonparametric (Mann-Whitney) analysis and data of radii was analysed by independent *t* test.

(Area and length: n = 3, Radii: n = 60 (20 radii from each of 3 samples),

*** *p*<0.001 when compared to 24 h)

a)
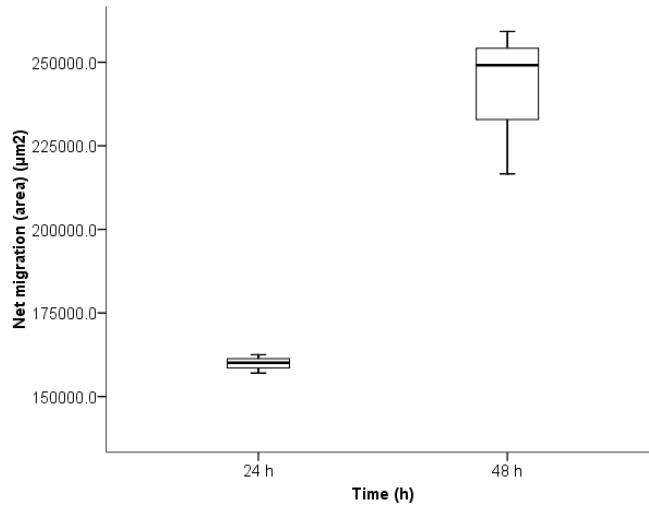
b)
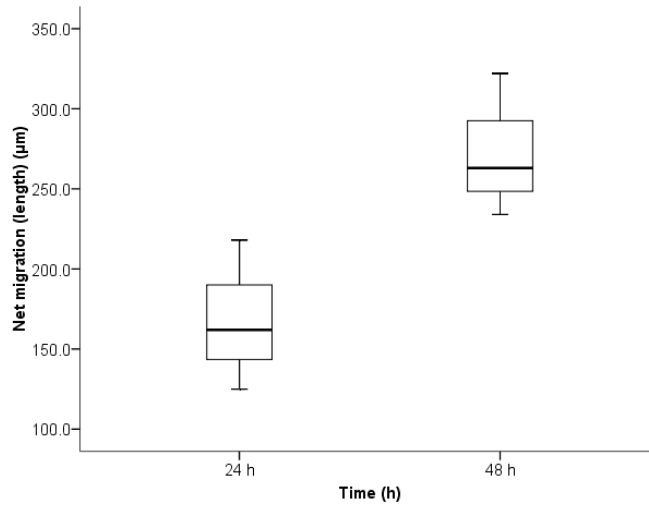
c)
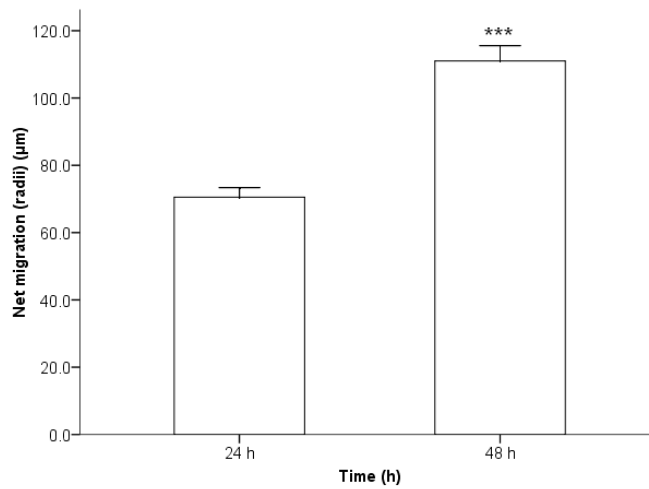
3.2.2.6 Single blind analysis of migration assay

The images of HMVECad captured as explained in section 2.2.2 were analysed before blinding (un-blinded) and after blinding (blinded) the samples to recognise the user induced bias, if any. The migration of cells was noted for totally eight test groups to compare between blinded and un-blinded samples (table 3.2). No significant difference ($p>0.05$) was found in any of the eight groups between the blinded and un-blinded samples. The coefficients of variation (CV) were calculated to assess the variation in a single test group for intra-experimental variation. The minimum value of CV was 1.0% for un-blinded samples of group 5 and maximum value was 3.1% for blinded samples of group 2. The lower values of CV indicate lesser variation in the measurement of radii of samples within an experiment. The effects of different conditions on the migration of endothelial cells are discussed in the next chapter.

Table 3.2 Single blind analysis of radial migration assay The circular HMVECad monolayers were grown as circular monolayers and images were captured. The images without coding were analysed as un-blind samples and after coding, the same images were analysed as blind samples. The coefficients of variation were calculated to analyse the reproducibility of the results within an experiment. The comparison between the un-blind and blind samples of a same condition was analysed by independent *t* test. (n=60 for all, except for test group 4 and 8 when n=40)

Test groups	Migration (mean ± SEM) (μm)		*p* value	Coefficient of Variation (%) (CV=(SEM/Mean)x100)	
	Blinded	Un-blinded		Blinded	Un-blinded
1	92.6 ± 1.9	95.8 ± 1.1	0.14	2.1	1.1
2	75.2 ± 2.3	78.3 ± 1.6	0.26	3.1	2.0
3	109.6 ± 2.1	111.8 ± 2.0	0.46	1.9	1.8
4	89.9 ± 1.6	90.0 ± 2.2	0.96	1.8	2.4
5	166.9 ± 2.2	168.9 ± 1.7	0.48	1.3	1.0
6	142.0 ± 2.3	144.7 ± 2.6	0.43	1.6	1.8
7	181.7 ± 3.0	184.5 ± 3.6	0.56	1.7	2.0
8	142.9 ± 2.3	147.2 ± 2.1	0.17	1.6	1.4

3.2.3 Summary

The following conclusions could be drawn from the different set of experiments of migration assay.

1. Net migration and not simple migration is an accurate indicator of the migration of cells.

2. Area and length are interdependent as they both are calculated by the software at a same time using a same image. One can not be used without the other in any of the methods explained.

3. Area and length could not be used as parameters of the migration of cells of a circular monolayer due to the

   3.1 limitation posed by the image frame. This limitation could have been possibly overcome by making either using lower magnification of 16x or by increasing the image frame by altering the C-mount (a hardware part of microscope camera) from 0.70x to 0.50x. However this would have been still a problem, if the monolayers were to grow larger than image frame at 48 h and the

   3.2 large errors associated with the values of area and length as large internal component does not vary.

4. The use radii of same samples for all the time points is an optimal method to measure the radial migration, as it makes the use of a same monolayer over the period of time.

5. Use of same sample for two time point method did not produce reproducible results for the migration in different condition suggesting the flaws of sampling technique.

6. Single blind study confirmed that the use of radii and same samples for all the time points is an optimal method.

In conclusion, it was decided to use radii from the same monolayer for all the time points in order to record the net migration of endothelial cells. All the observations of section 3.2 are summarised in the following table 3.3. The radial migration assay method was followed for the results presented in all other chapters; the method was explained as a general method in chapter 2. Using the radial migration assay the measurement of migration was carried out in different conditions varying the glucose and oxygen tension levels and the results are presented in next chapter.

Table 3.3 Summary of the sampling methods for migration assay

Section	Sampling method	Observations	Proposed reasons
3.2.2.1	Different samples at different time points	No change in the area or length or radii over the time	Variation in sampling technique
3.2.2.2	Same samples for two time points (i.e. at t_0 and t_{24} or t_0 and t_{48})	No change in area or length, but change in radii over the time	Image frame size, variation in sampling technique and small sample size of area and length
3.2.2.3	Same samples for two time points (i.e. t_0 and t_{24} or t_0 and t_{48}) with an extended incubation of 24h period before t_0	No change in area or length, but change in radii over the time	Image frame size, variation in sampling technique and small sample size of area and length
3.2.2.4	Same samples for two time points (i.e. t_0 and t_{24} or t_0 and t_{48}) in different conditions	Inter and intra experimental variability	Sampling technique
3.2.2.5	Same samples for all the time points	No change in area or length, but change in radii over the time	Image frame size and difference of values in net change compared to area and length
3.2.2.6	Same samples for all the time points	No difference between blinded and un-blinded samples	Optimal method

3.3 Wound healing assay

Two methods were employed to assess the migration of cells in the wound environment, termed for the purpose of this section as the scratch wound assay and the wound healing assay.

3.3.1 Scratch wound assay

3.3.1.1 Materials and Methods

The six well plates were seeded with 5×10^3 HUVECs per cm^2 as explained in section 2.2.1.4. When confluent, the monolayers were wounded by scratching with a sterile pipette tip drawn across the surface of the monolayers into four quadrants (Fig 3.7a). The detached cells were removed by washing with phosphate buffered saline (PBS) and the plates were replenished with fresh 2.5ml of media before returning them to either N5mM or H5mM incubation conditions for 24 or 48 h.

The monolayers were photographed using an inverted microscope (DMI 4000B, Leica Microsystems, Germany) at a magnification of 25x at 0 h before incubating cells in the above mentioned conditions and again images obtained at either 24 or 48 h. The photomicrographs were analysed using Leica (QWin Standard v 2.8, Image Processing and Analysing System) software by measuring the wound area of the cell monolayer. A circular loop generated using the software, was superimposed at the intersection of the monolayer where it was devoid of the cells (Fig. 3.7b). If, one loop was not big enough to cover the wounded region, more than one loop were used so as to cover the wounded region at the centre of the intersection (Fig.3.7c). The wound healing response presented as the median and was defined as the area (μm^2) remaining free of cells at 0, 24 and 48 h.

a)
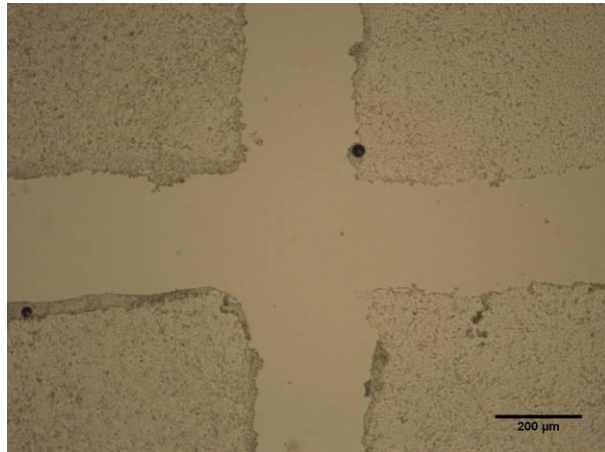
b)
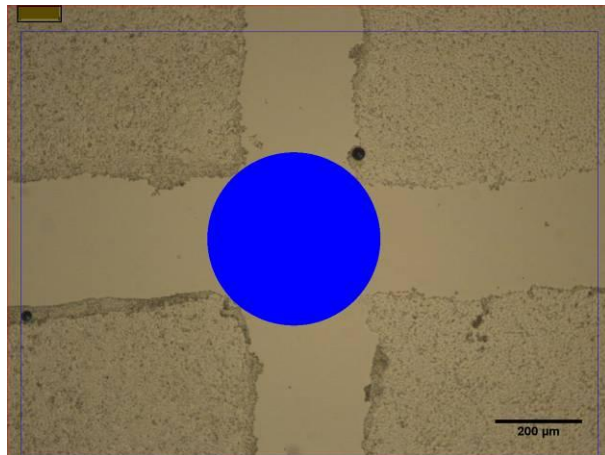
c)
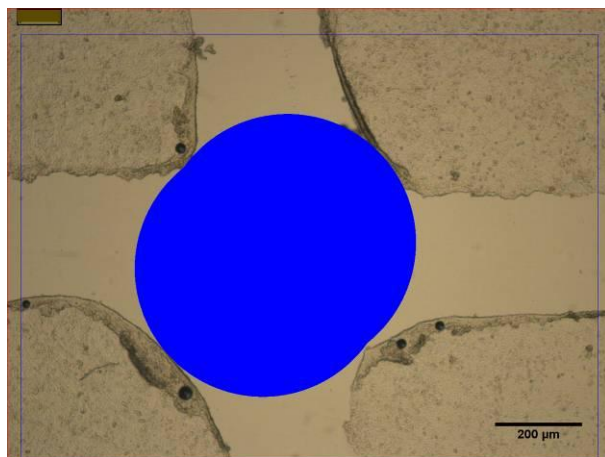
Fig. 3.7 Images of the scratch wound assay The confluent monolayer was scratched through to divide it into four quadrants (a). The wounded region was measured by recording the area of a software generated circular blue coloured loop superimposed at the intersection of quadrants. If a single circular loop (b) could not cover the central region of intersection, more than one loop (c) was superimposed to cover that region. The scale bar of photomicrographs represents 200μm (Magnification: 25x).

3.3.1.2 Results and Discussion

The wounded area (μm^2) in N5mM condition at 0, 24 and 48 h was 17404.3, 2260.0 and 0.0 respectively (Fig. 3.8). The wounded area in H5mM condition at 0, 24 and 48 h was 20956.3, 2776.8 and 0.0 respectively. There was no significant difference ($p>0.05$) in wounded area between the normoxic and hypoxic conditions at any of the time points. However, the wounded area was more confluent with cells at 24 h in N5mM ($p<0.001$) and H5mM ($p<0.05$) condition compared to 0 h. The monolayers continued to become confluent at 48 h compared to 24 h in N5mM ($p<0.01$) and H5mM ($p<0.05$) condition.
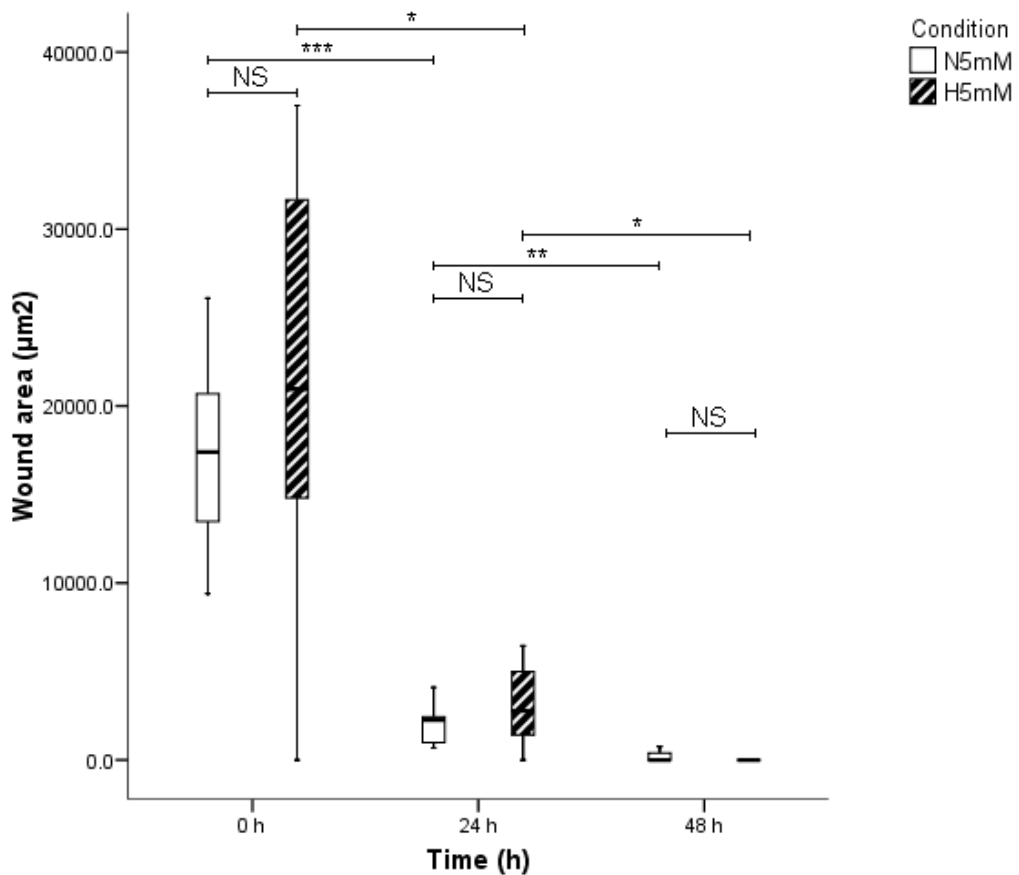
Fig. 3.8 Scratch wound model The monolayers of HUVECs were exposed to normoxic (20% O_2 tension) or hypoxic (5% O_2 tension) condition after wounding with a sterile pipette tip. The data were analysed by non parametric (Mann-Whitney) analysis.
(n=12 at 0 h and n=6 at 24 and 48 h; NS = not significant ($p>0.05$), *$p<0.05$, **$p<0.01$, ***$p<0.001$ when compared as indicated).

This method failed to detect the difference in the wound healing response to normoxic and hypoxic condition. However, the level of significance in the wound healing rate over different time points in normoxic and hypoxic condition were different. These can be attributed to the following reasons

a) HUVECs were detached from the surface unevenly while scratching, leading to variability in the level difference in the wounded area in different monolayers.

b) As the wounding was created in an already confluent monolayer, the monolayers were over confluent by the time the wound healing was measured at 24 and 48 h.

c) Like in the migration assay, the measurement of whole of area as a single value, rather than the multiple values of distance was an impediment in getting any meaningful results.

d) The sample size was too small and was an obstacle in getting any meaningful difference in wound healing rate between normoxic and hypoxic conditions.

e) This model did not provide the opportunity of assessing the migration of endothelial cells from both the wounded and unwounded edge of the same monolayer, which was one of the objectives of this project.

After considering all the above mentioned reasons, it was decided to design an experiment using HMVECad where the earlier explained radial migration assay would be brought together with the wound healing assay as explained in section 2.2.4 of the previous chapter.

3.3.2 Wound healing assay

3.3.2.1 Materials and methods

This method was developed with an aim of combining the wound healing assay with the migration assay, as one of the objectives of the project was to understand the migration of cells under the influence of a 'normal' and/or a 'wounded environment' on each other. The previously explained scratch wound method was not suitable to realise this objective. HMVECad cells were grown as a circular monolayer in 6-well plates and half of each monolayer was removed. The wound healing assay was carried out in N5mM and H5mM conditions and migration was assessed as explained in section 2.2.4 of chapter 2.

3.3.2.2 Results and discussion

The migration (µm) of HMVECad (Fig. 3.9a) from the intact edge in N5mM (24 h: 80.2 ± 1.4; 48 h: 153.7 ± 3.1) was significantly lower ($p<0.001$) than in H5mM (24 h: 92.9 ± 1.9; 48 h: 183 ± 2.8) condition. Similar to the intact edge, the migration of HMVECad from the wounded edge (Fig.3.9b) was significantly lower ($p<0.001$) in N5mM (24 h: 87.8 ± 1.8; 48 h: 170.5 ± 2.8) compared to H5mM (24 h: 105.1 ± 1.4; 48 h: 208.8 ± 2.8) condition. The migration in H5mM condition was significantly higher ($p<0.001$) compared to N5mM condition. The wound healing assay confirmed the increase in the migration of cells not only over time but also with decreasing oxygen tension.

a)
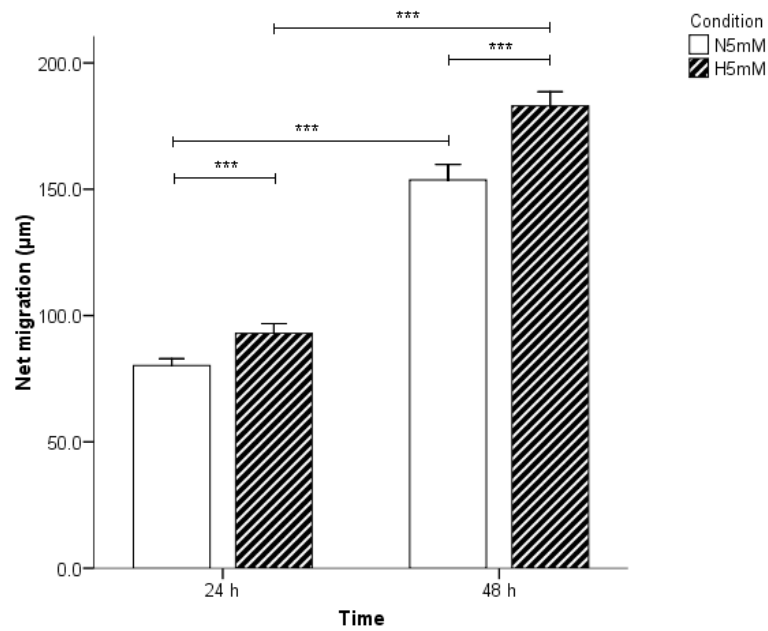
b)
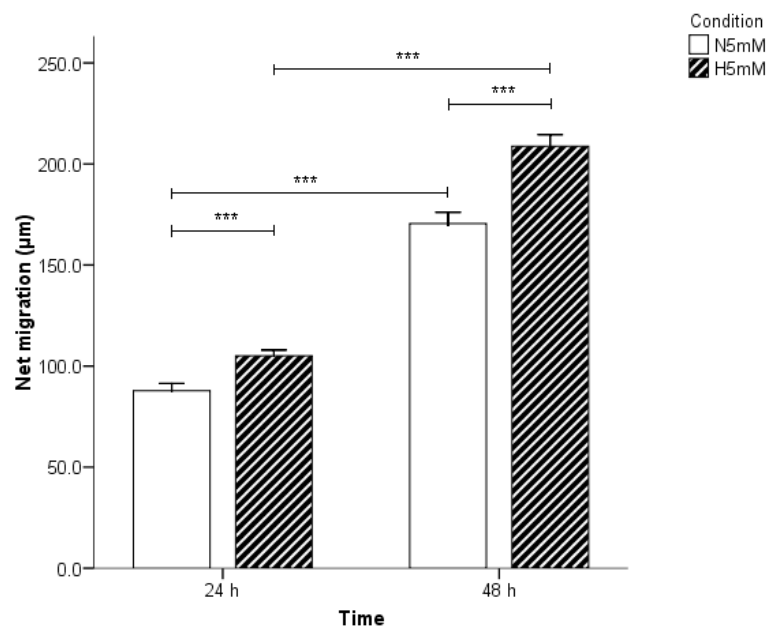
Fig. 3.9 Wound healing assay The migration of HMVECad in conditions of 5mM glucose and 20 (Normoxia – N) or 5% (Hypoxia – H) oxygen tension was assessed by the wound healing assay. The results are presented as net migration (mean ± SEM) of cells from the intact (a) and the wounded edge (b) of the monolayer. Independent *t* test was employed to compare the results between the two conditions and two time points.

(***p<0.001 when compared as indicated, n = 90 for each condition at 24 & 48 h, except for H5mM of intact edge, n = 80 at 24 h)

3.3.3 Summary

The following conclusions could be drawn from this different set of experiments of wound assays.

1. The scratch wound assay does not provide an opportunity to bring the wound healing and migration assay in a single model.

2. The scratch wound assay creates uneven areas of wound and involves small sample size due to measurement of area as a single observation. This would necessitate increase in the sample size to produce meaningful results. On the other hand wound healing assay not only combines the migration and wound healing together but also is able to meaningfully distinguish between the differences between the conditions and time points.

In conclusion, it was decided to use radial and normal distances from un-wounded and wounded edge of the monolayer respectively to record the net migration of endothelial cells. The wound healing assay method was followed for the results presented in all other chapters and the method has been explained in section 2.2.4 as a general method in chapter 2. A more detailed look at the effect of glucose concentration and oxygen tension using the validated methods was then undertaken and the results are presented in next chapter.

The work involving the development and validation of the migration/wound healing assay would benefit further if the cells seeded into a glass ring do not escape through a gap between the rings and surface of a plate. On few occasions, lack of sealing at the base of glass rings allowed the cells to escape through underneath of rings. This resulted in few cells residing at a little distance (few mm away) from the circumference of a circular monolayer. As the time progresses the cells at distance try to converge toward the monolayer and vice versa acting as a chemoattractants to each other. This could prove to be a hindrance to measure the migration and might lead to faulty measurements. Unlike Dolle et al. (2005), we avoided placing glass beads on the rings in order to provide the seal as we found it not only cumbersome and failed to prevent the cell leakage, but also resulted in falling off of beads creating more problem (Dolle et al. 2005). We also avoided using sterile silicone high vacuum grease at the base before placing the rings, as it would have possibly hindered capturing of clear images (Ryan 2010). However rare the occurrence might be, the method stands benefitted if the way to seal the gap is found.

3.4 Haematoxylin and eosin (H&E) staining of endothelial cells

3.4.1 Introduction

H&E staining uses two different stains, haematoxylin stains the nucleus and eosin stains the cytoplasm and connective tissue. Haematoxylin stains the chromatin of the nucleus leaving behind a deep purplish-blue colour. Eosin, an orangish-pink to red dye leaves an orange-pink colour after staining the cytoplasmic materials. Both act as counter stain to each other giving the sharp contrast colour.

H&E staining can be achieved by two commonly employed methods known as progressive and regressive staining. In progressive staining the slides are treated with haematoxylin, and then rinsed, followed by treatment with eosin. In the regressive staining procedure the slides are treated with Harris haematoxylin, and then differentiated in acid alcohol which takes out haematoxylin from everything except the nucleus, followed by treatment with eosin. The progressive staining employs Gill's 1, Gill's 2, Gill's 3 and Mayer's haematoxylin. On the other hand, the regressive staining employs a stronger form of haematoxylin called, Harris haematoxylin. Eosin of different strengths can be employed. Eosin Y being the mildest followed by Eosin Y Alcoholic and Eosin Y with Phloxine (Skip Brown 2010).

3.4.2 Materials and Methods

Previously prepared cells were removed from the -20^0C freezer, and allowed to thaw for 90 min to come up to room temperature. The cells were fixed in ice cold 70% ethanol in a fume hood before air drying for 10 minutes. The plates were equilibrated in tris-buffered saline (TBS) (50mM tris, 40mM HCl, 0.9% NaCl, pH7.6) for five minutes before removing the excess liquid. Another wash with TBS was given for five minutes. The cell monolayers were washed twice with absolute alcohol for five minutes followed by 70% alcohol for three minutes and finally with distilled water for two minutes to hydrate the cells. The plates were then treated with Harris haematoxylin for one minute followed by washing with water for two minutes. Haematoxylin was removed from the cytoplasm by washing with 0.5% acid alcohol {50ml of 5% HCl (2.5ml of Conc. HCl + 47.5ml of distilled H_2O) + 950ml of absolute ethanol} for a minute, followed by washing with distilled water for two minutes. The plates were then subjected to the blueing agent (Scott's tap water substitute - $MgSO_4.7H_2O$ - 20g, $NaHCO_3$ - 3.5g dissolved in 1l distilled water) for two minutes followed by washing with water for two minutes. The plates were then run through Eosin Y for 30 seconds followed by washing with water for two minutes. The plates were then taken back through water, 70% alcohol and absolute alcohol before applying the cover slip.

3.4.3 Results and Discussion

H&E staining in the following images (Fig. 3.10) show the cells migrating in a radial direction when seeded into a circular monolayer. The image (a) of Fig. 3.10 shows the cells at the edge of the monolayer emigrating outwardly (blue arrows) and some cells within the monolayer undergoing proliferation (green circles). The proliferating cells appear to be undergoing mitotic division which in few hours would divide into daughter cells. H&E staining revealed the morphology of the HUVECs and HMVECad. The HUVECs resembled cobble stones in appearance, whereas the HMVECad were more spindle shaped.

a)
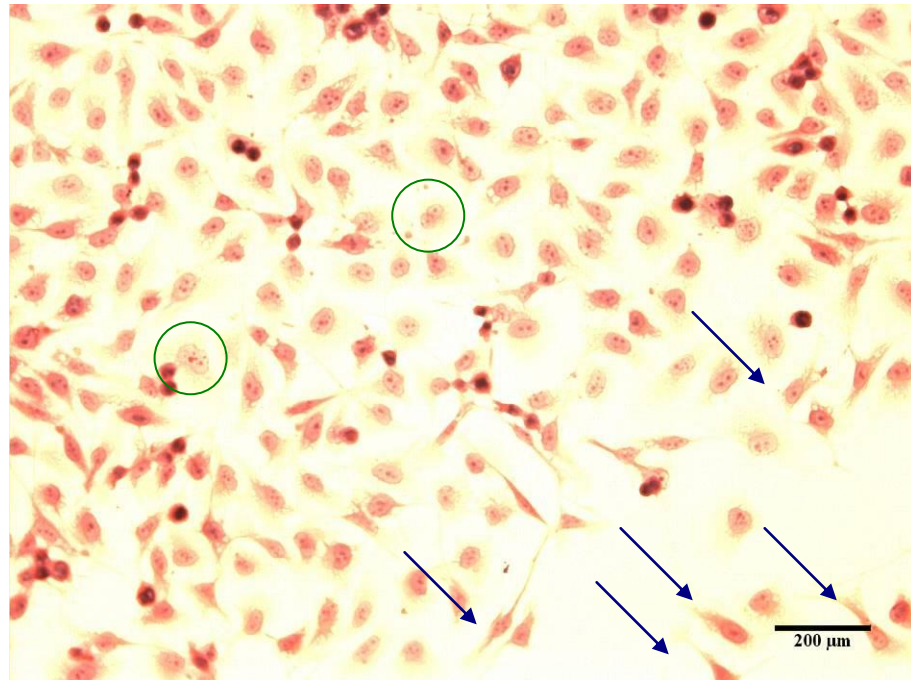
b)
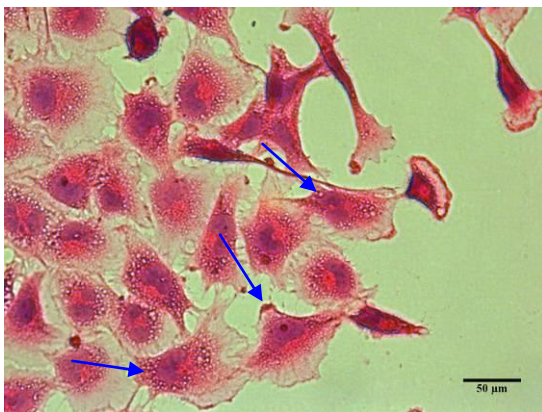
c)
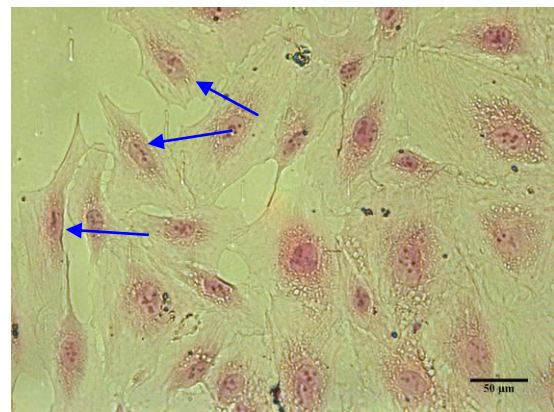
Fig. 3.10 Haematoxylin & Eosin staining The circular monolayers of HUVECs (a & b) and HMVECad (c) were stained with H&E staining. The blue arrows and green circles in photomicrographs indicate the migrating and proliferating cells respectively. The HUVECs are morphologically cobble stone shaped (b), whereas the some of HMVECad are spindle shaped (c). The images are representative of samples from 3 different occasions (n=3). The scale bar of photomicrograph represents 200 (a) and 50µm (b & c) (Magnification: 100x & 400x).

3.5 Expression of PECAM-1 and actin in HMVECad

3.5.1 Introduction

Platelet endothelial cell adhesion molecule-1 (PECAM-1) or CD31, a glycoprotein belonging to IgG super family has a molecular weight of 130kDa and is expressed constitutively by endothelial cells and on the surface of immune cells, platelets, monocytes and neutrophils, some T cells and megakaryocytes (Woodfin, Voisin and Nourshargh 2007). The role of PECAM-1 in leukocyte transmigration during the inflammatory reaction is well documented (Woodfin, Voisin and Nourshargh 2007). Apart from a role in inflammatory reaction, PECAM-1 has been implicated in modulating cell junctions, cell adhesion and cytoskeletal signalling pathways (Ilan and Madri 2003). PECAM-1 induces angiogenesis by enhancing tube formation by increasing the migration of endothelial cells (Cao et al. 2002). PECAM-1 knockout mice showed decreased angiogenesis due to low vascular density and less haemoglobin and laminin resulting in a fewer neutrophils accumulating at the site of foreign body implants (Solowiej et al. 2003). Further, PECAM-1 knockout endothelial cells showed a lack of formation of filopodia, decreased wound healing and cell motility in *in-vitro* models and decreased angiogenesis in PECAM-1 knockout mice (Cao et al. 2009).

There are not many reports indicating the role of PECAM-1 in any of the vascular complications of diabetes. Hyperinsulinaemia has been implicated in exacerbating atherosclerosis through increased expression of PECAM-1 which increases transendothelial migration of leukocytes (Okouchi et al. 2002). The *in vivo* and *in vitro* models of embryonic vasculogenesis in mice and embryo cells of mice suggest that the failure of PECAM-1 tyrosine dephosphorylation leads to the vasculopathy in the presence of hyperglycaemia or diabetes (Pinter et al. 1999). HUVECs when treated with advanced glycated fibronectin in the presence of inflammatory stimulants such as IL-1α, TNF-α, lipopolysaccharide and AGE-albumin increased the expression of PECAM-1 suggesting the involvement of PECAM-1 in the advancement of atherosclerosis in diabetes (Sengoelge et al. 1998). The anti-oxidants and PKC inhibitors blocked the diabetic red blood corpuscles (RBC) induced oxidative stress leading to PECAM-1 phosphorylation and transendothelial migration of monocytes (Rattan et al. 1997). However the contrasting reports suggesting no role for PECAM-1 in the presence of diabetes also exist in equal numbers. It has been reported that the expression of PECAM-1 remained unchanged in the presence of elevated glucose levels in HUVECs (Baumgartner-Parzer et al. 1995a). The possible beneficial use of PPAR-γ agonist in preventing diabetes induced atherosclerosis may be mediated by inhibiting the expression of some of adhesion

molecules but not through PECAM-1, as its expression remained unchanged in HUVECs as well as in myocardial infarction patients (Khare et al. 2005, Pasceri et al. 2000).

Actin rearrangement is central to the cell motility cycle. As hypoxia is central to angiogenesis, there are plenty of reports discussing the role of actin fibres in angiogenesis as discussed in section 1.8 of the chapter 1. However, the direct influence of diabetes or increased level of glucose on the actin filaments during migration of endothelial cells is very rare to find in the literature except for couple of reports. The increased levels of glucose impaired the cytoskeletal rearrangement through the prevention of phosphorylation of vasodilator stimulated phosphoprotein (VASP) which is a actin protein in HMVEC and EPC (Li Calzi et al. 2008). The higher glucose concentration is implicated in reduced migration by impairing the reorganization of actin fibres as a dense peripheral band in HMVEC (Hamuro et al. 2002). The metabolic products of glucose such as glyoxal and methylglyoxal have been reported to cause cytoskeletal rearrangement by increasing the formation of actin stress fibres and finally leading to the inhibition of tube formation in bovine pulmonary endothelial cells (Sliman et al. 2010).

3.4.2 Materials and Methods

HMVECad were stained for the expression of PECAM-1 and actin as a marker and to visualise the cytoskeletal arrangement in migrating cells respectively. The cells were stained for the expression of monoclonal anti-human CD31 (PECAM-1) (Sigma Aldrich, UK) and N-terminal polyclonal anti-actin (Sigma Aldrich, UK) primary antibodies at a dilution of 1:100. The detailed method of identification of proteins is explained in section 2.4.2. Actin stained cells were counterstained with Harris haematoxylin for a minute followed by washing with distilled water for two minutes.

3.4.3 Results and Discussion

PECAM-1 was expressed in HMVECad (Fig. 3.11) in all the four conditions of N5mM, N20mM, H5mM and H20mM at cell junctions as it is an EC-EC adhesion molecule (Woodfin, Voisin and Nourshargh 2007). The intensity of the stain was uniform across the monolayers as shown in photomicrographs (Fig. 3.11). The intensity of the stain corresponding to the confluence of the endothelial cells was observed by Raychaudhury et al. (2001) with help of immunocytochemical staining and northern blotting for mRNA levels of PECAM-1 (RayChaudhury et al. 2001). The same authors also suggest that newly migrating and sparse cells lack the expression of PECAM-1 until they establish contact with other cells (RayChaudhury et al. 2001). This could possibly explain the stain of PECAM-1 antibody being uniform across the confluent monolayer of cells. However the intensity of the stain differed depending on the conditions in which the cells were cultured. Although the expression of PECAM-1 was found predominantly at the cell junctions in

normoxic conditions (Fig. 3.11b), the stain was less intense in N20mM condition (Fig.3.11c) compared to N5mM condition (Fig.3.10b). This result is in contrast to Baumgartner-Parzer et al. (1995) who did not find any change in the expression of PECAM-1 in HUVECs cultured in 30mmol/l glucose levels (Baumgartner-Parzer et al. 1995a). The staining of PECAM-1 was expected to be higher in the presence of hypoxia as it acts as a stimulant for angiogenesis (Cao et al. 2002). On the contrary, the stain was found to be less intense in hypoxic conditions (Fig.3.11d&e) and found predominantly within the cytoplasm of the cells. The role of PECAM-1 in the wound environment of diabetes needs to be probed further as it was reported to be involved in angiogenesis by playing an active role in cell proliferation and migration in PECAM-1 null mice and in HUVEC and H5V endothelial cells (Cao et al. 2009).

The expression of actin was uniform across the different conditions hence only representative images are shown in Fig. 3.12 under lower magnification (Fig. 3.12a) and under higher magnification of intact edge (Fig. 3.12b) and wounded edge (Fig. 3.12c) of HMVECad monolayer. Migrating cells at the leading edge show intense staining for actin (yellow arrows in Fig. 3.12a) due to its accumulation and polymerization followed by protrusion (Vicente-Manzanares, Webb and Horwitz 2005). The localisation of the stain was less clear at the trailing edge and in cells at the centre of the monolayer. In the migrating cells of both the intact and wounded edge of the monolayer, the nucleus stained by haematoxylin can be clearly seen at the rear (yellow circular shapes in Fig. 3.12b&c). The movement of nucleus towards rear and the placement of the microtubule organising centre (MTOC) and Golgi apparatus (which were not visualized in the presented images of figure 3.12) at the front of the leading edge of a cell is indicative of the directionality of cell migration (Etienne-Manneville and Hall 2001). No difference in the expression of actin in cells migrating either at increased glucose levels and/or hypoxic conditions was expected as the cells migrated in all conditions with varying degree and actin is central to the cell motility. However it would be interesting to study the changes or regulation of actin involvement in the different aspects of cell motility due to increased glucose and/or hypoxic conditions.

a)
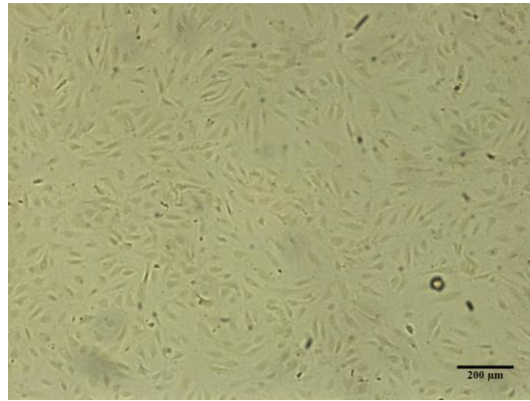
b)
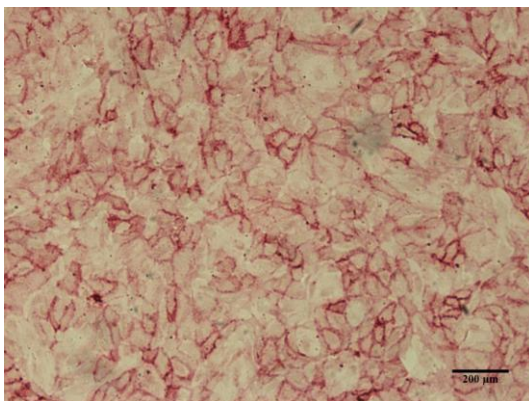
c)
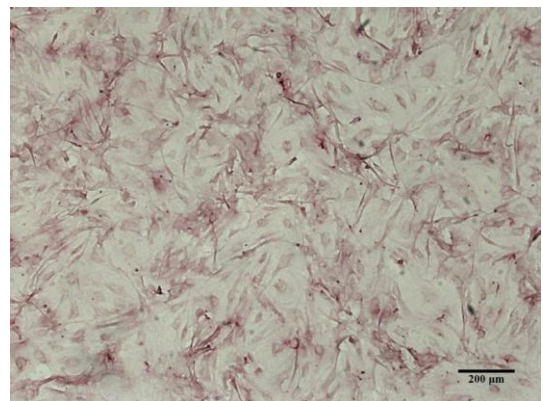
d)
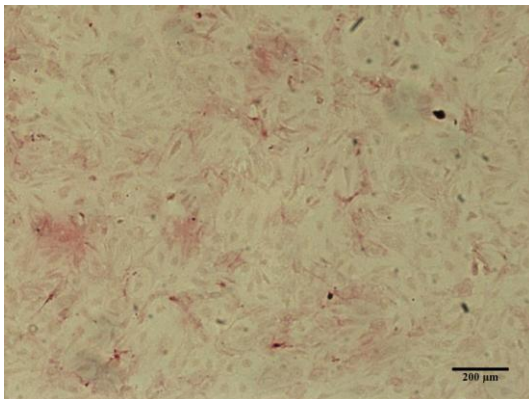
e)
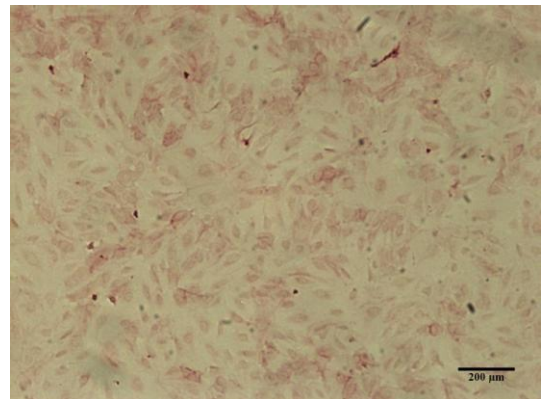
Fig. 3.11 Expression of PECAM-1 in HMVECad The HMVECad grown as circular monolayers were exposed to either 5mM or 20mM glucose and either normoxic (20% O_2) or hypoxic (5% O_2) condition for 48h. The cells in photomicrographs a) were treated with control antibody (IgG1) in order to determine the antibody specificity. The expression of PECAM-1 protein was detected in cells treated with b) N5mM, c) N20mM, d) H5mM and e) H20mM conditions. The images are representative of samples from 3 different occasions (n=3). The scale bar of each photomicrograph represents 200µm (Magnification: 100x).

a)
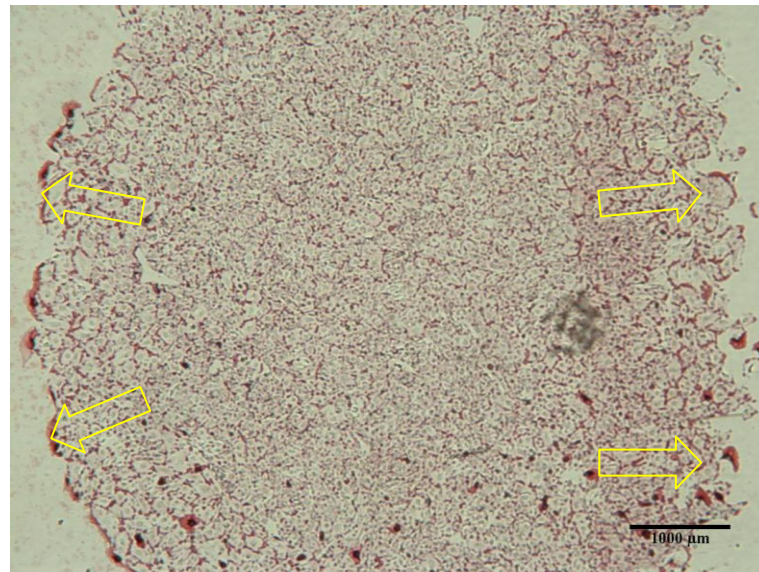
b)
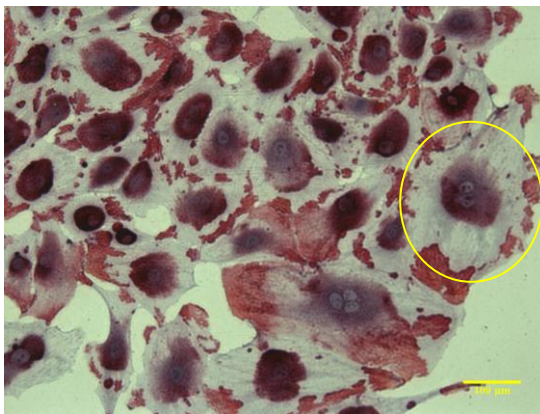
c)
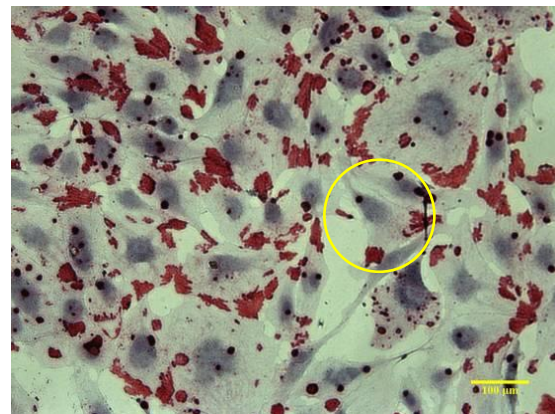
Fig. 3.12 Expression of actin in HMVECad The wounded monolayer of HMVECad exposed to four different conditions for 48 h was stained for actin followed by counterstaining with haematoxylin. No difference in the stain was observed in different conditions. Cells at the edge of the monolayer in photomicrographs a) show the intense expression of actin (yellow arrows) compared to the cells of other region. Cells at the edge (b) or other region (c) of the monolayer show the actin expression concentrated at the leading edge of a cell. The yellow circular shapes show the movement of nucleus towards rear indicating the direction of cell migration. The images are representative of samples from 3 different occasions (n=3). The scale bar of photomicrograph a) and of b) & c) represents 1mm and 100µm respectively [Magnification: a) - 25x; b) & c) – 200x].

Chapter 4 - Effect of hyperglycaemia and hypoxia on the migration of endothelial cells

4.1 Hypothesis

The varying concentration of glucose and oxygen tension has an effect on the migration of endothelial cells.

4.2 Introduction

Hyperglycaemia and hypoxia characterise the wound environment of diabetes. Impaired angiogenesis during diabetes deprives the tissues of essential nutrients and oxygen supply immediately after the injury. Sprouting of new blood vessels at the site of injury requires the proliferation and migration of endothelial cells. The effect of high glucose on the migration of endothelial cells is origin specific. Increase in the retinal endothelial cell proliferation and migration in the presence of elevated glucose level is a causative factor for the development of diabetic retinopathy (Duffy et al. 2006, Huang and Sheibani 2008). On the other hand, *in vitro* migration of human aortic endothelial cells and endothelial progenitor cells was impaired in the presence of elevated levels of glucose (Hamuro et al. 2002, Chen et al. 2007). Myocardial microvascular and aortic endothelial cells isolated from the diabetic rats showed decrease and increase respectively in the migration and proliferation compared to the corresponding cells isolated from age matched normal Wistar rats (Wang et al. 2009).

Hypoxia is a well known stimulant common to angiogenesis during undesirable carcinogenesis or during desirable wound healing (Carmeliet 2005). Endothelial cell migration and proliferation are essential steps of angiogenesis (Carmeliet 2005). Hypoxia induced angiogenesis is mainly mediated by hypoxia inducible factor (HIF) - 1 system by activating the endothelial cell migration through various angiogenic stimuli which include various cytokines (Pugh and Ratcliffe 2003, Yamakawa et al. 2003). Few reports have examined the combined effect of hypoxia and hyperglycaemia on endothelial cell migration. *In vivo* evidences suggest that the presence of diabetes impairs the migration of endothelial cells in diabetic animals (Liu et al. 2008). The fibroblasts isolated from diabetic mice showed less migration in the presence of hypoxia compared to wild type cells on a type I collagen coated surface (Lerman et al. 2003).

Donatis et al. (2010) suggests an interesting hypothesis of either migration or proliferation being exclusive at one given time for a single cell (De Donatis, Ranaldi and Cirri 2010). The same authors suggest that the fibroblasts migrate at a lower concentration of PDGF and make a phenotypic switch from migration to proliferation once the dose of PDGF is sufficient enough for the cells to undergo the cell division (De Donatis et al. 2008). In some other incidences, the endothelial cells were treated with an anti-proliferative agent in order to prevent the influence of proliferation on the migration of endothelial cells (Gade et al. 1997, Hamuro et al. 2002).

In this chapter an attempt is made to assess the migration in the presence of hyperglycaemia and/or hypoxia. An anti-proliferative agent was used to assess the influence of the proliferation on the migration itself. Finally, the migration was carried out in the presence of D-mannitol to address the possibility that osmolarity associated with the elevated glucose concentration was producing the observed effects.

4.3 Materials and methods

The migration assay and wound healing assay were carried out as detailed in section 2.2.3 and 2.2.4 respectively. Endothelial cells were supplemented with either 5 or 20mM D-glucose in 20 (N) or 5% (H) oxygen tension conditions creating four conditions for cell migration viz. N5mM, N20mM, H5mM and H20mM. To overrule the influence of proliferation on migration, an anti-proliferative agent hydroxyurea at 5mM concentration was used as previously described (Hamuro et al. 2002). HMVECad were treated with either 5 or 20mM of D-mannitol which served as an osmotic control. The migration data is presented in microns as mean ± SEM.

4.4 Results

4.4.1 Effect of varying glucose concentration and oxygen tension on the migration of endothelial cells assessed by radial migration assay

HUVECs incubated in an increased concentration of glucose (N20mM) (24 h: 45 ± 2.4; 48 h: 76.6 ± 2.8) resulted in a significant decrease ($p<0.001$) in the migration distance (μm) in comparison with normal glucose concentration (N5mM) (24 h: 73.7 ± 1.9; 48 h: 119 ± 3.2) condition (Fig. 4.1a). The cells in hypoxia with a normal glucose concentration (H5mM) (24 h: 120.1 ± 2.1; 48 h: 192.2 ± 0.8) migrated significantly faster ($p<0.001$) than in N5mM glucose and hypoxia with an elevated glucose concentration (H20mM) (24 h: 70.8 ± 1.8; 48 h: 141.2 ± 1.6).

The migration (μm) of HMVECad (Fig. 4.1b) in N5mM (24 h: 82.6 ± 1.4; 48 h: 133 ± 1.2) was significantly higher ($p<0.001$) compared to N20mM (24 h: 57.2 ± 1.0; 48 h: 105.2 ± 1.1) condition. The cells in H5mM (24 h: 105.8 ± 1.0; 48 h: 172.3 ± 1.1) condition migrated significantly faster ($p<0.001$) than in H20mM (24 h: 80.5 ± 0.9; 48 h: 124.5 ± 1.5) and N5mM conditions. The migration of HUVECs and HMVECad at 48 h was significantly higher ($p<0.001$) than at 24 h for all the test conditions (Fig. 4.1).

Fig. 4.1 Effect of glucose concentration and oxygen tension on endothelial cell migration The migration of HUVEC (a) and HMVECad (b) in conditions of 5 or 20mM glucose and 20 (Normoxia – N) or 5% (Hypoxia – H) oxygen tension was assessed by the radial migration assay. The results are presented as net migration (mean ± SEM) of cells at 24 and 48 h. The results between the conditions were analysed by analysis of variance (ANOVA) followed by Bonferroni post hoc test. Independent t test was employed to compare the results between the 24 and 48 h.

(***p<0.001 when compared as indicated; †††p<0.001 when compared with 24 h of a respective condition)

(HUVECs: n = 180 & 120 at 24 & 48 h respectively for every condition;

HMVECad: n =160 for N5mM; n = 140 for N20mM; n =180 for H5mM & H20mM at both 24 & 48 h)

a)
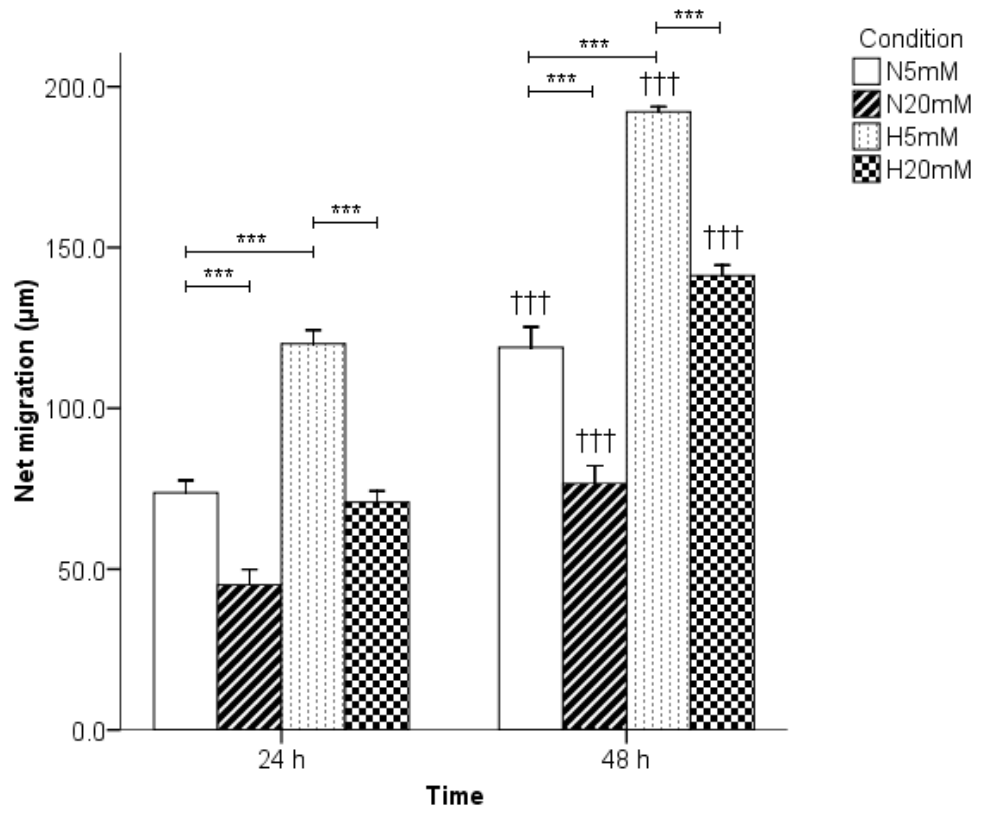
b)
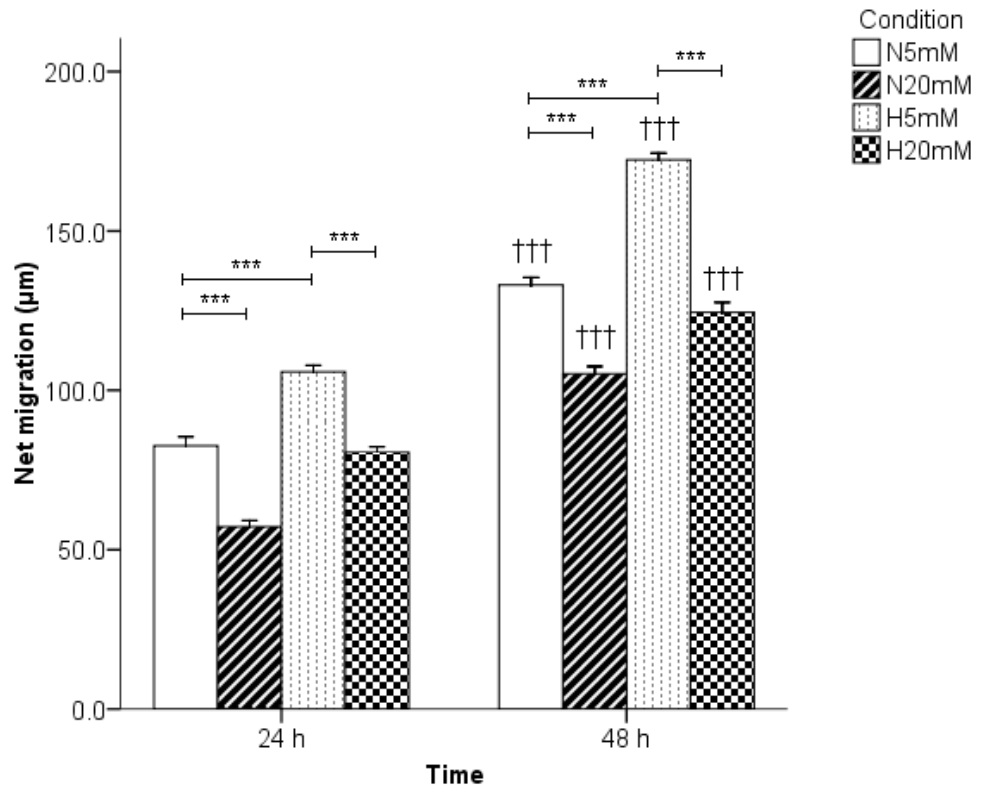
4.4.2 Effect of hydroxyurea on the migration of endothelial cells

To assess the effect of proliferation on migration, the endothelial cells were incubated with an anti-proliferative agent hydroxyurea at 5mM concentration along with varying concentrations of glucose and oxygen tension. Visual inspection indicated that the presence of hydroxyurea created gaps in the monolayers of both HUVEC and HMVECad at 48 h (Fig. 4.2). No major gaps in the monolayers were observed at 24 h. The migration with respect to each other conditions remained unaltered.

Similar to untreated cells, the migration (µm) of HUVECs (Fig. 4.3a) in the presence of hydroxyurea in N5mM (24 h: 80.4 ± 1.7; 48 h: 139.6 ± 1.2) and H5mM (24 h: 113.4 ± 2.8; 48 h: 152.4 ± 2.1) conditions was significantly higher ($p < 0.001$) than in N20mM (24 h: 62.1 ± 1.5; 48 h: 120.3 ± 0.5) and H20mM (24 h: 75.5 ± 2.1; 48 h: 114.3 ± 2.1) conditions respectively. The migration of cells in H5mM condition was significantly higher ($p < 0.001$) than in N5mM condition. The migration of HUVECs (Fig. 4.3a) in the presence of hydroxyurea in H5mM and H20mM conditions was not significantly different than in the absence of it at 24 h (Fig. 4.1a). However, the migration in N5mM ($p < 0.01$) and N20mM ($p < 0.001$) at 24 h and in all conditions ($p < 0.001$) at 48 h was significantly different between the presence (Fig. 4.3a) and absence (Fig. 4.1a) of hydroxyurea.

The migration (µm) of HMVECad in the presence hydroxyurea (5mM) (Fig. 4.3b) was similar to the migration of cells in its absence. The migration in N5mM (24 h: 76.0 ± 1.3; 48 h: 113.1 ± 1.2) and H5mM (24 h: 99.7 ± 1.8; 48 h: 149.4 ± 2.2) conditions was significantly higher ($p < 0.001$) than in N20mM (24 h: 61.0 ± 1.2; 48 h: 96.7 ± 1.4) and H20mM (24 h: 70.1 ± 0.8; 48 h: 110.0 ± 0.9) conditions respectively. The migration of cells in H5mM condition was significantly higher ($p < 0.001$) than in N5mM condition. The migration of HMVECad in N5mM ($p < 0.01$), N20mM ($p < 0.05$), H5mM ($p < 0.01$) and H20mM ($p < 0.001$) conditions at 24 h and in all above mentioned conditions ($p < 0.001$) at 48 h was significantly less in the presence of hydroxyurea (Fig. 4.3b) compared to those migrating in absence (Fig. 4.1b) of it.

a)
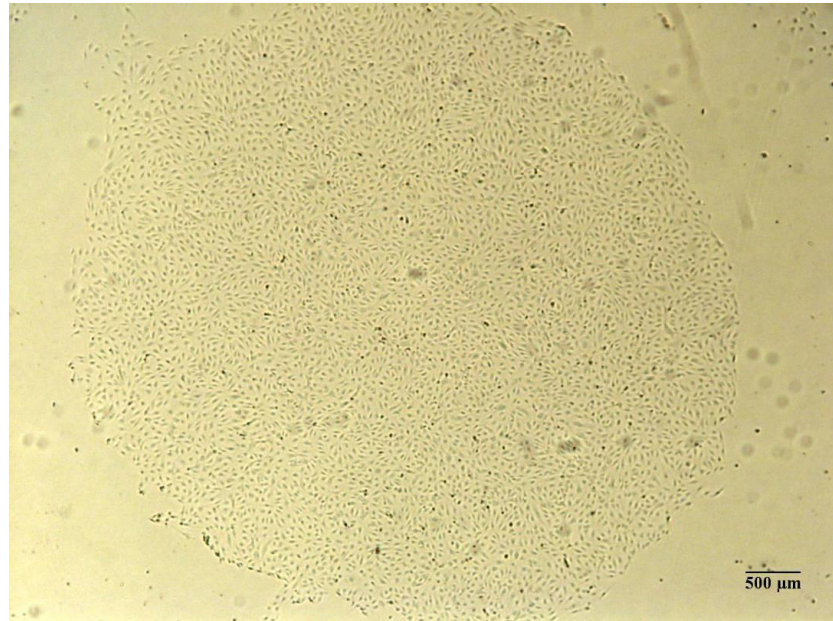
b)
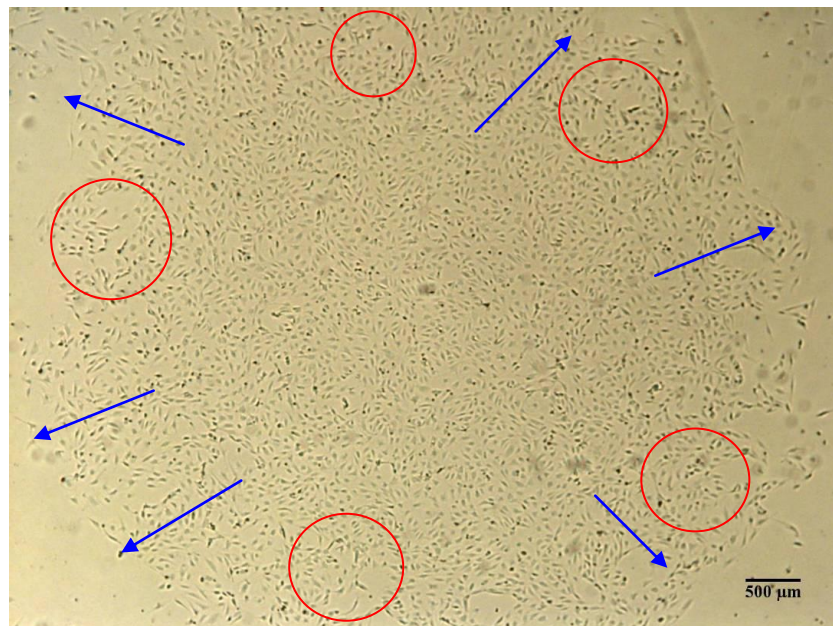
Fig. 4.2 Effect of hydroxyurea on the endothelial cell monolayer HMVECad were incubated in either 5mM or 20mM D-glucose and 20 or 5% oxygen tension in the presence of 5mM hydroxyurea. The images of the monolayer were captured at 0 h (a). After 48 h (b) of incubation, the hydroxyurea showed its effect by inhibiting the cell proliferation and thus creating the gaps in the monolayer. The gaps are marked by red circles and migrating cells are shown by blue arrow marks at the edge of the monolayer. Similar observation was also made from the monolayers of HUVECs. The images are representative of samples from 3 different occasions (n=3). The scale bar on each photomicrograph represents 500μm (Magnification: 25x).

Fig. 4.3 Effect of hydroxyurea on the migration of endothelial cells The migration of HUVECs (a) and HMVECad (b) in conditions of 5 or 20mM glucose and 20 (Normoxia – N) or 5% (Hypoxia – H) oxygen tension was assessed by the radial migration assay. The anti-proliferative agent hydroxyurea (5mM) was added to assess the relationship between proliferation and migration. The results are presented as net migration (mean ± SEM) of cells at 24 and 48 h. The results between the conditions were analysed by analysis of variance (ANOVA) followed by Bonferroni post hoc test. The independent t test was employed to compare the results between 24 and 48 h.

(***p<0.001 when compared as indicated; †††p<0.001 when compared with 24 h of respective condition)

(HUVECs: n = 180 & 120 at 24 & 48 h respectively for each condition;

HMVECad: n = 180 for each condition except for N20mM, where n=160 at 24 & 48 h)

a)
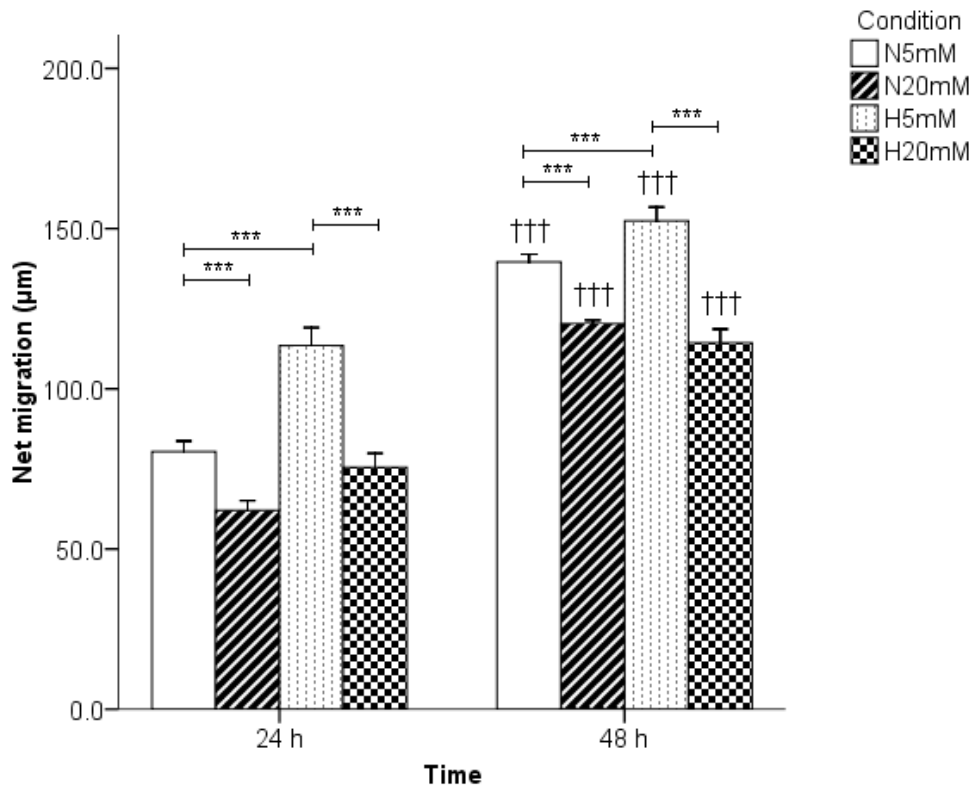
b)
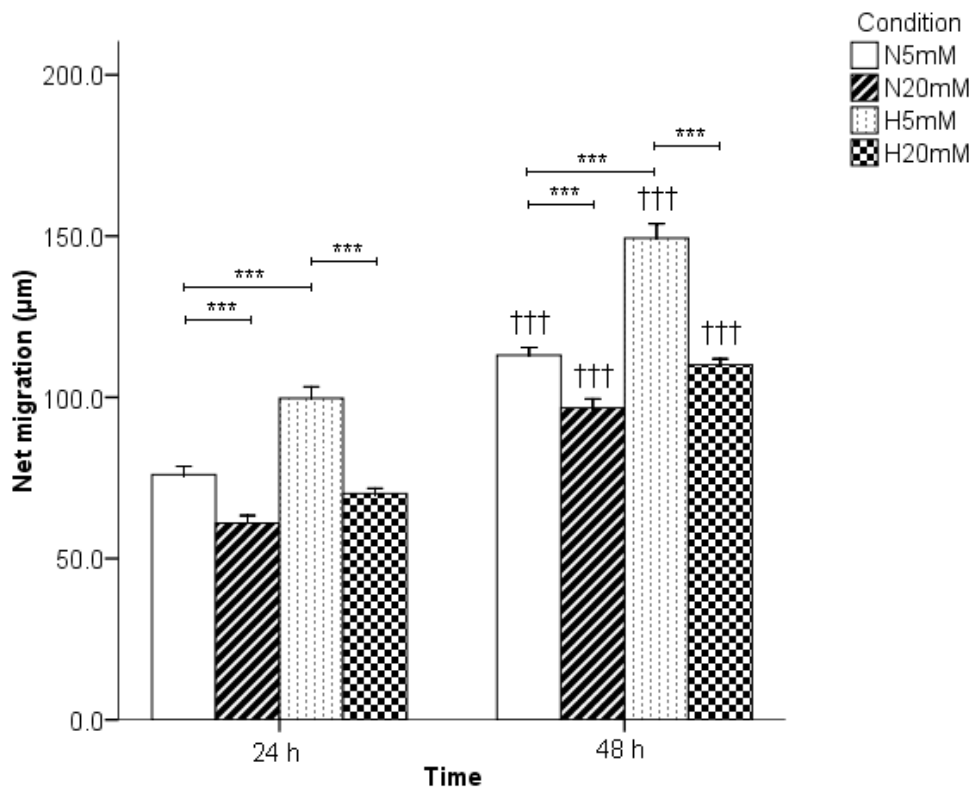
4.4.3 Effect of varying glucose concentration and oxygen tension on the migration of HMVECad assessed by wound healing assay

The migration experiments hereafter were studied using HMVECad only as the migration trend of HUVECs towards four different conditions was not different from that of HMVECad. The migration (μm) of HMVECad (Fig. 4.4) from the intact edge in N5mM (24 h: 80.2 ± 1.4; 48 h: 153.7 ± 3.1) was significantly higher ($p<0.001$) than in N20mM (24 h: 61.6 ± 1.3; 48 h: 129.9 ± 2.4) condition. The migration was significantly less ($p<0.001$) in H20mM (24 h: 81.8 ± 1.2; 48 h: 163.6 ± 2.1) compared to H5mM (24 h: 92.9 ± 1.9; 48 h: 183 ± 2.8) condition. The migration was significantly higher ($p<0.001$) in H5mM condition compared to N5mM condition.

Similar to the intact edge, the migration (μm) of HMVECad from the wounded edge was significantly higher ($p<0.001$) in N5mM (24 h: 87.8 ± 1.8; 48 h: 170.5 ± 2.8) and H5mM (24 h: 105.1 ± 1.4; 48 h: 208.8 ± 2.8) conditions compared to N20mM (24 h: 70.4 ± 1.7; 48 h: 143.4 ± 2.7) and H20mM (24 h: 87.4 ± 1.2; 48 h: 179.8 ± 2.3) conditions respectively. The migration in H5mM condition was significantly higher ($p<0.001$) compared to N5mM condition. The migration (μm) of cells from the wounded edge of the monolayer was significantly higher ($p<0.001$; except for N5mM and H20mM at 24 h where $p<0.01$) in all conditions compared to the migration from the intact edge of the monolayer.

Fig. 4.4 Effect of glucose concentration and oxygen tension on the migration of HMVECad The migration of HMVECad in conditions of 5 or 20mM glucose and 20 (Normoxia – N) or 5% (Hypoxia – H) oxygen tension was assessed by the wound healing assay. The results are presented as net migration (mean ± SEM) of cells at 24 (a) and 48 h (b). The results between the conditions were analysed by analysis of variance (ANOVA) followed by Bonferroni post hoc test. The independent t test was employed to compare the results between the intact and wounded edge of the monolayer.

(***p<0.001 when compared as indicated; ††p<0.01 and †††p<0.001 when compared with respective condition of intact edge cells)

(Intact edge: n = 90 for each condition at 24 & 48 h, except for H5mM where n=80 at 24 h; Wounded edge: n = 90 for each condition at 24 & 48 h)

a)
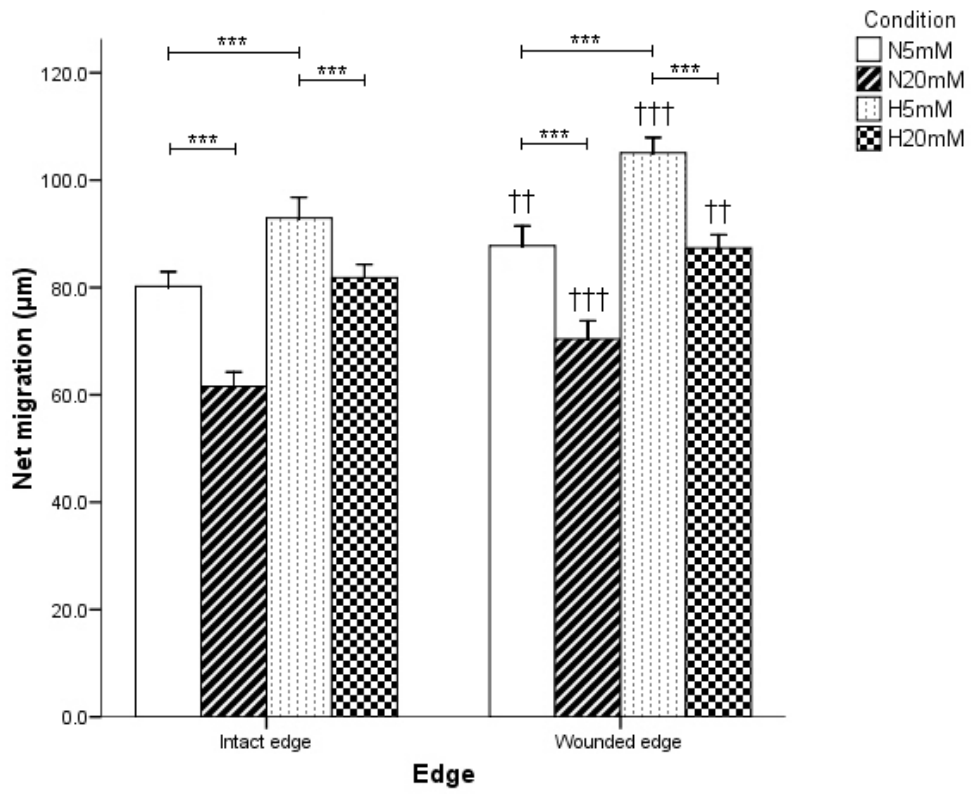
b)
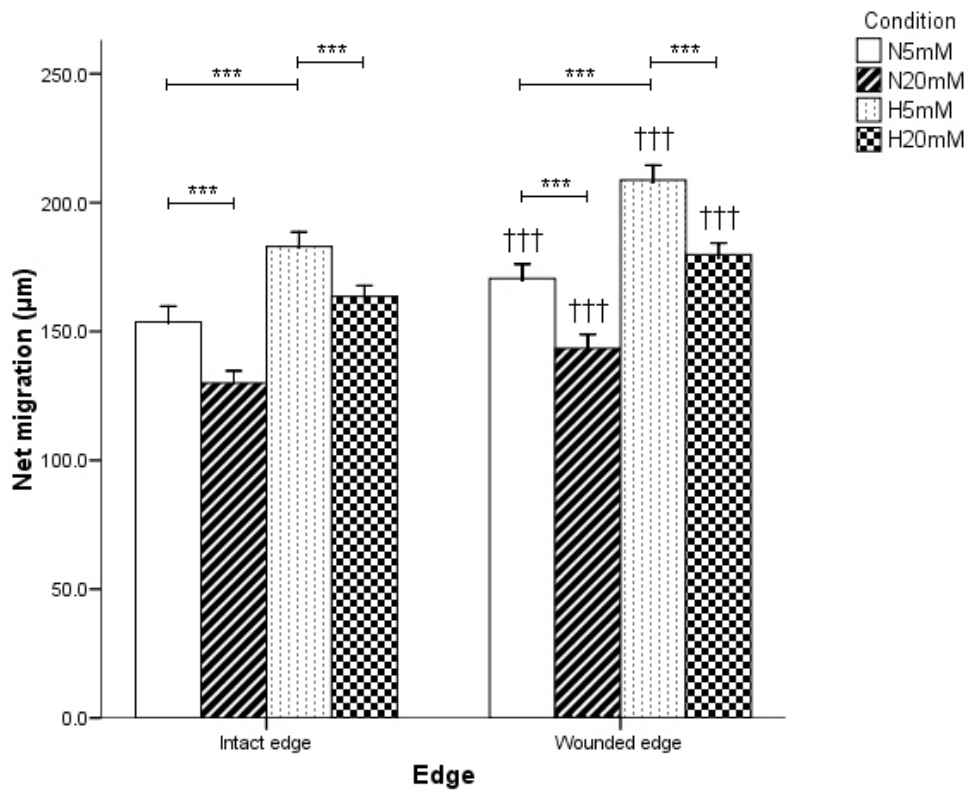
4.4.4 Effect of varying D-mannitol concentration and oxygen tension on the migration of HMVECad assessed by wound healing assay

D-mannitol (5 or 20mM) was used in order to overrule the role of osmotic pressure producing any effect on the migration. All the four conditions viz. N5mM, N20mM, H5mM and H20mM D-mannitol were incubated in medium containing 5.6mM D-glucose as this was already supplemented in the M131 medium. The migration (µm) of HMVECad (Fig. 4.5) from the intact edge in N5mM (24 h: 91.2 ± 1.8; 48 h: 146.1 ± 2.1) was not significantly different than in N20mM (24 h: 92.4 ± 1.8; 48 h: 152.8 ± 2.3) condition. The migration was not significantly different in H20mM (24 h: 106.7 ± 1.1; 48 h: 165.8 ± 1.7) condition compared to H5mM (24 h: 108.3 ± 1.7; 48 h: 169.7 ± 2.0) condition. However, the migration was significantly higher ($p<0.001$) in H5mM condition compared to N5mM condition.

Similar to the intact edge, the migration (µm) of cells from wounded edge (Fig. 4.5) was not significantly higher in N5mM (24 h: 110.1 ± 2.2; 48 h: 174.2 ± 3.1) and H5mM (24 h: 129.7 ± 1.8; 48 h: 203.8 ± 2.6) condition compared to N20mM (24 h: 113.3 ± 2.5; 48 h: 180.4 ± 3.1) and H20mM (24 h: 132.6 ± 1.6; 48 h: 206.4 ± 2.8) conditions respectively. The migration in H5mM condition was significantly higher ($p<0.001$) compared to N5mM condition. The cells migrated significantly faster ($p<0.001$) in all conditions from the wounded edge than those from the intact edge of the monolayer.

Fig. 4.5 Effect of D-Mannitol on the migration of HMVECad The migration of HMVECad in conditions of 5 or 20mM D-Mannitol and 20 (Normoxia – N) or 5% (Hypoxia – H) oxygen tension was assessed by the wound healing assay. The results are presented as net migration (mean ± SEM) of cells at 24 (a) and 48 h (b). The results between the conditions were analysed by analysis of variance (ANOVA) followed by Bonferroni post hoc test. The independent *t* test was employed to compare the results between the intact and wounded edge of the monolayer.

(***p<0.001 when compared as indicated; †††p<0.001 when compared with respective condition of intact edge cells and NS = not significant)

(Intact and wounded edge: n = 80, except at N20mM where n=90 at 24 & 48 h)

a)
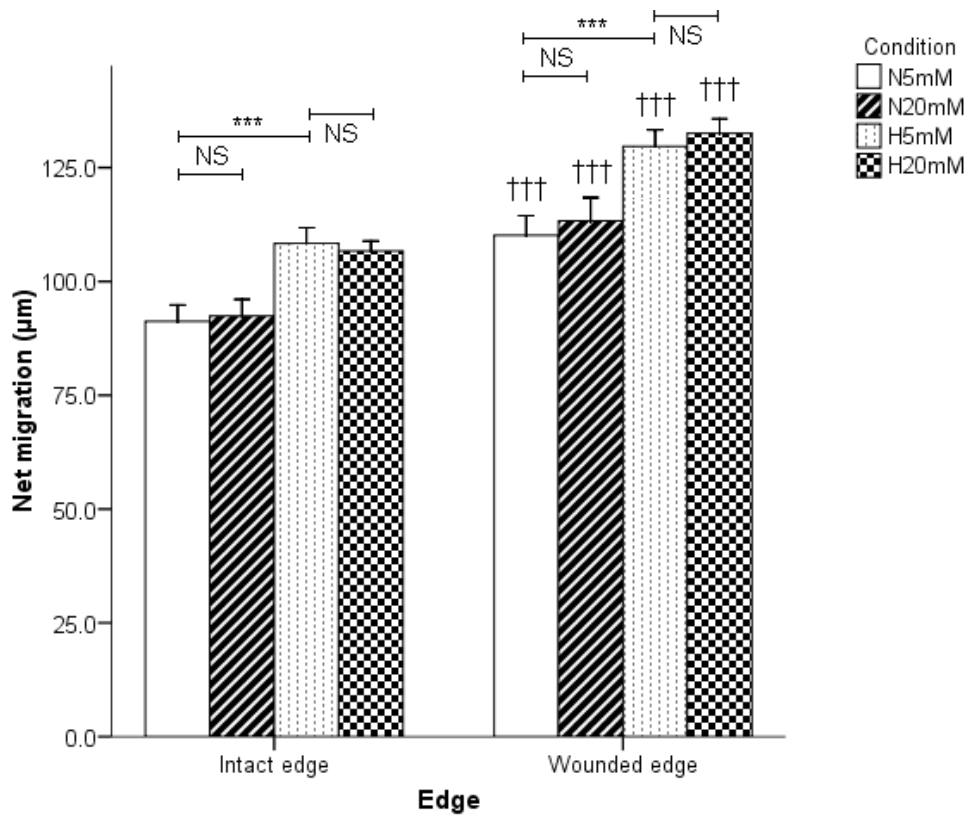
b)
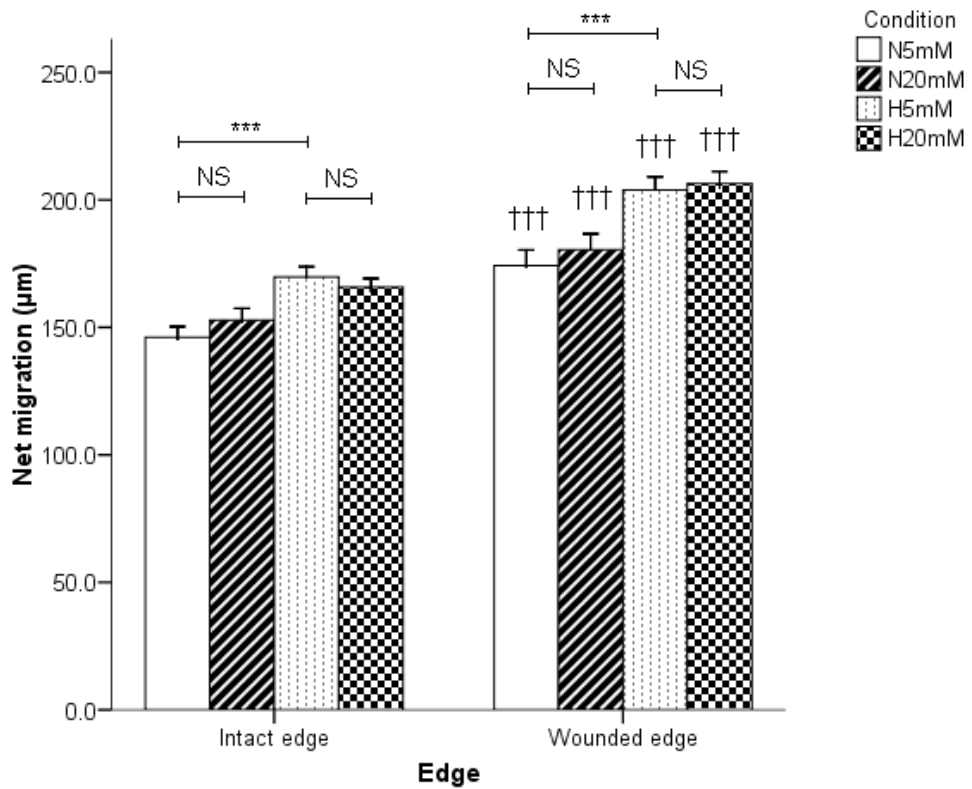
4.5 Discussion

The results indicate that the hyperglycaemia and hypoxia have opposing effects of decrease and increase respectively in the migration of endothelial cells. The migration was less when hyperglycaemia was combined with hypoxia compared to the hypoxia alone. HMVECad migrated faster from the wounded side than from the intact side of the monolayer. Osmotic control D-mannitol did not alter the emigrational trends of cells. The presence of an anti-proliferative agent reduced the migration at 48 h compared with the respective control.

The decrease in the migration of both HUVECs and HMVECad due to elevated levels of glucose is consistent with earlier findings where hyperglycaemia has been reported to cause dose dependant decrease in the migration of endothelial cells (Gade et al. 1997, Hamuro et al. 2002, Mascardo 1988, Yu et al. 2006). Results also confirmed that the reduction in the migration was not a result of osmotic pressure (Fig. 4.5) as increased D-mannitol did not alter the migration distance compared to lower concentration of D-mannitol. Hyperglycaemia has been reported to cause the reduction in the migration of microvascular endothelial cells by dephosphorylation of vasodilator stimulated phosphoprotein (VASP) resulting in its decrease in the redistribution at the leading edge (Li Calzi et al. 2008). Carbon monoxide and NO lost their ability to induce phosphorylation of VASP at Ser-157 and Ser-239 respectively in the presence of elevated levels of glucose (Li Calzi et al. 2008). The role of NO has been implicated by other studies as well. The reduced migration of endothelial cells in elevated levels of glucose is attributed to NO mediated impairment in actin polymerization (Gade et al. 1997) and further eNOS expression and intracellular production of NO was shown to be mediated by NF-κβ (Hamuro et al. 2002, Murohara et al. 1999). Yu et.al. (2006) suggest that the reduction in the proliferation and migration of HUVECs in the presence of higher glucose concentration was a result of PI3K and Akt inhibition (Yu et al. 2006). Increased glucose is known to produce its deleterious effects by increasing the production of reactive oxygen species (Brownlee 2005). Hence, hyperglycaemia induced reduction in the migration of endothelial cells was overcome by the complementing the media with an anti-oxidant, thiamine (Ascher et al. 2001).

HUVECs and HMVECad were used as a model of macro and microvascular cells to measure the migration. The migration response towards increased concentrations of glucose has been reported to be cell specific (Wang et al. 2009, Duffy et al. 2006). Contrary to these reports, HUVECs and HMVECad responded similarly to the elevated levels of glucose by decreasing the migration (Fig.4.1). These contradictory results could possibly be due to the difference in the experimental models, cell type used and/or origin of cells. Wang et al. (2009) used the scratch wound assay and transwell inserts to

measure the migration of myocardial microvascular and aortic endothelial cells isolated from diabetic rats (Wang et al. 2009). Doffy et al. (2006) did not measure migration but found that the cell viability and apoptosis to be different in response to elevated glucose levels in human aortic and retinal endothelial cells.

In various cell culture systems the hypoxia starts from 5% to downward reaching anoxia at 0.1 to 0.2% (1% = 8mm Hg) (Pouyssegur, Dayan and Mazure 2006). Hypoxia inducible factor (HIF) system activates pleiotropic actions by inducing various genes controlling cell migration, angiogenesis, erythropoiesis, energy metabolism and others as a part of cellular adaptation in response to the oxygen deprivation (Wang and Semenza 1995, Semenza 2004). Results clearly indicated that the hypoxia increased the migration of both HUVEC and HMVECad over the period of 48 h (Fig. 4.1). ECs adapt to the decreasing oxygen tension and accordingly increase the accumulation of HIF-1α and its target genes such as VEGF, angiopoietins and GLUT-1 (Abaci et al. 2010). Hypoxia induced HIF-1α dependant bFGF and VEGF autocrine activity could be responsible for the *in vitro* migration of endothelial cells as they have been implicated in vessel formation (Calvani et al. 2006, Takata et al. 2008). The effect of hypoxia through HIF-1α activation is well documented as HIF-1α gene therapy has proved to be beneficial in healing the wounds of diabetic mice (Liu et al. 2008, Mace et al. 2007).

The migration of HUVECs and HMVECad was reduced when hyperglycaemia was combined with hypoxia in comparison with hypoxia alone (Fig. 4.1). These results are consistent with clinical manifestations of the people with diabetes suffering from chronic wounds as they experience delayed wound healing due to impaired angiogenesis. Hyperglycaemia induced formation of free radicals impaired the formation of ischemia driven vessel formation in diabetic mice. Further, hyperglycaemia prevented the dimerization of HIF-1α with HIF-1β and thus reduced the HIF-1 dependant transcription of VEGF and stormal cell derived factor-1 (SDF-1) in hypoxic mouse fibroblasts (Ceradini et al. 2008). In another study in diabetic fibroblasts, hyperglycaemia interfered with the transactivational activity of HIF-1 by impairing the interaction of HIF-1α with the coactivator p300 (Thangarajah et al. 2009). Hyperglycaemia has been reported to decrease the hypoxia induced expression of HIF-1α and its target gene VEGF, VEGFR, HSP-90, SDF-1 and stormal cell factor (SCF) by destabilisation of transctivational domains of HIF-1α (Botusan et al. 2008, Catrina et al. 2004).

Hydroxyurea, an anti-proliferative agent was used to understand the influence of proliferation on the migration as both processes are essential for angiogenesis. The dose of hydroxyurea at 5mM has been found to be anti-proliferative but not cytotoxic by previous users (Hamuro et al. 2002). The results (Fig. 4.3) indicated that hydroxyurea reduced the migration only after 48 h of its introduction and did not completely prevent the

migration. These are consistent with previous reports where it was found that the cessation of proliferation did not adversely affect the migration of endothelial cells (Gade et al. 1997, Hamuro et al. 2002). Although there is scant evidence differentiating the proliferation from migration and vice versa with respect to angiogenesis, it has been known for some time now that migration precedes the proliferation of endothelial cells in *in vitro* wound healing models (Coomber and Gotlieb 1990). It has been suggested that the migration was initiated due to VEGFR2 present on long filopodia of migrating retinal endothelial cells at the edge (tip cells) of a monolayer which sense the angiogenic stimulant (Gerhardt et al. 2003). Further unlike stalk cells, tip cells failed to stain for either phospho-histone or Ki-67 (markers for mitosis) indicating that tip cells were not proliferating whereas stalk cells were (Gerhardt et al. 2003). It was also suggested that the place vacated within a monolayer by a migrating tip cell is filled with proliferation of stalk cells to maintain cell-cell contact (Farooqui and Fenteany 2005). This could be the reason we witnessed the gap in the monolayer in stalk cells region than in the region of tip cells due to inhibition of proliferation of stalk cells by hydroxyurea (Fig. 4.2). Further, cells in the presence of the right quantity of soluble cues are known to make a phenotypic switch from migration to proliferation (De Donatis et al. 2008). This could be the possible reason in spite of using an anti-proliferative agent the migration persisted; however, was not equivalent to the cells which did not receive hydroxyurea (Fig. 4.1 vs. 4.3) as stalk cells might have failed to proliferate to fill the gap in the monolayer and keep up the pace of migration.

The wound healing assay (Fig.4.4) was carried out in order to bring the migration of cells from the wounded and intact edge in a single model to test the effect of wounding on the intact edge. The wound healing assay made use of only HMVECad and not the HUVECs as both exhibited similar migration trends under different conditions and treatments. The results (Fig. 4.4) clearly showed that cells from the wounded side migrate faster than those from intact edge. Although there is no direct explanation available in the literature to be compared, the faster re-endothelialization could be due to faster rearrangement of cytoskeleton at the wound edge (Lee and Gotlieb 2003). Similar to epithelial cells, the migration of endothelial cells as a sheet at the wounded edge may be helped by the formation of lamellopodia and active crawling of the cells behind the edge (Farooqui and Fenteany 2005). This could be further assisted by release of the mitogenic/angiogenic substances from the wounded cells acting as chemotactants and/or the denuded region acting as a coated surface inducing haptotaxis.

4.6 Conclusion

It is clearly evident from the results that the basal migration was altered in the presence of high glucose and/or low oxygen tension. Although proliferation has not been shown to adversely affect the migration, the role of cell cycle regulator such as cyclin dependant kinase inhibitor p27^{Kip1} in the migration is explored in the next chapter. The role of transcription factor HIF-1α in carrying out the effect of hypoxia and hyperglycaemia along with any signalling pathways such as MAPK p42/44, PI3K and PKC$_{βII}$ are explored in next chapter.

Chapter 5 - Molecular mechanisms of endothelial cell migration

5.1 Hypothesis

The expression of transcription factor HIF-1 and cyclin dependant kinase inhibitor p27^{Kip1} have a role to play in the migration of HMVECad. The effect of hypoxia and hyperglycaemia are mediated by HIF-1α and through various signalling molecules such as protein kinase C (PKC), mitogen activated protein kinase (MAPK) and/or phosphotidylinositol 3-kinase (PI3K) during the migration of microvascular endothelial cells.

5.2 Introduction

Cell division and migration, essential steps of angiogenesis during the wound healing process, are known to be regulated by around 1249 and 360 genes respectively (Neumann et al. 2010). Cyclin dependant kinase inhibitor (CKI) - p27^{Kip1} acts as a check point or negative regulator preventing cell cycle progression from G_1 to S phase (Toyoshima and Hunter 1994). Although a great amount of evidence has been recorded regarding the role of p27^{Kip1} with respect to cancer development, there is little indicating the role of p27^{Kip1} in the development of diabetic complications. The granulation tissue consisting mainly of fibroblasts showed considerable decrease in proliferation due to up regulation of p27^{Kip1} delaying the wound healing in diabetic mice (Altavilla et al. 2010). Similarly, proliferation of retinal neuronal cells of hypertensive rats with diabetes decreased due to increased expression of p27^{Kip1} (Lopes de Faria et al. 2008). In another study, TGF-β induced a decrease in HUVEC number and impaired cell cycle progression in hyperglycaemia was attributed to the over expression of p27^{Kip1} (McGinn et al. 2003a). Most of the work involving p27^{Kip1} and diabetes has focussed on diabetic nephropathy. The p27^{Kip1} protein expression increased consistently in podocytes and mesangial cells and occasionally in glomerular endothelial cells of diabetic mice and in the mesangial cells of normal mice in the presence of hyperglycaemia causing cell cycle arrest and hypertrophy (Wolf et al. 1998). Further, it was suggested that the hyperglycaemia in mesangial cells increased the expression of p27^{Kip1} by activating ERK1/2 which directly phosphorylates p27^{Kip1} at Ser^{178} (Wolf et al. 2003).

Increasingly the evidence for the role of cytoplasmic p27^{Kip1} in regulating cell migration particularly in the backdrop of metastasis of cancerous cells is emerging (McAllister et al. 2003). Cell cycle independent migratory stimulant role of p27^{Kip1} was illustrated when p27^{Kip1} was knocked out in mouse embryonic fibroblasts led to the reduced migration due to increased RhoA activation with subsequent increase in the focal adhesions and stress fibres (Besson et al. 2004). Over expression of p90 ribosomal S6 kinase 1 (RSK1), a serine/threonine kinase activated downstream of MAPK and PI3K, increased cytoplasmic localisation of p27^{Kip1} which in turn increased the migration by

inhibition of RhoA activation (Larrea et al. 2009). In contrast, other reports suggest that p27^{Kip1} mediates decrease in the cell motility. Elevated glucose level has been implicated in the increased migration and proliferation of aortic smooth muscle cells mediated by decreased expression of p27^{Kip1} and increased production of ROS (Yoon et al. 2010). Vascular smooth muscle cells cultured in high glucose have shown an increase in the proliferation and migration and this was inhibited by the use of simavistatin, a lipid lowering drug by increased expression of p27^{Kip1} (Chan et al. 2010). The migration of HUVECs, tube formation by HUVECs and by coronary artery endothelial cells (HCAECs) and blood flow recovery and vessel density in mice were inhibited due to the over expression of p27^{Kip1} establishing its role not only on the cell cycle progression but also during *in vitro* as well as *in vivo* migration (Goukassian et al. 2001, Moss et al. 2010). Further, over expression of p27^{Kip1} resulted in the disruption of lamellopodia formation, actin re-organization and focal adhesions in vascular smooth muscle cells and fibroblasts leading to the decrease in the migration (Diez-Juan and Andres 2003).

Transcription factor HIF-1 mediates many biological activities including cell proliferation, migration/angiogenesis or invasion and metastasis through a cocktail of cytokines and growth factors (Semenza 2007). Deletion of HIF-1α resulted in reduced proliferation and migration of endothelial cells and HIF-1α null mice exhibited delayed wound healing due to impairment in the angiogenesis owing to decreased expression of VEGF (Tang et al. 2004). On one hand if hypoxia is known to stabilize HIF-1α, on other hand hyperglycaemia is known to destabilize or inactivate the HIF-1α in diabetic wound environment (Botusan et al. 2008, Thangarajah et al. 2010). Hyperglycaemia has been reported to interfere with the stability of HIF-1α in multiple ways. In a recent work, Thangarajah et al. (2010) suggest that hyperglycaemia produces reactive oxygen species which subsequently impair the binding of HIF-1 complex with co-activator p300 by methylglyoxal, a glycolytic end product thus preventing the transcription of downstream target genes leading to impaired wound healing in diabetic mice (Thangarajah et al. 2009, Thangarajah et al. 2010). Hyperglycaemia has also been shown to cause the destabilisation of HIF-1α stability by proteasomal degradation (Catrina et al. 2004). In another study by Botusan et al. (2008), hyperglycaemia has been shown to interfere with a) the stability of HIF-1α by causing VHL dependant degradation and b) translational activity by modifying the caroboxy terminal transactivation domain of HIF-1 (Botusan et al. 2008). Decrease in the hypoxia responsive element (HRE) promoter transactivation too has also been held responsible for producing the deleterious effects of glucose on HIF-1α expression (Gao et al. 2007). The effects of hyperglycaemia and hypoxia may also be mediated through various signalling pathways including PKC$_{βII}$, p42/p44 MAPK and PI3K-Akt.

5.2.1 Protein Kinase C (PKC) pathway

Diacylglycerol (DAG)/Protein kinase C (PKC) activation is implicated in mediating the vascular complications of diabetes (Das Evcimen and King 2007). Ruboxistaurin (LY333531), a PKC β antagonist inhibited AGE induced expression of TGF-β1 and ICAM-1 reducing macrophage adhesion to HUVECs via anti-oxidant property by increasing superoxide dismutase/malondialdehyde (SOD/MDA) level (Xu et al. 2010a). The same antagonist inhibited the VEGF induced proliferation, migration and tube formation by HUVECs and inhibition of VSMC too with partial inhibition of p42/p44 MAPK and Akt (Andrassy et al. 2005, Nakamura et al. 2010). Decrease in the glomerular endothelial cell numbers and VEGF over expression was over come by PKC β inhibitor in diabetic Ren-2 rats proving its role in the prevention of nephropathic complication of diabetes as well (Kelly et al. 2007). Diabetes induced a decrease in sciatic motor and saphaneous nerve sensory conduction velocity with blood flow along with thermal hyperalgesia was overcome by the use of ruboxistaurin in streptozotocin induced diabetic rats (Cotter, Jack and Cameron 2002). Protein kinase C β has also been reported to be involved with wound healing by modulating the F-actin activity in HUVECs (Jensen and Larsson 2004). All the above mentioned evidence suggests that over activation of PKC β actively precipitates the vascular complication of diabetes. ROS mediated over expression of HIF-1α mRNA in cancerous cells is known to subsequently activate PI3K-Akt and PKC signalling pathways (Koshikawa et al. 2009). Hypoxia independent activation of HIF-1α by angiotensin II was dependent on the production of ROS and activation of PKC in VSMC (Page et al. 2002). However the role of PKC β in either mediating the effects of hypoxia or HIF-1α on wound healing or cell proliferation and migration is not completely elucidated.

5.2.2 p42/p44 mitogen activated protein kinase (MAPK)

p42/p44, also known as extracellular regulated kinase (ERK) 1/2 MAPK is one of the evolutionarily conservative four MAPK cascades along with c-Jun N-terminal kinase 1-3 (JNK1-3), p38MAPK α, β, γ, δ and ERK5 (Keshet and Seger 2010). Various mitogens such as growth factors activate the ERK cascade by an upstream kinase called MAPK/ERK kinase (MEK) in an order to initiate vital cell functions such as proliferation and differentiation (Keshet and Seger 2010). The evidence involving the role of MAPK in precipitating the complications of diabetes is accumulating. Advanced glycation end products (AGE) induce apoptosis in endothelial progenitor cells which was reversed by the use of MPAK inhibitors confirms the MAPK pathways involvement in deleterious effects of high glucose (Shen et al. 2010). The expression of phosphorylated ERK1/2 was found in the subcutaneous microvascular endothelial cells isolated from human tissue of T2DM patients (Gogg, Smith and Jansson 2009). The migration of human coronary artery

endothelial cells due to VEGF by inducing the formation of stress fibres and adhesion molecules was mediated by the activation of ERK 1/2 MAPK and Akt (Mahadev et al. 2008). Glycated bFGF resulted in the reduced capillary formation by bovine aortic endothelial cells with a reduction in the activation of ERK 1/2, which suggests that high glucose produces its deleterious effect on angiogenesis and hence wound healing via deactivation of ERK 1/2 MAPK (Duraisamy et al. 2001). PD98059, a p42/p44 MAPK inhibitor blocked the high glucose induced stimulation of L-arginine transport, membrane hyperpolarisation and eNOS phosphorylation resulting in NO production in HUVECs which could lead to the vasodilation during gestational diabetes (Flores et al. 2003). Topical administration of rhPDGF on skin wounds of diabetic rats improved the wound healing with increased phosphorylation of ERK 1/2 at the wound site (Cheng et al. 2007).

ERK1/2 MAPK has also been implicated in mediating HIF-1α induced activities. Hypoxia induced the migration and proliferation in VSMC through the activation of HIF-1α, ROS and ERK (Fu et al. 2010). Hypoxia induced VEGF expression was mediated by the activation of ERK, whereas PI3K mediated hypoxia induced HIF-1α and VEGF expression confirming PI3K and ERK1/2 MAPK role as an upstream mediators for the expression of HIF-1α and VEGF in animals (Yang et al. 2009). HIF-1α was phosphorylated by p42/p44 MAPK *in vitro* as well as *in vivo* and the activation of p42/p44 MAPK increased the transcription activity of HIF-1α (Richard et al. 1999). It has been suggested that p42/p44 MAPK although may not have any effect either on the stabilization or DNA binding activity of HIF-1α, but mediates the transcriptional activity of HIF-1α (Hur et al. 2001).

5.2.3 Phosphatidylinoisitol 3-Kinase (PI3K)/adenosine-triphosphate dependant tyrosine kinase (Akt) Pathway

The PI3K-Akt signalling pathway controls many cellular activities including cell proliferation and activation of angiogenesis by controlling the expression of VEGF in endothelial cells (Jiang et al. 2000). Further, inhibition of PI3K-Akt pathway has been implicated in the inhibition of VEGF induced HUVEC migration as well (Matsunaga et al. 2008). Activation of PI3K-Akt pathway is also believed to mediate high glucose induced retinal endothelial cell migration contributing towards the proliferative retinopathy of diabetes (Huang and Sheibani 2008). On the other hand, the PI3K-Akt signalling pathway was suppressed in the EPCs obtained from diabetic patients leading to a decrease in migration and cell count. The effect was more pronounced if EPCs were treated with both glucose and oxidized LDL (Hamed et al. 2010). Increased glucose levels caused a decrease in cell proliferation and an increase in apoptosis and senescent activity of HUVECs and this effect was associated with the inhibition of the PI3K-Akt pathway (Varma et al. 2005, Zhong et al. 2010). Apoptosis induced by high glucose has been

reported to be due to an increase in the production of ROS mediated by PI3K-Akt pathway (Sheu et al. 2005). All this evidence made it clear that activation of PI3K-Akt pathway leads to increased migration and a reduction in the migration results due to its suppression in the presence of glucose.

Various studies have reported the involvement of PI3K-Akt pathway in regulating the expression of HIF-1α. Ferulic acid, a natural compound produced its angiogenic effects by increasing the expression of HIF-1α with subsequent increase in the production of VEGF and PDGF via activation of PI3K-Akt pathway along with p42/p44 MAPK pathway in HUVECs (Lin et al. 2010). Another natural product, apigenenin a dietary flavanoid inhibited the formation of tubes via decreasing the expression of HIF-1α and subsequent expression of VEGF via PI3K-Akt pathway (Fang et al. 2005). The choroidal blood vessel formation in rats and retinal pigment epithelial cells *in vitro* up regulated the expression of HIF-1α and VEGF production in the presence of hypoxia with the activation of PI3K-Akt pathway (Yang et al. 2009). In tumour cells, hypoxia stabilised the HIF-1α with simultaneous increased production of ROS and this was negated by the use of a PI3K inhibitor leading to the conclusions that the production of ROS and HIF-1α are mediated by PI3K-Akt pathway in cancer cells (Koshikawa et al. 2009, Zhong et al. 2000). However, the role of PI3K-Akt in regulating HIF-1α remains unclear as short duration hypoxia stabilized and accumulated HIF-1α depending on the activation of PI3K-Akt whereas prolonged hypoxia resulted in the inactivation of Akt and down regulation of HIF-1α via glycogen synthase kinase (GSK) 3β pathway (Mottet et al. 2003).

5.3 Materials and methods

5.3.1 Immunocytochemistry and wound healing assay

Expression of the cyclin dependent kinase inhibitor p27[Kip1] and hypoxia inducible factor–1α (HIF-1α) was carried out by immunocytochemistry as explained in chapter 2 (section 2.4.2). Unconjugated polyclonal anti-phospho-p27 (Ser10) at 1:100 and monoclonal anti-HIF-1α at 1:50 were used for identifying p27[Kip1] and HIF-1α in HMVECad after incubation of cells for 48 h in four conditions (viz. N5mM, N20mM, H5mM and H20mM). The expression of HIF-1α was assessed for HMVECad at 48 h in the presence of different signal inhibitors as mentioned in the relevant segments and legends of the figures. The quantification of the stain is explained below in section 5.3.2.

The molecular mechanisms of hypoxia and/or hyperglycaemia mediated migration of HMVECad was assessed by the addition of signal inhibitors at the beginning of the wound healing assay. The wound healing assay was carried out as explained in section 2.2.4 using HMVECad. Different signal inhibitors such as PKC$_{βII}$/EGFR inhibitor (PKC$_{βII}$/EGFRi) [4,5-bis(4-Fluoroanilino)-phthalimide] 1μM (Calbiochem, Merck Chemicals,

Nottingham), p42/p44 MAPK Inhibitor (P42/p44 MAPKi) (2′-Amino-3′-methoxyflavone) (PD98059) 2µM (Calbiochem, Merck Chemicals, Nottingham) and PI3K Inhibitor (PI3Ki) [2-(4-Morpholinyl)-8-phenyl-4H-1-benzopyran-4-one] (LY294002) 10µM (Invitrogen, UK) were used. DMSO of molecular biology grade was used as a solvent for these signal inhibitors at a final concentration of ≤ 0.7% v/v and an equivalent concentration was used for each control.

5.3.2 Quantification of the protein expression

The images stained for the expression of $p27^{Kip1}$ and HIF-1α were quantified using the Image J freeware (Image J 2010) developed by the National Institute of Health of Bethesda, USA. The quantification of stained images involved four steps

    a) Changing the scale of measurement from pixels to micrometers

    b) Converting the image to gray scale

    c) Segmenting the red stained cells using the threshold

    d) Measuring the threshold area at a fixed value

Conversion of the scale from pixels to micrometers was done by using *Analyse>Set>Scale* command to set the scale to micrometers. As all the images were captured at the magnification of 100x, the conversion ratio was 0.74pixels/µm. This ratio was used for all the images.
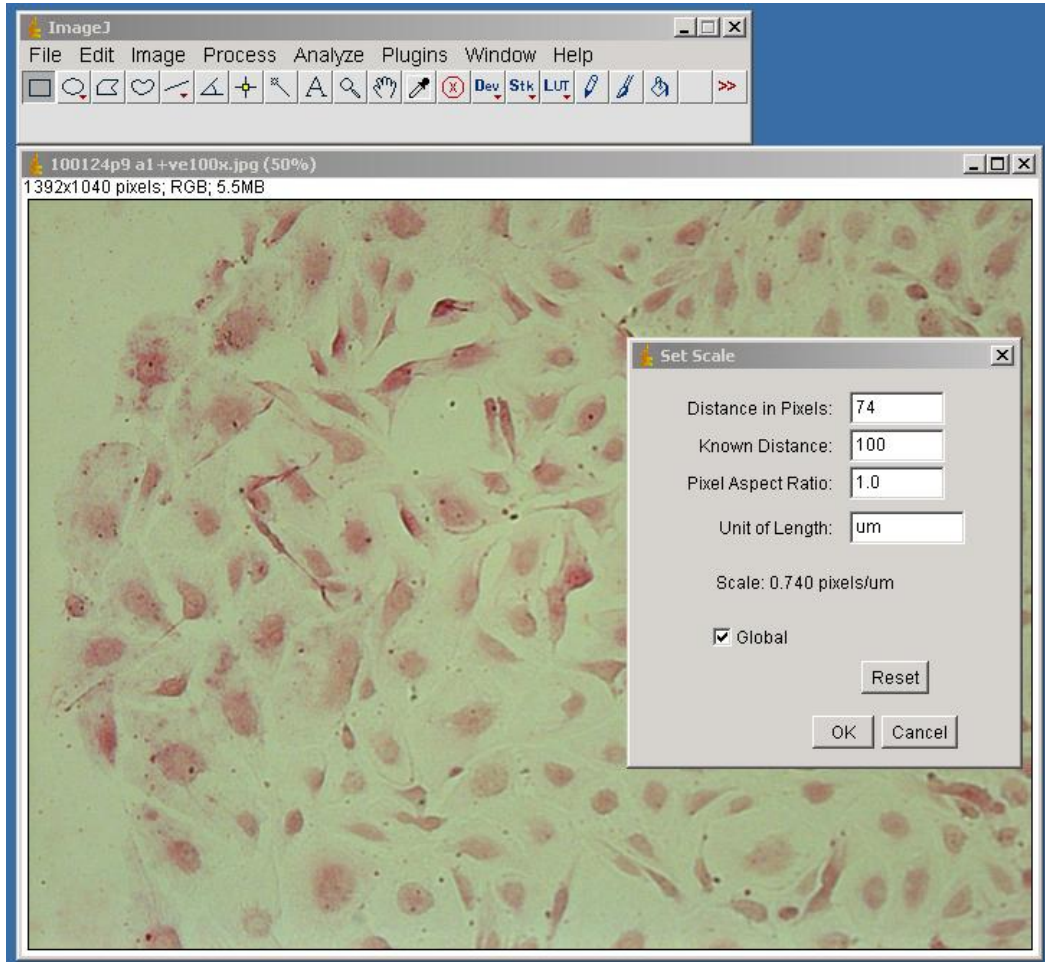
Fig. 5.1a Quantification of stain An image of which the stain was to be quantified was opened and the scale was converted to pixels

Conversion of the images to gray scale was done using the *Image>Type>RGB stack* command to split the image into red, green and blue channels. It is essential to stack the image in gray scale in order to measure the threshold. The green channel of the RGB stack was selected to get the best separation.
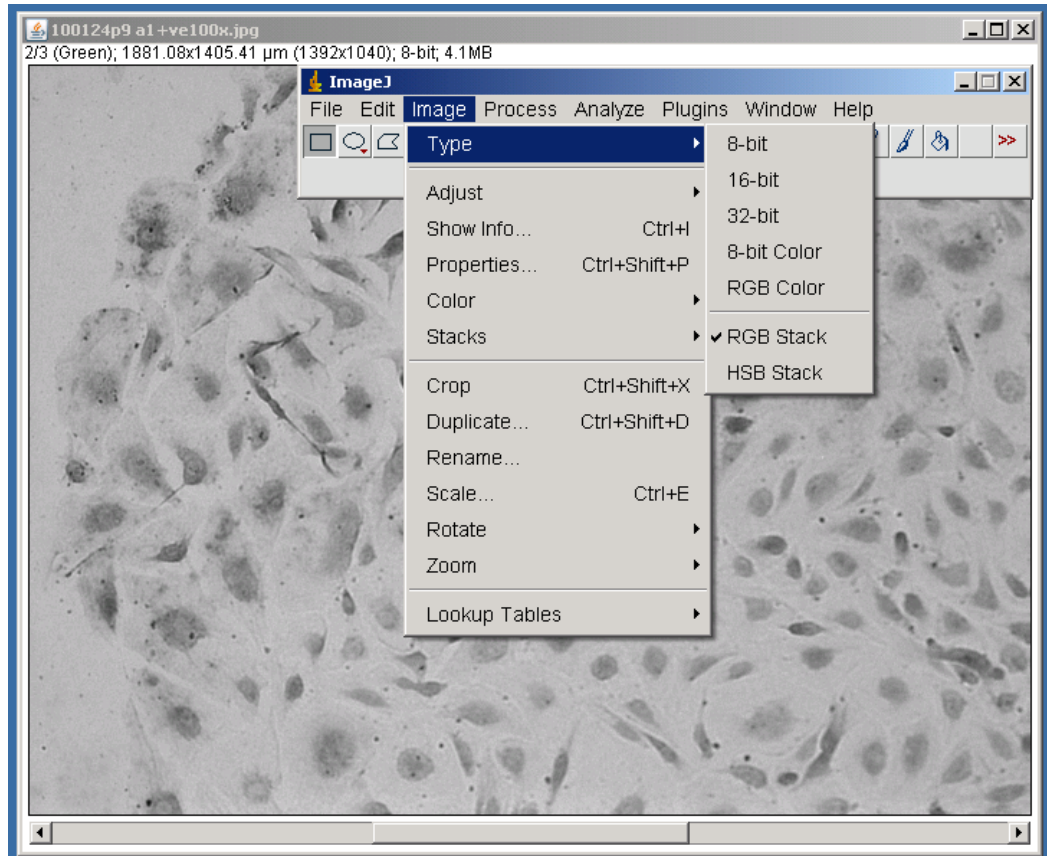
Fig.5.1b Quantification of stain Image was converted to gray scale

Next *Image>Adjust>Threshold* tool was used for thresholding the image. As image J cannot correctly threshold the image, it was manually adjusted. Using the 'Threshold' tool, the upper level of the threshold was fixed at 150 for all images barring a few images whose maximum threshold was either equal to or less than 150. For such images the adjusted threshold was slightly less than 150.
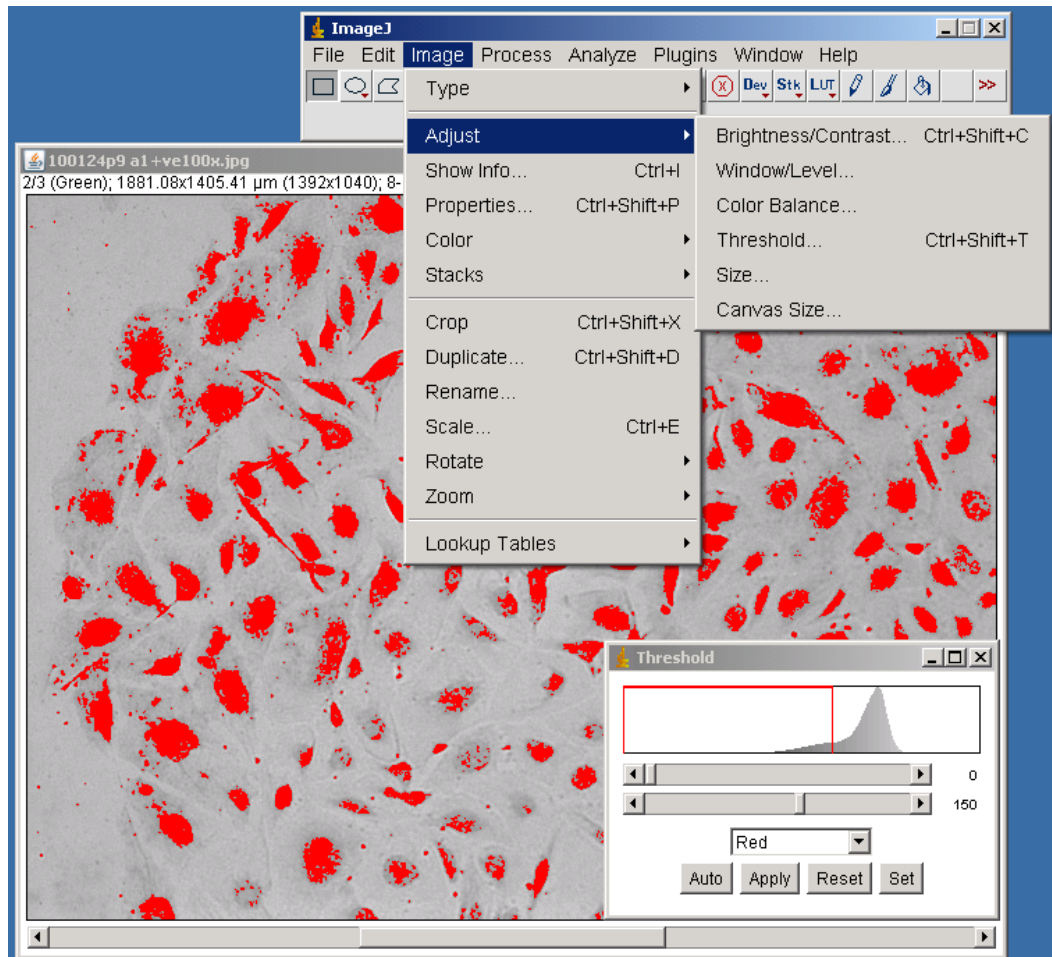
Fig.5.1c Quantification of stain Image was thresholded to reflect accurate staining

Analyse>Set Measurement dialog was used to select the 'Area', 'Area Fraction', 'Limit to threshold' and 'Display Label' so that image J measured the percentage of stained area and displayed it as a result.
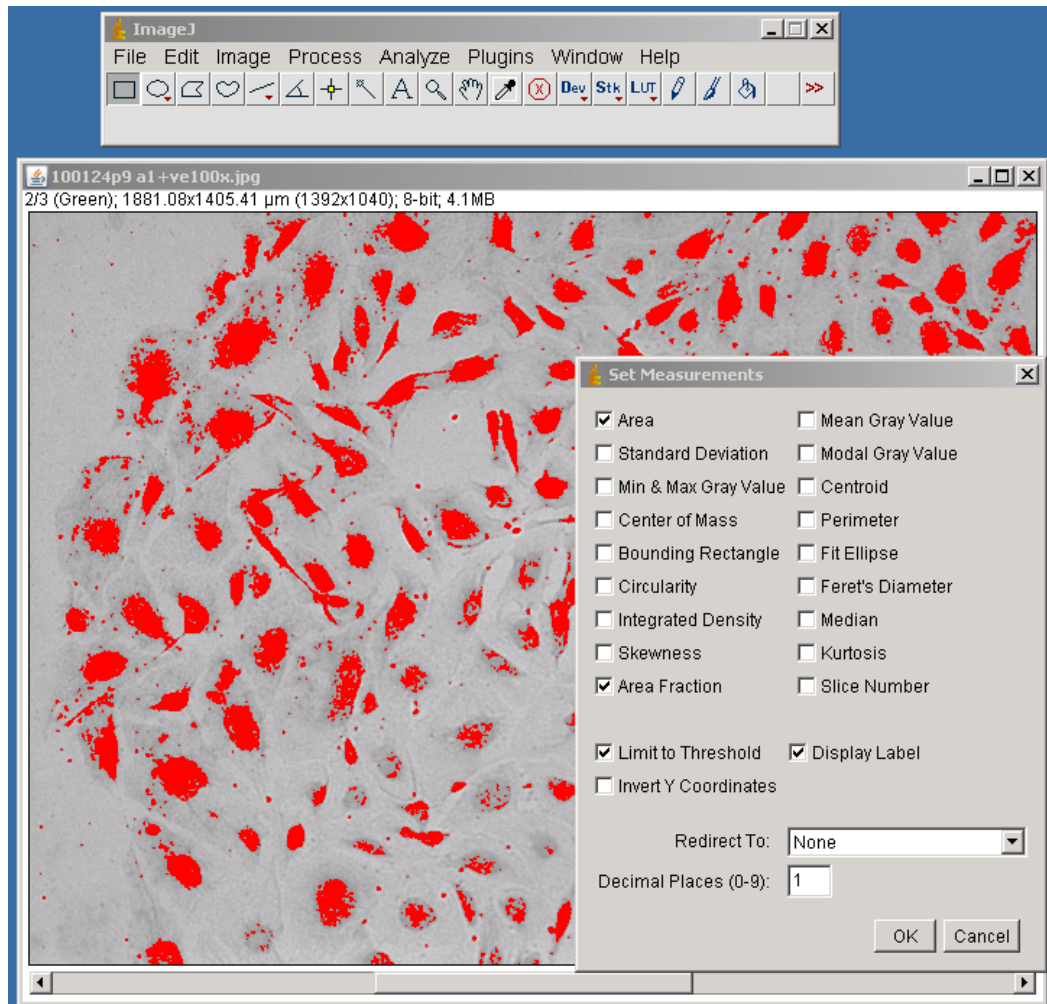
Fig.5.1d Quantification of image Parameter such as area of a defined square was selected to be displayed

The *rectangular selections* icon on the image J tool bar was selected to draw a square of 229.7 x 229.7 μm^2. These dimensions were drawn on the image with the aim of measuring the threshold within six identical sized areas along the edges of the monolayer. These squares (229.7 x 229.7 μm^2) were drawn along the edges of the layer to quantify the expression of proteins in migrating cells. However while quantifying HIF-1α expression in the images captured from the radial migration assay (Fig. 5.6 from section 5.4.2), the squares were drawn randomly as the cells were stained uniformly across the image. After drawing each of the six squares, the *Analyse>Measure* command was selected to display the area and percent area in the 'Results' window. These results were copied to the excel worksheet for subsequent analysis. The results were expressed as mean ± SEM of percent of stained area of six observations for each image (n=6) from each condition. All the results were analysed using SPSS 15.0.
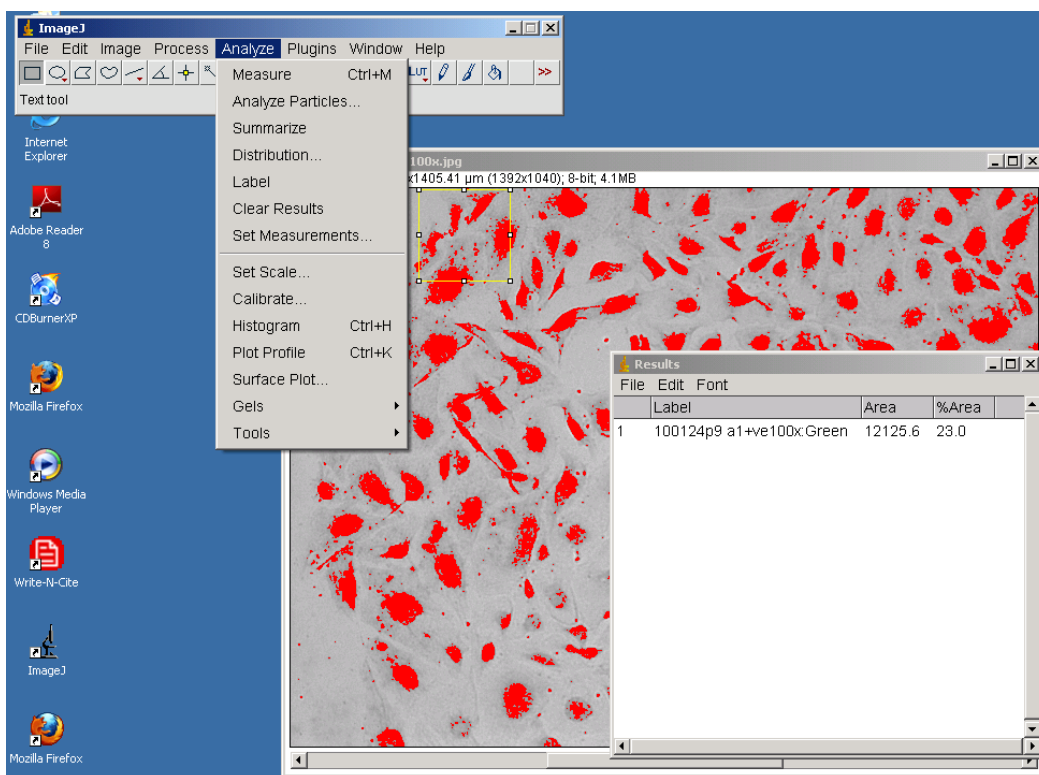
Fig. 5.1e Quantification of stain Total of six squares of defined area were measured for each image

5.4 Results

5.4.1 Expression of p27^{Kip1} protein in HMVECad

HMVECad expressed p27^{Kip1} protein at N5mM, N20mM, H5mM and H20mM conditions at 48 h. The p27^{Kip1} was predominantly expressed in the nuclei of the cells at the migrating edges of the monolayer for all of the test conditions (Fig. 5.2c-f). It was very rarely found anywhere other than the edges of the monolayer. Interestingly, in some of the cells migrating in 5mM glucose in both normoxia and hypoxia the p27^{Kip1} expression was localised, along with nuclei, in the cytoplasm of cells (Fig. 5.2c&e). No difference in the intensity of the expression of p27^{Kip1} was found between N5mM and N20mM or between H5mM and H20mM conditions. However, the cells incubated in 5% oxygen (Fig. 5.2e&f) expressed more p27^{Kip1} than those of their normoxic (Fig. 5.2c&d) counterparts.

The expression of p27^{Kip1} was also assessed for migrating cells of the wound healing assay model at 48 h. Similar to those of the circular monolayer; the HMVECad migrating from the intact edge of the semicircular monolayer expressed p27^{Kip1} in the nuclei and in some cases (i.e. N5mM and H5mM) in the cytoplasm of cells at the leading edges (Fig. 5.3c&e). The intact edge of HMVECad (Fig. 5.3) was more intensely stained for p27^{Kip1} in N5mM and H5mM compared to N20mM and H20mM conditions respectively. Cells migrating under N20mM and H20mM conditions showed only weak staining. On the other hand HMVECad migrating from the wounded edge expressed very little p27^{Kip1} for all the four conditions (Fig. 5.4).

The influence of varying glucose concentration and oxygen tension on the intensity of the p27^{Kip1} staining was quantified using image J freeware (Fig. 5.5). The intensity of p27^{Kip1} expression by HMVECad of the intact and wounded edge of the semicircular monolayer was assessed. The percent area of stained cells at the intact edge was found to be significantly less for N20mM (1.3 ± 0.7) and H20mM (3.2 ± 0.7) compared to those of N5mM (9.0 ± 2.3) and H5mM (18.9 ± 7.5) conditions respectively. The HMVECad of the intact edge under H5mM conditions expressed significantly higher quantities of p27^{Kip1} when compared to the N5mM condition ($p<0.001$). However, the difference in the p27^{Kip1} expression in cells migrating from the wounded edge was not found to reach statistical significance ($p>0.05$) for N5mM (3.0 ± 2.1), N20mM (1.5 ± 0.6), H5mM (2.2 ± 1.8) and H20mM (4.6 ± 2.2) conditions.

When the intensity of the expression of p27^{Kip1} is compared between the intact and wounded edge, it was found to be significantly different for N5mM ($p<0.05$) and H5mM ($p<0.001$) only. The intensity of the stain for cells in both N20mM and H20mM was not significantly different between the intact and wounded edge.

a)   b)

c)   d)

e)   f)
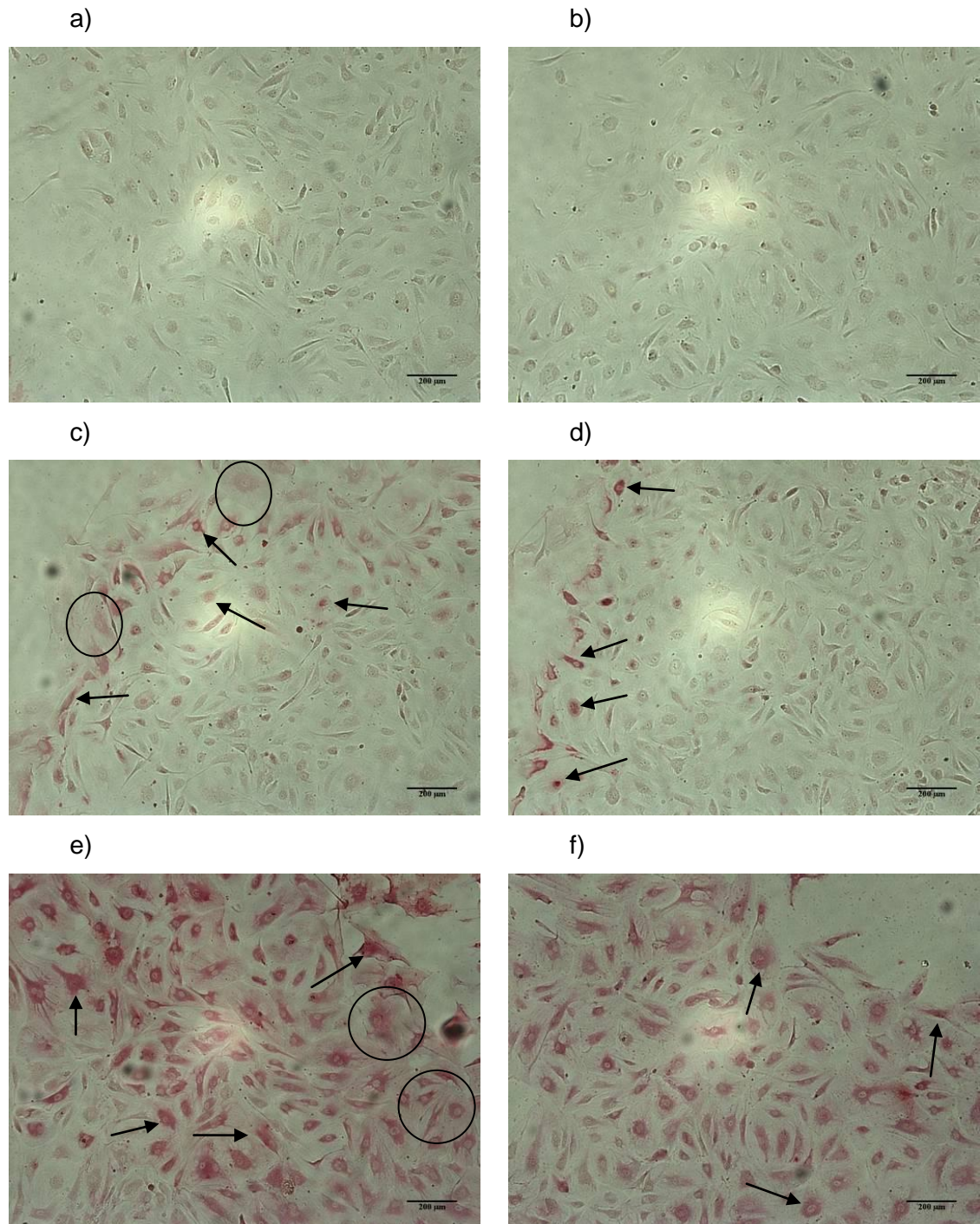
Fig. 5.2 Expression of p27^{Kip1} in HMVECad of the circular monolayer The circular monolayers of HMVECad were exposed to four different conditions for 48 h. The cells of a) and b) were treated with control antibody (IgG1) and TBS alone in order to determine the antibody specificity and as buffer control respectively. The expression of p27^{Kip1} protein was detected in the cells treated with c) N5mM, d) N20mM, e) H5mM and f) H20mM conditions. The arrows and circles indicate nuclear and cytoplasmic staining respectively. The images are representative of samples from 3 different occasions (n=3). The scale bar on each photomicrograph represents 200µm (Magnification: 100x).

a)

b)

c)

d)

e)

f)
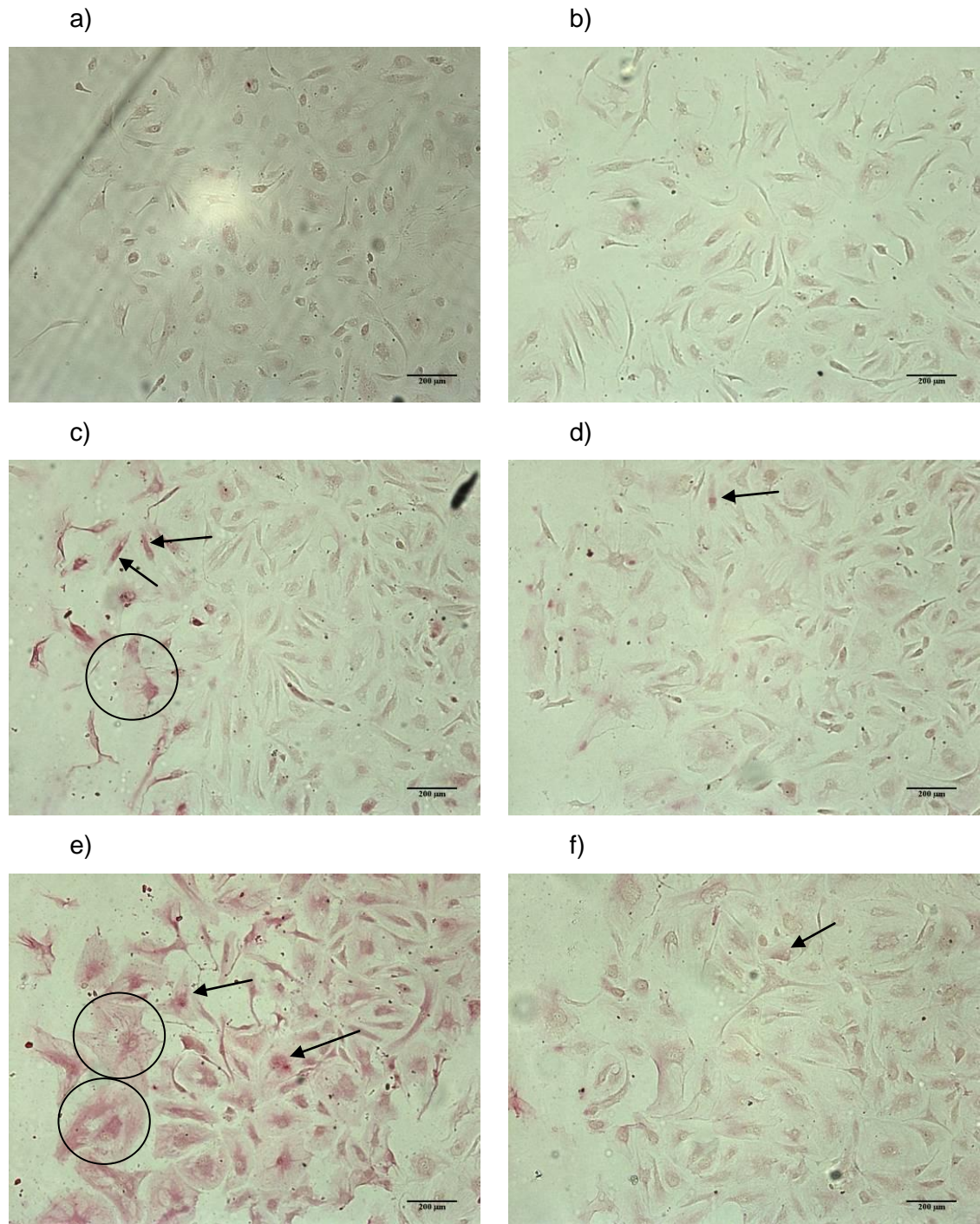
Fig. 5.3 Expression of p27^{Kip1} in HMVECad of the intact edge The intact edges of the semicircular monolayer of HMVECad were exposed to four different conditions for 48h. The cells were treated with control antibody (IgG1) (a) and TBS alone (b) in order to determine the antibody specificity and as buffer control respectively. The expression of p27^{Kip1} protein was detected in cells treated with c) N5mM, d) N20mM, e) H5mM and f) H20mM conditions. The arrows and circles indicate nuclear and cytoplasmic staining respectively. The images are representative of samples from 3 different occasions (n=3). The scale bar on each photomicrograph represents 200µm (Magnification: 100x).

a)

b)

c)

d)

e)

f)
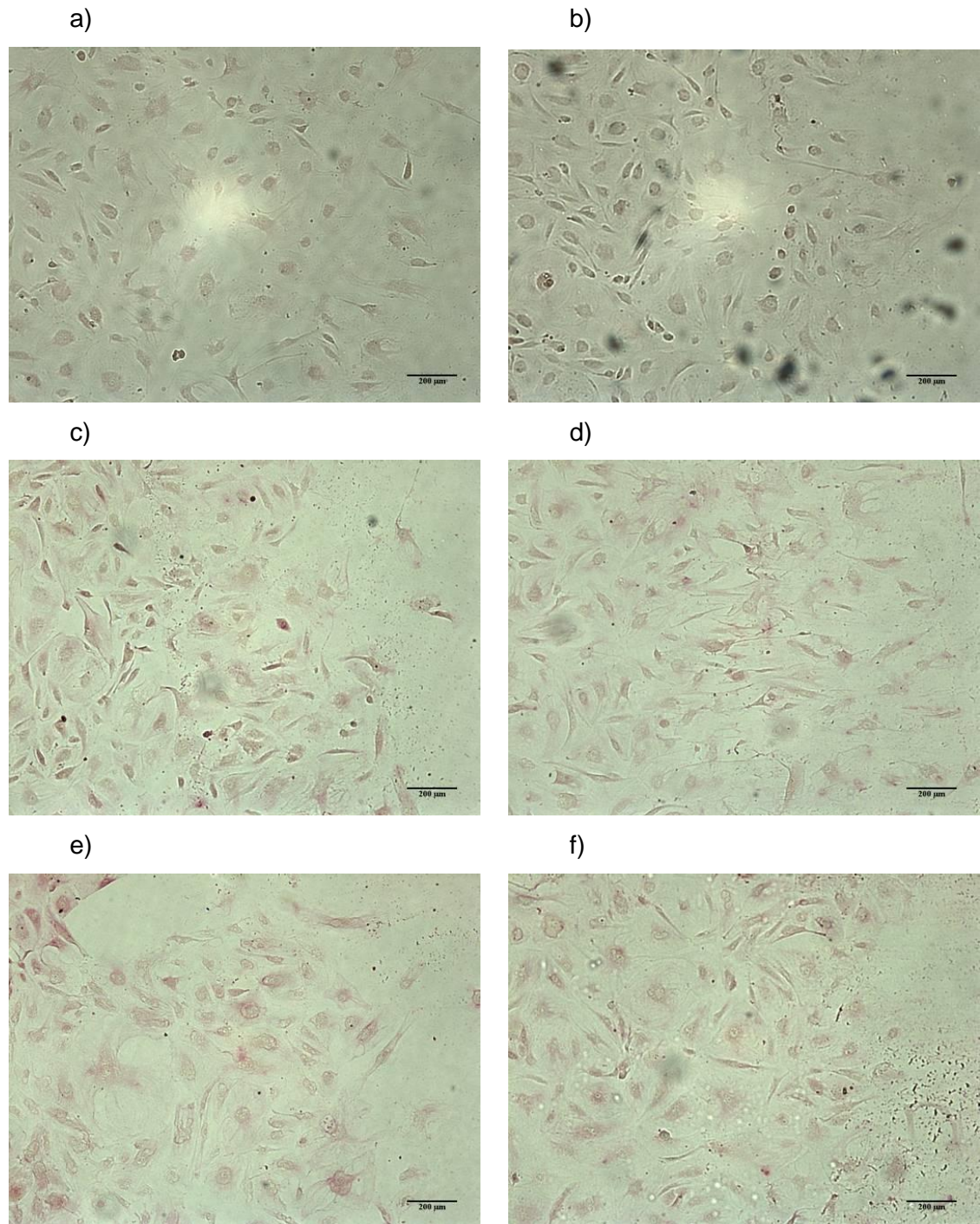
Fig. 5.4 Expression of p27^{Kip1} in HMVECad of the wounded edge The wounded edges of the semicircular monolayer of HMVECad were exposed to four different conditions for 48 h. The cells were treated with a) control antibody (IgG1) and b) TBS alone in order to determine the antibody specificity and as buffer control respectively. The expression of p27^{Kip1} protein was detected in cells treated with c) N5mM, d) N20mM, e) H5mM and f) H20mM conditions. The images are representative of samples from 3 different occasions (n=3). The scale bar on each photomicrograph represents 200μm (Magnification: 100x).
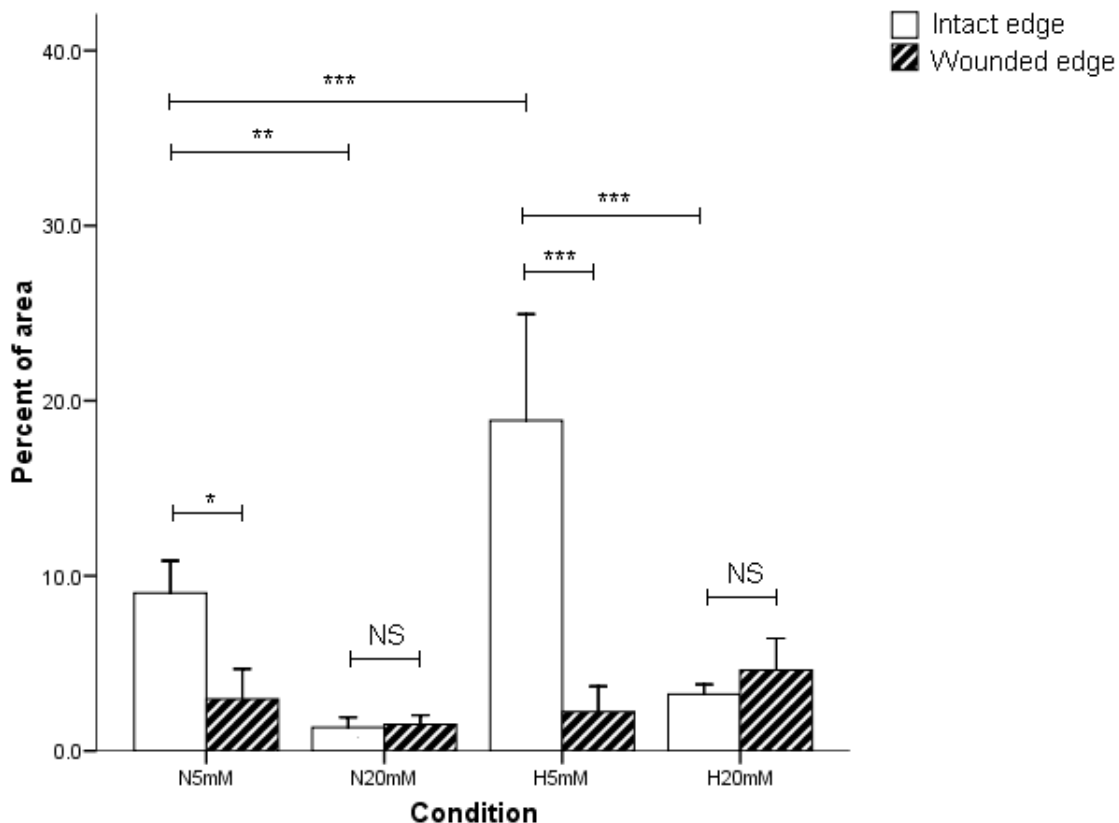
Fig. 5.5 Expression of p27^{Kip1} in HMVECad in response to glucose concentration and oxygen tension The semicircular monolayers were incubated at 5mM or 20mM glucose concentration in either normoxic (20% O_2) or hypoxic (5% O_2) condition for 48 h. The cells were stained for the expression of p27^{Kip1} on both the intact and wounded edge of the semicircular monolayer. Intensity of the expression was quantified as percent area using Image J freeware. The results are presented as mean ± SEM of 6 identical sized regions (n=6) at either intact or wounded edge from a single monolayer. The results for different conditions were analysed by analysis of variance (ANOVA) followed by Bonferroni post hoc test. The comparison between the intact and wounded edge was analysed by Independent t test.

($*p<0.05$, $**p<0.01$, $***p<0.001$ and NS = not significant when compared as indicated)

5.4.2 Expression of HIF-1α in HMVECad

The circular monolayers of HMVECad in N5mM, N20mM, H5mM and H20mM conditions were stained for the detection of HIF-1α (Fig. 5.6) protein after measuring the migration at 48 h. The expression was found to be uniform across the given monolayer. The HIF-1α staining was more intense in cells exposed to hypoxic conditions compared to normoxic conditions (Fig.5.6e&f vs. c&d). The expression was weak in N5mM (Fig.5.6c) than in N20mM (Fig.5.6d) condition. Hypoxia induced expression of HIF-1α was predominantly found to be concentrated in the nuclei of the cells which were cultured in 5mM glucose concentration (Fig.5.6c&e) and in the perinuclear region for those which were cultured in 20mM glucose concentration (Fig.5.6d&f).

The expression of HIF-1α in the migrating cells of the intact edge of the semicircular monolayer was found to be higher (Fig. 5.7) in hypoxic conditions than normoxic conditions at 48 h, similar to that of the circular monolayer. However, the cells sitting at the edge expressed more HIF-1α than any other part of the layer for all the conditions (Fig. 5.7). The distinction between the nuclear and perinuclear localisation of HIF-1α expression was not clear for N5mM and N20mM conditions. For cells migrating in H5mM conditions, the expression of HIF-1α was greater than any other conditions and was localised predominately in the nuclei. The cells incubated in H20mM expressed HIF-1α more at the perinuclear region than within the nucleus.

The cells migrating from the wounded edge of the semicircular monolayer (Fig. 5.8) expressed HIF-1α across the layer uniformly for any given condition. The cells migrating under H5mM condition expressed more HIF-1α than those in any other conditions.

HIF-1α expression in HMVECad located in the intact or the wounded edges due to the changes in concentration of glucose and oxygen tension was quantified by image J (Fig. 5.9). The cells migrating from the intact edge expressed significantly ($p<0.001$) more HIF-1α for H5mM (21.2 ± 8.3) than H20mM (7.2 ± 2.6) and N5mM (5.5 ± 2.4) conditions. However, no significant ($p>0.05$) difference in the percent area of stained cells was observed between N5mM and N20mM (3.8 ± 2.3) conditions. The HIF-1α expression pattern was similar for the wounded edge. The intensity of the stain was significantly higher ($p<0.001$) for H5mM (14.1 ± 3.5) than H20mM (2.5 ± 1.7) and N5mM (3.0 ± 1.0). No significant difference ($p>0.05$) was found between N5mM and N20mM (2.6 ± 1.2).

No significant difference in the level of HIF-1α protein was found between the intact and wounded edge for any of the conditions except for H20mM, where cells of the intact edge expressed more ($p<0.05$) HIF-1α than those of wounded edge.

a)

b)

c)

d)

e)

f)

Fig. 5.6 Expression of HIF-1α in HMVECad of the circular monolayer The circular monolayer of HMVECad were exposed to four different conditions for 48 h. The cells were treated with a) control antibody (IgG1) and b) TBS alone in order to determine the antibody specificity and as buffer control respectively. The expression of HIF-1α protein was detected in cells treated with c) N5mM, d) N20mM, e) H5mM and f) H20mM conditions. The arrows and circles indicate nuclear and perinuclear staining respectively. The images are representative of samples from 3 different occasions (n=3). The scale bar of each photomicrograph represents 200μm (Magnification: 100x).

a)

b)

c)

d)

e)

f)

Fig. 5.7 Expression of HIF-1α in HMVECad of the intact edge The intact edges of the semicircular monolayer of HMVECad were exposed to four different conditions for 48 h. The cells were treated with a) control antibody (IgG1) and b) TBS alone in order to determine the antibody specificity and as buffer control respectively. The expression of HIF-1α protein was detected in cells treated with c) N5mM, d) N20mM, e) H5mM and f) H20mM conditions. The arrows and circles indicate nuclear and perinuclear staining respectively. The images are representative of samples from 3 different occasions (n=3). The scale bar of each photomicrograph represents 200μm (Magnification: 100x).

a)

b)

c)

d)

e)

f)

Fig. 5.8 Expression of HIF-1α in HMVECad of the wounded edge The wounded edges of the semicircular monolayer of HMVECad were exposed to four different conditions for 48 h. The cells were treated with a) control antibody (IgG1) and b) TBS alone in order to determine the antibody specificity and as buffer control respectively. The expression of HIF-1α protein was detected in cells treated with c) N5mM, d) N20mM, e) H5mM and f) H20mM conditions. The arrows and circles indicate nuclear and perinuclear staining respectively. The images are representative of samples from 3 different occasions (n=3). The scale bar of each photomicrograph represents 200μm (Magnification: 100x).

Fig. 5.9 Expression of HIF-1α in HMVECad in response to altered glucose and oxygen concentration The semicircular monolayers were incubated at either 5mM or 20mM glucose concentration and either normoxic (ambient O_2) or hypoxic (5% O_2) condition for 48 h. The cells were stained for the expression of HIF-1α. Intensity of the expression was quantified as percent area using Image J freeware. The results are presented as mean ± SEM of six identical sized regions (n=6) at either intact or wounded edge from a single monolayer. The results for different conditions were analysed by analysis of variance (ANOVA) followed by Bonferroni post hoc test. The comparison between the intact and wounded edge was analysed by Independent t test. (**$p<0.01$, ***$p<0.001$ and NS = not significant when compared as indicated)

5.4.3 Effect of intracellular signal inhibitors on the migration of HMVECad in hypoxia

The migration (µm) of HMVECad from the intact edge for H5mM condition (Fig.5.10) was greater than for the cells incubated in H20mM amongst all treatments viz. untreated cells (166.5 ± 3.9 vs. 147.0 ± 3.2), p42/p44 MAPKi (163.0 ± 4.1 vs. 118.0 ± 3.9) and PI3Ki treatment (124.8 ± 3.5 vs. 104.5 ± 3.8) except for PKC$_{\beta II}$/EGFRi treated cells (169.0 ± 3.9 vs. 163.4 ± 4.1) at 48 h. However, the migration of cells from the wounded edge for H5mM condition was faster than those for H20mM condition for all the treatments (untreated cells: 212.7 ± 4.6 vs. 183.1 ± 4.2, p42/p44 MAPKi treated cells: 194.8 ± 4.1 vs. 156.7 ± 7.4, PKC$_{\beta II}$/EGFRi treated cells: 210.0 ± 4.0 vs. 193.0 ± 4.5 and PI3Ki treatment: 169.7 ± 4.9 vs. 130.3 ± 5.0).

The PI3Ki treated cells of the intact edge (Fig. 5.10) migrated significantly lesser ($p < 0.001$) than those of the other three treatments under H5mM condition. No difference ($p > 0.05$) in the migration was recorded for either PKC$_{\beta II}$/EGFRi treated or p42/p44 MAPKi treated cells when compared with those of untreated cells for H5mM condition. The PI3Ki treated cells were not significantly different ($p > 0.05$) from p42/p44 MAPKi treated cells in the migration under H20mM condition. However along with PI3Ki treated cells, p42/p44 MAPKi treated cells also migrated significantly less ($p < 0.001$) than those of untreated and PKC$_{\beta II}$/EGFRi treated cells for H20mM condition.

The cells of the wounded edge (Fig. 5.10) migrated significantly less when they received PI3Ki compared to no treatment ($p < 0.001$) or p42/p44 MAPKi ($p < 0.05$) or PKC$_{\beta II}$/EGFRi ($p < 0.001$) treatment for H5mM condition. No difference ($p > 0.05$) was observed in the migration between untreated, p42/p44 MAPKi treated or PKC$_{\beta II}$/EGFRi treated cells for H5mM condition. The inhibition of PI3K treatment significantly prevented the cells from migrating on par with the other treatments ($p < 0.001$ against untreated and PKC$_{\beta II}$/EGFRi, $p < 0.01$ against p42/p44 MAPKi) under H20mM condition too. The p42/p44 MAPKi treated cells also migrated significantly less than those of untreated ($p < 0.01$) and PKC$_{\beta II}$/EGFRi treated ($p < 0.001$) cells under H20mM condition. However, like those from the intact edge, the cells from the wounded edge showed no significant ($p > 0.05$) difference in the migration of PKC$_{\beta II}$/EGFRi treatment from those of no treatment. The migration of the HMVECad (Fig. 5.10) from the wounded edge was significantly greater ($p < 0.001$) than that from intact edge for all the treatments and both the conditions.

Fig. 5.10 Effect of specific intracellular signal inhibitors on the migration of HMVECad The semi circular monolayers of HMVECad were treated with either p42/p44 MAPK inhibitor (PD98059) (2µM) or PKC$_{\beta II}$/EGFR inhibitor (1µM) or PI3K inhibitor (LY294002) (10µM). The migration of HMVECad of the semicircular monolayer in the presence of the above mentioned treatments due to the conditions induced by both 5mM or 20mM glucose concentration and hypoxia (5% oxygen tension) at 48 h was assessed by the wound healing assay. The results represent 10 observations from each of 3 samples of one occasion (n=30, unless mentioned below). The results are presented as net migration (mean ± SEM) of cells. The comparison between treatments was analysed by analysis of variance (ANOVA) followed by Bonferroni post hoc test. The comparison among conditions and edges was analysed by Independent student's t test. The migration was significantly lower ($p<0.001$) at the intact edge for both the conditions and all the treatments compared to respective condition and treatment of the wounded edge.

(††$p<0.01$, ††† $p<0.001$ when compared with H5mM condition of respective edge; *$p<0.05$, **$p<0.01$, and ***$p<0.001$ when compared as indicated)

(Intact and wounded edges: n = 20 for both PD98059 and LY294002 in H5mM and for PKC$_{\beta II}$/EGFRi in H20mM)
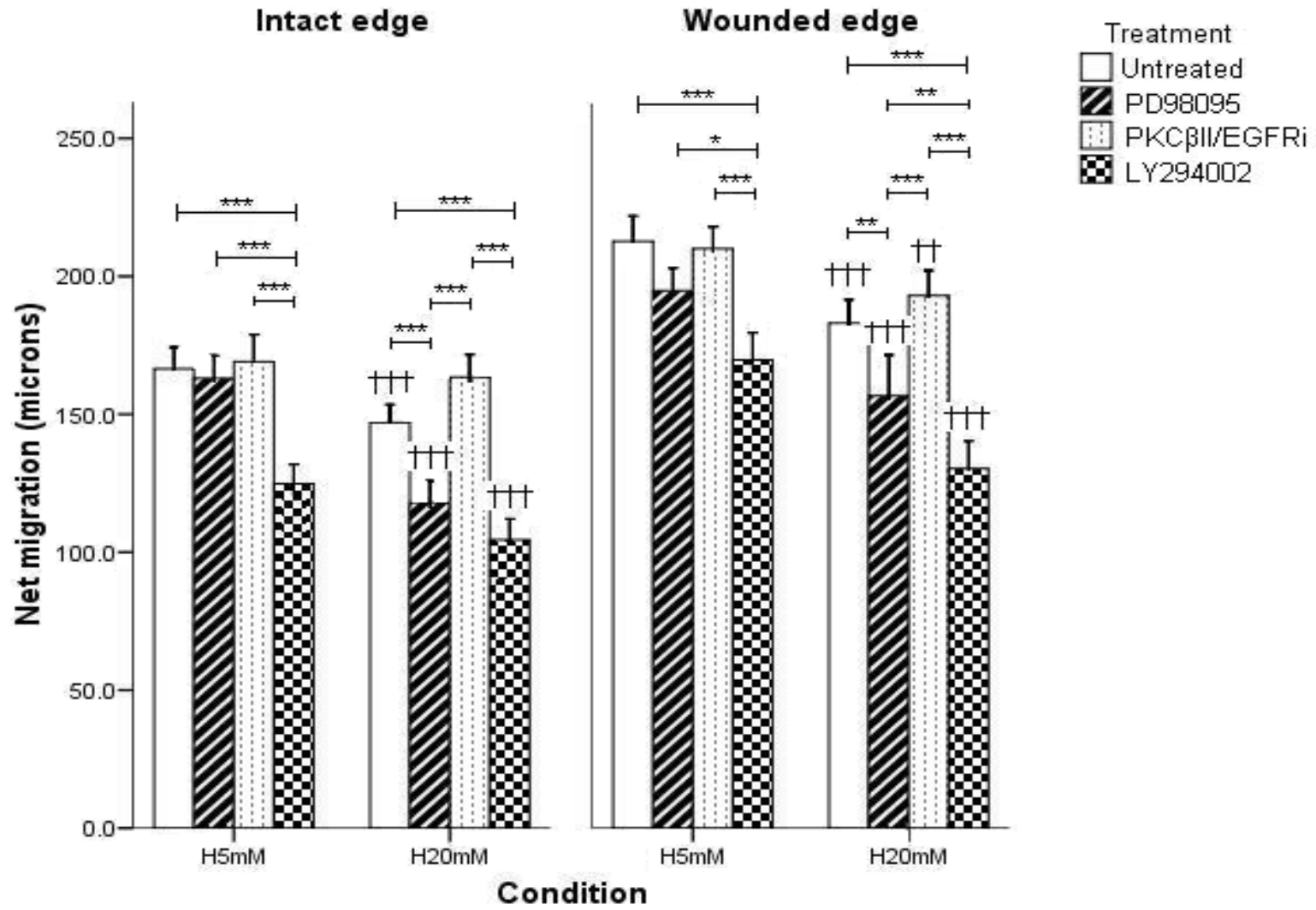
5.4.4 Effect of intracellular signal inhibitors on the expression of HIF-1α

The HMVECad were treated with p42/44 MAPKi or PKC$_{\beta II}$/EGFRi or PI3Ki to understand their role in regulating the expression of HIF-1α. The semicircular monolayers were incubated in H5mM and H20mM conditions for 48 h before staining for the expression of HIF-1α. The expression of HIF-1α was localised in the nucleus for H5mM treatments (Fig. 5.11Aa and 5.12Aa), and both nucleus and the perinuclear region in H20mM (Fig. 5.11Ba & 5.12Ba) and in PI3Ki treated cells (Fig.5.11d (A&B) & 5.12d (A&B)). HIF-1α was predominantly perinuclear in cells treated with p42/p44 MAPKi (Fig.5.11b (A&B) & 5.12b (A&B)) and PKC$_{\beta II}$/EGFRi (Fig.5.11c (A&B) & 5.12c (A&B)) in H5mM and H20mM conditions. HIF-1α staining was more intense in untreated cells of the intact and wounded edge compared to treated cells in both H5mM (Fig. 5.11Aa & 5.12Aa) and H20mM (Fig. 5.11Ba & 5.12Ba) conditions.

The HIF-1α expression in the presence of different signal inhibitors was quantified using image J (Fig. 5.13). Untreated (7.6 ± 2.2) HMVECad of the intact edge expressed significantly more HIF-1α than p42/p44 MAPKi (2.1 ± 0.3) ($p<0.001$) or PKC$_{\beta II}$/EGFRi (2.2 ± 0.4) ($p<0.001$) or PI3Ki (2.1 ± 0.4) ($p<0.001$) treatment for H5mM condition. No significant difference ($p>0.05$) was observed amongst the treated cells for H5mM condition. The H20mM conditions followed the trend of H5mM as the untreated cells (9.4 ± 1.2) expressed more of HIF-1α than p42/p44 MAPKi (2.1 ± 0.3) ($p<0.001$) or PKC$_{\beta II}$/EGFRi (5.1 ± 0.7) ($p<0.01$) or PI3Ki (2.9 ± 0.5) ($p<0.001$) treatment. Among the different treatments, the level of HIF-1α protein was more ($p<0.05$) in PKC$_{\beta II}$/EGFRi treated cells compared to p42/p44 MAPKi treated cells. There was no difference ($p>0.05$) between H5mM and H20mM condition for any of the treatments except for PKC$_{\beta II}$/EGFRi. The PKC$_{\beta II}$/EGFRi treated cells expressed more ($p<0.01$) HIF-1α in H20mM than in H5mM condition of intact edge.

The level of expression of HIF-1α in the wounded edge was different ($p<0.01$) between the untreated cells (9.4 ± 1.7) and PI3Ki treated cells (2.6 ± 0.5) for H5mM condition. No difference ($p>0.05$) was observed between the untreated cells and p42/p44 MAPKi (6.1 ± 1.1) or PKC$_{\beta II}$/EGFRi treated (5.1 ± 1.1) cells for H5mM condition. No difference ($p>0.05$) among the treatments was observed. For H20mM condition, p42/p44 MAPKi treatment (2.4 ± 0.4) significantly reduced ($p<0.001$) the expression of HIF-1α compared to either no treatment (10.5 ± 1.1) or PKC$_{\beta II}$/EGFRi treatment (8.3 ± 0.9). A significant difference ($p<0.01$) was also found between the untreated and PI3Ki treated cells (5.4 ± 0.9). The level of the protein was significantly less ($p<0.01$) for p42/p44 MAPKi and more ($p<0.05$) for PKC$_{\beta II}$/EGFRi and PI3Ki treatment at H20mM compared to H5mM condition.

The HMVECad of the wounded edge expressed more HIF-1α for p42/p44 MAPKi ($p<0.01$) and PKC$_{\beta II}$/EGFRi ($p<0.05$) treatment than those of intact edge in H5mM condition. No difference ($p>0.05$) was detected for untreated and PI3Ki treated cells. However, for H20mM condition, PKC$_{\beta II}$/EGFRi ($p<0.01$) and PI3Ki ($p<0.05$) treatment increased the expression of HIF-1α in the cells of the wounded edge compared to intact edge. No difference ($p>0.05$) between the two edges was observed in untreated as well as for p42/p44 MAPKi treated cells.
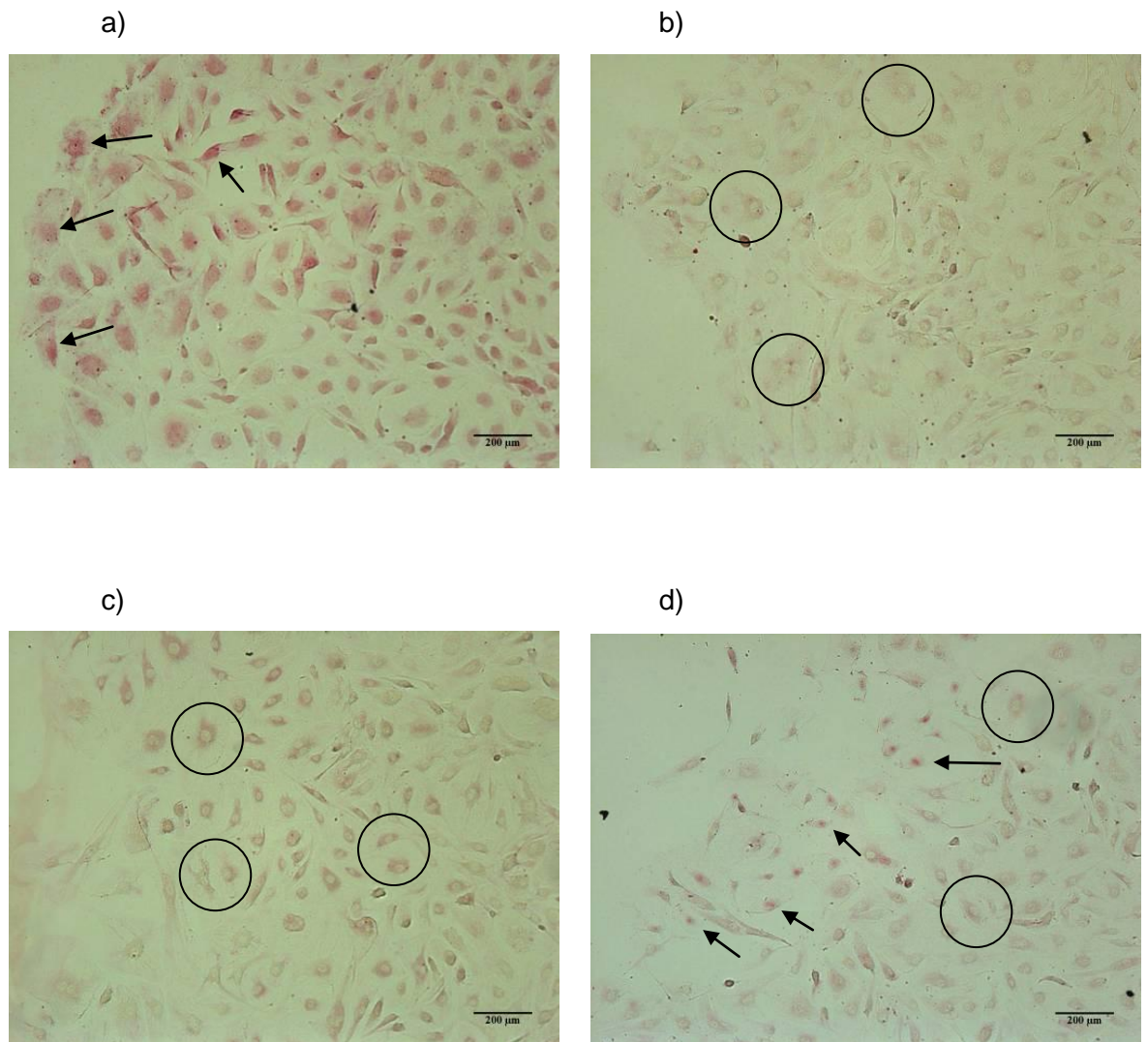
Fig. 5.11A Effect of inhibitors on the expression of HIF-1α in HMVECad of the intact edge The HMVECad of intact edges of the semicircular monolayer were treated with signal inhibitors and exposed to 5mM glucose under hypoxic (5% O$_2$) condition for 48 h. The expression of HIF-1α protein was detected in cells treated with a) no treatment, b) p42/p44 MAPKi (PD98059) (2µM), c) PKC$_{\beta II}$/EGFRi (1µM) and d) PI3Ki (LY294002) (10µM) treatment. The arrows and circles indicate nuclear and perinuclear staining respectively. The images are representative of 3 samples (n=3). The scale bar of each photomicrograph represents 200µm (Magnification: 100 x).

Fig. 5.11B Effect of inhibitors on the expression of HIF-1α in HMVECad of the intact edge The HMVECad of the intact edges of the semicircular monolayer were treated with signal inhibitors and exposed to 20mM glucose under hypoxic (5% O_2) condition for 48 h. The expression of HIF-1α protein was detected in cells treated with a) no treatment, b) p42/p44 MAPKi (PD98059) (2μM), c) PKC$_{βII}$/EGFRi (1μM) and d) PI3Ki (LY294002) (10μM) treatment. The arrows and circles indicate nuclear and perinuclear staining respectively. The images are representative of 3 samples (n=3). The scale bar of each photomicrograph represents 200μm (Magnification: 100 x).

a)

b)

c)

d)

Fig. 5.12A Effect of inhibitors on the expression of HIF-1α in HMVECad of the wounded edge The HMVECad of wounded edges of the semicircular monolayer were treated with signal inhibitors and exposed to 5mM glucose under hypoxic (5% O_2) condition for 48 h. The expression of HIF-1α protein was detected in cells treated with a) no treatment, b) p42/p44 MAPKi (PD98059) (2µM), c) PKC$_{\beta II}$/EGFRi (1µM) and d) PI3Ki (LY294002) (10µM) treatment. The arrows and circles indicate nuclear and perinuclear staining respectively. The images are representative of 3 samples (n=3). The scale bar of each photomicrograph represents 200µm (Magnification: 100 x).

Fig. 5.12B Effect of inhibitors on the expression of HIF-1α in HMVECad of the wounded edge The HMVECad of the wounded edges of the semicircular monolayer were treated with signal inhibitors and exposed to 20mM glucose under hypoxic (5% O_2) condition for 48 h. The expression of HIF-1α protein was detected in cells treated with a) no treatment, b) p42/p44 MAPKi (PD98059) (2µM), c) PKC$_{\beta II}$/EGFRi (1µM) and d) PI3Ki (LY294002) (10µM) treatment. The arrows and circles indicate nuclear and perinuclear staining respectively. The images are representative of 3 samples (n=3). The scale bar of each photomicrograph represents 200µm (Magnification: 100 x).

Fig. 5.13 Expression of HIF-1α in HMVECad in response to the specific intracellular signal inhibitors Intensity of the stain for the expression of HIF-1α was quantified as percent area using Image J freeware. The semicircular monolayer was incubated at 5mM or 20mM glucose concentration and hypoxic (5% O_2) condition for 48 h. The cells were treated with either p42/44 MAPK inhibitor (PD98059) (2µM) or $PKC_{\beta II}$/EGFR inhibitor (1µM) or PI3K inhibitor (LY294002) (10µM) at the beginning of the incubation. The results are presented as mean ± SEM of 6 identical sized regions from 3 samples (n=18, unless mentioned below). The comparison between the treatments within a condition was analysed by analysis of variance (ANOVA) followed by Bonferroni post hoc test. Independent student's *t* test was employed to compare amongst the conditions and edges.

(†$p<0.05$, †† $p<0.01$ when compared with intact edge of the respective treatment, *$p<0.05$, **$p<0.01$ and ***$p<0.001$ when compared as indicated)

(Intact & wounded edge: n = 12 for both p42/p44 MAPKi and PI3Ki in H5mM condition)
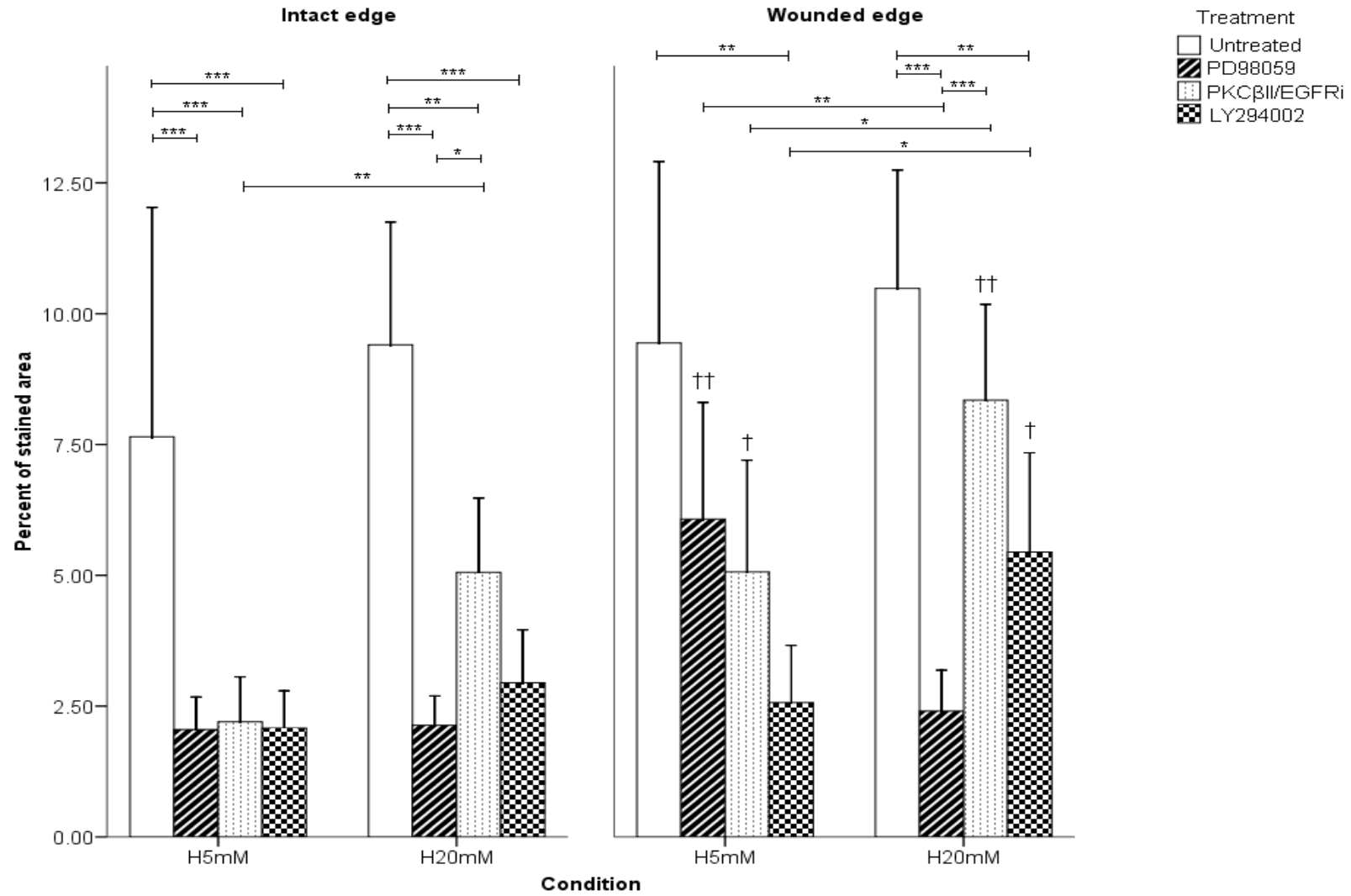
5.5 Discussion

HMVECad incubated in hypoxia expressed more p27^{Kip1} compared to normoxia (Fig.5.2c&d vs. 5.2e&f) as hypoxia has been reported to activate various cell cycle regulators. The expression of p27^{Kip1} has been found to be activated in hypoxic cells (Gardner et al. 2001). The expression of p27^{Kip1} in the nuclei of some of HMVECad only at the migrating edge of a monolayer (Fig. 5.2) could indicate that those cells might be actively under the consideration of not transiting from G$_1$ to S phase of cell cycle. However this observation, although correct might not have any bearing on the migration of cells, as the migration has been observed in the presence of anti-proliferative agent (Fig. 4.3). The expression of p27^{Kip1} in the cytoplasm (Fig. 5.2c&e, 5.3c&e) could indicate its role in the migration as the evidence has started emerging in its favour. It has been proved that MAPK/PI3K downstream effector p90 ribosomal S6 kinase (RSK1) increased the migration via accumulation of p27^{Kip1} in cytoplasm (Besson et al. 2004, Larrea et al. 2009). On the contrary, over expression of p27^{Kip1} is implicated in negatively regulating the migration along with proliferation (Diez-Juan and Andres 2003, Goukassian et al. 2001). It is also worth remembering that the cells might be making the phenotypic switch from migration to proliferation (De Donatis et al. 2008). However, there is a need to confirm this further. Surprisingly, either no difference in the p27^{Kip1} nuclear expression was found between the normal and elevated glucose concentration or cells incubated in low glucose concentration expressed more p27^{Kip1} protein compared to higher glucose level (Fig.5.2c&e vs. d&f). These observations are contrary to previous observation wherein high glucose leads to the induction of p27^{Kip1} mediated hypertrophy of mesengial cells (Wolf et al. 2003). The cells at the middle of the monolayer (Fig.5.2-5.4) have not, as expected, expressed the p27^{Kip1}. This could be explained on the basis that the cells in the middle of the monolayer are neither at the forefront of the migration nor undergoing active proliferation irrespective of the conditions.

The lack of expression of p27^{Kip1} in elevated glucose levels in intact edge cells was clearly demonstrated when the stain was quantified using image J freeware (Fig.5.5). Surprisingly, the intensity of the stain differed between the cells cultured in normal glucose levels of intact edge and wounded edge but not for those cultured in higher glucose levels (Fig.5.5). It is further surprising that the cells at the wounded edge failed to express p27^{Kip1} either in nuclei or cytoplasm suggesting no role for it either in proliferation (expected) or migration (unexpected). As no difference in the expression of p27^{Kip1} between any of the conditions in HMVECad of wounded edge (Fig.5.5) was found, it is plausible to understand the lack of nuclear expression considering that the proliferation might be taking place and aiding the increased migration at the wounded edge. However the lack of

cytoplasmic expression of p27^{Kip1} in the cells of wounded edge raises the question about activated p27^{Kip1} having any role in the migration of cells. This dichotomy in the role of cytoplasmic p27^{Kip1} in regulating the migration of cells could be the reason behind the contradicting evidences being reported. Taken together there is a need for more work to elucidate the role of p27^{Kip1} in proliferation and/or migration of microvascular endothelial cells in diabetic milieu.

The immunostain being more intense in the presence of hypoxia (Fig.5.6e, 5.7e and 5.8e) is very much expected as HIF-1α is a well known angiogenic stimulant under the control of oxygen tension. Hypoxia is essential not only for the stabilization of HIF-1α but also for the nuclear translocation and its accumulation in the nucleus, so that it can perform its transcriptional activity (Kallio et al. 1998). The expression of HIF-1α was found to be nuclei specific in large number of HMVECad cultured in normal glucose condition as against the perinuclear localisation in elevated glucose levels (Fig.5.6c&e vs. d&f). The perinuclear localization suggests that HIF-1α although stabilized due to hypoxia and hence getting expressed, might not be translocated into nuclei as the high glucose might be interfering with that process. Apart from this, there are reports suggesting the degradation of HIF-1α in the presence of higher glucose. Catrina et el. (2004) suggest that hyperglycaemia interferes with the stability of HIF-1α in hypoxia against the proteasomal degradation in spite of the inhibition of PHDs and with the transcriptional activity of HIF-1α (Catrina et al. 2004). Further, stabilization and activation of HIF-1α rectified the diabetes induced impairment of wound healing by restoring the activation of many essential target genes such as VEGF, VEGFR, HSP-90, SDF-1α, SCF and Tie-2 (Botusan et al. 2008). The degradation of HIF-1α and its failure to undergo nuclear translocation in the presence of high glucose could be the reasons for the decreased migration of HMVECad. The expression of HIF-1α in normoxia (Fig.5.6c&d) although weak could have been regulated not by oxygen tension but by other factors such as growth factors and cytokines which are also known to regulate HIF-1 (Webb, Coleman and Pugh 2009). It was interesting to note the uniformity of the stain across the circular monolayer as against the expectation of cells at the edge having more stain (Fig. 5.6). The expectation that the cells at the edge of monolayer express more HIF-1α was based on the proposition that HIF-1 being a transcription factor for many mitogenic agents such as VEGF would be instrumental in driving the migration up (Pugh and Ratcliffe 2003).

HMVECad at the intact and wounded edge in hypoxia (Fig.5.7e&f and 5.8e&f) stained slightly more intensely than the cells at the centre of the monolayer. This could indicate that HIF-1α activation is essential for the migration of cells. The quantification of the intensity of the stain using image J freeware (Fig.5.9) found no difference among any of the conditions except in H20mM condition between the intact and wounded edge,

although the migration of the wounded edge was greater than the intact edge (chapter 4, Fig.4.4). Contrary to the expectation HIF-1α level was found to be more intense at the intact edge than at the wounded edge.

We wanted to assess the role of possible signalling pathway/s in mediating the HIF-1α and hyperglycaemia regulated migration of HMVECad. Hence, the migration was assessed using p42/p44 MAPK, PKC$_{βII}$ and PI3K signal inhibitors in hypoxia as it was well established that hypoxia not only stimulates the migration but also activates HIF-1 system. Further, HMVECad were stained in the presence of inhibitors for the expression of HIF-1α in order to understand how different signalling pathways regulated the expression of HIF-1α in H5mM (Fig.5.11 A&B) and H20mM (Fig.5.12 A&B) conditions. HIF-1α was localised as expected in the nuclei of untreated cells (Fig.5.11Aa & 5.12Aa) in H5mM condition in both intact and wounded edges. Unlike previous set of experiments, equal number of cells if not more, expressed nuclear localisation than perinuclear localisation of HIF-1α in the presence of H20mM condition (Fig.5.11Ba & 5.12Ba). Further, when the stain was quantified (Fig. 5.13) no difference in the quantity of HIF-1α was observed between H5mM and H20mM conditions in untreated cells.

The PI3Ki treated cells from both the intact and wounded edge, migrated significantly less than other treatments and untreated cells (Fig.5.10). This clearly indicates that PI3K activation is central to the migration and re-endothelialisation induced by hypoxia and this observation is consistent with previous reports (Fitsialos et al. 2008, Woodward et al. 2009). The involvement of PI3K in mediating the HIF-1α dependant migration of endothelial cells was confirmed by the consistent decrease in the expression of HIF-1α in PI3Ki treated cells compared to untreated cells (Fig.5.13). The mediatory role of PI3K in regulating the expression of HIF-1α has been reported by other workers as well (Mottet et al. 2003, Yang et al. 2009). Inhibition of PI3K-Akt pathway could be aggravating the decrease in the migration induced by high glucose through degrading the HIF-1α as few PI3Ki treated cells expressed HIF-1α in nucleus (Fig.5.11Bd &5.12Bd), not the extent of untreated cells (Fig.5.13). This observation is consistent with previous reports where the inhibition of PI3K pathway has been reported to be detrimental in mediating the effects of high glucose in migration of cells (Yu et al. 2006). Interestingly, more of HIF-1α was expressed by the re-endothelializing PI3K inhibited cells from the wounded edge in H20mM compared to their counterparts in H5mM condition (Fig.5.13).

Although many reports support the role of p42/p44 MAPK pathway in mediating the effects of hypoxia and HIF-1α (Richard et al. 1999), p42/p44 MAPK inhibition did not impact the migration (Fig.5.10) in hypoxia alone in HMVECad. The presence of elevated glucose levels continued to decrease the migration further when treated with p42/p44 MAPKi or PI3Ki (Fig. 5.10). This indicates that the inhibition of MAPK along with PI3K

pathway aggravates the deleterious effect of glucose on the migration in the presence of hypoxia. The decreased activation of p42/p44 MAPK has been implicated in reducing the tube formation by glycated bFGF (Duraisamy et al. 2001). The decrease in the migration due to inhibition of p42/p44 MAPK could be due to reduced production of VEGF and decreased activity of HIF-1α during hyperglycaemia (Gupta et al. 1999, Yun et al. 2009). The role of p42/p44 MAPK pathway in mediating the effects of hypoxia and/or hyperglycaemia remain unclear as it did not produce any conclusive effect either on the migration or on the expression of HIF-1α. These results are not surprising as p42/p44 MAPK is known to mediate proliferation and differentiation effects and p38 MAPK pathway has been implicated in mediating the migration of cells (Rousseau et al. 1997). However, regulation of HIF-1α remained puzzling as it has been reported to be regulated by p42/p44 MAPK (Richard et al. 1999). This population of cells could possibly were affected by different set of signalling pathways than p42/p44 MAPK.

The inhibition of PKC pathway led to the reversal of high glucose effects in migration indicating that glucose caused HIF-1α degradation via activation of PKC pathway as PKC$_{\beta II}$/EGFRi treated cells expressed HIF-1α in high glucose compared to normal glucose levels. These results confirm that the production of ROS via *de novo* synthesis of DAG and subsequent activation of PKC pathway is central to the harmful effects of high glucose (Brownlee 2005). The perinuclear HIF-1α expression in PKC$_{\beta II}$/EGFRi treated cells suggests that the phopsphorylation of PKC$_{\beta II}$ may have a role in the nuclear translocation of HIF-1α into the nucleus. Hyperglycaemia is known to not only induce the activation of PKC$_{\beta II}$ pathway but also the formation of ROS in HUVECs (Gallo et al. 2005). Further, the beneficial effects of PKC inhibitor was demonstrated when it reduced the microvascular complications of hind limbs in STZ induced diabetic mice through the increased expression of PDGF (Tanii et al. 2006). Although the migration of PKC$_{\beta II}$/EGFRi treated cells from wounded edge decreased, the expression of HIF-1α did not diminish in comparison to untreated cells in H20mM condition. This clearly indicates that deleterious effects of glucose in decreasing the migration were mediated at least partially through the activation of PKC pathway via HIF-1α.

5.6 Conclusion

Hyperglycaemia results in decreasing the migration compared to hypoxia alone due to retarded transcriptional activity of HIF-1 either because of failure in nuclear translocation or degradation of HIF-1α. This activity was mediated by PKC$_{\beta II}$ pathway. The p42/p44 MAPK pathway aggravated the effects of high glucose whereas PI3K pathway might be a mediator for either aggravating the effects of high glucose and/or for the inhibition of angiogenic stimulant effects of hypoxia. The role of cytoplasmic expression of

p27^{Kip1} during the migration of cells needs a further probing. As ROS are known to be a common source of both hypoxia and hyperglycaemia, in the next chapter effect of silymarin, an antioxidant on the migration of HMVECad is evaluated.

Chapter 6 - Effect of silymarin on the migration of endothelial cells

6.1 Hypothesis

Antioxidant, silymarin [*Silybum marianum* (L.)] will have a beneficial effect on high glucose induced decrease in the migration of HMVECad.

6.2 Introduction

Silymarin complex consisting of seven different flavonolignans and a flavanoid has been in use as a hepatoprotective agent and as an antioxidant for many years (Comelli et al. 2007, Post-White, Ladas and Kelly 2007). Silymarin produces its anti-oxidant effects through various ways. It has been shown to increase many anti-oxidant enzymes such as superoxide dismutase (SOD), glutathione peroxidase (GSHPx), glutathione reductase (GR) and catalase (CAT) as well as decreasing the levels of serum alanine aminotransferase (ALT), aspartate amino transferase (AST), alkaline phosphatase (ALP) and total bilirubin which help in the elimination of ROS (Comelli et al. 2007, Eminzade, Uraz and Izzettin 2008). Silymarin has started to receive attention not only as a hepatoprotective adjuvant for cancer therapy but also because of its antiangiogenic effects (Ramasamy and Agarwal 2008, Singh, Gu and Agarwal 2008). Silibinin, the main component of silymarin has been shown to produce antiangiogenic effects by decreasing the expression of many angiogenic stimulants such as HIF-1α, iNOS, PECAM-1, VEGF, down regulation of VEGFR1 (Raina et al. 2008) and by increasing the expression of TIMP-1 and 2 which are inhibitors of MMPs and ANG-2 and Tie-2 (Tyagi et al. 2009). The anticancerous effects were mediated by the inhibition of the phosphorylation of p38, JNK1/2 and ERK1/2 MAPK and PI3K-Akt pathway (Garcia-Maceira and Mateo 2009, Gu et al. 2005). However, beneficial effects of silibinin in non-cancerous cells such as glial cells, cardiac myocytes and neutrophils are regulated by PKC activity along with other pathways (Tsai et al. 2010, Varga et al. 2004, Zhou et al. 2007).

The anti-diabetic effects of silymarin remain untested to a large extent. Silymarin is known to produce its anti-diabetic effects by acting as a cytoprotectant of pancreatic cells, as an anti-oxidant and by inhibition of hepatic glucose formation (Guigas et al. 2007, Soto et al. 2003, Soto et al. 2004 and Soto et al. 2010). Silymarin has also been proved to provide the cytoprotective effect to HUVECs against hypoxia as well as high glucose (Weidmann 2008). Hypoxia and high glucose are known to produce their effects by inducing the production of ROS (Li et al. 2010). As silymarin is a known antioxidant, the effects of silymarin on the migration of endothelial cells in the presence of high glucose and/or low oxygen tension are tested in this chapter.

6.3 Materials and methods

The migration of HMVECad was assessed in the presence of silymarin (SM) (50µM) (in 0.5% v/v of DMSO) and α-lipoic acid (aLA) (100 µM) (in 0.5% v/v of ethanol)

(Weidmann 2008). Alpha lipoic acid was used as a positive control to compare with silymarin treatment. DMSO and ethanol were used as a vehicle control for SM and aLA treatment respectively. The migration was assessed by both the radial migration assay and wound healing assay as explained in section 2.2.3 and 2.2.4 respectively. The migration of endothelial cells was assessed in 20% O_2 tension and 5mM glucose (N5mM), 20% O_2 tension and 20mM glucose (N20mM), 5% O_2 tension and 5mM glucose (H5mM) and 5% O_2 tension and 20mM glucose (H20mM) conditions. All the results are presented as net migration (mean ± SEM) in micrometers and analysed using SPSS 15.0.

6.4 Results

6.4.1 Effect of silymarin on the migration of HMVECad by radial migration assay

The vehicle control (DMSO) for silymarin, did not significantly alter endothelial cell migration (Fig. 6.1a & b) when compared to control. The migration pattern was found to be similar to that explained in section 4.4.1.; the migration (μm) of untreated endothelial cells was lower ($p<0.001$) for N20mM (24 h: 57 ± 1.3; 48 h: 117.2 ± 1.5) in comparison to that of N5mM (24 h: 78.4 ± 0.8; 48 h: 133.9 ± 0.9) condition for both 24 and 48 h. The migration was high ($p<0.001$) for H5mM (24 h: 101.4 ± 1.1; 48 h: 174.6 ± 1.5) compared to N5mM condition for 24 and 48 h. When hypoxia and high glucose concentration (H20mM) (24 h: 72.2 ± 1.1; 48 h: 136.3 ± 1.3) were combined the migration was lower ($p<0.001$) than that of hypoxic and normal glucose (H5mM) level for both 24 and 48 h.

The results show that the addition of silymarin (50μM) increased the migration of cells in N20mM (24 h: 100.4 ± 1.0; 48 h: 178.3 ± 1.6) condition and was found to bring the migration (μm) level to those in N5mM (24 h: 99.9 ± 0.8; 48 h: 172.7 ± 2.0) condition. However, the migration of cells in H5mM (24 h: 117.9 ± 1.4; 48 h: 208.9 ± 5.6) condition was found to be more ($p<0.001$) than those in N5mM condition as with the untreated cells. Like in normoxia, the migration of cells in H20mM (24 h: 115.5 ± 1.3; 48 h: 198.5 ± 2.0) condition was brought to the level of H5mM condition and no significant difference was found between the two conditions. The number of observations (n = 40) recorded for H5mM and H20mM at 48 h was less due to the limitation of image size that could have been captured within the image frame, which was explained in section 3.2.3. The migration of untreated cells in all conditions was significantly ($p<0.001$) lower compared to respective condition of silymarin treated cells. The silymarin treatment increased the migration level of HMVECad in 20mM condition under both normoxia and hypoxia to that of 5mM condition. These results confirm the ability of the silymarin to overcome the high glucose induced decrease in the migration of microvascular endothelial cells.

Fig. 6.1 Effect of silymarin (50µM) on the migration HMVECad were cultured in conditions of 5 or 20mM glucose and 20 (Normoxia – N) or 5% (Hypoxia – H) oxygen tension. The migration was assessed by the radial migration assay. The silymarin significantly increased (p<0.001) the migration for all the conditions compared to respective condition of untreated cells. The results are presented as net migration (mean ± SEM) of cells at 24 (a) and 48h (b) and analysed by analysis of variance (ANOVA) followed by Bonferroni post hoc test.

(***p<0.001 when compared as indicated; NS = not significant)

v.c. (DMSO) 24 & 48h: N5mM=160; N20mM=120; H5mM=180; H20mM=180

SM 24 & 48h: N5mM=180 & 120; N20mM=180; H5mM=180 & 40; H20mM=140 & 40)

a)

b)
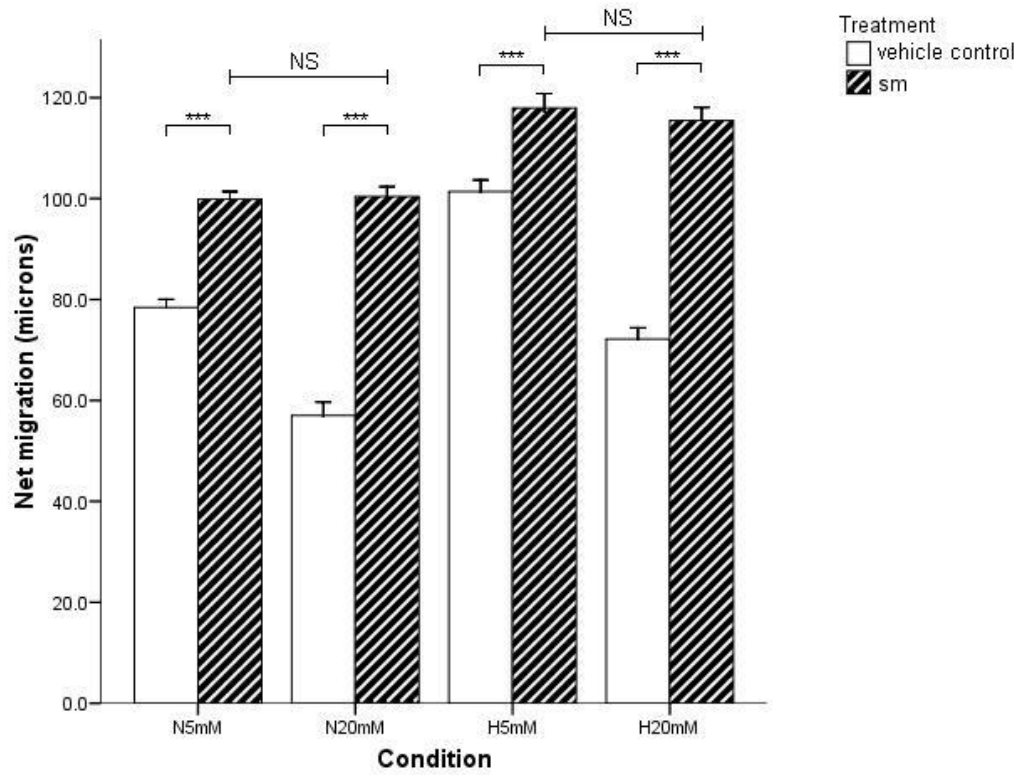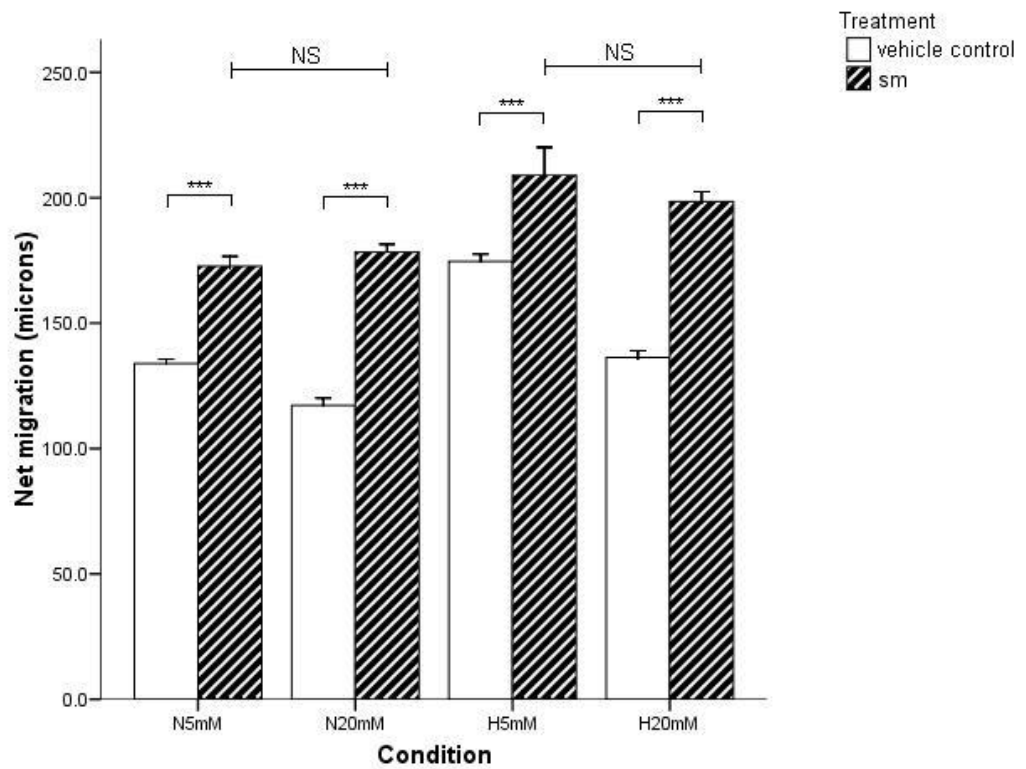
6.4.2 Effect of α - lipoic acid on the migration of HMVECad by radial migration assay

The migration of HMVECad in the presence of vehicle control (ethanol) (Fig. 6.2a & b) was comparable to those found with DMSO. The migration (μm) in N20mM condition (24 h: 62.1 ± 1.3; 48 h: 110.5 ± 1.6) was lower ($p<0.001$) and that of H5mM (24 h: 105.9 ± 1.9; 48 h: 175.5 ± 2.6) condition was higher ($p<0.001$) in comparison with the N5mM (24 h: 73.7 ± 0.8; 48 h: 136.8 ± 1.7) condition for both 24 and 48 h. When hypoxia and high glucose concentration (H20mM) were combined (24 h: 74.1 ± 0.6; 48 h: 138.3 ± 0.9) the migration was lower ($p<0.001$) than that of hypoxic and normal glucose level (H5mM) at 24 and 48 h.

Unlike silymarin, aLA (100μM) failed to overcome the decrease in the migration (μm) of N20mM (24 h: 73.8 ± 0.8; 48 h: 129 ± 1.2) cells compared to those of N5mM (24 h: 77.4 ± 0.8; 48 h: 144.4 ± 0.9) cells (24 h: $p<0.05$; 48 h: $p<0.001$). Similarly, there was a significant decrease ($p<0.001$) for both 24 and 48 h in the migration of cells incubated in H20mM (24 h: 82.5 ± 0.9; 48 h: 144.1 ± 1.3) condition compared to H5mM (24 h: 92.2 ± 1.3; 48 h: 165.8 ± 2.0) condition. However, hypoxia (H5mM) was still able to drive the migration of the cells further ($p<0.001$) than those of normoxia (N5mM).

Alpha lipoic acid treatment was found to significantly (N5mM: 24 h - $p<0.01$ & 48 h - $p<0.001$, N20mM: 24 & 48 h - $p<0.001$) increase the migration under normoxic condition when compared to those of untreated cells of same conditions. However, in H5mM condition the migration at 24 ($p<0.001$) and 48 h ($p<0.01$) was found to be less than that of untreated cells. For the cells incubated in H20mM condition, the migration due to aLA treatment was again found to be high at 24 ($p<0.001$) and 48 h ($p<0.001$) compared to those of untreated cells of the same condition. As aLA failed to overcome the high glucose induced decrease in the migration, it was decided to continue to work with silymarin and the aLA was not used any further.

Fig. 6.2 Effect of α- lipoic acid (100µM) (aLA) on the migration HMVECad were cultured in conditions of 5 or 20mM glucose and 20 (Normoxia – N) or 5% (Hypoxia – H) oxygen tension. The migration was assessed by the radial migration assay. Alpha lipoic acid significantly increased the migration of all conditions except H5mM condition, compared to the respective condition of untreated cells. The results are presented as net migration (mean ± SEM) of cells at 24 (a) and 48 h (b) and analysed by analysis of variance (ANOVA) followed by Bonferroni post hoc test.

(*$p<0.05$, **$p<0.01$ & ***$p<0.001$ when compared as indicated)

(v. c. (ethanol) 24 & 48 h: N5mM=180; N20mM=160; H5mM=140; H20mM=180

aLA 24 & 48 h: N5mM = 180; N20mM = 180; H5mM = 160; H20mM = 160)

a)
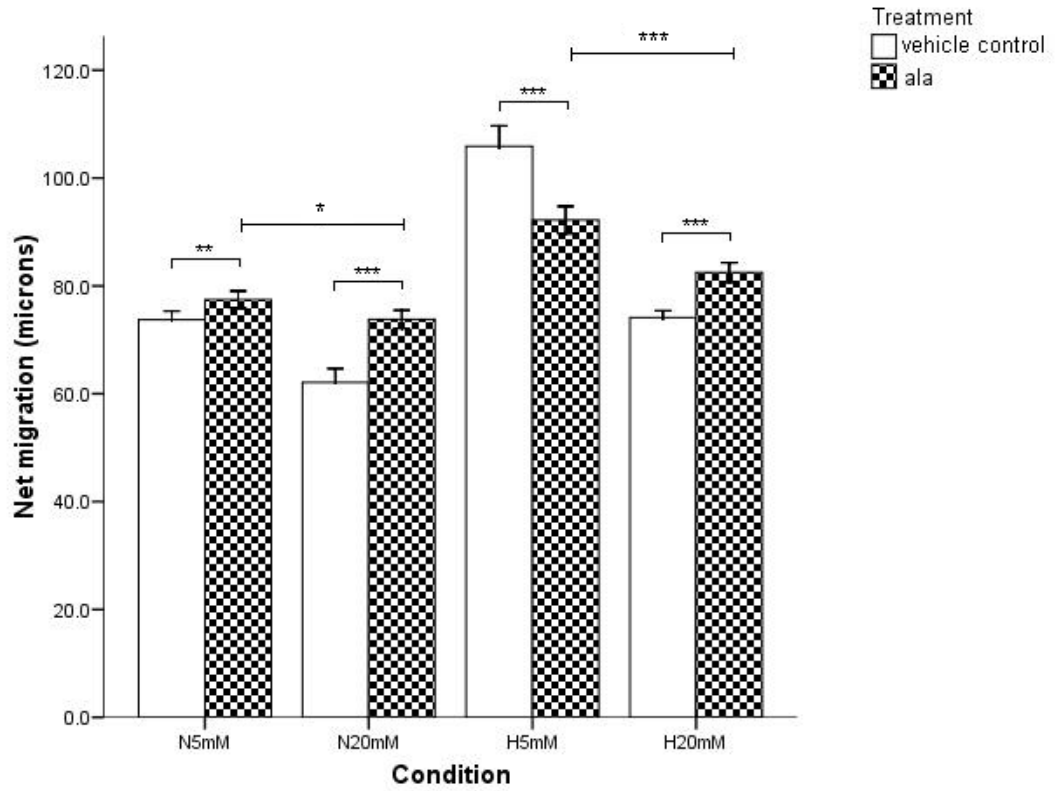
b)
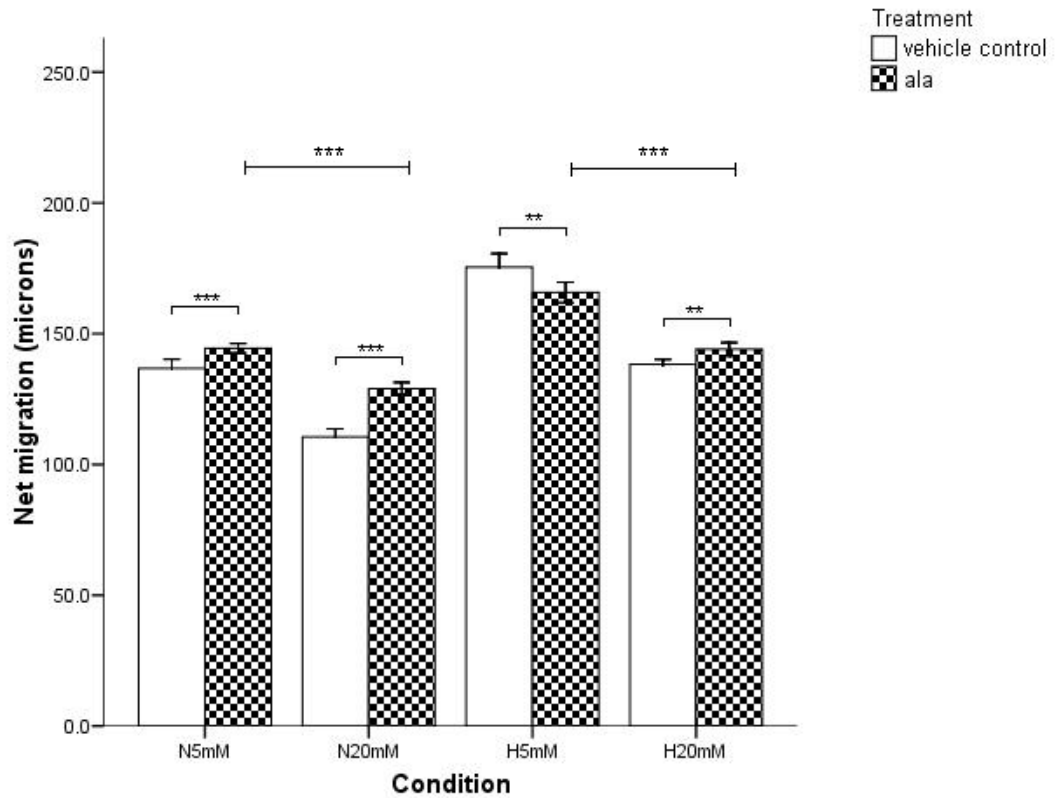
6.4.3 Effect of silymarin on the migration of HMVECad by the wound healing assay

The effect of silymarin (50μM) on HMVECad migrating from the intact and wounded edges of the semicircular monolayer was assessed by the wound healing assay.

Like with the radial migration assay, the vehicle control (DMSO) for SM on its own did not alter the trends of endothelial cell migration (Fig 6.3a & b) from intact or wounded edge of the layer. The migration pattern for vehicle control was found to be similar to that explained in the earlier section (6.4.1) of this chapter. The migration (μm) of endothelial cells from the intact edge was lower ($p<0.001$) under N20mM (24 h: 82.4 ± 1.9; 48 h: 160.3 ± 3.2) condition in comparison to that of N5mM (24 h: 100.2 ± 2; 48 h: 192.2 ± 4.7) condition for both 24 and 48 h. The migration was higher ($p<0.001$) in H5mM (24 h: 136.6 ± 2.7; 48 h: 237.6 ± 3.9) condition compared to that of N5mM condition at both 24 and 48h. When hypoxia and high glucose level were combined (H20mM) (24h: 95.6 ± 3.9; 48h: 191.5 ± 4.5) the migration was lower ($p<0.001$) than that of hypoxic and normal glucose level (H5mM) for 24 and 48 h.

The migration (μm) of cells from the wounded edge of the same monolayer was measured. The same patter of migration (N5mM; 24 h: 131.9 ± 4.2; 48 h: 227.9 ± 4.6, N20mM; 24 h: 107.5 ± 2.9; 48 h: 187.7 ± 4.2, H5mM; 24 h: 165 ± 3.3; 48 h: 262.7 ± 4.3 and H20mM; 24 h: 125.5 ± 4.3; 48 h: 224.2 ± 4.5) was observed for cells migrating from the wounded edge of the layer (Fig. 6.3a & b). When the migration of untreated cells were compared between the intact and wounded edges of the monolayer, it was observed that the wounded edge cells migrated significantly ($p<0.001$) faster than those on non wounded edge for all the conditions and time points.

The results (Fig. 6.3a & b) for the intact edge of the layer show that the silymarin treatment increased the migration (μm) in N20mM condition (24 h: 95.9 ± 3.3; 48 h: 190.5 ± 4.2) and was found to be on par with those of N5mM (24 h: 97.4 ± 3.9; 48 h: 169.1 ± 5.3) at 24 h. However, the migration of cells from the intact edge in N20mM condition was significantly increased ($p<0.01$) beyond the migration in N5mM condition after 48 h. The migration of cells incubated in H5mM (24 h: 120.2 ± 2.6; 48 h: 208.6 ± 3.9) condition was found to be significantly higher ($p<0.001$) than those of N5mM condition. Under hypoxic conditions, silymarin halted the effect of hyperglycaemia on the migration of cells in H20mM (24 h: 122.2 ± 3.1; 48 h: 221.5 ± 4.3) condition at 24 and 48 h and brought it to the level of H5mM condition.

The silymarin treated cells migrating from the wounded edge of the layer followed the same pattern as those from the intact edge for all the conditions and time points (N5mM; 24 h: 122.4 ± 2.1; 48 h: 215.1 ± 3.5, N20mM; 24 h: 129.5 ± 3; 48 h: 235.5 ± 3.1, H5mM; 24 h: 148.7 ± 2.8; 48 h: 266.5 ± 4.1 and H20mM; 24 h: 159.6 ± 4; 48 h: 269.1 ± 4.3). Like with the cells of intact edge, the silymarin treatment caused an increase in the

migration of cells in N20mM condition beyond that in N5mM condition of the wounded edge at 48 h. Like untreated cells, it was observed that the silymarin treated cells of the wounded edge migrated faster ($p<0.001$) than those of unwounded edge of the same monolayers for all conditions and time points.

The difference in the migration of the untreated and silymarin treated cells from intact edge did not reach significance at 24 h in N5mM condition. However by the end of 48 h the silymarin treated cells from the intact edge had migrated less ($p<0.01$) than those of untreated cells. The difference in the migration of the untreated and treated cells migrating from the wounded edge did not reach significance at both time points. In N20mM condition, the migration of cells in the presence of SM was significantly higher than those of untreated cells for both the intact (24 h: $p<0.01$ 48 h: $p<0.001$) and wounded edges (24 & 48 h: $p<0.001$) and for both time points. In H5mM condition at 24 and 48 h, SM treated cells migrated slower from the intact edge (24 h: $p<0.01$, 48 h: $p<0.001$) compared to those of untreated cells. Surprisingly, SM treated cells from the wounded edge migrated slower at 24 h ($p<0.01$), but covered more distance in the next 24 h hence no difference was found between the treated and untreated cells at the end of 48 h. Similar to N20mM condition there was a significant difference ($p<0.001$) between the untreated and treated cells at H20mM condition at both time points as silymarin negated the effect of hyperglycaemia on reducing migration distance. It was noted that the migration of untreated cells from the intact edge of the wounded semicircular monolayer (Fig. 6.3a & b) was significantly ($p<0.001$) higher than that of intact circular monolayer (Fig. 6.1a & b)

Fig. 6.3 Effect of silymarin (50μM) on the migration of HMVECad from intact and wounded edges Migration in conditions of 5 or 20mM glucose and 20 (Normoxia – N) or 5% (Hypoxia – H) oxygen tension was assessed by the wound healing assay. The silymarin significantly increased ($p<0.001$) the migration of 20mM conditions compared to respective conditions of untreated cells. The results are presented as net migration (mean ± SEM) of cells at 24 (a) and 48 h (b) and analysed by analysis of variance (ANOVA) followed by Bonferroni post hoc test.

(**$p<0.01$, *** $p<0.001$ when compared as indicated; NS = not significant)

(v.c. intact edge and wounded edge (24 & 48h): N5mM = 60 & 90; N20mM = 60 & 90; H5mM = 60 & 90; H20mM = 40 & 70

SM intact edge (24 & 48h): N5mM = 40 & 70; N20mM = 40 & 60; H5mM = 50 & 70; H20mM = 50 & 70

SM wounded edge (24 & 48h): N5mM = 50 & 70; N20mM = 40 & 70; H5mM = 60; H20mM = 60 & 80)

a)
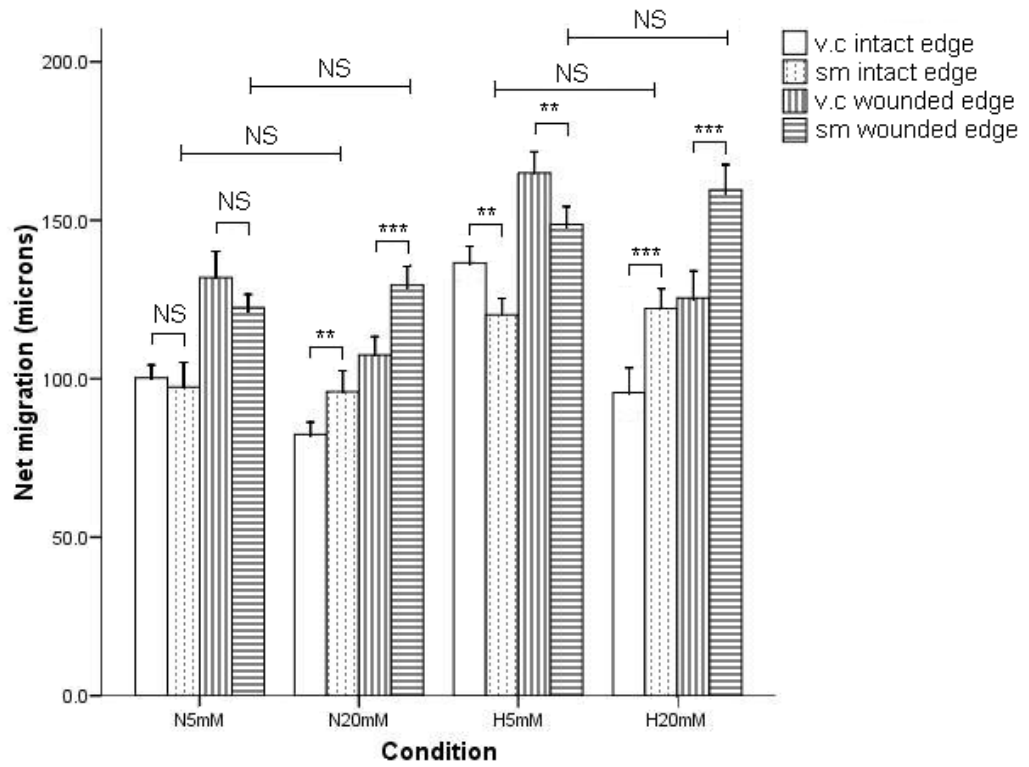
b)
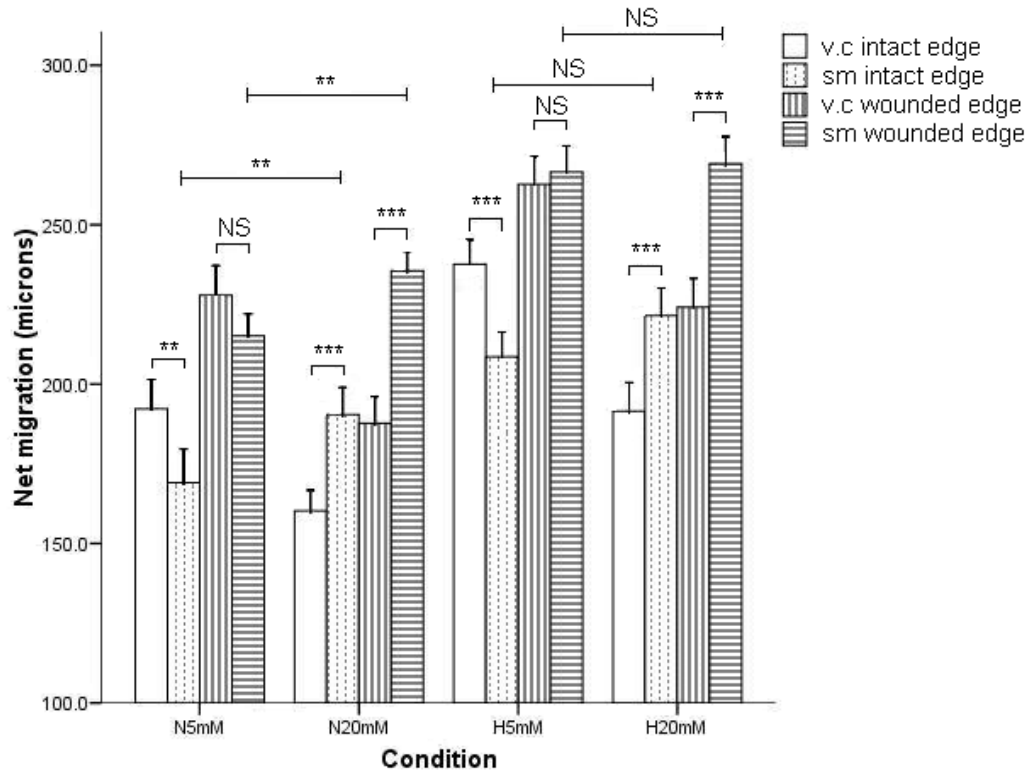
6.5 Discussion

Silymarin successfully restored the high glucose induced decrease in the migration of HMVECad in the presence of both normoxia and hypoxia. This observation was true for both radial migration and the wound healing assay. The migration of silymarin treated HMVECad in hypoxia compared to normoxia was not consistent as it was contradictory between the radial migration and wound healing assay. Further, the results indicated that α-lipoic acid was not sufficiently effective in restoring the negative trend of migration due to high glucose.

It has been proven from the data presented in chapter 4 that high glucose and low oxygen tension have opposing effects on the migration of HMVECad. The migration of cells treated with vehicles (untreated) (Fig.6.1 & 6.2) resembled the trends explained in chapter 4. However, there are no reports to the best of our knowledge, detailing the role of silymarin in endothelial cell migration or angiogenesis during diabetes, although it has been proved to have beneficial effects in diabetes (Soto et al. 2010). It has been confirmed from chapter 5 that the over activation of PKC pathway mediated the deleterious effects of high glucose whereas activation of PI3K is essential to induce the migration in hypoxia.

Hyperglycaemia is known to cause the production of ROS which in turn over activates different pathways including DAG dependant PKC pathway which leads to glucotoxicity (Brownlee 2001). High glucose causes not only the production of ROS via over activation of $PKC_{\beta II}$ but also its translocation from cytosol to the membrane (Gallo et al. 2005). Silibinin has been proved to produce its anti-oxidant activity by inhibition of DAG dependant PKC translocation and NADPH activity (Varga et al. 2004). It is also known that the inhibitors of PKC prevent the formation of various ROS in endothelial cells (Pricci et al. 2003). Further, increased production of ROS in hyperglycaemia leads to the dysfunction of HIF-1α with subsequent impairment in the expression of target genes such as VEGF and PDGF (Thangarajah et al. 2010). This could possibly suggest that silymarin restored the migration of HMVECad (Fig.6.1 &6.3) in high glucose by inhibition of the production of ROS via reduced activation of $PKC_{\beta II}$ pathway and restoration of HIF-1α activity. However, it was surprising to note the inability of aLA (Fig.6.2) to produce any effect on the high glucose induced decrease in the migration, as it is a established strong anti-oxidant capable of interfering with the production of ROS and subsequent activation of $PKC_{\beta II}$ along with other oxidative markers (Ihnat et al. 2007).

The results (Fig.6.1) suggest that silymarin treated cells increased the migration compared to untreated cells in both normoxia and hypoxia. Hypoxia causes an increase in the production of ROS and activation of PI3K leading to the increase in the migration of cancer cells due to increased transcriptional activity of HIF-1α (Koshikawa et al. 2009).

However, during the normal wound healing process hypoxia is desirable as it stimulates angiogenesis in order to re-establish the supply of oxygen and nutrients to the wounded tissue (Falanga 2005). The inhibition of PI3K attenuated hypoxia induced migration as noticed in chapter 5. Hence, silymarin could be causing the increase in the migration by either by its ability to scavenge the free radicals or through the mechanisms other than PI3K-Akt pathway. However, the increased migration was not consistent when the wounded monolayers were treated with silymarin (Fig.6.3). The cells in hypoxia from intact and wounded edge migrated significantly lesser than untreated cells. These conflicting results make the interpretation difficult. Further, there are no reported evidences about the pro-angiogenic effects of silymarin. On the contrary, the anti-angiogenic effects of silymarin find reasoning in the literature, which suggest that silymarin or its main constituent silibinin decreases the migration. Singh et al. (2005) suggests that silibinin produces its anti-angiogenic effects through multiple ways in both HUVEC and HMVEC (Singh et al. 2005). It has been suggested that silibinin inhibits the proliferation of HUVECs by the over expression of p27^{Kip1}, p21^{Cip1} and p53 and causes apoptosis by increasing the activity of caspase 3 and 7 and decreasing survivin activity (Singh et al. 2005). Further, silibinin has also been shown to cause a decrease in angiogenic stimuli by decreased MMP-2 mediated migration and tube formation through the inhibition of the Akt pathway and NF-κβ pathways (Singh et al. 2005). Anti-angiogenic effects of silymarin or silibinin are attributed to inactivation or inhibition of HIF-1α, PI3K-Akt pathway, ERK1/2, JNK1/2 and p38 MAPK (Chen et al. 2005, Garcia-Maceira and Mateo 2009, Gu et al. 2005).

6.6 Conclusion

It could be possible that silymarin is restoring the high glucose induced decrease in the migration through its free radical scavenging activity via PKC$_{βII}$ inhibition and restoration of HIF-1α activity. Successful restoration of the migration in high glucose by silymarin suggests that it could be a candidate for therapeutic angiogenesis, hence formulated as a topical application with an aim of developing it as a therapeutic agent for delayed wound healing of diabetes.

Chapter 7 - Formulation of silymarin wafers

7.1 Hypothesis

Gamma ray irradiated lyophilised wafer discs containing silymarin restore the high glucose induced reduction of endothelial cell migration compared to control wafer discs.

7.2 Introduction

Wound dressings developed over many years are classified into different categories depending on their content, physical form and their function (Boateng et al. 2008). Different agents such antimicrobials, growth factors and supplements are used to medicate the wound dressings (Boateng et al. 2008). Freeze-dried fibrin discs containing growth factors were reported to enhance endothelialisation (Kumar and Krishnan 2002) and those containing tetracyclins were successfully used as subcutaneous implants to control infection during wound healing in mice with steady release of the drug into the serum (Kumar, Vasantha Bai and Krishnan 2004). Similarly topical application of vitamins A, E and C has shown to improve wound healing in rats (Porto da Rocha et al. 2002). Lyophilised or freeze-dried formulations are a promising topical drug deliver system for the application of therapeutic agents used to treat recalcitrant diabetic wounds. Wafers can be developed to contain a variety of medication using freeze-dried polymers as topical vehicles (Matthews et al. 2005, Matthews et al. 2008). Silymarin or silibinin has been used topically to treat contact dermatitis and photocarcinogenesis in experimental animals (Han et al. 2007, Mallikarjuna et al. 2004). However, freeze-dried products containing silymarin for the topical treatment of diabetic wounds has not been reported.

Natural polymers are widely used as vehicles in many different formulations. Selection of a vehicle is critical as some vehicles themselves may have a therapeutic effect. A freeze-dried chitosan film with and without bFGF was beneficial when applied on full-thickness wounds created on the backs of genetically diabetic mice until day five indicating that the vehicle itself may also have an effect on the wound healing (Mizuno et al. 2003). TGF-β1 was incorporated in phosphate buffered saline/poloxamer gel formulations, duoDERM hydroactive paste and in a poly (ethylene oxide) hydrogel and tested for wound healing activity in diabetic rats. Poloxamer gel formulations containing TGF-β1 showed improved wound healing in diabetic rats with sustained release of drug suggesting the importance of the carrier used in drug delivery (Puolakkainen et al. 1995). Polymers can also be used as vehicles for RNA interference constructs (Werth et al. 2006). Xanthan gum and sodium alginate with methylcellulose have been successfully used to prepare freeze-dried wafers for wound models (Matthews et al. 2005, Matthews et al. 2006).

Characterisation of physical properties of freeze-dried formulations is essential in order to understand drug/vehicle interactions, flow properties and drug release profile.

Some of the procedures such as thermal analysis and rheology are helpful in understanding the physical properties of freeze dried wafers and their contents (Matthews et al. 2008). The flow properties of the vehicle and other contents of topical applications determine the residence time of a drug when applied to the wound surface. The formulations for wound treatment would be effective if they establish an adherence to the wound site with prolonged residence time (Jones, Lawlor and Woolfson 2003). Other physical properties such as water vapour transmission, gaseous exchange, water absorption (from the wound surface) and adherence (to the wound site) are also of interest (Gatti, Pinchiorri and Monari 1994). These properties also serve as valuable guidance dictating the selection of materials.

Therapeutic agents used in the treatment of chronic wounds of diabetes needs to be sterile in order to keep the bacterial load to the minimum at the wound site. Any topical application desirous of containing either anti-bacterial or proteinaceous growth factor or any other medication sensitive to heat can not be autoclaved or heat sterilised as the contents may not remain stable after sterilisation (Traub and Leonhard 1995). However the preparations can be sterilised by other method such as gamma irradiation while maintaining the stability of heat labile contents (Matthews et al. 2006). Gamma rays generated from Co-60 are widely used in industry to sterilise many pharmaceutical preparations, surgical instruments and cell culture materials. Gamma irradiation has been reported to affect stability and properties of few materials. The viscosity of extruded products containing xanthan gum increased when irradiated and those containing starch displayed increased expansion when exposed to ionising radiation (Hanna et al. 1997). The viscosity and molecular weight was reduced and chain breaking increased, with a change in colour, when alginate solution was exposed to gamma rays (Lee et al. 2003). The rheological properties of freeze-dried wafers containing xanthan gum remained largely unaffected when exposed to 40kGy of gamma radiation where as those composed of sodium alginate displayed reduced viscosity (Matthews et al. 2006). The ability of xanthan gum to withstand ionising radiation and its ability to potentially produce enhanced residence time at a wound site due to its viscous nature makes it an ideal vehicle for freeze dried products.

This chapter deals with the preparation of freeze dried wafer discs composed of xanthan gum as a vehicle and silymarin and α-lipoic acid as active ingredients. The pre- and post-lyophilised gels were rheologically characterised by continuous flow measurements. Freeze dried wafer discs were tested on the wound healing model following gamma ray sterilisation.

7.3 Materials and methods

7.3.1 Preparation of lyophilised wafers

Polymer gels of xanthan gum (XG), guar gum (GG), ghatti gum (GhG), locust bean gum (LbG), karaya gum (KG) and sodium alginate (SA) were prepared at concentrations of 1.5, 2, 7, 1.5, 3 and 5% (w/v) respectively. The gels containing these polymers were prepared by dissolving them in pre-heated (~ 40 ^{0}C) distilled water in a stainless steel beaker. Distilled water was heated by placing the beaker on a hot plate and the polymer was added and stirred with a mechanical overhead stirrer at 500rpm. The resulting gel was used for rheological characterisation as explained in 7.3.2.

XG (1.5% w/v) was chosen as a vehicle to prepare the lyophilised wafers containing silymarin (SM) or α-lipoic acid (aLA). Wafers were prepared at concentration of 50 and 100 µM of SM and aLA respectively, for further testing with endothelial cells. Pluronic F68 was used to aid suspension of SM and aLA as they are insoluble in water. Gels were prepared by dissolving Pluronic F68 (0.2% w/v) in distilled water in a stainless steel beaker, followed by the addition of SM (0.07% w/v) or aLA (0.06% w/v). Different components and their ratio in gels used for the preparation of the wafers are tabulated in Table 7.1. The contents were stirred using a Silverson turbine mixer for 0.5 h at room temperature (22 ^{0}C). XG (1.5% w/v) was added and the beaker was left overnight in the fridge at ~4 ^{0}C to form a weak gel. Roller mixture was used to get homogenous suspension of SM and aLA gels.

Samples of prepared gel suspensions (4g) were poured to each well of a 6-well plate, avoiding the formation of bubbles for freeze drying. Gel suspensions were lyophilised in a laboratory scale freeze drier (VirTis adVantage, Biopharma Process Systems, Hampshire, UK) with shelf cooling. Gels were cooled to -50 ^{0}C and then heated to room temperature by a series of thermal ramps under reduced pressure. Primary drying removed the frozen water by sublimation and the remaining non-freezing water was removed by desorption to the gas phase. The freeze drying process was carried out over 26 hours and a temperature profile of the process is charted in Fig. 7.1 Resulting lyophilized wafers were pressed to a paper-thin size and punched to make discs using a paper punch. Wafer discs (~5mm in size and ~1.5mg in weight) were placed in self-sealable polythene bags and stored at room temperature.

Table 7.1 Contents of gels used to prepare lyophilised wafers The wafers containing silymarin (SM) or α-lipoic acid (aLA) as active pharmaceutical ingredient (API) were prepared using xanthan gum (XG) as a vehicle and non-ionic surfactant Pluronic F68 as a suspending agent. Vehicle control (v.c.) wafers contained no API.

Batch No.	Component ratio (%) in gels XG : F68 : API (API=SM/aLA)	Calculated solids in each wafer gel (4g) (mg)				Mean (± S.D) weight of wafer (mg) (n=6)
		XG	F68	API	Total	
1 (v.c.)	1.5 : 0.2 : 0.0	60	8	-	68	65.7 (±2.6)
2 (v.c.)	1.5 : 0.2 : 0.0	60	8	-	68	67.7 (±1.1)
3 (SM)	1.5 : 0.2 : 0.07	60	8	2.8	70.8	67.7 (±0.6)
4 (SM)	1.5 : 0.2 : 0.07	60	8	2.8	70.8	68.8 (±1.5)
5 (aLA)	1.5 : 0.2 : 0.06	60	8	2.4	70.4	68.5 (±0.8)
6 (aLA)	1.5 : 0.2 : 0.06	60	8	2.4	70.4	69.2 (±0.5)
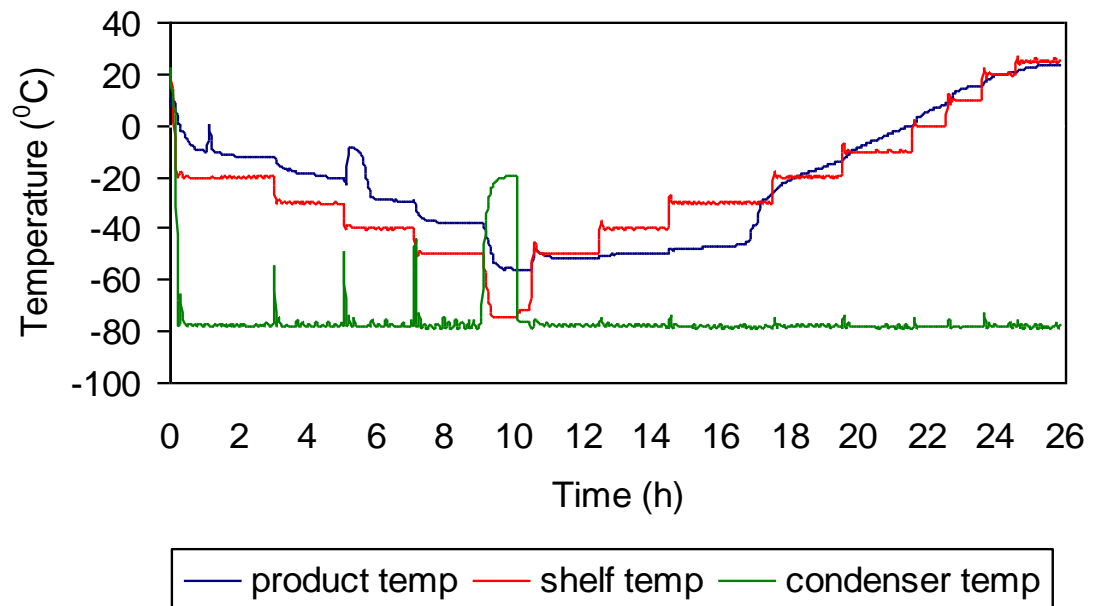
Fig. 7.1 Freeze-drying cycle The temperature profile of the freeze drying cycle for 26h was obtained during the preparation of the wafers. The pre-lyophilised gels were cooled to -50 °C and then heated to room temperature by a series of thermal ramps under reduced pressure.

7.3.2 Rheological properties of polymer gels

The rheological properties of pre-lyophilised polymer gels were measured using a dynamic rheometer (*AR1000*, TA Instruments). Gels formed from lyophilised wafers by the addition of volumetric amounts of distilled water to their original weight (i.e. 4g per well) were also rheologically characterised. Continuous flow rheometry tests were conducted at 25 ^{0}C. This test depends on the viscous drag exerted on the geometry, when it is rotated on the fluid to determine the apparent viscosity of the fluid. The geometry is composed of a wide-angle cone which spins centrally above a stationary plate giving torsional shear. A cone and plate geometry of 40mm/2^0 (steel) and truncation value of 57µm was used. Flow measurements were carried out at continuous shear rates ranging from 0 to 600s^{-1}. The results (rheograms) were a plot of shear rate vs. shear stress. The rheograms were analysed by the system software using the Herschel-Bulkley equation

$$\sigma = \eta'\gamma^n + \sigma_0$$

where σ is shear stress (Pa), η' the viscosity coefficient or consistency (Pa.s), γ the shear rate (s^{-1}), n the rate index (flow behaviour index) and σ_0 the yield stress (Pa).

7.3.3 Sterilisation of wafers

Wafers prepared as detailed in section 7.3.1 were irradiated with ultra violet rays (UVitec CROSSLINKER CL-500). Wafers were irradiated with UV rays at 0.36, 0.72, 1.5, 3.0, 6.0 and 12.0 J/cm^2. As the UV rays failed to sterilise the wafers, they were sterilised by gamma irradiation. Each batch of the control, SM and aLA wafers was divided into three lots packed as wafer discs in self-sealable plastic pouches. One lot was not irradiated to compare with other irradiated lots. One lot was irradiated with 25KGy, another with 40KGy of gamma rays (Isotron Plc, Swindon, UK) using Cobalt-60 as a source with an approximate dose rate of 5kGy/h.

After irradiation wafers were tested for the presence of bacteria and fungi. To test for the presence of bacteria, wafers were incubated in tryptone soya agar (TSA) (Oxoid, UK)[40g/l of TSA made up of tryptone 15g/l, soyapeptone 5g/l, sodium chloride 5g/l and agar 15g/l poured into Petri dishes and sterilised at 121^{0}C for 15 minutes] plates for 24h (Landry et al. 2001). To test for the presence of fungi wafers were incubated with sabouraud dextrose agar (SAB) (Oxoid, UK)[65g/l of SAB made up of mycologicalpeptone 10g/l, glucose 40g/l and agar 15g/l is poured into Petri dishes and sterilised at 121^{0}C for 15 minutes] plates for 48h (Landry et al. 2001).

7.3.4 Quantification of silymarin in the wafers

High performance liquid chromatography (HPLC) was used to quantify SM (Quaglia et al. 1999) present in non-irradiated, 25 and 40kGy irradiated wafer discs. The HPLC system used for the quantification of silymarin content was as follows:

Table 7.2 Components of HPLC equipment

	Components	Make
1	Pump	Jasco PU-1580
2	Column	Agilent Eclipse XDB-C18
3	Degasser	Jasco DG-980-50
4	Gradient Unit	Jasco – 1580 -02
5	UV-Visible Detector	Jasco UV-1500
6	Data acquisition and evaluation	Jasco Borwin 15.0

The standard (or calibration) curve was obtained by running SM solution, prepared by dissolving 0.0112g of silymarin in 50ml of solvent in a volumetric flask. The solvent (50ml) was composed of 32ml of solvent A (0.01% formic acid in deionised water), 6ml of solvent B (HPLC grade methanol) and 12ml of solvent C (HPLC grade acetonitrile). Solution was injected into a valve using a 50µl sample loop. Analyte produces five well defined peaks at λ value of 289nm and a flow rate of 1ml/min using the following gradient elution:

Table 7.3 HPLC gradient elution used to analyse silymarin

Time	% water	% methanol	% acetonitrile
0	68	12	20
10	68	12	20
15	50	20	30
20	50	20	30
25	68	12	20

Standard solution from SM neat and sample solutions of non-irradiated, 25 and 40kGy irradiated SM wafer discs were prepared in the above mentioned HPLC solvent to carry out the quantification of SM.

7.3.5 Effect of silymarin wafers on the migration of HMVECad

Gamma irradiated sterile wafer discs with and without silymarin were tested for their effect on the migration of human microvascular endothelial cells of adult dermis (HMVECad). The migration of cells in the presence of discs in four different conditions of normoxia in absence and presence of elevated glucose (N5mM and N20mM) and in hypoxia in absence and presence of elevated glucose concentration (H5mM and H20mM) was measured according to the method explained in 2.2.4. The results are expressed as net migration in microns (µm) and expressed as mean ± SEM.

7.4 Results

7.4.1 Rheological characterisation of the gels

The gels made from 2% GG and 1.5% XG exhibited plastic (i.e. a clear yield stress followed by a decrease in apparent viscosity as a function of increased shear rate) flow (Fig. 7.2a). The viscosity coefficient (consistency) and yield stress (inability of the gel to flow at lower shear rate) of the GG was found to be more than that of XG (table 7.4). Plastic flow exhibits a dramatic 'shear thinning' effect when a shear stress in excess of the minimum yielding stress is applied. The gels from other gums viz. 5% SA, 3% KG, 1.5% LbG and 7% GhG exhibited pseudoplastic (i.e. decreased apparent viscosity with increasing shear rate) flow (Fig. 7.2b). The flow charts of these polymer gums suggest that the gels exhibited pseudoplastic flow as they started to flow as soon as the shear stress was applied, making the flow curves pass through the origin. Pseudoplastic flow also exhibits shear thinning although less dramatically than plastic flow. The viscosity coefficient of 5% SA was found highest whereas 7% GhG exhibited the lowest (table 7.4). The freeze dried wafer discs of SM and aLA were prepared using 1.5% XG and sterilised by gamma rays. The freeze drying process did not change the flow properties of the post-lyophilised reconstituted wafer gels from that of corresponding pre-lyophilised gels (Fig. 7.3). Sterilisation by gamma rays increased the viscosity coefficient and yield stress of post-lyophilised control and SM wafers. On the contrary, viscosity coefficient decreased for sterilised aLA wafers and yield stress remained unchanged. Alpha lipoic acid pre- and post-lyophilised gels before sterilisation were more viscous with higher viscosity coefficient values and exhibited a higher yield stress compared to either control or SM wafer gels (table 7.4).

a)

b)
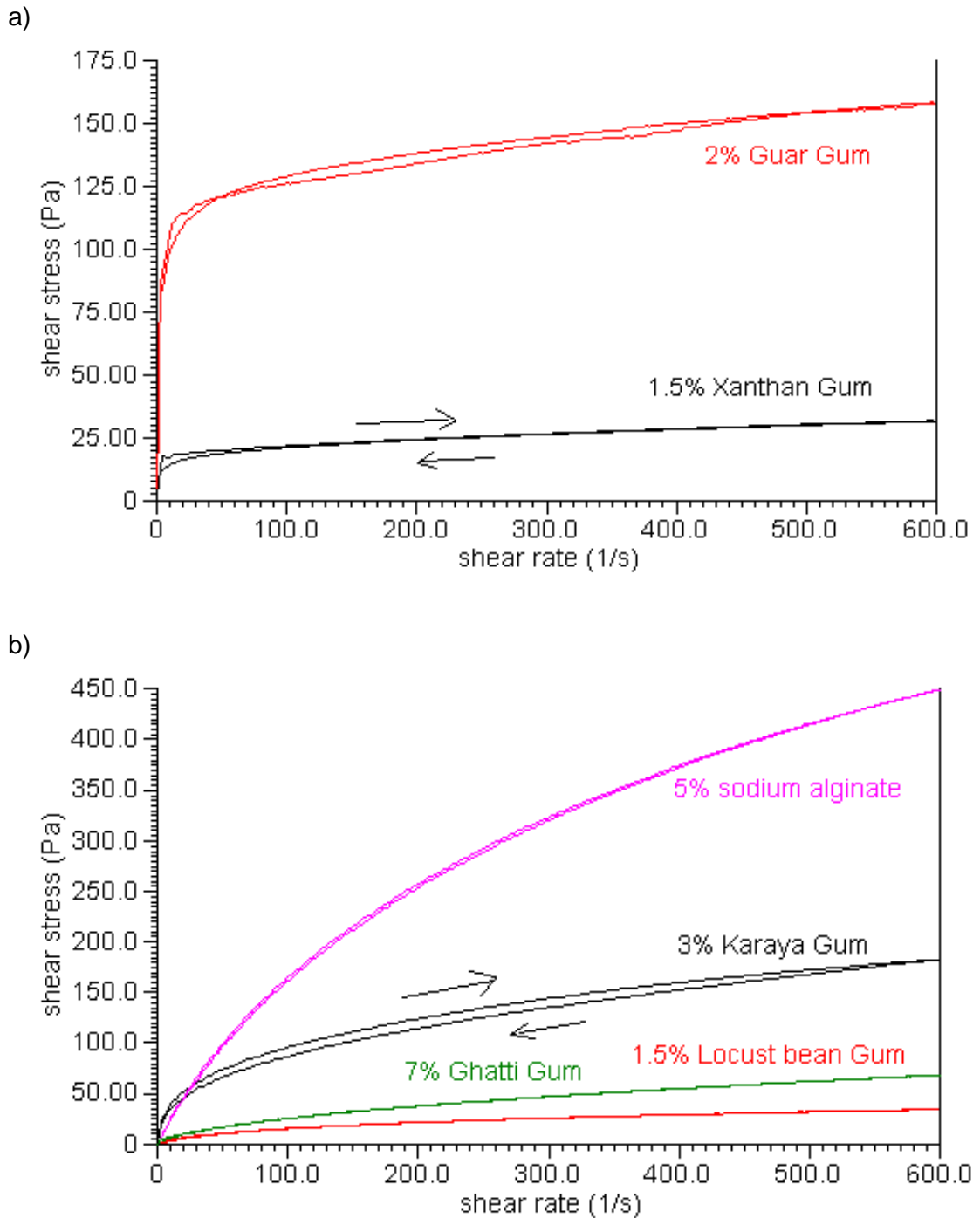
Fig. 7.2 Rheograms of gels The flow charts were obtained from gels composed of a) 2% GG and 1.5% XG and b) 5% SA, 3% KG, 1.5% LbG and 7% GhG. The XG and GG exhibited (a) plastic flow and the others (b) pseudoplastic flow. Arrows indicate ascending (→) and descending (←) cycles.

a)

b)

c)
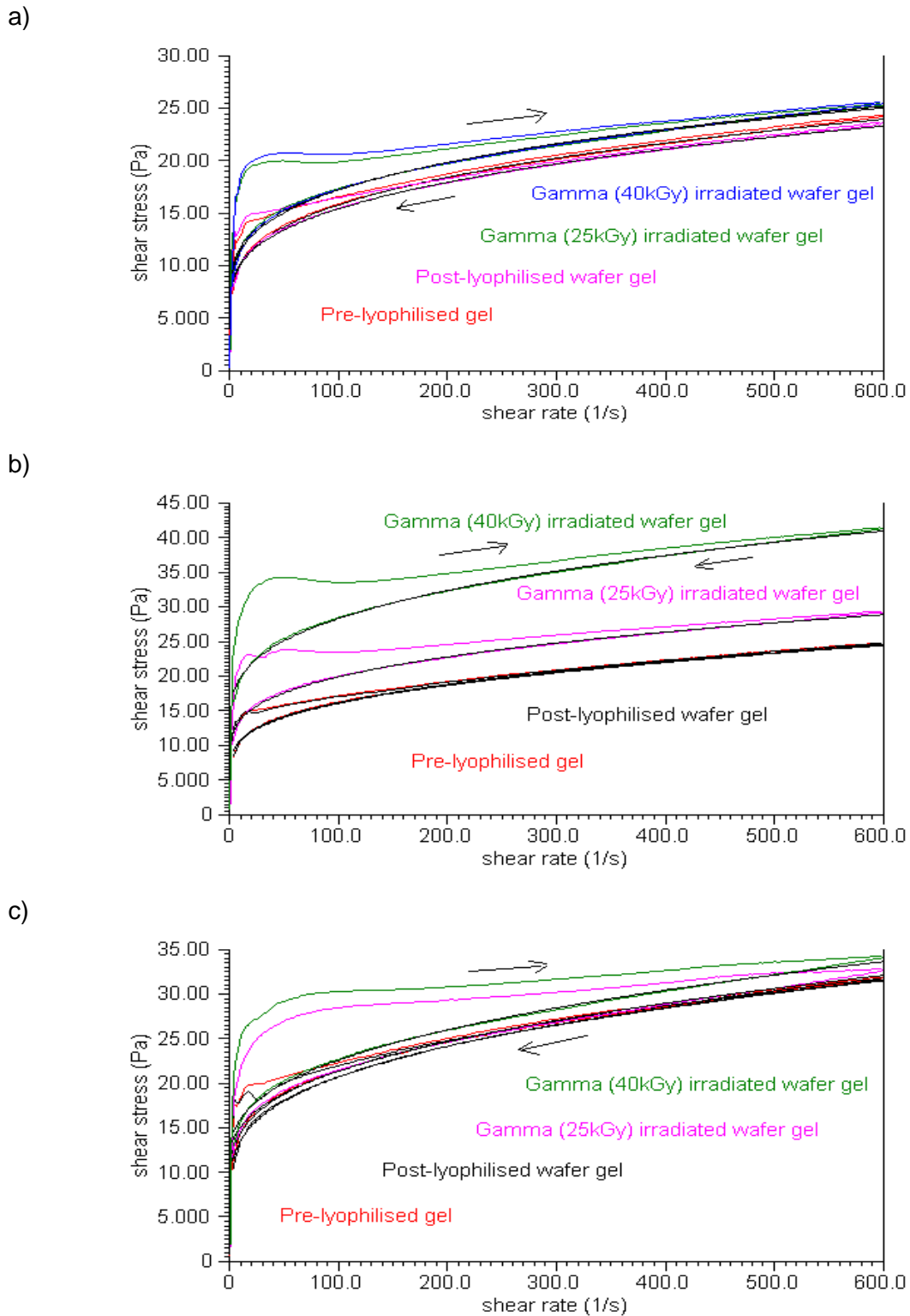
Fig. 7.3 The rheograms of pre-lyophilised and post-lyophilised wafer gels Flow charts of gels of irradiated and non-irradiated reconstituted post-lyophilised a) control wafers, b) silymarin (SM) wafers and c) α-lipoic acid (aLA) wafers. The wafers were composed of 0.07%w/v of SM or 0.06% w/v of aLA, 1.5% w/v of xanthan gum (XG) as a vehicle and non-ionic surfactant, Pluronic F68. Arrows indicate ascending (⟶) and descending (⟵) cycles.

Table 7.4 Viscosity coefficients and yield stress The viscosity coefficients (consistency) and yield stress (inability to flow at lower shear rates) of polymer gels, pre-lyophilised wafer gels and post-lyophilised wafer gels were calculated using the Herschel-Bulkley model.

Fig. No.	Gels	Viscosity coefficient (Pa.s)	Rate index	Yield stress (Pa.s)
7.2a	2.0% GG	74.9	0.11	139.8
	1.5% XG	1.8	0.39	24.6
7.2b	5.0% SA	31.9	0.44	-
	3.0% KG	23.7	0.33	-
	7.0% GhG	2.7	0.51	-
	1.5% LbG	4.7	0.34	-
7.3a	Pre-lyophilised control gel	2.5	0.31	18.9
	Post-lyophilised control wafer gel	2.3	0.32	18.4
	Gamma (25kGy) irradiated gel	2.9	0.29	20.2
	Gamma (40kGy) irradiated gel	3.2	0.28	20.3
7.3b	Pre-lyophilised SM gel	2.2	0.33	19.3
	Post-lyophilised SM wafer gel	1.9	0.35	19.2
	Gamma (25kGy) irradiated gel	2.8	0.31	23.2
	Gamma (40kGy) irradiated gel	3.6	0.32	33.0
7.3c	Pre-lyophilised aLA gel	3.3	0.31	25.2
	Post-lyophilised aLA wafer gel	3.0	0.33	24.8
	Gamma (25kGy) irradiated gel	1.7	0.39	25.0
	Gamma (40kGy) irradiated gel	1.9	0.38	26.5

7.4.2 Sterilisation of wafers

Lyophilized wafers composed of 1.5% XG, 5% SA, 2% hydroxypropyl methyl cellulose (HPMC) and 4% methyl cellulose (MC) were subjected to UV irradiation from 0 to 12 J/cm^2. Gels of HPMC and MC were prepared by slowly adding these polymers with continuous stir to pre-heated (~70 ^{0}C) distilled water in a glass beaker. The wafers were prepared by the same method to that of XG wafers. After UV irradiation, these wafers were tested for the presence of bacteria and fungi (table 7.5). Microbial colonies were counted to grade the level of contamination. The complete absence of colonies was considered as no contamination. One to 5 colonies, 6 to 20 colonies and more than 20 colonies were graded as +, ++ and +++ respectively. Bacteria were found to be present in all wafers and the presence of fungi was detected in all wafers except in those made from MC. Gamma irradiated wafers were also tested for the presence of bacteria and fungi (Fig. 7.4). Bacteria and fungi were both absent in wafers irradiated with 25 and 40kGy of gamma rays, but present in non-irradiated control samples.

Table 7.5 UV irradiation Wafers prepared from different polymers were treated with UV radiation of different strengths and tested for the presence of a) bacteria and b) fungi.

a)

	Control (0J/cm^2)	0.36 J/cm^2	0.72 J/cm^2	1.5 J/cm^2	3.0 J/cm^2	6.0 J/cm^2	12.0 J/cm^2
XG	+++	++	++	++	++	++	++
HPMC	+	+	++	+	+++	+++	+
MC	+	++	++	-	-	-	+
SA	+++	+++	+++	+	+++	+++	+

b)

	Control (0J/cm^2)	0.36 J/cm^2	0.72 J/cm^2	1.5 J/cm^2	3.0 J/cm^2	6.0 J/cm^2	12.0 J/cm^2
XG	++	-	-	+	-	-	-
HPMC	-	-	+	-	-	-	-
MC	-	-	-	-	-	-	-
SA	-	-	+	+	-	-	-

- No contamination (0 colonies)

+   -   1 – 5 colonies

++   -   6 – 20 colonies

+++   -   >20 colonies

a)
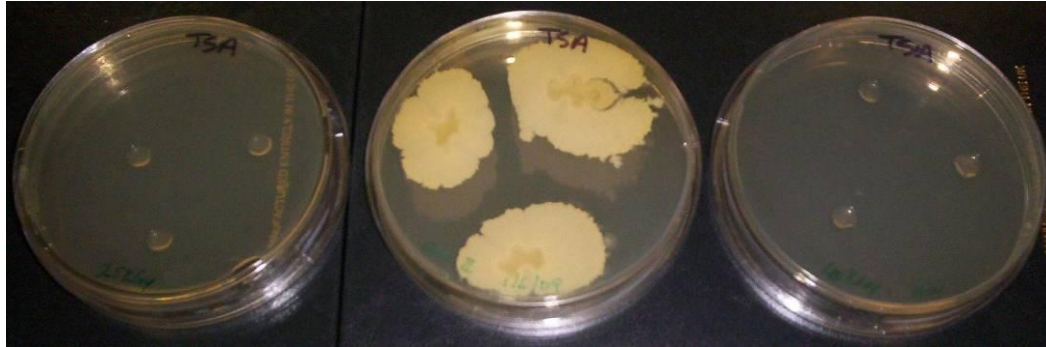
| 25kGy | 0kGy | 40kGy |

b)

| 25kGy | 0kGy | 40kGy |

Fig. 7.4 Sterilisation by gamma irradiation The control, silymarin and α-lipoic acid wafers were prepared using 1.5% w/v of XG as a vehicle with 0.2% w/v of Pluronic F68 as non-ionic surfactant. They were successfully sterilised by treating with 25 and 40kGy gamma radiation. The gamma irradiated wafer discs did not show any presence of either a) bacteria or b) fungi, whereas untreated (0kGy) wafer discs were contaminated.

7.4.3 Quantification of silymarin in the wafers by HPLC

The concentration of silymarin present in gamma irradiated wafer discs was quantified by HPLC. The standard reference solution of silymarin was prepared by dissolving 0.0112g neat silymarin in 50ml of HPLC solvent as explained in 7.3.4. A series of solutions at different concentrations was prepared by diluting a standard reference solution. The range of standard solution concentrations obtained by a series of dilutions was between 8.96 and 89.6µg/ml. These standard solutions were used to obtain chromatograms with five distinguishable peaks (Fig. 7.5). The area under the curve (AUC) for each of the five peaks and total peak area was measured using the software (Table 7.6). The AUC of peak 2 obtained from the different standard solutions was used to plot the calibration curve (Fig. 7.6). Peak 2 data was used as it was the most prominent of all peaks. The calibration curve of the standard solutions showed good linearity (correlation coefficient = 0.986).

The molecular weight of SM and aLA is 482.44 and 206.33Da respectively. Each small disc added to 2.5ml of medium in a well weighs ~1.5mg. This 1.5mg wafer disc contained either 0.06mg of SM or 0.052mg of aLA in order to achieve the final concentration of 50 or 100µM respectively in 2.5ml of media. Silymarin alone was quantified as it was used in measuring the migration of HMVECad (Chapter 6).

The sample solutions were prepared by dissolving SM wafer discs in HPLC solvent. Weight of two each of non-irradiated, 25 and 40kGy irradiated wafer discs was noted and dissolved in 5ml of HPLC solvent so that they have a theoretical or expected concentration of 79.7, 78.05 and 85.37µg/ml respectively (Table 7.7). These sample solutions were run through the HPLC and AUC of peak 2 was used to quantify the silymarin present. The regression equation ($y = 15994x - 45718$) obtained from the calibration curve suggests that the silymarin present in non irradiated, 25 and 40kGy irradiated wafer discs was 71.7, 69.5 and 76.5µg/ml respectively.
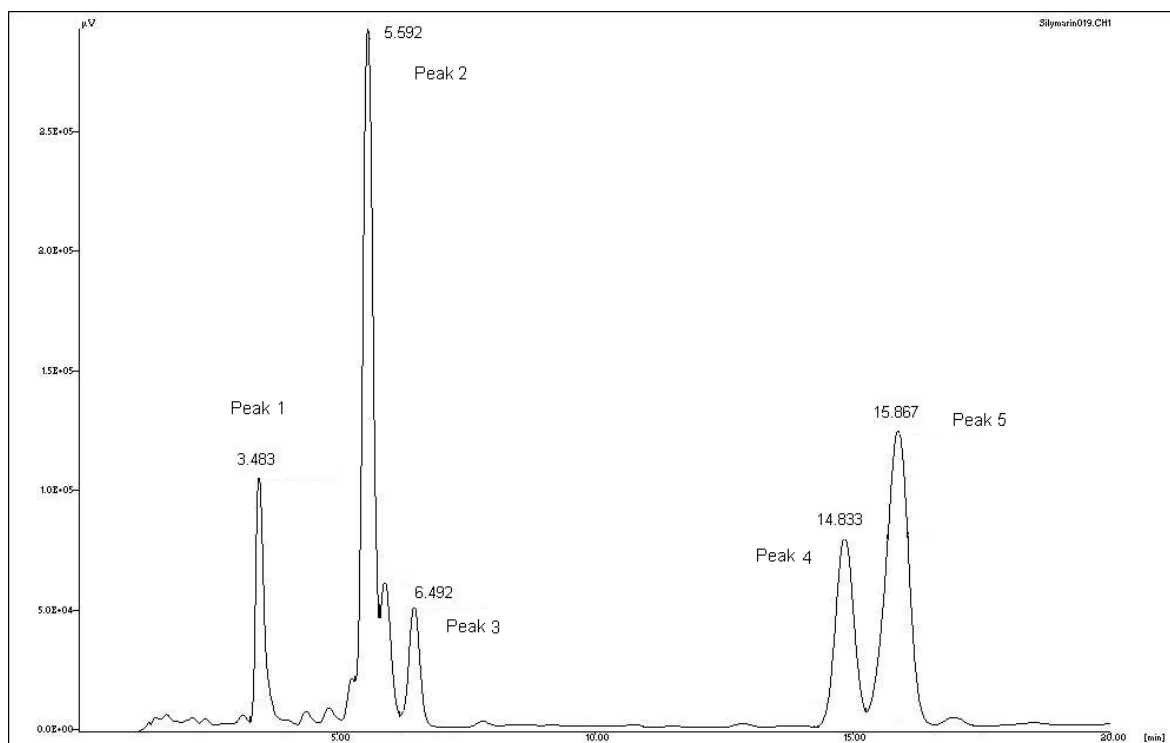
Fig. 7.5 Chromatogram obtained from silymarin by HPLC The chromatogram was obtained by running a volumetric solution of silymarin (0.0112g) dissolved in 50ml of a solvent composed of 0.01% v/v formic acid in deionised water (32ml); methanol (6ml); and acetonitrile (12ml). The silymarin (50µl) solution was injected at a flow rate of 1ml/min to obtain five clear and distinguishable peaks at 289nm by the UV Visible detector. Numbers at each peak indicate the retention time (minutes) at which a peak appears on the chromatogram.

Table 7.6 Calculation of area under curve (AUC) The chromatograms obtained by HPLC contain five peaks due to standard and sample wafer disc solutions. The AUC for these peaks was calculated using Jasco Borwin 15.0 software.

	Concentration of silymarin (µg/ml)	AUC (data in thousands)					
		Total area	Peak 1	Peak 2	Peak 3	Peak 4	Peak 5
Std 1	8.96	449.1	31.9	155.6	24.4	86.8	150.4
Std 2	17.92	602.9	30.4	262.1	27.2	91.4	191.8
Std 3	26.88	860.9	50.4	378.1	44.5	125.0	262.6
Std 4	35.84	1164.2	72.9	489.4	66.4	180.1	355.4
Std 5	44.8	1382.4	82.7	586.8	77.2	209.7	425.9
Std 6	89.6	3570.5	234.7	1436.4	219.8	579.4	1100.0
Sample 1 0kGy	-	3271.6	217.9	1102.3	173.4	544.6	1233.4
Sample 2 25kGy	-	2934.0	142.1	1066.1	103.3	679.7	942.6
Sample 3 40kGy	-	3503.8	183.2	1178.2	150.2	676.4	1315.8
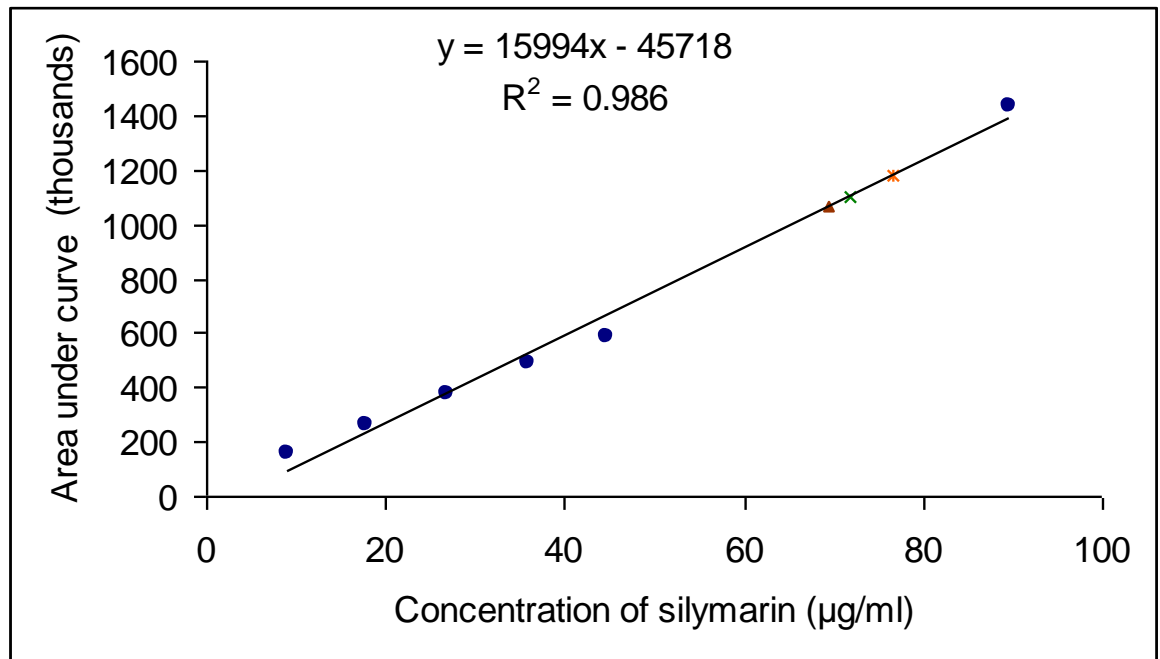
Fig. 7.6 Quantification of silymarin in lyophilised wafer discs The calibration curve was obtained from silymarin standard solutions. The data from peak 2 was used to plot the calibration curve. The concentration of the silymarin present in the sample wafer discs was calculated from the regression equation.

(Key: ● standard solutions, ▲ 25kGy irradiated SM wafer discs, x non-irradiated wafer discs and ж 40kGy irradiated wafer discs)

Table 7.7 Quantification of silymarin Peak 2 AUC was used to quantify the silymarin present in sample wafer disc solutions. The sample wafer disc solutions were prepared from non-irradiated, 25 and 40kGy irradiated wafer discs.

	Weight of the wafer discs in solvent (mg/ml)	Measured concentration of silymarin (µg/ml) (y = 15994x – 45718)	Theoretical concentration of silymarin (µg/ml)	Area under the curve for peak 2
Std 1	-	-	8.96	155644.2
Std 2	-	-	17.92	262053.5
Std 3	-	-	26.88	378076
Std 4	-	-	35.84	489391.8
Std 5	-	-	44.8	586805
Std 6	-	-	89.6	1436422
Sample1 (0kGy)	2.0	71.7	79.7	1102258
Sample2 (25kGy)	1.9	69.5	78.1	1066145
Sample3 (40kGy)	2.1	76.5	85.4	1178273

7.4.4 Effect of silymarin wafer discs on the migration of HMVECad

The control and silymarin wafer discs were prepared as detailed in 7.3.1. Gamma irradiated wafer discs were used to assess their effect on the migration of HMVECad. The effect of the control wafer discs on the migration was assessed by placing 1 or 3 or 5 discs in each well of a 6 well plate seeded with a circular monolayer of HMVECad.

The net migration (µm) of endothelial cells (Fig. 7.7) in N5mM condition with no discs (24 h: 105.8 ± 0.6, 48 h: 160.9 ± 1.7), 1 disc (24 h: 101.4 ± 1.1, 48 h: 175.1 ± 1.1), 3 discs (24 h: 101.9 ± 0.6, 48 h: 165.2 ± 1.2) and 5 discs (24 h: 111.8 ± 1.9, 48 h: 172.9 ± 1.2) was found to be significantly ($p<0.001$) more than that of N20mM condition for no discs (24 h: 96.6 ± 1.1, 48 h: 138.7 ± 1.1), 1 disc (24 h: 92.6 ± 0.9, 48 h: 155.3 ± 0.7), 3 discs (24 h: 86.1 ± 0.9, 48 h: 155.9 ± 0.5) and 5 discs (24 h: 90.9 ± 1.3, 48 h: 146.5 ± 1.1). These results confirm that the control wafers (i.e. 1.5% w/v XG + 0.2% w/v F68) on their own did not alter the migration when glucose concentration was altered.

The migration (µm) of cells (Fig. 7.8) from the intact edge in the presence of silymarin wafer discs in N5mM (24 h: 82.7 ± 2.1, 48 h: 143.3 ± 3.0) condition was not different ($p>0.05$) than in N20mM (24 h: 89.7 ± 1.7, 48 h: 156.7 ± 3.1) condition. Similarly, the migration of cells was not different ($p>0.05$) in H5mM (24 h: 103.7 ± 1.9, 48 h: 168.7 ± 2.5) condition compared to H20mM (24 h: 98.7 ± 1.7, 48 h: 171 ± 2.5) condition. However, the migration in H5mM condition was significantly higher ($p<0.001$) than in N5mM condition. A similar pattern of migration was observed for cells migrating from the wounded edge of the same monolayer (N5mM; 24 h: 101.6 ± 2.6, 48 h: 194 ± 4.6, N20mM; 24 h: 109.6 ± 2.3, 48 h: 184.6 ± 2.8, H5mM; 24 h: 132.4 ± 2.9, 48 h: 207.8 ± 3.6 and H20mM; 24 h: 129.7 ± 2.4, 48 h: 203.4 ± 2.8). Unlike the intact edge, the migration from the wounded edge in N20mM condition was higher ($p<0.05$) compared to N5mM condition.

Control wafer discs produced a migration (µm) similar to that of the vehicle controls detailed in previous chapter 6. The migration of HMVECad (Fig. 7.8) from the intact edge of the semicircular monolayer in N5mM condition (24 h: 89 ± 2.1, 48 h: 139.8 ± 1.9) was significantly ($p<0.001$) higher than in N20mM (24 h: 77.4 ± 1.8, 48 h: 125.6 ± 2.6) condition. The migration in H5mM (24 h: 112.1 ± 3.1, 48 h: 165.5 ± 4.9) condition was much higher ($p<0.001$) than in N5mM condition. High glucose concentration combined with hypoxia (H20mM) (24 h: 93.9 ± 1.8, 48 h: 145.1 ± 2.8) significantly reduced ($p<0.001$) the migration of cells compared to those in H5mM condition. The migration of endothelial cells from the wounded edge of the monolayer (N5mM; 24 h: 115.7 ± 2.6, 48 h: 174.1 ± 3.6, N20mM; 24 h: 100.8 ± 2.3, 48 h: 152.7 ± 2.6, H5mM; 24 h: 136.2 ± 2.9, 48 h: 203.4 ± 4.5 and H20mM; 24 h: 117.6 ± 1.8, 48 h: 172.5 ± 2.2) was similar to that from the intact edge with similar levels of significance.

Fig. 7.7 Effect of control wafer discs on the migration of HMVECad The migration due to control wafer discs (1.5%w/v XG + 0.2%w/v Fluronic F68) was carried out in conditions of 5mM or 20mM glucose and 20% (Normoxia – N) oxygen tension. The migration was assessed by the radial migration assay. The control wafer discs did not alter the migration when the glucose level was increased. The results are presented in microns as net migration (mean ± SEM) (n=60) of cells at 24 (a) and 48 h (b) and analysed by independent t test.

(***p<0.001 when compared with N5mM condition of respective disc numbers)

a)
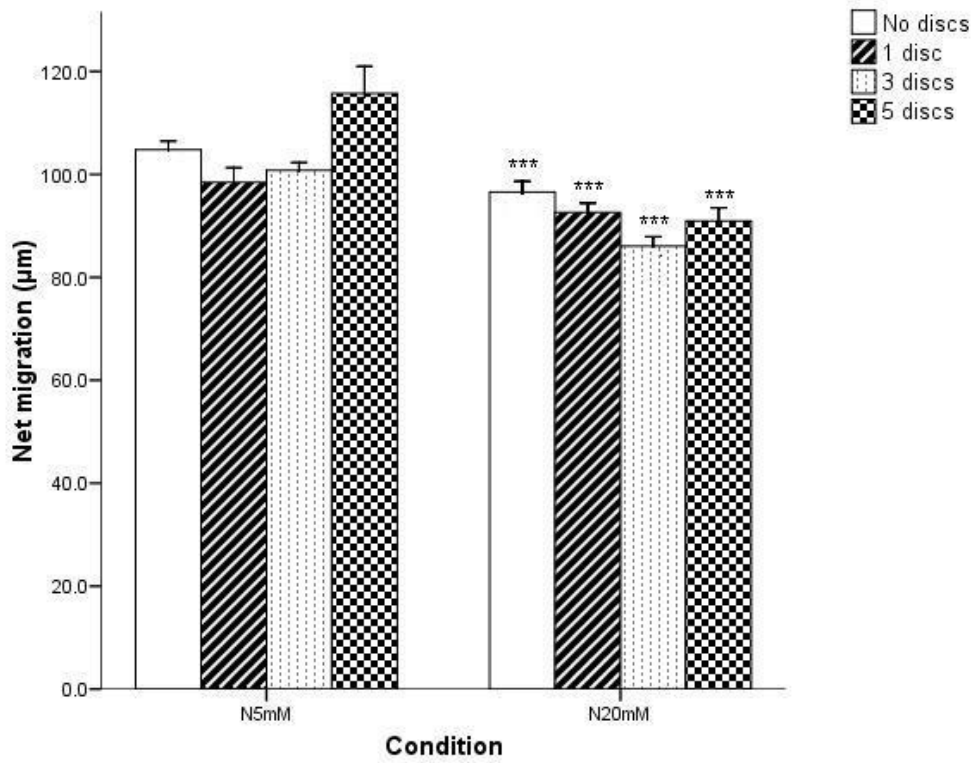
b)
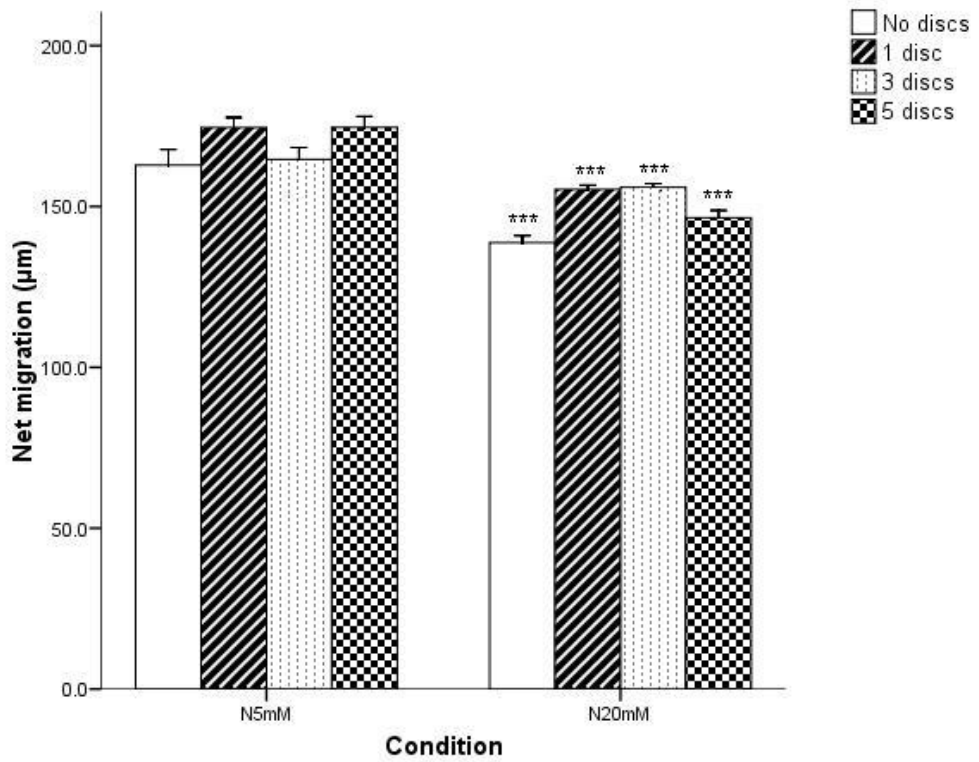
Fig. 7.8 Effect of silymarin wafer discs on the migration of HMVECad The migration of cells from intact and wounded edges in conditions of 5mM or 20mM glucose and 20% (Normoxia – N) or 5% (Hypoxia – H) oxygen tension was assessed by the wound healing assay. The silymarin wafer discs successfully overcame the negative effects of high glucose. The cells migrating from the wounded edge were significantly faster ($p<0.001$) than their counterparts from the intact edge for all the conditions and treatments. The migration due to control wafer discs resulted in trends similar to those of vehicle control wherein high glucose resulted in the reduction during both normoxia and hypoxia. The results are presented in microns as net migration (mean ± SEM) (n=90) of cells at 24 (a) and 48 h (b) and analysed by analysis of variance (ANOVA) followed by Bonferroni post hoc test.

(*$p<0.05$ and NS = not significant when compared as indicated)

(Control wafers: Intact & wounded edge, 24&48 h, N5mM = 80, H5mM = 60, H20mM = 80; SM wafers: Intact & wounded edge; 24&48 h, N5mM = 60, H5mM = 80 and H20mM = 80)

a)
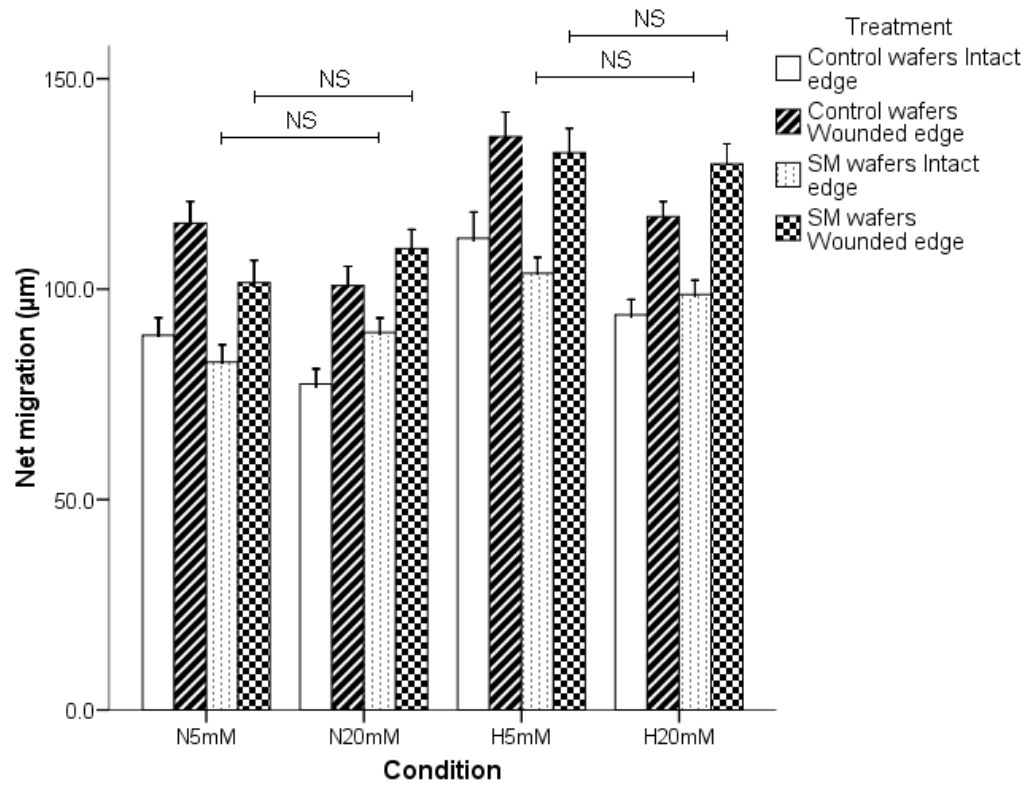
b)
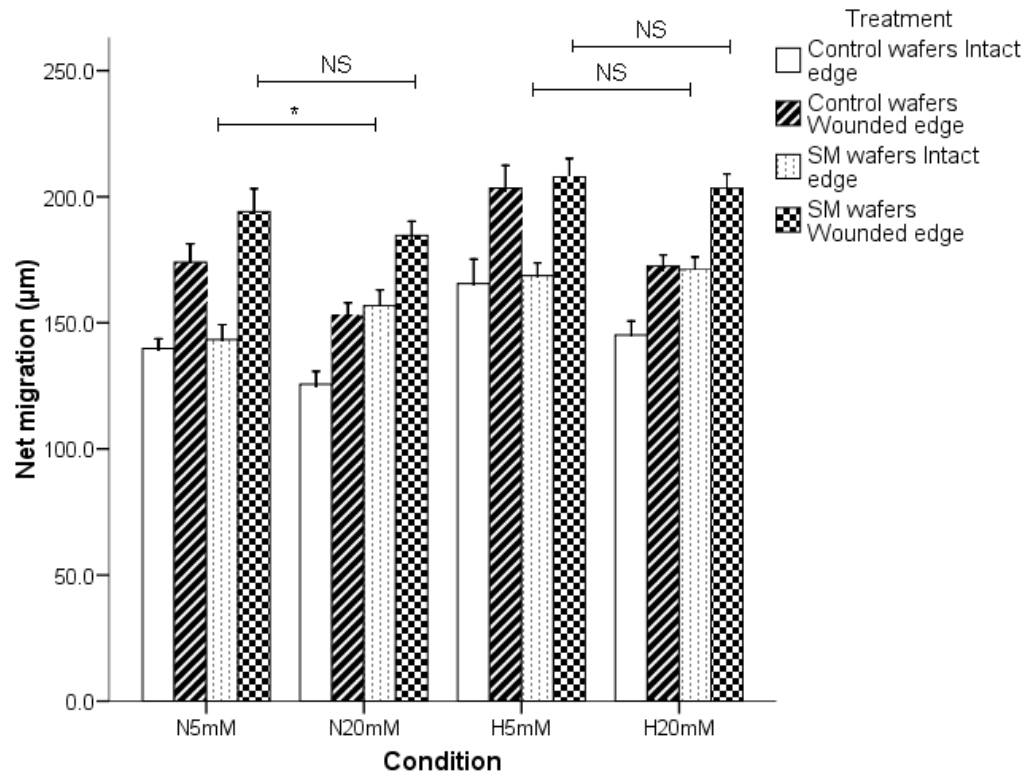
7.5 Discussion

The viscosity coefficient and yield stress of freeze dried silymarin wafers increased after gamma ray sterilisation. Sterilised wafers containing silymarin exhibited plastic flow and the drug content remained largely unaffected by ionising gamma rays. High performance liquid chromatography was used to quantify the silymarin present in sterile and non-sterile wafer discs. The migration due to silymarin present in the wafer discs was comparable to that of neat drug.

The preparation of freeze dried wafer discs involved XG as a vehicle and non-ionic surfactant Pluronic F68 as both silymarin and aLA are water insoluble drugs (table 7.1). Matthews et al. (2008) successfully used XG along with non-ionic surfactant to prepare the freeze dried wafers of a water insoluble MMP-3 inhibitor (Matthews et al. 2008). The discrepancies observed between the calculated contents with that of mean weight of each (table 7.1) freeze dried wafer might be due to either a combination of residual water content and absorbed moisture as observed in a previous study (Matthews et al. 2005) or due to the loss of a part of wafer while peeling the wafer out of a well in which they were cast. The doses were calculated so that each wafer disc of SM and aLA produced 50 and 100µM respectively when placed in 2.5ml of medium of a well of six well plate.

The rheological studies help to design the freeze dried products to achieve suitable consistency when applied to the wound site. Gels prepared from XG and GG exhibited plastic flow whereas other gums including SA exhibited psuedoplastic flow (Fig. 7.2). This is consistent with earlier findings where flow curves of XG gel alone and in combination with varying concentration of methyl cellulose have a small yield value and flow curves of SA pass through origin (Matthews et al. 2005). Although the viscosity coefficient and yield stress exhibited by XG was much lower than that of GG, XG was used as a vehicle to prepare the lyophilised wafers. Xanthan gum was chosen over other natural polymers as it produces the right amount of consistency so that the topical application will have sufficient residence time at the wound site. Sufficient residence time of topical application is critical in the delivery of a drug (Jones, Lawlor and Woolfson 2003). The expected enhancement in residence time by XG could be due to yield stress exhibited by XG which delays or inhibits viscous flow (Matthews et al. 2006). The pre-lyophilised gel of the control wafer containing XG and Pluronic F68 was more viscous than XG alone but the yield value was lower. This indicates that non-ionic surfactant could be acting as a viscosity enhancer. Another added advantage of using XG as a vehicle in the preparation intended for wound management is its ability to withstand ionising gamma rays while undergoing sterilisation.

Sterilisation of potable water and clothing in operating theatres by UV irradiation has been in use for some time now (Taylor, Bannister and Leeming 1995, Zimmer and Slawson 2002). Attempts to sterilise the wafers by UV rays however, did not yield the desired results (table 7.5). The reason for this needs further assertion. This could possibly be due to either the failure of UV rays to penetrate wafers or the failure of polysaccharides to absorb UV rays and disrupt the microbes. This necessitated the search for other sterilisation methods.

Silymarin and aLA wafer discs (Fig. 7.4) were sterilised at 25 and 40kGy of gamma rays which are normal dose rates for sterilising medical devices. However, lower doses used in sterilising products such as bone allografts can be explored (Nguyen, Morgan and Forwood 2007). The flow properties were investigated after gamma ray sterilisation in order to understand the possible changes ionisation might inflict on the polymers and active constituents. It is evident from the results (Fig. 7.3 & table 7.4) that reconstituted gels from XG wafers and SM wafers showed a small dose dependant increase in their viscosity coefficient and yield stress values upon gamma irradiation. These observations are in agreement with previous observations where gamma irradiation of XG resulted in a small increase in yield stress (Hanna et al. 1997). The antioxidant activity of SM might be acting synergistically in avoiding polymer chain scission by gamma rays, as antioxidant such as ascorbate are known to protect blood products against degradation by gamma rays (Zbikowska, Nowak and Wachowicz 2006). In contrast, the viscosity coefficient of reconstituted gels of sterile aLA wafers was decreased compared to non-sterile gels, but yield stress remained unchanged. This anomaly, along with the full potentials of other polymers as a suitable vehicle in preparing freeze dried products and their ability to remain stable during the sterilization process remains to be explored.

It has been observed from chapter 6 that silymarin produces its effects against glucose induced decrease in cell migration at 50µM concentration. The quantity of silymarin present in individual wafer discs was assessed by comparing the sample solutions against the standard curve of known concentrations of silymarin by HPLC (Table 7.6 & 7.7). HPLC has been used to quantify the different components of silymarin and further to establish its pharmacokinetic profile in human plasma in conjunction with other analytical methods (Quaglia et al. 1999, Wen et al. 2008). The different components of silymarin were separated and detected as five separate peaks (Fig. 7.5) at retention times of 3-18min which was different from earlier observations at 289nm (Quaglia et al. 1999). Peaks were not assigned to the components of silymarin due to their complex chemical nature and were simply referred as peak 1 to 5. Area under the curve of peak 2 was used to establish the standard curve and to calculate the concentration of silymarin in samples

as it was a predominant peak among others even at lower concentrations (Table 7.6, 7.7 and Fig. 7.6).

Neither the presence of a single control wafer disc or an increase in their number altered the migration trends as the presence of high glucose continued to decrease the migration (Fig. 7.7 & 7.8). This confirms that unlike chitosan which has been reported to induce changes in wound healing (Mizuno et al. 2003), XG did not produce any effect on its own. The silymarin wafer discs were prepared so that each disc contained silymarin equivalent to 50µM when placed in a well containing 2.5ml of medium. However, the concentration of silymarin present in the wafer discs quantified by HPLC (table 7.7) suggested that one disc with an average weight of 1.5mg contained 10-11% less silymarin than expected. This could possibly be due to faulty readings obtained by HPLC as a result of non-homogenous dispersion of silymarin in xanthan gel or due to water content of wafers. It has been proved that water or moisture content in lyophilised wafers could be as high as 10-15% w/w (Matthews et al. 2005). This would mean that silymarin content could possibly be 10-15% less than expected. However, this decrease in the dose of silymarin did not adversely affect the migration of cells (Fig. 7.8). Similar to neat silymarin, as found in chapter 6, wafer discs containing the drug successfully prevented the decrease in endothelial cell migration due to elevated glucose levels both in normoxia and hypoxia.

7.6 Conclusion

Silymarin was successfully formulated as freeze dried wafer discs and sterilized by gamma radiation. The sterile freeze-dried discs containing silymarin retained their effect of restoring the migration of cells against the elevated glucose concentration both in normoxia and hypoxia.

7.7 Further work

This pilot study established the method of formulating the silymarin into a freeze dried product. Qualitative and quantitative analysis of silymarin would be aided further by characterisation of wafers and gels by the use of differential scanning calorimetry (DSC) for thermal analysis, particle size distribution, vapour content and physical structure of wafers by scanning electron microscopy. The project would also benefit from studies on long term stability and drug release profile of silymarin in the freeze dried form. Furthermore, the effect of gamma sterilisation on the stability of the active ingredients needs further investigation by different analytical methods such as nuclear magnetic resonance (NMR) and liquid chromatography - mass spectra (LC-MS).

Chapter 8 – General discussion

8.1 Discussion

The Diabetes Control and Complication Study (DCCT) and the United Kingdom Prospective Diabetes Study (UKPDS) have established that elevated glucose concentration is responsible for the onset and progression of the vascular complications of diabetes (DCCT Group 1993, UKPDS Group 1998). The presence of elevated glucose concentration interferes with hypoxia induced angiogenesis leading to a delay in wound healing for patients suffering from diabetes mellitus (Falanga 2005). Hypoxia is an essential stimulant for angiogenesis including endothelial cell migration during wound healing as well as cancer (Carmeliet 2005). The findings of this thesis suggest that the hypoxia and hyperglycaemia have opposing effects on the migration of endothelial cells. Hypoxia, as expected, increased the migration whereas the presence of higher concentration of glucose hindered the migration of endothelial cells. The deleterious effects of high glucose were mediated through HIF-1α protein and the migration was restored by the use of an anti-oxidant, silymarin. The strategy of developing a topical application resulted in a successful development of freeze dried wafer discs containing silymarin which prevented the deleterious effects of high glucose on migration.

In vitro migration of cells can be investigated using different methods (Auerbach et al. 2003, Eccles, Box and Court 2005). The scratch wound assay is one of the most widely used assays. We were interested in developing a method which would help to understand the influence of wounding a cell monolayer on the migration of cells not only from the wounded edge but also from the intact edge. A scratch wound assay is of no help in this regard as there is no intact edge as the scratch wound would be made on a confluent monolayer. Recently Dolle et al. (2005) used an omni-directional migration assay which was an improvement of previously designed assays by others (Dolle et al. 2005). The omni-directional assay depends on the accuracy of placing glass rings on pre-marked circles underneath each well of a six well plate and any changes would lead to non usability of the data generated. This omni-directional assay was based on optimising a method explained by Dixit and co-workers (Dixit et al. 2001). Dixit et al. (2001) measured the area of a circularly seeded monolayer at the starting time point and seven days later at an end time point. The radii were calculated from the difference in the *approximate* area of a monolayer at an end time point and area of a steel ferrule (used to cast the cells into a circular monolayer) at a starting time point (Dixit et al. 2001). The authors considered the approximation of area of a circular monolayer at an end time point possibly due to the lack of image analysis tools to analyse the exact area during the time of their study. The radial migration assay detailed in section 2.2.3 of chapter 2 of this study is a further improvement of the omni-directional assay explained by Dolle et al. (2005) and Dixit et al. (2001). Unlike the earlier methods, the radial migration assay

method developed in this thesis provides the flexibility of seeding the cells anywhere within a confined area of a glass ring and allows the measurement of an *exact* area or radii of monolayer using image analysis software. Once the radial migration assay was developed (after numerous trials and errors as discussed in chapter 3), it easily lent itself to develop the wound healing assay as explained in section in 2.2.4 of chapter 2. The wound healing assay explained in this thesis was able to not only determine the migration of cells from the intact and wounded edge together in one model as envisioned but to the best of our knowledge is also a novel method. Furthermore, the choice of 5% oxygen tension for the hypoxic conditions used in this study was chosen as the upper limit at which hypoxia mediated responses were operating and prior to induction of anoxia (Pouyssegur, Dayan and Mazure 2006). The results presented here demonstrate that this was sufficient to enhance cell migration and also activate HIF-1α. So these conditions were used throughout the study.

The results of all the chapters clearly suggest that the ECs from the wounded edge migrated faster than their counterparts from the intact edge. In the light of these results, it could be argued that the wounded surface and un-wounded surface on which cells migrate, influences the rate and direction of migration. The migration of cells from the intact edge resembles endothelialisation simulating neo-angiogenesis or vasculogenesis whereas that from the wounded edge resembles re-endothelialisation simulating angiogenesis. Endothelial cells participating in endothelialisation demonstrated directionality with a basal speed (i.e. velocity) whereas those participating in re-endothelialisation have directionality and increased speed (i.e. increased velocity). The increased velocity in endothelial cell migration from the wounded edge could be due to active crawling of stalk cells lining up behind tip cells at the edge, faster formation of lamellopodia and rearrangement of cytoskeletal structure in the leading edge of the migrating tip cells (Farooqui and Fenteany 2005, Lee and Gotlieb 2003). Along with these factors we suspect that the denuded surface might be acting as a 'matrix' and induces or enhances the haptotaxis. Furthermore, the release of soluble cues from 'wounded' cells might also be influencing the chemotaxis which needs further exploration. Chemotaxis and haptotaxis could be acting additively to increase the migration from the wounded edge compared to that from the intact edge. It would of interest to develop this by characterisation of the factors involved in inducing cell migration.

The glucose dependent decrease in endothelial cell migration observed in this study contrasts with enhanced migration of retinal endothelial cells due to high glucose observed during diabetic retinopathy (Aiello et al. 1994, Huang and Sheibani 2008). This illustrates the importance of the source of endothelial cells and also demonstrates a rationale for the variety of vascular complications exhibited in the diabetes. In this study,

the intracellular processes that are involved in the observed changes in cell migration due to hypoxia and/or high glucose demonstrated the following;

- The role of p27^{Kip1} in cell migration was inconclusive but the differences in expression profile of cells within the wound healing model highlight the need for further in-depth investigation.

- Activation of PKC$_{βII}$ was central to the hyperglycaemia induced decrease in the migration of ECs and supports the notion of glucose mediated activation of ROS (This was further supported by the work using silymarin).

- Activation of p42/p44 MAPK was required for high glucose mediated changes in cell migration.

- The PI3K pathway was required for the hypoxia induced increase in EC migration. This could be due to the hypoxia induced activation of growth factors.

- HIF-1α appeared to be a common factor between both hypoxia and hyperglyaecemia affected cell migration.

Increased concentration of glucose is known to lead to the production of ROS in endothelial cells and has been proposed as a unifying mechanism for four different metabolic pathways of excessive glucose metabolism which are increased flux of glucose through polyol and hexosamine pathway, increased production of AGEs and activation of the PKC (Brownlee 2005, Nishikawa et al. 2000). Use of anti-oxidants has successfully prevented some of the deleterious effects of high glucose produced by ROS which were mediated through the over activation of PKC$_{βII}$ (Gallo et al. 2005, Kunisaki et al. 1994). Therefore we also used an anti-oxidant, silymarin which was able to prevent the glucose mediated decrease in the cell migration. To our knowledge, there are no reports of using silymarin in preventing the deleterious effects of glucose on the migration although another anti-oxidant, thiamine has been successfully used in bovine aortic endothelial cells to overcome the glucose induced decrease in cell migration (Ascher et al. 2001).

Silymarin was formulated as a freeze dried wafer once it was confirmed to restore the reduced migration due to high glucose. This has potential for more direct therapeutic use as a topical application to wounds. The ability of freeze dried wafers to retain the effectiveness of the drug is an important finding and will be further investigated in future projects to realize the larger goal of a development of a suitable formulation for chronic wounds of diabetes. The following cartoon summarizes the findings of this thesis;
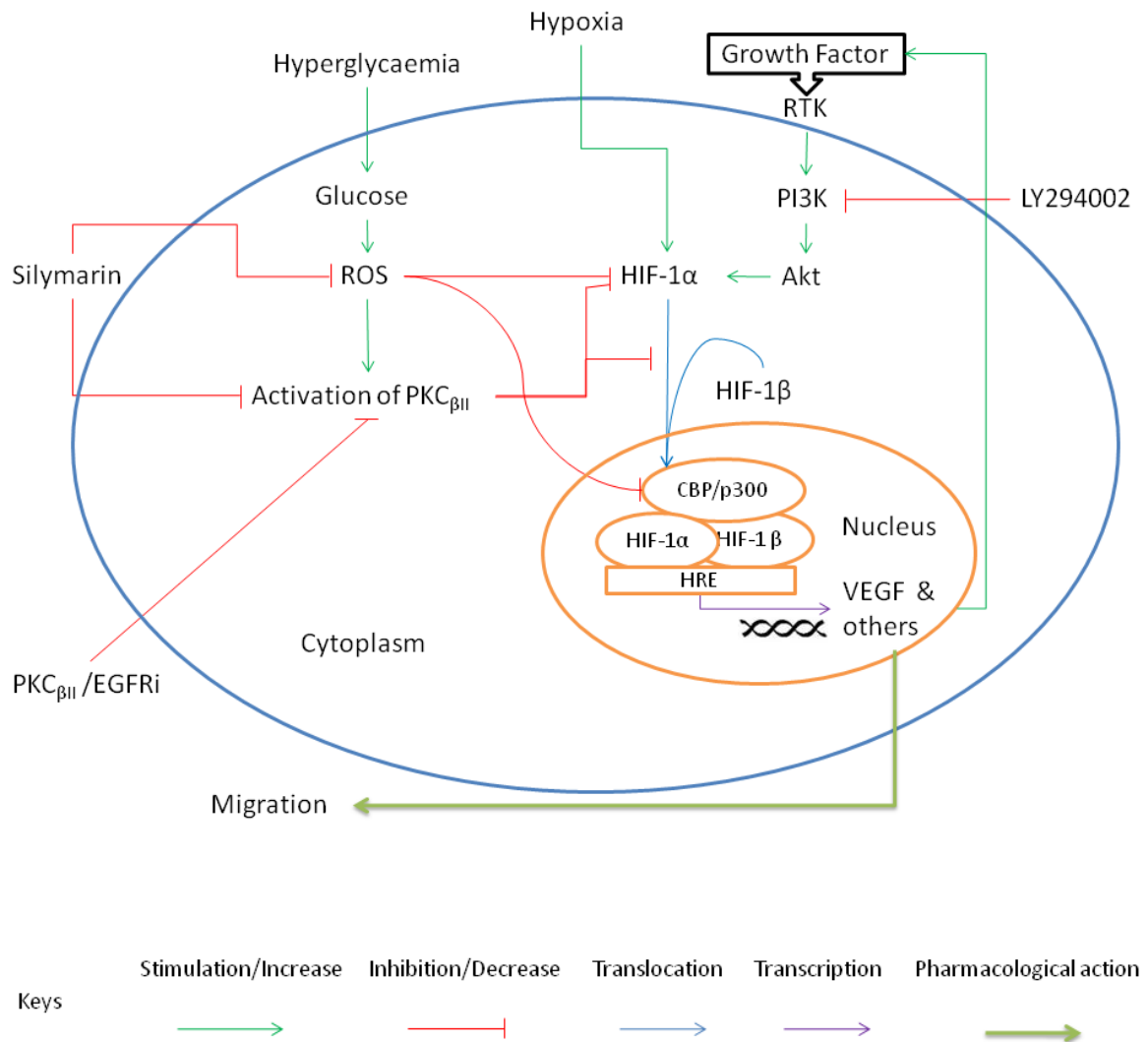
Fig. 8.1 Summary of the findings High glucose concentration attenuates the migration of HMVECad by over production of ROS and over activation of PKC$_{\beta II}$ which could be interfering with the stabilisation, translocation and transcriptional activities of HIF-1α. Silymarin treatment mimicked the effect of PKC$_{\beta II}$ inhibitor by restoring the migration of cells via its anti-oxidant activities. On the other hand, hypoxia and growth factors such as VEGF increase the migration by increasing the stability and transcriptional activity of HIF-1α, which might be mediated through PI3K-Akt pathway.

8.2 Conclusion

Hypoxia and hyperglycaemia have an opposing effect of the migration of microvascular endothelial cells of dermal origin. Hypoxia increased and hyperglycaemia decreased the migration of cells. The change in migration response to varying concentration of glucose and oxygen tension appears to be mediated via multiple molecular pathways. Hypoxia appears to increase the migration via activating PI3K pathway whereas hyperglycaemia appears to decrease the migration due to the overproduction of ROS and activation of PKC$_{\beta II}$ pathway. HIF-1α seems to be a common link between the two which is activated in presence of hypoxia and its activity is hindered in the presence of high glucose. Anti-oxidant effects of silymarin seem to be successful in restoring the high glucose induced reduction in the migration of cells. Silymarin formulated as a freeze dried wafer disc retained its effectiveness against the deleterious effects of high glucose concentration.

8.3 Future work

a) Relationship between the migration and proliferation need further investigation as we and others observed that the migration and proliferation although interlinked might not be occurring simultaneously in a cell of a monolayer (Gerhardt et al. 2003). This could be further ascertained by staining the cells for mitosis markers such as phospho-histone or Ki67 which would help to understand the proliferation status of stalk and tip cells of a monolayer.

b) The link between HIF-1α and hypoxia/hyperglycaemia affected migration, although established to some extent, would benefit further by the use of other molecular biology techniques such as anti-sense technology or use of siRNA to establish a direct link between them.

c) The role of HIF-1α and small GTPases such as RhoA, Rac1 and cdc42 in mediating the migration may not be independent of each other. Establishing a link between these two would enhance the understanding of the effects of the diabetic milieu on the angiogenesis of wound healing.

d) Mechanistically, on reflection, it would have been beneficial to assess the role of both p38 along with p42/p44 MAPK pathways in mediating the migration/proliferation during hyperglycaemia. As the role of PI3K-Akt pathway produced pro-migratory effects in hypoxia was established, it would be interesting to understand the effect that different isoforms of PI3K have in the regulation of migration. Further, the role of PI3K-Akt in mediating the high glucose induced decrease in cell migration should be further explored. The greatest paradox about the effect of hyperglycaemia on the migration and by

that extension on angiogenesis is that of the contrast between decrease in wound healing process and increase in proliferative diabetic retinopathy. Clearly, the environment and cell origin will have some bearing but it may be that the relative levels of hypoxia and hyperglycaemia differs between the two conditions. It would be of a great interest to study the effect of hyperglycaemia on the migration/proliferation of microvascular endothelial cells of dermal and simultaneously of retinal origin. In this respect the role of $PKC_{\beta II}$ would be interesting to ascertain as ruboxistaurin (a PKC_β inhibitor – developed by Eli Lilly) came up to the stage of approval before it was withdrawn by the company for its use in proliferative retinopathy (Anonymous 2007).

e) Molecular mechanism/s through which silymarin produces its effect also needs investigation. The development of freeze dried wafers as a suitable formulation would benefit from future work of testing them on an *in vivo* model of wound healing.

It is a continuous and arduous task to develop a suitable formulation containing a therapeutic agent (á la magic pill) for chronic wounds of diabetes, as wound healing itself is a complex process and the presence of diabetes further complicates the picture. While it is recognised that this complexity exists and has also been demonstrated by this study, it also illustrates that the combination of mechanistic and therapeutic study provides some hope for resolution in a clinical context. This is a challenge for the combination of multiple disciplines of biomedical sciences, but it may also be paraphrased as a 'juggernaut' which takes a lot of energy to initiate movement, but once moving, the power of its size and impact fully evident.

Chapter 9 - References

References

A
ANONYMUS, 2007. Ruboxistaurin: LY 333531. 2007. *Drugs in R&D,* 8(3), pp. 193-199

ABACI, H.E., TRUITT, R., LUONG, E., DRAZER, G. and GERECHT, S., 2010. Adaptation to oxygen deprivation in cultures of human pluripotent stem cells, endothelial progenitor cells, and umbilical vein endothelial cells. *American journal of physiology.Cell physiology,* 298(6), pp. C1527-37

ADLER, A.I., STEVENS, R.J., NEIL, A., STRATTON, I.M., BOULTON, A.J. and HOLMAN, R.R., 2002. UKPDS 59: hyperglycemia and other potentially modifiable risk factors for peripheral vascular disease in type 2 diabetes. *Diabetes care,* 25(5), pp. 894-899

AGARWAL, R., AGARWAL, C., ICHIKAWA, H., SINGH, R.P. and AGGARWAL, B.B., 2006. Anticancer potential of silymarin: from bench to bed side. *Anticancer Research,* 26(6B), pp. 4457-4498

AHN, J.D., MORISHITA, R., KANEDA, Y., LEE, K.U., PARK, J.Y., JEON, Y.J., SONG, H.S. and LEE, I.K., 2001. Transcription factor decoy for activator protein-1 (AP-1) inhibits high glucose- and angiotensin II-induced type 1 plasminogen activator inhibitor (PAI-1) gene expression in cultured human vascular smooth muscle cells. *Diabetologia,* 44(6), pp. 713-720

AIELLO, L.P., AVERY, R.L., ARRIGG, P.G., KEYT, B.A., JAMPEL, H.D., SHAH, S.T., PASQUALE, L.R., THIEME, H., IWAMOTO, M.A. and PARK, J.E., 1994. Vascular endothelial growth factor in ocular fluid of patients with diabetic retinopathy and other retinal disorders. *The New England journal of medicine,* 331(22), pp. 1480-1487

ALBERTS, B., JOHNSON, A., LEWIS, J., RAFF, M., ROBERTS, K. and WALTER, P., 2008. *Molecular biology of the cell.* New York NY10016, Abingdon OX4 4RN: Garland Science, Taylor and Francis Group.

ALTANNAVCH, T.S., ROUBALOVA, K., KUCERA, P. and ANDEL, M., 2004. Effect of high glucose concentrations on expression of ELAM-1, VCAM-1 and ICAM-1 in HUVEC with and without cytokine activation. *Physiological Research / Academia Scientiarum Bohemoslovaca,* 53(1), pp. 77-82

ALTAVILLA, D., SQUADRITO, F., POLITO, F., IRRERA, N., CALO, M., LO CASCIO, P., GALEANO, M., LA CAVA, L., MINUTOLI, L., MARINI, H. and BITTO, A., 2010. Activation of adenosine A2(A) receptors restores the altered cell-cycle machinery during impaired wound healing in genetically diabetic mice. *Surgery,*

ANDRASSY, M., BELOV, D., HARJA, E., ZOU, Y.S., LEITGES, M., KATUS, H.A., NAWROTH, P.P., YAN, S.D., SCHMIDT, A.M. and YAN, S.F., 2005. Central role of PKCbeta in neointimal expansion triggered by acute arterial injury. *Circulation research,* 96(4), pp. 476-483

ARAGONES, J., JONES, D.R., MARTIN, S., SAN JUAN, M.A., ALFRANCA, A., VIDAL, F., VARA, A., MERIDA, I. and LANDAZURI, M.O., 2001. Evidence for the involvement of diacylglycerol kinase in the activation of hypoxia-inducible transcription factor 1 by low oxygen tension. *The Journal Of Biological Chemistry,* 276(13), pp. 10548-10555

ASCHER, E., GADE, P.V., HINGORANI, A., PUTHUKKERIL, S., KALLAKURI, S., SCHEINMAN, M. and JACOB, T., 2001. Thiamine reverses hyperglycemia-induced dysfunction in cultured endothelial cells. *Surgery,* 130(5), pp. 851-858

AUERBACH, R., LEWIS, R., SHINNERS, B., KUBAI, L. and AKHTAR, N., 2003. Angiogenesis assays: a critical overview. *Clinical chemistry,* 49(1), pp. 32-40

B
BAE, S.H., JEONG, J.W., PARK, J.A., KIM, S.H., BAE, M.K., CHOI, S.J. and KIM, K.W., 2004. Sumoylation increases HIF-1alpha stability and its transcriptional activity. *Biochemical and biophysical research communications,* 324(1), pp. 394-400

BAEK, J.H., LIU, Y.V., MCDONALD, K.R., WESLEY, J.B., ZHANG, H. and SEMENZA, G.L., 2007. Spermidine/spermine N(1)-acetyltransferase-1 binds to hypoxia-inducible

factor-1alpha (HIF-1alpha) and RACK1 and promotes ubiquitination and degradation of HIF-1alpha. *The Journal of biological chemistry,* 282(46), pp. 33358-33366

BALKAU, B. and ESCHWEGE, E., 2003. The diagnosis and classification of diabetes and impaired glucose regulation. In: J.C. PICKUP and G. WILLIAMS, eds. *Textbook of Diabetes.* 3rd ed. Oxford: Blackwell Science. pp. 2.1-2.13

BARRIENTOS, S., STOJADINOVIC, O., GOLINKO, M.S., BREM, H. and TOMIC-CANIC, M., 2008. Growth factors and cytokines in wound healing. *Wound repair and regeneration: official publication of the Wound Healing Society [and] the European Tissue Repair Society,* 16(5), pp. 585-601

BAUMGARTNER-PARZER, S.M., WAGNER, L., PETTERMANN, M., GESSL, A. and WALDHAUSL, W., 1995a. Modulation by high glucose of adhesion molecule expression in cultured endothelial cells. *Diabetologia,* 38(11), pp. 1367-1370

BAUMGARTNER-PARZER, S.M., WAGNER, L., PETTERMANN, M., GRILLARI, J., GESSL, A. and WALDHAUSL, W., 1995b. High-glucose--triggered apoptosis in cultured endothelial cells. *Diabetes,* 44(11), pp. 1323-1327

BERRIER, A.L. and YAMADA, K.M., 2007. Cell-matrix adhesion. *Journal of cellular physiology,* 213(3), pp. 565-573

BERTHIER, C.C., ZHANG, H., SCHIN, M., HENGER, A., NELSON, R.G., YEE, B., BOUCHEROT, A., NEUSSER, M.A., COHEN, C.D., CARTER-SU, C., ARGETSINGER, L.S., RASTALDI, M.P., BROSIUS, F.C. and KRETZLER, M., 2009. Enhanced expression of Janus kinase-signal transducer and activator of transcription pathway members in human diabetic nephropathy. *Diabetes,* 58(2), pp. 469-477

BESSON, A., GURIAN-WEST, M., SCHMIDT, A., HALL, A. and ROBERTS, J.M., 2004. p27Kip1 modulates cell migration through the regulation of RhoA activation. *Genes & development,* 18(8), pp. 862-876

BLANCHOIN, L., POLLARD, T.D. and MULLINS, R.D., 2000. Interactions of ADF/cofilin, Arp2/3 complex, capping protein and profilin in remodeling of branched actin filament networks. *Current biology : CB,* 10(20), pp. 1273-1282

BOATENG, J.S., MATTHEWS, K.H., STEVENS, H.N. and ECCLESTON, G.M., 2008. Wound healing dressings and drug delivery systems: a review. *Journal of pharmaceutical sciences,* 97(8), pp. 2892-2923

BOERI, D., ALMUS, F.E., MAIELLO, M., CAGLIERO, E., RAO, L.V. and LORENZI, M., 1989. Modification of tissue-factor mRNA and protein response to thrombin and interleukin 1 by high glucose in cultured human endothelial cells. *Diabetes,* 38(2), pp. 212-218

BOTUSAN, I.R., SUNKARI, V.G., SAVU, O., CATRINA, A.I., GRUNLER, J., LINDBERG, S., PEREIRA, T., YLA-HERTTUALA, S., POELLINGER, L., BRISMAR, K. and CATRINA, S.B., 2008. Stabilization of HIF-1alpha is critical to improve wound healing in diabetic mice. *Proceedings of the National Academy of Sciences of the United States of America,* 105(49), pp. 19426-19431

BOUCHE, C., SERDY, S., KAHN, C.R. and GOLDFINE, A.B., 2004. The cellular fate of glucose and its relevance in type 2 diabetes. *Endocrine reviews,* 25(5), pp. 807-830

BRAHIMI-HORN, M.C. and POUYSSEGUR, J., 2009. HIF at a glance. *Journal of cell science,* 122(Pt 8), pp. 1055-1057

BROWNLEE, M., 2001. Biochemistry and molecular cell biology of diabetic complications. *Nature,* 414, pp. 813-820

BROWNLEE, M., 2005. The pathobiology of diabetic complications: a unifying mechanism. *Diabetes,* 54(6), pp. 1615-1625

C

CACICEDO, J.M., YAGIHASHI, N., KEANEY, J.F.,JR, RUDERMAN, N.B. and IDO, Y., 2004. AMPK inhibits fatty acid-induced increases in NF-kappaB transactivation in cultured human umbilical vein endothelial cells. *Biochemical and biophysical research communications,* 324(4), pp. 1204-1209

CAGLIERO, E., MAIELLO, M., BOERI, D., ROY, S. and LORENZI, M., 1988. Increased expression of basement membrane components in human endothelial cells cultured in high glucose. *The Journal of clinical investigation,* 82(2), pp. 735-738

CALVANI, M., RAPISARDA, A., URANCHIMEG, B., SHOEMAKER, R.H. and MELILLO, G., 2006. Hypoxic induction of an HIF-1alpha-dependent bFGF autocrine loop drives angiogenesis in human endothelial cells. *Blood,* 107(7), pp. 2705-2712

CAMPOS, S.B., ASHWORTH, S.L., WEAN, S., HOSFORD, M., SANDOVAL, R.M., HALLETT, M.A., ATKINSON, S.J. and MOLITORIS, B.A., 2009. Cytokine-induced F-actin reorganization in endothelial cells involves RhoA activation. *American journal of physiology.Renal physiology,* 296(3), pp. F487-95

CAO, G., FEHRENBACH, M.L., WILLIAMS, J.T., FINKLESTEIN, J.M., ZHU, J.X. and DELISSER, H.M., 2009. Angiogenesis in platelet endothelial cell adhesion molecule-1-null mice. *The American journal of pathology,* 175(2), pp. 903-915

CAO, G., O'BRIEN, C.D., ZHOU, Z., SANDERS, S.M., GREENBAUM, J.N., MAKRIGIANNAKIS, A. and DELISSER, H.M., 2002. Involvement of human PECAM-1 in angiogenesis and in vitro endothelial cell migration. *American journal of physiology.Cell physiology,* 282(5), pp. C1181-90

CARLIER, M.F., NIOCHE, P., BROUTIN-L'HERMITE, I., BOUJEMAA, R., LE CLAINCHE, C., EGILE, C., GARBAY, C., DUCRUIX, A., SANSONETTI, P. and PANTALONI, D., 2000. GRB2 links signaling to actin assembly by enhancing interaction of neural Wiskott-Aldrich syndrome protein (N-WASp) with actin-related protein (ARP2/3) complex. *The Journal of biological chemistry,* 275(29), pp. 21946-21952

CARMELIET, P., 2005. Angiogenesis in life, disease and medicine. *Nature,* 438(7070), pp. 932-936

CATRINA, S.B., OKAMOTO, K., PEREIRA, T., BRISMAR, K. and POELLINGER, L., 2004. Hyperglycemia regulates hypoxia-inducible factor-1alpha protein stability and function. *Diabetes,* 53(12), pp. 3226-3232

CELL MIGRATION GATEWAY, 2010. *Overview of the migration process.* [online] Cell migration consortium of NIH and Nature publishing group of Macmillan publishers. Available from: http://cellmigration.org/science/#overview [Accessed 09/10 2010]

CERADINI, D.J., YAO, D., GROGAN, R.H., CALLAGHAN, M.J., EDELSTEIN, D., BROWNLEE, M. and GURTNER, G.C., 2008. Decreasing intracellular superoxide corrects defective ischemia-induced new vessel formation in diabetic mice. *The Journal of biological chemistry,* 283(16), pp. 10930-10938

CHAN, K.C., WU, C.H., HUANG, C.N., LAN, K.P., CHANG, W.C. and WANG, C.J., 2010. Simvastatin Inhibits Glucose-Stimulated Vascular Smooth Muscle Cell Migration Involving Increased Expression of RhoB and a Block of Ras/Akt Signal. *Cardiovascular therapeutics,*

CHANDEL, N.S., MALTEPE, E., GOLDWASSER, E., MATHIEU, C.E., SIMON, M.C. and SCHUMACKER, P.T., 1998. Mitochondrial reactive oxygen species trigger hypoxia-induced transcription. *Proceedings Of The National Academy Of Sciences Of The United States Of America,* 95(20), pp. 11715-11720

CHEN, P.N., HSIEH, Y.S., CHIOU, H.L. and CHU, S.C., 2005. Silibinin inhibits cell invasion through inactivation of both PI3K-Akt and MAPK signaling pathways. *Chemico-biological interactions,* 156(2-3), pp. 141-150

CHEN, Y.H., LIN, S.J., LIN, F.Y., WU, T.C., TSAO, C.R., HUANG, P.H., LIU, P.L., CHEN, Y.L. and CHEN, J.W., 2007. High glucose impairs early and late endothelial progenitor cells by modifying nitric oxide-related but not oxidative stress-mediated mechanisms. *Diabetes,* 56(6), pp. 1559-1568

CHENG, B., LIU, H.W., FU, X.B., SUN, T.Z. and SHENG, Z.Y., 2007. Recombinant human platelet-derived growth factor enhanced dermal wound healing by a pathway involving ERK and c-fos in diabetic rats. *Journal of dermatological science,* 45(3), pp. 193-201

CHRISTIAN, L.M., GRAHAM, J.E., PADGETT, D.A., GLASER, R. and KIECOLT-GLASER, J.K., 2006. Stress and wound healing. *Neuroimmunomodulation,* 13(5-6), pp. 337-346

CHRISTIANSEN, V.J., JACKSON, K.W., LEE, K.N. and MCKEE, P.A., 2007. Effect of fibroblast activation protein and alpha2-antiplasmin cleaving enzyme on collagen types I, III, and IV. *Archives of Biochemistry and Biophysics,* 457(2), pp. 177-186

CINES, D.B., POLLAK, E.S., BUCK, C.A., LOSCALZO, J., ZIMMERMAN, G.A., MCEVER, R.P., POBER, J.S., WICK, T.M., KONKLE, B.A., SCHWARTZ, B.S., BARNATHAN, E.S., MCCRAE, K.R., HUG, B.A., SCHMIDT, A.M. and STERN, D.M., 1998. Endothelial cells in physiology and in the pathophysiology of vascular disorders. *Blood,* 91(10), pp. 3527-3561

CLARK, R.J., MCDONOUGH, P.M., SWANSON, E., TROST, S.U., SUZUKI, M., FUKUDA, M. and DILLMANN, W.H., 2003. Diabetes and the accompanying hyperglycemia impairs cardiomyocyte calcium cycling through increased nuclear O-GlcNAcylation. *The Journal of biological chemistry,* 278(45), pp. 44230-44237

CLIFFORD, S.C., ASTUTI, D., HOOPER, L., MAXWELL, P.H., RATCLIFFE, P.J. and MAHER, E.R., 2001. The pVHL-associated SCF ubiquitin ligase complex: molecular genetic analysis of elongin B and C, Rbx1 and HIF-1alpha in renal cell carcinoma. *Oncogene,* 20(36), pp. 5067-5074

CLYNE, A.M., ZHU, H. and EDELMAN, E.R., 2008. Elevated fibroblast growth factor-2 increases tumor necrosis factor-alpha induced endothelial cell death in high glucose. *Journal of cellular physiology,* 217(1), pp. 86-92

COMELLI, M.C., MENGS, U., SCHNEIDER, C. and PROSDOCIMI, M., 2007. Toward the definition of the mechanism of action of silymarin: activities related to cellular protection from toxic damage induced by chemotherapy. *Integrative cancer therapies,* 6(2), pp. 120-129

CONWAY, E.M., COLLEN, D. and CARMELIET, P., 2001. Molecular mechanisms of blood vessel growth. *Cardiovascular research,* 49(3), pp. 507-521

COOK, K.M. and FIGG, W.D., 2010. Angiogenesis inhibitors: current strategies and future prospects. *CA: a cancer journal for clinicians,* 60(4), pp. 222-243

COOMBER, B.L. and GOTLIEB, A.I., 1990. In vitro endothelial wound repair. Interaction of cell migration and proliferation. *Arteriosclerosis (Dallas, Tex.),* 10(2), pp. 215-222

COOPER, J.A. and SCHAFER, D.A., 2000. Control of actin assembly and disassembly at filament ends. *Current opinion in cell biology,* 12(1), pp. 97-103

COTTER, M.A., JACK, A.M. and CAMERON, N.E., 2002. Effects of the protein kinase C beta inhibitor LY333531 on neural and vascular function in rats with streptozotocin-induced diabetes. *Clinical science (London, England : 1979),* 103(3), pp. 311-321

D

DAI, Y. and GRANT, S., 2003. Cyclin-dependent kinase inhibitors. *Current Opinion in Pharmacology,* 3(4), pp. 362-370

DAS EVCIMEN, N. and KING, G.L., 2007. The role of protein kinase C activation and the vascular complications of diabetes. *Pharmacological research : the official journal of the Italian Pharmacological Society,* 55(6), pp. 498-510

DCCT GROUP, 1993. The effect of intensive treatment of diabetes on the development and progression of long-term complications in insulin-dependent diabetes mellitus. The Diabetes Control and Complications Trial Research Group. *The New England journal of medicine,* 329(14), pp. 977-986

DCCT/EDIC STUDY RESEARCH GROUP, NATHAN, D.M., CLEARY, P.A., BACKLUND, J.Y., GENUTH, S.M., LACHIN, J.M., ORCHARD, T.J., RASKIN, P. and ZINMAN, B., 2005. Intensive diabetes treatment and cardiovascular disease in patients with type 1 diabetes. *The New England journal of medicine,* 353(25), pp. 2643-2653

DE DONATIS, A., COMITO, G., BURICCHI, F., VINCI, M.C., PARENTI, A., CASELLI, A., CAMICI, G., MANAO, G., RAMPONI, G. and CIRRI, P., 2008. Proliferation versus

migration in platelet-derived growth factor signaling: the key role of endocytosis. *The Journal of biological chemistry,* 283(29), pp. 19948-19956

DE DONATIS, A., RANALDI, F. and CIRRI, P., 2010. Reciprocal control of cell proliferation and migration. *Cell communication and signaling : CCS,* 8, pp. 20

DETAILLE, D., SANCHEZ, C., SANZ, N., LOPEZ-NOVOA, J.M., LEVERVE, X. and EL-MIR, M.Y., 2008. Interrelation between the inhibition of glycolytic flux by silibinin and the lowering of mitochondrial ROS production in perifused rat hepatocytes. *Life Sciences,* 82(21-22), pp. 1070-1076

DIABETES TRIALS UNIT, 2010a. *UK prosepctive diabetes study - home page.* [online] Oxford: University of Oxford. Available from: http://www.dtu.ox.ac.uk/ukpds_trial/index.php [Accessed 07/14 2010]

DIABETES TRIALS UNIT, 2010b. *UKPDS - post trial monitoring - home page.* [online] Oxford: University of Oxford. Available from: http://www.dtu.ox.ac.uk/ukpds/index.php [Accessed 07/14 2010]

DIEZ-JUAN, A. and ANDRES, V., 2003. Coordinate control of proliferation and migration by the p27Kip1/cyclin-dependent kinase/retinoblastoma pathway in vascular smooth muscle cells and fibroblasts. *Circulation research,* 92(4), pp. 402-410

DING, Z., LAMBRECHTS, A., PAREPALLY, M. and ROY, P., 2006. Silencing profilin-1 inhibits endothelial cell proliferation, migration and cord morphogenesis. *Journal of cell science,* 119(Pt 19), pp. 4127-4137

DINH, T.L. and VEVES, A., 2005. A review of the mechanisms implicated in the pathogenesis of the diabetic foot. *The international journal of lower extremity wounds,* 4(3), pp. 154-159

DIXIT, P., HERN-ANDERSON, D., RANIERI, J. and SCHMIDT, C.E., 2001. Vascular graft endothelialization: comparative analysis of canine and human endothelial cell migration on natural biomaterials. *Journal of Biomedical Materials Research,* 56(4), pp. 545-555

DOLLE, J.P., REZVAN, A., ALLEN, F.D., LAZAROVICI, P. and LELKES, P.I., 2005. Nerve growth factor-induced migration of endothelial cells. *The Journal of pharmacology and experimental therapeutics,* 315(3), pp. 1220-1227

DU, X., MATSUMURA, T., EDELSTEIN, D., ROSSETTI, L., ZSENGELLER, Z., SZABO, C. and BROWNLEE, M., 2003. Inhibition of GAPDH activity by poly(ADP-ribose) polymerase activates three major pathways of hyperglycemic damage in endothelial cells. *The Journal of clinical investigation,* 112(7), pp. 1049-1057

DU, X.L., EDELSTEIN, D., ROSSETTI, L., FANTUS, I.G., GOLDBERG, H., ZIYADEH, F., WU, J. and BROWNLEE, M., 2000. Hyperglycemia-induced mitochondrial superoxide overproduction activates the hexosamine pathway and induces plasminogen activator inhibitor-1 expression by increasing Sp1 glycosylation. *Proceedings of the National Academy of Sciences of the United States of America,* 97(22), pp. 12222-12226

DUFFY, A., LIEW, A., O'SULLIVAN, J., AVALOS, G., SAMALI, A. and O'BRIEN, T., 2006. Distinct effects of high-glucose conditions on endothelial cells of macrovascular and microvascular origins. *Endothelium : journal of endothelial cell research,* 13(1), pp. 9-16

DUNN, E.J. and GRANT, P.J., 2005. Type 2 diabetes: an atherothrombotic syndrome. *Current Molecular Medicine,* 5(3), pp. 323-332

DURAISAMY, Y., SLEVIN, M., SMITH, N., BAILEY, J., ZWEIT, J., SMITH, C., AHMED, N. and GAFFNEY, J., 2001. Effect of glycation on basic fibroblast growth factor induced angiogenesis and activation of associated signal transduction pathways in vascular endothelial cells: possible relevance to wound healing in diabetes. *Angiogenesis,* 4(4), pp. 277-288

E

ECCLES, S.A., BOX, C. and COURT, W., 2005. Cell migration/invasion assays and their application in cancer drug discovery. *Biotechnology annual review,* 11, pp. 391-421

EL-OSTA, A., BRASACCHIO, D., YAO, D., POCAI, A., JONES, P.L., ROEDER, R.G., COOPER, M.E. and BROWNLEE, M., 2008. Transient high glucose causes persistent

epigenetic changes and altered gene expression during subsequent normoglycemia. *The Journal of experimental medicine,* 205(10), pp. 2409-2417

EMA, M., TAYA, S., YOKOTANI, N., SOGAWA, K., MATSUDA, Y. and FUJII-KURIYAMA, Y., 1997. A novel bHLH-PAS factor with close sequence similarity to hypoxia-inducible factor 1alpha regulates the VEGF expression and is potentially involved in lung and vascular development. *Proceedings of the National Academy of Sciences of the United States of America,* 94(9), pp. 4273-4278

EMERLING, B.M., WEINBERG, F., LIU, J.L., MAK, T.W. and CHANDEL, N.S., 2008. PTEN regulates p300-dependent hypoxia-inducible factor 1 transcriptional activity through Forkhead transcription factor 3a (FOXO3a). *Proceedings of the National Academy of Sciences of the United States of America,* 105(7), pp. 2622-2627

EMINZADE, S., URAZ, F. and IZZETTIN, F.V., 2008. Silymarin protects liver against toxic effects of anti-tuberculosis drugs in experimental animals. *Nutrition & metabolism,* 5, pp. 18

ENDERS, G.H., 2010. Gauchos and ochos: a Wee1-Cdk tango regulating mitotic entry. *Cell division,* 5, pp. 12

ETIENNE-MANNEVILLE, S. and HALL, A., 2001. Integrin-mediated activation of Cdc42 controls cell polarity in migrating astrocytes through PKCzeta. *Cell,* 106(4), pp. 489-498

F

FALANGA, V., 2005. Wound healing and its impairment in the diabetic foot. *The Lancet,* 366(9498), pp. 1736-1743

FANG, J., XIA, C., CAO, Z., ZHENG, J.Z., REED, E. and JIANG, B.H., 2005. Apigenin inhibits VEGF and HIF-1 expression via PI3K/AKT/p70S6K1 and HDM2/p53 pathways. *The FASEB journal : official publication of the Federation of American Societies for Experimental Biology,* 19(3), pp. 342-353

FAROOQUI, R. and FENTEANY, G., 2005. Multiple rows of cells behind an epithelial wound edge extend cryptic lamellipodia to collectively drive cell-sheet movement. *Journal of cell science,* 118(Pt 1), pp. 51-63

FERENCI, P., DRAGOSICS, B., DITTRICH, H., FRANK, H., BENDA, L., LOCHS, H., MERYN, S., BASE, W. and SCHNEIDER, B., 1989. Randomized controlled trial of silymarin treatment in patients with cirrhosis of the liver. *Journal of hepatology,* 9(1), pp. 105-113

FERRARA, N. and KERBEL, R.S., 2005. Angiogenesis as a therapeutic target. *Nature,* 438(7070), pp. 967-974

FIGUEROA-ROMERO, C., SADIDI, M. and FELDMAN, E.L., 2008. Mechanisms of disease: the oxidative stress theory of diabetic neuropathy. *Reviews in endocrine & metabolic disorders,* 9(4), pp. 301-314

FITSIALOS, G., BOURGET, I., AUGIER, S., GINOUVES, A., REZZONICO, R., ODORISIO, T., CIANFARANI, F., VIROLLE, T., POUYSSEGUR, J., MENEGUZZI, G., BERRA, E., PONZIO, G. and BUSCA, R., 2008. HIF1 transcription factor regulates laminin-332 expression and keratinocyte migration. *Journal of cell science,* 121(Pt 18), pp. 2992-3001

FLETCHER, D.A. and MULLINS, R.D., 2010. Cell mechanics and the cytoskeleton. *Nature,* 463(7280), pp. 485-492

FLORES, C., ROJAS, S., AGUAYO, C., PARODI, J., MANN, G., PEARSON, J.D., CASANELLO, P. and SOBREVIA, L., 2003. Rapid stimulation of L-arginine transport by D-glucose involves p42/44(mapk) and nitric oxide in human umbilical vein endothelium. *Circulation research,* 92(1), pp. 64-72

FLUGEL, D., GORLACH, A., MICHIELS, C. and KIETZMANN, T., 2007. Glycogen synthase kinase 3 phosphorylates hypoxia-inducible factor 1alpha and mediates its destabilization in a VHL-independent manner. *Molecular and cellular biology,* 27(9), pp. 3253-3265

FOLKMAN, J., 1971. Tumor angiogenesis: therapeutic implications. *The New England journal of medicine,* 285(21), pp. 1182-1186

FU, H., LUO, F., YANG, L., WU, W. and LIU, X., 2010. Hypoxia stimulates the expression of macrophage migration inhibitory factor in human vascular smooth muscle cells via HIF-1alpha dependent pathway. *BMC cell biology,* 11, pp. 66

G
GADE, P.V., ANDRADES, J.A., NIMNI, M.E., BECERRA, J., LONGORIA, J., ASEMANFAR, N. and SORGENTE, N., 1997. Nitric oxide mediates hyperglycemia-induced defective migration in cultured endothelial cells. *Journal of vascular surgery : official publication, the Society for Vascular Surgery [and] International Society for Cardiovascular Surgery, North American Chapter,* 26(2), pp. 319-326

GALLO, A., CEOLOTTO, G., PINTON, P., IORI, E., MURPHY, E., RUTTER, G.A., RIZZUTO, R., SEMPLICINI, A. and AVOGARO, A., 2005. Metformin prevents glucose-induced protein kinase C-beta2 activation in human umbilical vein endothelial cells through an antioxidant mechanism. *Diabetes,* 54(4), pp. 1123-1131

GAO, W., FERGUSON, G., CONNELL, P., WALSHE, T., MURPHY, R., BIRNEY, Y.A., O'BRIEN, C. and CAHILL, P.A., 2007. High glucose concentrations alter hypoxia-induced control of vascular smooth muscle cell growth via a HIF-1α-dependent pathway. *Journal of Molecular and Cellular Cardiology,* 42(3), pp. 609-619

GARCIA-MACEIRA, P. and MATEO, J., 2009. Silibinin inhibits hypoxia-inducible factor-1alpha and mTOR/p70S6K/4E-BP1 signalling pathway in human cervical and hepatoma cancer cells: implications for anticancer therapy. *Oncogene,* 28(3), pp. 313-324

GARDINER, T.A., ANDERSON, H.R. and STITT, A.W., 2003. Inhibition of advanced glycation end-products protects against retinal capillary basement membrane expansion during long-term diabetes. *The Journal of pathology,* 201(2), pp. 328-333

GARDNER, L.B., LI, Q., PARK, M.S., FLANAGAN, W.M., SEMENZA, G.L. and DANG, C.V., 2001. Hypoxia inhibits G1/S transition through regulation of p27 expression. *The Journal of biological chemistry,* 276(11), pp. 7919-7926

GATTI, A.M., PINCHIORRI, P. and MONARI, E., 1994. Physical properties of a new biomaterial for wound management. *Journal of material science: Materials in medicine,* 5, pp. 190-193

GERHARDT, H., GOLDING, M., FRUTTIGER, M., RUHRBERG, C., LUNDKVIST, A., ABRAMSSON, A., JELTSCH, M., MITCHELL, C., ALITALO, K., SHIMA, D. and BETSHOLTZ, C., 2003. VEGF guides angiogenic sprouting utilizing endothelial tip cell filopodia. *The Journal of cell biology,* 161(6), pp. 1163-1177

GNUDI, L., GRUDEN, G. and VIBERTI, G.F., 2003. Pathogenesis of diabetic nephropathy. In: J.C. PICKUP and W. GARETH, eds. *Textbook of diabetes.* 3rd ed. Oxford: Blackwell Sciences. pp. 52.1-52.21

GODA, N., RYAN, H.E., KHADIVI, B., MCNULTY, W., RICKERT, R.C. and JOHNSON, R.S., 2003. Hypoxia-inducible factor 1alpha is essential for cell cycle arrest during hypoxia. *Molecular and cellular biology,* 23(1), pp. 359-369

GOGG, S., SMITH, U. and JANSSON, P.A., 2009. Increased MAPK activation and impaired insulin signaling in subcutaneous microvascular endothelial cells in type 2 diabetes: the role of endothelin-1. *Diabetes,* 58(10), pp. 2238-2245

GOMES, E.R., JANI, S. and GUNDERSEN, G.G., 2005. Nuclear movement regulated by Cdc42, MRCK, myosin, and actin flow establishes MTOC polarization in migrating cells. *Cell,* 121(3), pp. 451-463

GONG, C., STOLETOV, K.V. and TERMAN, B.I., 2004. VEGF treatment induces signaling pathways that regulate both actin polymerization and depolymerization. *Angiogenesis,* 7(4), pp. 313-321

GOUKASSIAN, D., DIEZ-JUAN, A., ASAHARA, T., SCHRATZBERGER, P., SILVER, M., MURAYAMA, T., ISNER, J.M. and ANDRES, V., 2001. Overexpression of p27(Kip1) by doxycycline-regulated adenoviral vectors inhibits endothelial cell proliferation and migration and impairs angiogenesis. *The FASEB journal : official publication of the Federation of American Societies for Experimental Biology,* 15(11), pp. 1877-1885

GRAIER, W.F., GRUBENTHAL, I., DITTRICH, P., WASCHER, T.C. and KOSTNER, G.M., 1995. Intracellular mechanism of high D-glucose-induced modulation of vascular cell proliferation. *European journal of pharmacology,* 294(1), pp. 221-229

GREENLEE, H., ABASCAL, K., YARNELL, E. and LADAS, E., 2007. Clinical applications of Silybum marianum in oncology. *Integrative cancer therapies,* 6(2), pp. 158-165

GRIFFIOEN, A.W. and MOLEMA, G., 2000. Angiogenesis: potentials for pharmacologic intervention in the treatment of cancer, cardiovascular diseases, and chronic inflammation. *Pharmacological reviews,* 52(2), pp. 237-268

GU, M., DHANALAKSHMI, S., MOHAN, S., SINGH, R.P. and AGARWAL, R., 2005. Silibinin inhibits ultraviolet B radiation-induced mitogenic and survival signaling, and associated biological responses in SKH-1 mouse skin. *Carcinogenesis,* 26(8), pp. 1404-1413

GU, Y.Z., MORAN, S.M., HOGENESCH, J.B., WARTMAN, L. and BRADFIELD, C.A., 1998. Molecular characterization and chromosomal localization of a third alpha-class hypoxia inducible factor subunit, HIF3alpha. *Gene expression,* 7(3), pp. 205-213

GUHAGARKAR, S.A., MALSHE, V.C. and DEVARAJAN, P.V., 2009. Nanoparticles of polyethylene sebacate: a new biodegradable polymer. *AAPS PharmSciTech,* 10(3), pp. 935-942

GUIGAS, B., NABOULSI, R., VILLANUEVA, G.R., TALEUX, N., LOPEZ-NOVOA, J.M., LEVERVE, X.M. and EL-MIR, M.Y., 2007. The flavonoid silibinin decreases glucose-6-phosphate hydrolysis in perfused rat hepatocytes by an inhibitory effect on glucose-6-phosphatase. *Cellular physiology and biochemistry : international journal of experimental cellular physiology, biochemistry, and pharmacology,* 20(6), pp. 925-934

GUPTA, K., KSHIRSAGAR, S., LI, W., GUI, L., RAMAKRISHNAN, S., GUPTA, P., LAW, P.Y. and HEBBEL, R.P., 1999. VEGF prevents apoptosis of human microvascular endothelial cells via opposing effects on MAPK/ERK and SAPK/JNK signaling. *Experimental Cell Research,* 247(2), pp. 495-504

GUMY, L.F., BAMPTON, E.T. and TOLKOVSKY, A.M., 2008. Hyperglycaemia inhibits Schwann cell proliferation and migration and restricts regeneration of axons and Schwann cells from adult murine DRG. *Molecular and cellular neurosciences,* 37(2), pp. 298-311

GUO, S. and DIPIETRO, L.A., 2010. Factors affecting wound healing. *Journal of dental research,* 89(3), pp. 219-229

GUTIERREZ, G.J., TSUJI, T., CROSS, J.V., DAVIS, R.J., TEMPLETON, D.J., JIANG, W. and RONAI, Z.A., 2010. JNK-mediated phosphorylation of Cdc25C regulates cell cycle entry and G(2)/M DNA damage checkpoint. *The Journal of biological chemistry,* 285(19), pp. 14217-14228

H

HAMED, S., BRENNER, B., ABASSI, Z., AHARON, A., DAOUD, D. and ROGUIN, A., 2010. Hyperglycemia and oxidized-LDL exert a deleterious effect on endothelial progenitor cell migration in type 2 diabetes mellitus. *Thrombosis research,* 126(3), pp. 166-174

HAMURO, M., POLAN, J., NATARAJAN, M. and MOHAN, S., 2002. High glucose induced nuclear factor kappa B mediated inhibition of endothelial cell migration. *Atherosclerosis,* 162(2), pp. 277-287

HAN, M.H., YOON, W.K., LEE, H., HAN, S.B., LEE, K., PARK, S.K., YANG, K.H., KIM, H.M. and KANG, J.S., 2007. Topical application of silymarin reduces chemical-induced irritant contact dermatitis in BALB/c mice. *International immunopharmacology,* 7(13), pp. 1651-1658

HANNA, M.A., CHINNSWAMY, R., GRAY, D.R. and MILADINOV, V.D., 1997. *Extrudates of Starch-Xanthan Gum Mixtures as Affected by Chemical Agents and Irradiation.* - Blackwell Publishing Ltd.

HANNON, G.J. and BEACH, D., 1994. p15INK4B is a potential effector of TGF-beta-induced cell cycle arrest. *Nature,* 371(6494), pp. 257-261

HERBACH, N., SCHAIRER, I., BLUTKE, A., KAUTZ, S., SIEBERT, A., GOKE, B., WOLF, E. and WANKE, R., 2009. Diabetic kidney lesions of GIPRdn transgenic mice: podocyte hypertrophy and thickening of the GBM precede glomerular hypertrophy and glomerulosclerosis. *American journal of physiology.Renal physiology,* 296(4), pp. F819-29

HERVÉ, M., BUTEAU-LOZANO, H., MOURAH, S., CALVO, F. and PERROT-APPLANAT, M., 2005. VEGF189 stimulates endothelial cells proliferation and migration in vitro and up-regulates the expression of Flk-1/KDR mRNA. *Experimental Cell Research,* 309(1), pp. 24-31

HINSHAW, D.B., BURGER, J.M., MILLER, M.T., ADAMS, J.A., BEALS, T.F. and OMANN, G.M., 1993. ATP depletion induces an increase in the assembly of a labile pool of polymerized actin in endothelial cells. *The American Journal of Physiology,* 264(5 Pt 1), pp. C1171-9

HIRAI, H., ROUSSEL, M.F., KATO, J.Y., ASHMUN, R.A. and SHERR, C.J., 1995. Novel INK4 proteins, p19 and p18, are specific inhibitors of the cyclin D-dependent kinases CDK4 and CDK6. *Molecular and cellular biology,* 15(5), pp. 2672-2681

HIROTA, K. and SEMENZA, G.L., 2006. Regulation of angiogenesis by hypoxia-inducible factor 1. *Critical reviews in oncology/hematology,* 59(1), pp. 15-26

HOLMAN, R.R., PAUL, S.K., BETHEL, M.A., MATTHEWS, D.R. and NEIL, H.A., 2008. 10-Year Follow-Up of Intensive Glucose Control in Type 2 Diabetes. *The New England journal of medicine,* 359(15), pp. 1577-1589

HOSOYA, M., OHASHI, J., SAWADA, A., TAKAKI, A. and SHIMOKAWA, H., 2010. Combination therapy with olmesartan and azelnidipine improves EDHF-mediated responses in diabetic apolipoprotein E-deficient mice. *Circulation journal : official journal of the Japanese Circulation Society,* 74(4), pp. 798-806

HSU, S., THAKAR, R. and LI, S., 2007. Haptotaxis of endothelial cell migration under flow. *Methods in Molecular Medicine,* 139, pp. 237-250

HUANG, J., ZHAO, Q., MOONEY, S.M. and LEE, F.S., 2002. Sequence determinants in hypoxia-inducible factor-1alpha for hydroxylation by the prolyl hydroxylases PHD1, PHD2, and PHD3. *The Journal of biological chemistry,* 277(42), pp. 39792-39800

HUANG, L.E., GU, J., SCHAU, M. and BUNN, H.F., 1998. Regulation of hypoxia-inducible factor 1alpha is mediated by an O2-dependent degradation domain via the ubiquitin-proteasome pathway. *Proceedings of the National Academy of Sciences of the United States of America,* 95(14), pp. 7987-7992

HUANG, Q. and SHEIBANI, N., 2008. High glucose promotes retinal endothelial cell migration through activation of Src, PI3K/Akt1/eNOS, and ERKs. *American journal of physiology.Cell physiology,* 295(6), pp. C1647-57

HUBNER, G., BRAUCHLE, M., SMOLA, H., MADLENER, M., FASSLER, R. and WERNER, S., 1996. Differential regulation of pro-inflammatory cytokines during wound healing in normal and glucocorticoid-treated mice. *Cytokine,* 8(7), pp. 548-556

HUFNER, K., HIGGS, H.N., POLLARD, T.D., JACOBI, C., AEPFELBACHER, M. and LINDER, S., 2001. The verprolin-like central (vc) region of Wiskott-Aldrich syndrome protein induces Arp2/3 complex-dependent actin nucleation. *The Journal of biological chemistry,* 276(38), pp. 35761-35767

HUNG, C.F., LIN, Y.K., ZHANG, L.W., CHANG, C.H. and FANG, J.Y., 2010. Topical delivery of silymarin constituents via the skin route. *Acta Pharmacologica Sinica,* 31(1), pp. 118-126

HUR, E., CHANG, K.Y., LEE, E., LEE, S.K. and PARK, H., 2001. Mitogen-activated protein kinase kinase inhibitor PD98059 blocks the trans-activation but not the stabilization or DNA binding ability of hypoxia-inducible factor-1alpha. *Molecular pharmacology,* 59(5), pp. 1216-1224

HUSEINI, H.F., LARIJANI, B., HESHMAT, R., FAKHRZADEH, H., RADJABIPOUR, B., TOLIAT, T. and RAZA, M., 2006. The efficacy of Silybum marianum (L.) Gaertn. (silymarin) in the treatment of type II diabetes: a randomized, double-blind, placebo-controlled, clinical trial. *Phytotherapy Research : PTR,* 20(12), pp. 1036-1039

HUSSAIN, S.A., 2007. Silymarin as an adjunct to glibenclamide therapy improves long-term and postprandial glycemic control and body mass index in type 2 diabetes. *Journal of medicinal food,* 10(3), pp. 543-547

HUVENEERS, S. and DANEN, E.H., 2009. Adhesion signaling - crosstalk between integrins, Src and Rho. *Journal of cell science,* 122(Pt 8), pp. 1059-1069

HYNES, R.O., 2002. Integrins: Bidirectional, Allosteric Signaling Machines. *Cell,* 110(6), pp. 673-687

I

IDRIS, I. and DONNELLY, R., 2006. Protein kinase C beta inhibition: A novel therapeutic strategy for diabetic microangiopathy. *Diabetes & vascular disease research : official journal of the International Society of Diabetes and Vascular Disease,* 3(3), pp. 172-178

IHNAT, M.A., THORPE, J.E., KAMAT, C.D., SZABO, C., GREEN, D.E., WARNKE, L.A., LACZA, Z., CSELENYAK, A., ROSS, K., SHAKIR, S., PICONI, L., KALTREIDER, R.C. and CERIELLO, A., 2007. Reactive oxygen species mediate a cellular 'memory' of high glucose stress signalling. *Diabetologia,* 50(7), pp. 1523-1531

IIDA, T., MINE, S., FUJIMOTO, H., SUZUKI, K., MINAMI, Y. and TANAKA, Y., 2002. Hypoxia-inducible factor-1alpha induces cell cycle arrest of endothelial cells. *Genes to cells : devoted to molecular & cellular mechanisms,* 7(2), pp. 143-149

ILAN, N. and MADRI, J.A., 2003. PECAM-1: old friend, new partners. *Current opinion in cell biology,* 15(5), pp. 515-524

IM, E., CHOI, Y.J., KIM, C.H., FIOCCHI, C., POTHOULAKIS, C. and RHEE, S.H., 2009. The angiogenic effect of probiotic Bacillus polyfermenticus on human intestinal microvascular endothelial cells is mediated by IL-8. *American journal of physiology.Gastrointestinal and liver physiology,* 297(5), pp. G999-G1008

IMAGE J, 2010. *Quantifying stained liver tissue.* [online] Available from: http://rsbweb.nih.gov/ij/docs/examples/stained-sections/index.html 2010]

INNOCENTI, M., GERBOTH, S., ROTTNER, K., LAI, F.P., HERTZOG, M., STRADAL, T.E., FRITTOLI, E., DIDRY, D., POLO, S., DISANZA, A., BENESCH, S., DI FIORE, P.P., CARLIER, M.F. and SCITA, G., 2005. Abi1 regulates the activity of N-WASP and WAVE in distinct actin-based processes. *Nature cell biology,* 7(10), pp. 969-976

INTERNATIONAL DIABETES FEDERATION, 2009. *Diabetes atlas 4th edition.* [online] Brussels, Belgium: IDF. Available from: http://www.diabetesatlas.org/ [Accessed 07/07 2010]

J

JAAKKOLA, P., MOLE, D.R., TIAN, Y.M., WILSON, M.I., GIELBERT, J., GASKELL, S.J., KRIEGSHEIM, A., HEBESTREIT, H.F., MUKHERJI, M., SCHOFIELD, C.J., MAXWELL, P.H., PUGH, C.W. and RATCLIFFE, P.J., 2001. Targeting of HIF-alpha to the von Hippel-Lindau ubiquitylation complex by O2-regulated prolyl hydroxylation. *Science (New York, N.Y.),* 292(5516), pp. 468-472

JENSEN, P.V. and LARSSON, L.I., 2004. Actin microdomains on endothelial cells: association with CD44, ERM proteins, and signaling molecules during quiescence and wound healing. *Histochemistry and cell biology,* 121(5), pp. 361-369

JEONG, J.W., BAE, M.K., AHN, M.Y., KIM, S.H., SOHN, T.K., BAE, M.H., YOO, M.A., SONG, E.J., LEE, K.J. and KIM, K.W., 2002. Regulation and destabilization of HIF-1alpha by ARD1-mediated acetylation. *Cell,* 111(5), pp. 709-720

JIANG, B.H., RUE, E., WANG, G.L., ROE, R. and SEMENZA, G.L., 1996. Dimerization, DNA binding, and transactivation properties of hypoxia-inducible factor 1. *The Journal of biological chemistry,* 271(30), pp. 17771-17778

JIANG, B.H., ZHENG, J.Z., AOKI, M. and VOGT, P.K., 2000. Phosphatidylinositol 3-kinase signaling mediates angiogenesis and expression of vascular endothelial growth factor in endothelial cells. *Proceedings of the National Academy of Sciences of the United States of America,* 97(4), pp. 1749-1753

JIANG, C., AGARWAL, R. and LU, J., 2000. Anti-angiogenic potential of a cancer chemopreventive flavonoid antioxidant, silymarin: inhibition of key attributes of vascular endothelial cells and angiogenic cytokine secretion by cancer epithelial cells. *Biochemical and biophysical research communications,* 276(1), pp. 371-378

JOBERTY, G., PETERSEN, C., GAO, L. and MACARA, I.G., 2000. The cell-polarity protein Par6 links Par3 and atypical protein kinase C to Cdc42. *Nature cell biology,* 2(8), pp. 531-539

JONES, D.S., LAWLOR, M.S. and WOOLFSON, A.D., 2003. Rheological and mucoadhesive characterization of polymeric systems composed of poly(methylvinylether-co-maleic anhydride) and poly(vinylpyrrolidone), designed as platforms for topical drug delivery. *Journal of pharmaceutical sciences,* 92(5), pp. 995-1007

JUNG, C.R., HWANG, K.S., YOO, J., CHO, W.K., KIM, J.M., KIM, W.H. and IM, D.S., 2006. E2-EPF UCP targets pVHL for degradation and associates with tumor growth and metastasis. *Nature medicine,* 12(7), pp. 809-816

K

KALLIO, P.J., OKAMOTO, K., O'BRIEN, S., CARRERO, P., MAKINO, Y., TANAKA, H. and POELLINGER, L., 1998. Signal transduction in hypoxic cells: inducible nuclear translocation and recruitment of the CBP/p300 coactivator by the hypoxia-inducible factor-1alpha. *The EMBO journal,* 17(22), pp. 6573-6586

KAMURA, T., SATO, S., IWAI, K., CZYZYK-KRZESKA, M., CONAWAY, R.C. and CONAWAY, J.W., 2000. Activation of HIF1alpha ubiquitination by a reconstituted von Hippel-Lindau (VHL) tumor suppressor complex. *Proceedings of the National Academy of Sciences of the United States of America,* 97(19), pp. 10430-10435

KANEIDER, N.C., LEGER, A.J. and KULIOPULOS, A., 2006. Therapeutic targeting of molecules involved in leukocyte-endothelial cell interactions. *The FEBS journal,* 273(19), pp. 4416-4424

KANG, H., WANG, J., LONGLEY, S.J., TANG, J.X. and SHAW, S.K., 2010. Relative actin nucleation promotion efficiency by wasp and wave proteins in endothelial cells. *Biochemical and biophysical research communications,* 400(4), pp. 661-666

KANTERS, S.D., BANGA, J.D., ALGRA, A., FRIJNS, R.C., BEUTLER, J.J. and FIJNHEER, R., 2001. Plasma levels of cellular fibronectin in diabetes. *Diabetes care,* 24(2), pp. 323-327

KASHYAP, S.R. and DEFRONZO, R.A., 2007. The insulin resistance syndrome: physiological considerations. *Diabetes & vascular disease research : official journal of the International Society of Diabetes and Vascular Disease,* 4(1), pp. 13-19

KATSILAMBROS, N. and TENTOLOURIS, N., 2003. Type 2 diabetes: an overview. In: J.C. PICKUP and WILLIAMS GARETH, eds. *Textbook of Diabetes.* 3rd ed. Oxford: Blackwell Science. pp. 4.1-4.19

KAUR, M., VELMURUGAN, B., TYAGI, A., DEEP, G., KATIYAR, S., AGARWAL, C. and AGARWAL, R., 2009. Silibinin suppresses growth and induces apoptotic death of human colorectal carcinoma LoVo cells in culture and tumor xenograft. *Molecular cancer therapeutics,* 8(8), pp. 2366-2374

KE, Q. and COSTA, M., 2006. Hypoxia-inducible factor-1 (HIF-1). *Molecular pharmacology,* 70(5), pp. 1469-1480

KELLY, D.J., BUCK, D., COX, A.J., ZHANG, Y. and GILBERT, R.E., 2007. Effects on protein kinase C-beta inhibition on glomerular vascular endothelial growth factor expression and endothelial cells in advanced experimental diabetic nephropathy. *American journal of physiology.Renal physiology,* 293(2), pp. F565-74

KESHET, Y. and SEGER, R., 2010. The MAP kinase signaling cascades: a system of hundreds of components regulates a diverse array of physiological functions. *Methods in molecular biology (Clifton, N.J.),* 661, pp. 3-38

KHARE, A., SHETTY, S., GHOSH, K., MOHANTY, D. and CHATTERJEE, S., 2005. Evaluation of markers of endothelial damage in cases of young myocardial infarction. *Atherosclerosis,* 180(2), pp. 375-380

KIM, N.C., GRAF, T.N., SPARACINO, C.M., WANI, M.C. and WALL, M.E., 2003. Complete isolation and characterization of silybins and isosilybins from milk thistle (Silybum marianum). *Organic & biomolecular chemistry,* 1(10), pp. 1684-1689

KIM, S., CHOI, M.G., LEE, H.S., LEE, S.K., KIM, S.H., KIM, W.W., HUR, S.M., KIM, J.H., CHOE, J.H., NAM, S.J., YANG, J.H., KIM, S., LEE, J.E. and KIM, J.S., 2009. Silibinin suppresses TNF-alpha-induced MMP-9 expression in gastric cancer cells through inhibition of the MAPK pathway. *Molecules (Basel, Switzerland),* 14(11), pp. 4300-4311

KIM, W.Y. and SHARPLESS, N.E., 2006. The regulation of INK4/ARF in cancer and aging. *Cell,* 127(2), pp. 265-275

KINLEY, A.W., WEED, S.A., WEAVER, A.M., KARGINOV, A.V., BISSONETTE, E., COOPER, J.A. and PARSONS, J.T., 2003. Cortactin interacts with WIP in regulating Arp2/3 activation and membrane protrusion. *Current biology : CB,* 13(5), pp. 384-393

KITAGAWA, K., KOTAKE, Y. and KITAGAWA, M., 2009. Ubiquitin-mediated control of oncogene and tumor suppressor gene products. *Cancer science,* 100(8), pp. 1374-1381

KLIMOVA, T. and CHANDEL, N.S., 2008. Mitochondrial complex III regulates hypoxic activation of HIF. *Cell death and differentiation,* 15(4), pp. 660-666

KNOTT, R.M. and FORRESTER, J.V., 2003. Pathogenesis of diabetic eye disease. In: J.C. PICKUP and W. GARETH, eds. *Textbook of diabetes.* 3rd ed. Oxford: Blackwell sciences. pp. 48.1-48.17

KNOTT, R.M., HECTOR, E., COTTER, M., CAMERON, N.E., FORDYCE, I., FERGUSON, S. and MOIR, D., 2003. Alpha lipoic acid reduces expression of hypoxia inducible factor Type 1 alpha in the sciatic nerve of streptozotocin induced diabetic rats. In: W. WALDHAUSL, ed. *The International Diabetes Federation Abstract Volume of the 18th Congress.* 24-29 August 2003. Springer. pp. A401

KNOTT, R.M., HECTOR, E., ZAMPOULIS, V., COTTER, M., CAMERON, N.E., FORDYCE, I. and STEEL, L., 2002. Diabetes-induced expression of hypoxia inducible factor Type 1-alpha in the sciatic nerve. *Diabetic Medicine,* 19(Supplement 2), pp. 86-P234

KNOTT, R.M., PASCAL, M.M., FERGUSON, C., LEIPER, J., OLSON, J., MUCKERSIE, E., ROBERTSON, M. and FORRESTER, J.V., 1999. Regulation of transforming growth factor-beta, basic fibroblast growth factor, and vascular endothelial cell growth factor mRNA in peripheral blood leukocytes in patients with diabetic retinopathy. *Metabolism,* 48(9), pp. 1172-1178

KOBAYASHI, T., NOGAMI, T., TAGUCHI, K., MATSUMOTO, T. and KAMATA, K., 2008. Diabetic state, high plasma insulin and angiotensin II combine to augment endothelin-1-induced vasoconstriction via ETA receptors and ERK. *British journal of pharmacology,* 155(7), pp. 974-983

KOFLER, S., NICKEL, T. and WEIS, M., 2005. Role of cytokines in cardiovascular diseases: a focus on endothelial responses to inflammation. *Clinical science (London, England : 1979),* 108(3), pp. 205-213

KOH, W., MAHAN, R.D. and DAVIS, G.E., 2008. Cdc42- and Rac1-mediated endothelial lumen formation requires Pak2, Pak4 and Par3, and PKC-dependent signaling. *Journal of cell science,* 121(Pt 7), pp. 989-1001

KOHDA, Y., KANEMATSU, M., KONO, T., TERASAKI, F. and TANAKA, T., 2009. Protein O-glycosylation induces collagen expression and contributes to diabetic cardiomyopathy in rat cardiac fibroblasts. *Journal of pharmacological sciences,* 111(4), pp. 446-450

KOSHIKAWA, N., HAYASHI, J., NAKAGAWARA, A. and TAKENAGA, K., 2009. Reactive oxygen species-generating mitochondrial DNA mutation up-regulates hypoxia-inducible factor-1alpha gene transcription via phosphatidylinositol 3-kinase-Akt/protein kinase C/histone deacetylase pathway. *The Journal of biological chemistry,* 284(48), pp. 33185-33194

KOWLURU, R.A., 2005. Effect of advanced glycation end products on accelerated apoptosis of retinal capillary cells under in vitro conditions. *Life Sciences,* 76(9), pp. 1051-1060

KOYA, D., HANEDA, M., NAKAGAWA, H., ISSHIKI, K., SATO, H., MAEDA, S., SUGIMOTO, T., YASUDA, H., KASHIWAGI, A., WAYS, D.K., KING, G.L. and KIKKAWA, R., 2000. Amelioration of accelerated diabetic mesangial expansion by treatment with a PKC beta inhibitor in diabetic db/db mice, a rodent model for type 2 diabetes. *The FASEB journal : official publication of the Federation of American Societies for Experimental Biology,* 14(3), pp. 439-447

KROLL, D.J., SHAW, H.S. and OBERLIES, N.H., 2007. Milk thistle nomenclature: why it matters in cancer research and pharmacokinetic studies. *Integrative cancer therapies,* 6(2), pp. 110-119

KRUGER, E.A., BLAGOSKLONNY, M.V., DIXON, S.C. and FIGG, W.D., 1998. UCN-01, a protein kinase C inhibitor, inhibits endothelial cell proliferation and angiogenic hypoxic response. *Invasion & metastasis,* 18(4), pp. 209-218

KUBES, P., SUZUKI, M. and GRANGER, D.N., 1991. Nitric oxide: an endogenous modulator of leukocyte adhesion. *Proceedings of the National Academy of Sciences of the United States of America,* 88(11), pp. 4651-4655

KUBOKI, K., JIANG, Z.Y., TAKAHARA, N., HA, S.W., IGARASHI, M., YAMAUCHI, T., FEENER, E.P., HERBERT, T.P., RHODES, C.J. and KING, G.L., 2000. Regulation of endothelial constitutive nitric oxide synthase gene expression in endothelial cells and in vivo : a specific vascular action of insulin. *Circulation,* 101(6), pp. 676-681

KUEH, H.Y. and MITCHISON, T.J., 2009. Structural plasticity in actin and tubulin polymer dynamics. *Science (New York, N.Y.),* 325(5943), pp. 960-963

KUMAR, T.R. and KRISHNAN, L.K., 2002. A stable matrix for generation of tissue-engineered nonthrombogenic vascular grafts. *Tissue engineering,* 8(5), pp. 763-770

KUMAR, T.R., VASANTHA BAI, M. and KRISHNAN, L.K., 2004. A freeze-dried fibrin disc as a biodegradable drug release matrix. *Biologicals : journal of the International Association of Biological Standardization,* 32(1), pp. 49-55

KUNG, A.L., WANG, S., KLCO, J.M., KAELIN, W.G. and LIVINGSTON, D.M., 2000. Suppression of tumor growth through disruption of hypoxia-inducible transcription. *Nature medicine,* 6(12), pp. 1335-1340

KUNISAKI, M., BURSELL, S.E., UMEDA, F., NAWATA, H. and KING, G.L., 1994. Normalization of diacylglycerol-protein kinase C activation by vitamin E in aorta of diabetic rats and cultured rat smooth muscle cells exposed to elevated glucose levels. *Diabetes,* 43(11), pp. 1372-1377

KUPFER, A., LOUVARD, D. and SINGER, S.J., 1982. Polarization of the Golgi apparatus and the microtubule-organizing center in cultured fibroblasts at the edge of an experimental wound. *Proceedings of the National Academy of Sciences of the United States of America,* 79(8), pp. 2603-2607

KVASNICKA, F., BIBA, B., SEVCIK, R., VOLDRICH, M. and KRATKA, J., 2003. Analysis of the active components of silymarin. *Journal of chromatography.A,* 990(1-2), pp. 239-245

L

LAH, J.J., CUI, W. and HU, K.Q., 2007. Effects and mechanisms of silibinin on human hepatoma cell lines. *World journal of gastroenterology : WJG,* 13(40), pp. 5299-5305

LAMPUGNANI, M.G., ORSENIGO, F., RUDINI, N., MADDALUNO, L., BOULDAY, G., CHAPON, F. and DEJANA, E., 2010. CCM1 regulates vascular-lumen organization by inducing endothelial polarity. *Journal of cell science,* 123(Pt 7), pp. 1073-1080

LANDO, D., PEET, D.J., GORMAN, J.J., WHELAN, D.A., WHITELAW, M.L. and BRUICK, R.K., 2002a. FIH-1 is an asparaginyl hydroxylase enzyme that regulates the transcriptional activity of hypoxia-inducible factor. *Genes & development,* 16(12), pp. 1466-1471

LANDO, D., PEET, D.J., WHELAN, D.A., GORMAN, J.J. and WHITELAW, M.L., 2002b. Asparagine hydroxylation of the HIF transactivation domain a hypoxic switch. *Science (New York, N.Y.),* 295(5556), pp. 858-861

LANDRY, C., BUSSIERES, J.F., LEBEL, P., FOREST, J.M., HILDGEN, P. and LAFERRIERE, C., 2001. Factors affecting the sterility of work areas in barrier isolators and a biological safety cabinet. *American Journal of Health-System Pharmacy : AJHP : Official Journal of the American Society of Health-System Pharmacists,* 58(11), pp. 1009-1014

LARREA, M.D., HONG, F., WANDER, S.A., DA SILVA, T.G., HELFMAN, D., LANNIGAN, D., SMITH, J.A. and SLINGERLAND, J.M., 2009. RSK1 drives p27Kip1 phosphorylation at T198 to promote RhoA inhibition and increase cell motility. *Proceedings of the National Academy of Sciences of the United States of America,* 106(23), pp. 9268-9273

LAUFFENBURGER, D.A. and HORWITZ, A.F., 1996. Cell Migration: A Physically Integrated Molecular Process. *Cell,* 84(3), pp. 359-369

LE CLAINCHE, C. and CARLIER, M.F., 2008. Regulation of actin assembly associated with protrusion and adhesion in cell migration. *Physiological Reviews,* 88(2), pp. 489-513

LEASK, A., SHI-WEN, X., KHAN, K., CHEN, Y., HOLMES, A., EASTWOOD, M., DENTON, C.P., BLACK, C.M. and ABRAHAM, D.J., 2008. Loss of protein kinase Cepsilon results in impaired cutaneous wound closure and myofibroblast function. *Journal of cell science,* 121(Pt 20), pp. 3459-3467

LEE, D.W., CHOI, W.S., BYUN, M.W., PARK, H.J., YU, Y.M. and LEE, C.M., 2003. Effect of gamma-irradiation on degradation of alginate. *Journal of Agricultural and Food Chemistry,* 51(16), pp. 4819-4823

LEE, D.Y. and LIU, Y., 2003. Molecular structure and stereochemistry of silybin A, silybin B, isosilybin A, and isosilybin B, isolated from Silybum marianum (milk thistle). *Journal of natural products,* 66(9), pp. 1171-1174

LEE, J.S. and GOTLIEB, A.I., 2003. Understanding the role of the cytoskeleton in the complex regulation of the endothelial repair. *Histology and histopathology,* 18(3), pp. 879-887

LEE, J.S., KANG DECKER, N., CHATTERJEE, S., YAO, J., FRIEDMAN, S. and SHAH, V., 2005. Mechanisms of nitric oxide interplay with Rho GTPase family members in modulation of actin membrane dynamics in pericytes and fibroblasts. *The American journal of pathology,* 166(6), pp. 1861-1870

LEE, J.W., BAE, S.H., JEONG, J.W., KIM, S.H. and KIM, K.W., 2004. Hypoxia-inducible factor (HIF-1)alpha: its protein stability and biological functions. *Experimental & molecular medicine,* 36(1), pp. 1-12

LEE, J.W., PARK, J.A., KIM, S.H., SEO, J.H., LIM, K.J., JEONG, J.W., JEONG, C.H., CHUN, K.H., LEE, S.K., KWON, Y.G. and KIM, K.W., 2007. Protein kinase C-delta regulates the stability of hypoxia-inducible factor-1 alpha under hypoxia. *Cancer science,* 98(9), pp. 1476-1481

LEE, M.H., REYNISDOTTIR, I. and MASSAGUE, J., 1995. Cloning of p57KIP2, a cyclin-dependent kinase inhibitor with unique domain structure and tissue distribution. *Genes & development,* 9(6), pp. 639-649

LERMAN, O.Z., GALIANO, R.D., ARMOUR, M., LEVINE, J.P. and GURTNER, G.C., 2003. Cellular dysfunction in the diabetic fibroblast: impairment in migration, vascular endothelial growth factor production, and response to hypoxia. *The American journal of pathology,* 162(1), pp. 303-312

LI CALZI, S., PURICH, D.L., CHANG, K.H., AFZAL, A., NAKAGAWA, T., BUSIK, J.V., AGARWAL, A., SEGAL, M.S. and GRANT, M.B., 2008. Carbon monoxide and nitric oxide mediate cytoskeletal reorganization in microvascular cells via vasodilator-stimulated phosphoprotein phosphorylation: evidence for blunted responsiveness in diabetes. *Diabetes,* 57(9), pp. 2488-2494

LI, J., WANG, J.J., YU, Q., CHEN, K., MAHADEV, K. and ZHANG, S.X., 2010. Inhibition of reactive oxygen species by Lovastatin downregulates vascular endothelial growth factor expression and ameliorates blood-retinal barrier breakdown in db/db mice: role of NADPH oxidase 4. *Diabetes,* 59(6), pp. 1528-1538

LI, J., ZHOU, L., TRAN, H.T., CHEN, Y., NGUYEN, N.E., KARASEK, M.A. and MARINKOVICH, M.P., 2006. Overexpression of laminin-8 in human dermal microvascular

endothelial cells promotes angiogenesis-related functions. *The Journal of investigative dermatology,* 126(2), pp. 432-440

LI, L., GAO, Y., ZHANG, L., ZENG, J., HE, D. and SUN, Y., 2008. Silibinin inhibits cell growth and induces apoptosis by caspase activation, down-regulating survivin and blocking EGFR-ERK activation in renal cell carcinoma. *Cancer letters,* 272(1), pp. 61-69

LI, S., BUTLER, P., WANG, Y., HU, Y., HAN, D.C., USAMI, S., GUAN, J.L. and CHIEN, S., 2002. The role of the dynamics of focal adhesion kinase in the mechanotaxis of endothelial cells. *Proceedings of the National Academy of Sciences of the United States of America,* 99(6), pp. 3546-3551

LI, Z., WANG, D., MESSING, E.M. and WU, G., 2005. VHL protein-interacting deubiquitinating enzyme 2 deubiquitinates and stabilizes HIF-1alpha. *EMBO reports,* 6(4), pp. 373-378

LIN, C.M., CHIU, J.H., WU, I.H., WANG, B.W., PAN, C.M. and CHEN, Y.H., 2010. Ferulic acid augments angiogenesis via VEGF, PDGF and HIF-1 alpha. *The Journal of nutritional biochemistry,* 21(7), pp. 627-633

LIN, F., BALDESSARI, F., GYENGE, C.C., SATO, T., CHAMBERS, R.D., SANTIAGO, J.G. and BUTCHER, E.C., 2008. Lymphocyte electrotaxis in vitro and in vivo. *Journal of immunology (Baltimore, Md.: 1950),* 181(4), pp. 2465-2471

LIRUSSI, F., BECCARELLO, A., ZANETTE, G., DE MONTE, A., DONADON, V., VELUSSI, M. and CREPALDI, G., 2002. Silybin-beta-cyclodextrin in the treatment of patients with diabetes mellitus and alcoholic liver disease. Efficacy study of a new preparation of an anti-oxidant agent. *Diabetes, nutrition & metabolism,* 15(4), pp. 222-231

LIU, L., MARTI, G.P., WEI, X., ZHANG, X., ZHANG, H., LIU, Y.V., NASTAI, M., SEMENZA, G.L. and HARMON, J.W., 2008. Age-dependent impairment of HIF-1alpha expression in diabetic mice: Correction with electroporation-facilitated gene therapy increases wound healing, angiogenesis, and circulating angiogenic cells. *Journal of cellular physiology,* 217(2), pp. 319-327

LIU, Y., VEENA, C.K., MORGAN, J.B., MOHAMMED, K.A., JEKABSONS, M.B., NAGLE, D.G. and ZHOU, Y.D., 2009. Methylalpinumisoflavone inhibits hypoxia-inducible factor-1 (HIF-1) activation by simultaneously targeting multiple pathways. *The Journal of biological chemistry,* 284(9), pp. 5859-5868

LIU, Y.V., BAEK, J.H., ZHANG, H., DIEZ, R., COLE, R.N. and SEMENZA, G.L., 2007a. RACK1 competes with HSP90 for binding to HIF-1alpha and is required for O(2)-independent and HSP90 inhibitor-induced degradation of HIF-1alpha. *Molecular cell,* 25(2), pp. 207-217

LIU, Y.V., HUBBI, M.E., PAN, F., MCDONALD, K.R., MANSHARAMANI, M., COLE, R.N., LIU, J.O. and SEMENZA, G.L., 2007b. Calcineurin promotes hypoxia-inducible factor 1alpha expression by dephosphorylating RACK1 and blocking RACK1 dimerization. *The Journal of biological chemistry,* 282(51), pp. 37064-37073

LOCK, J.G., WEHRLE-HALLER, B. and STROMBLAD, S., 2008. Cell-matrix adhesion complexes: master control machinery of cell migration. *Seminars in cancer biology,* 18(1), pp. 65-76

LOOTS, M.A.M., KENTER, S.B., AU, F.L., VAN GALEN, W.J.M., MIDDELKOOP, E., BOS, J.D. and MEKKES, J.R., 2002. Fibroblasts derived from chronic diabetic ulcers differ in their response to stimulation with EGF, IGF-I, bFGF and PDGF-AB compared to controls. *European Journal of Cell Biology,* 81(3), pp. 153-160

LOPES DE FARIA, J.M., SILVA, K.C., BOER, P.A., CAVALCANTI, T.C., ROSALES, M.A., FERRARI, A.L. and LOPES DE FARIA, J.B., 2008. A decrease in retinal progenitor cells is associated with early features of diabetic retinopathy in a model that combines diabetes and hypertension. *Molecular vision,* 14, pp. 1680-1691

LORINCZ, A.T. and REED, S.I., 1984. Primary structure homology between the product of yeast cell division control gene CDC28 and vertebrate oncogenes. *Nature,* 307(5947), pp. 183-185

M

MACE, K.A., YU, D.H., PAYDAR, K.Z., BOUDREAU, N. and YOUNG, D.M., 2007. Sustained expression of Hif-1alpha in the diabetic environment promotes angiogenesis and cutaneous wound repair. *Wound repair and regeneration : official publication of the Wound Healing Society [and] the European Tissue Repair Society,* 15(5), pp. 636-645

MACIVER, S.K. and HUSSEY, P.J., 2002. The ADF/cofilin family: actin-remodeling proteins. *Genome biology,* 3(5), pp. reviews 3007

MACKINNON, J.R., KNOTT, R.M. and FORRESTER, J.V., 2004. Altered L-selectin expression in lymphocytes and increased adhesion to endothelium in patients with diabetic retinopathy. *The British journal of ophthalmology,* 88(9), pp. 1137-1141

MACKINNON, S.L., HODDER, M., CRAFT, C. and SIMMONS-BOYCE, J., 2007. Silyamandin, a new flavonolignan isolated from milk thistle tinctures. *Planta Medica,* 73(11), pp. 1214-1216

MACPHERSON, I. and STOKER, M., 1962. Polyoma transformation of hamster cell clones—an investigation of genetic factors affecting cell competence. *Virology,* 16(2), pp. 147-151

MAHADEV, K., WU, X., DONNELLY, S., OUEDRAOGO, R., ECKHART, A.D. and GOLDSTEIN, B.J., 2008. Adiponectin inhibits vascular endothelial growth factor-induced migration of human coronary artery endothelial cells. *Cardiovascular research,* 78(2), pp. 376-384

MAIELLO, M., BOERI, D., PODESTA, F., CAGLIERO, E., VICHI, M., ODETTI, P., ADEZATI, L. and LORENZI, M., 1992. Increased expression of tissue plasminogen activator and its inhibitor and reduced fibrinolytic potential of human endothelial cells cultured in elevated glucose. *Diabetes,* 41(8), pp. 1009-1015

MAKINO, H., MIYAMOTO, Y., SAWAI, K., MORI, K., MUKOYAMA, M., NAKAO, K., YOSHIMASA, Y. and SUGA, S., 2006. Altered gene expression related to glomerulogenesis and podocyte structure in early diabetic nephropathy of db/db mice and its restoration by pioglitazone. *Diabetes,* 55(10), pp. 2747-2756

MAKINO, Y., CAO, R., SVENSSON, K., BERTILSSON, G., ASMAN, M., TANAKA, H., CAO, Y., BERKENSTAM, A. and POELLINGER, L., 2001. Inhibitory PAS domain protein is a negative regulator of hypoxia-inducible gene expression. *Nature,* 414(6863), pp. 550-554

MALINDA, K.M., GOLDSTEIN, A.L. and KLEINMAN, H.K., 1997. Thymosin beta 4 stimulates directional migration of human umbilical vein endothelial cells. *The FASEB journal : official publication of the Federation of American Societies for Experimental Biology,* 11(6), pp. 474-481

MALINDA, K.M., SIDHU, G.S., MANI, H., BANAUDHA, K., MAHESHWARI, R.K., GOLDSTEIN, A.L. and KLEINMAN, H.K., 1999. Thymosin beta4 accelerates wound healing. *The Journal of investigative dermatology,* 113(3), pp. 364-368

MALLIKARJUNA, G., DHANALAKSHMI, S., SINGH, R.P., AGARWAL, C. and AGARWAL, R., 2004. Silibinin protects against photocarcinogenesis via modulation of cell cycle regulators, mitogen-activated protein kinases, and Akt signaling. *Cancer research,* 64(17), pp. 6349-6356

MANSOUR, H.H., HAFEZ, H.F. and FAHMY, N.M., 2006. Silymarin modulates Cisplatin-induced oxidative stress and hepatotoxicity in rats. *Journal of biochemistry and molecular biology,* 39(6), pp. 656-661

MARFELLA, R., D'AMICO, M., DI FILIPPO, C., PIEGARI, E., NAPPO, F., ESPOSITO, K., BERRINO, L., ROSSI, F. and GIUGLIANO, D., 2002. Myocardial infarction in diabetic rats: role of hyperglycaemia on infarct size and early expression of hypoxia-inducible factor 1. *Diabetologia,* 45(8), pp. 1172-1181

MARFELLA, R., ESPOSITO, K., NAPPO, F., SINISCALCHI, M., SASSO, F.C., PORTOGHESE, M., DI MARINO, M.P., BALDI, A., CUZZOCREA, S., DI FILIPPO, C., BARBOSO, G., BALDI, F., ROSSI, F., D'AMICO, M. and GIUGLIANO, D., 2004. Expression of angiogenic factors during acute coronary syndromes in human type 2 diabetes. *Diabetes,* 53(9), pp. 2383-2391

MARRERO, M.B., BANES-BERCELI, A.K., STERN, D.M. and EATON, D.C., 2006. Role of the JAK/STAT signaling pathway in diabetic nephropathy. *American journal of physiology.Renal physiology,* 290(4), pp. F762-8

MARTIN, P., 1997. Wound healing--aiming for perfect skin regeneration. *Science (New York, N.Y.),* 276(5309), pp. 75-81

MASCARDO, R.N., 1988. The effects of hyperglycemia on the directed migration of wounded endothelial cell monolayers. *Metabolism: clinical and experimental,* 37(4), pp. 378-385

MASSON, N., WILLAM, C., MAXWELL, P.H., PUGH, C.W. and RATCLIFFE, P.J., 2001. Independent function of two destruction domains in hypoxia-inducible factor-alpha chains activated by prolyl hydroxylation. *The EMBO journal,* 20(18), pp. 5197-5206

MATSUDA, T., FERRERI, K., TODOROV, I., KURODA, Y., SMITH, C.V., KANDEEL, F. and MULLEN, Y., 2005. Silymarin protects pancreatic beta-cells against cytokine-mediated toxicity: implication of c-Jun NH2-terminal kinase and janus kinase/signal transducer and activator of transcription pathways. *Endocrinology,* 146(1), pp. 175-185

MATSUNAGA, N., SHIMAZAWA, M., OTSUBO, K. and HARA, H., 2008. Phosphatidylinositol inhibits vascular endothelial growth factor-A--induced migration of human umbilical vein endothelial cells. *Journal of pharmacological sciences,* 106(1), pp. 128-135

MATSUO, J., OKU, H., KANBARA, Y., KOBAYASHI, T., SUGIYAMA, T. and IKEDA, T., 2009. Involvement of NADPH oxidase and protein kinase C in endothelin-1-induced superoxide production in retinal microvessels. *Experimental eye research,* 89(5), pp. 693-699

MATTHEWS, K.H., STEVENS, H.N.E., AUFFRET, A.D., HUMPHREY, M.J. and ECCLESTON, G.M., 2005. Lyophilised wafers as a drug delivery system for wound healing containing methylcellulose as a viscosity modifier. *International Journal of Pharmaceutics,* 289(1-2), pp. 51-62

MATTHEWS, K.H., STEVENS, H.N.E., AUFFRET, A.D., HUMPHREY, M.J. and ECCLESTON, G.M., 2006. Gamma-irradiation of lyophilised wound healing wafers. *International Journal of Pharmaceutics,* 313(1-2), pp. 78-86

MATTHEWS, K.H., STEVENS, H.N.E., AUFFRET, A.D., HUMPHREY, M.J. and ECCLESTON, G.M., 2008. Formulation, stability and thermal analysis of lyophilised wound healing wafers containing an insoluble MMP-3 inhibitor and a non-ionic surfactant. *International Journal of Pharmaceutics,* 356(1-2), pp. 110-120

MATTILA, P.K. and LAPPALAINEN, P., 2008. Filopodia: molecular architecture and cellular functions. *Nature reviews.Molecular cell biology,* 9(6), pp. 446-454

MAXWELL, P.H., WIESENER, M.S., CHANG, G.W., CLIFFORD, S.C., VAUX, E.C., COCKMAN, M.E., WYKOFF, C.C., PUGH, C.W., MAHER, E.R. and RATCLIFFE, P.J., 1999. The tumour suppressor protein VHL targets hypoxia-inducible factors for oxygen-dependent proteolysis. *Nature,* 399(6733), pp. 271-275

MCALLISTER, S.S., BECKER-HAPAK, M., PINTUCCI, G., PAGANO, M. and DOWDY, S.F., 2003. Novel p27(kip1) C-terminal scatter domain mediates Rac-dependent cell migration independent of cell cycle arrest functions. *Molecular and cellular biology,* 23(1), pp. 216-228

MCGINN, S., PORONNIK, P., KING, M., GALLERY, E.D. and POLLOCK, C.A., 2003a. High glucose and endothelial cell growth: novel effects independent of autocrine TGF-beta 1 and hyperosmolarity. *American journal of physiology.Cell physiology,* 284(6), pp. C1374-86

MCGINN, S., SAAD, S., PORONNIK, P. and POLLOCK, C.A., 2003b. High glucose-mediated effects on endothelial cell proliferation occur via p38 MAP kinase. *American journal of physiology.Endocrinology and metabolism,* 285(4), pp. E708-17

MEERAN, S.M. and KATIYAR, S.K., 2008. Cell cycle control as a basis for cancer chemoprevention through dietary agents. *Frontiers in bioscience : a journal and virtual library,* 13, pp. 2191-2202

MIN, J.H., YANG, H., IVAN, M., GERTLER, F., KAELIN, W.G.,JR and PAVLETICH, N.P., 2002. Structure of an HIF-1alpha -pVHL complex: hydroxyproline recognition in signaling. *Science (New York, N.Y.),* 296(5574), pp. 1886-1889

MINAMI, T. and AIRD, W.C., 2005/7. Endothelial Cell Gene Regulation. *Trends in Cardiovascular Medicine,* 15(5), pp. 174.e1-174.e24

MINET, E., ARNOULD, T., MICHEL, G., ROLAND, I., MOTTET, D., RAES, M., REMACLE, J. and MICHIELS, C., 2000/2/18. ERK activation upon hypoxia: involvement in HIF-1 activation. *FEBS Letters,* 468(1), pp. 53-58

MIZUNO, K., YAMAMURA, K., YANO, K., OSADA, T., SAEKI, S., TAKIMOTO, N., SAKURAI, T. and NIMURA, Y., 2003. Effect of chitosan film containing basic fibroblast growth factor on wound healing in genetically diabetic mice. *Journal of biomedical materials research.Part A,* 64(1), pp. 177-181

MORGAN, D.O., 1997. Cyclin-dependent kinases: engines, clocks, and microprocessors. *Annual Review of Cell and Developmental Biology,* 13, pp. 261-291

MORIGI, M., ANGIOLETTI, S., IMBERTI, B., DONADELLI, R., MICHELETTI, G., FIGLIUZZI, M., REMUZZI, A., ZOJA, C. and REMUZZI, G., 1998. Leukocyte-endothelial interaction is augmented by high glucose concentrations and hyperglycemia in a NF-kB-dependent fashion. *The Journal of clinical investigation,* 101(9), pp. 1905-1915

MORISHIMA, C., SHUHART, M.C., WANG, C.C., PASCHAL, D.M., APODACA, M.C., LIU, Y., SLOAN, D.D., GRAF, T.N., OBERLIES, N.H., LEE, D.Y., JEROME, K.R. and POLYAK, S.J., 2010. Silymarin inhibits in vitro T-cell proliferation and cytokine production in hepatitis C virus infection. *Gastroenterology,* 138(2), pp. 671-81, 681.e1-2

MOSS, S.C., LIGHTELL, D.J.,JR, MARX, S.O., MARKS, A.R. and WOODS, T.C., 2010. Rapamycin regulates endothelial cell migration through regulation of the cyclin-dependent kinase inhibitor p27Kip1. *The Journal of biological chemistry,* 285(16), pp. 11991-11997

MOTTET, D., DUMONT, V., DECCACHE, Y., DEMAZY, C., NINANE, N., RAES, M. and MICHIELS, C., 2003. Regulation of hypoxia-inducible factor-1alpha protein level during hypoxic conditions by the phosphatidylinositol 3-kinase/Akt/glycogen synthase kinase 3beta pathway in HepG2 cells. *The Journal of biological chemistry,* 278(33), pp. 31277-31285

MULLINS, R.D., HEUSER, J.A. and POLLARD, T.D., 1998. The interaction of Arp2/3 complex with actin: nucleation, high affinity pointed end capping, and formation of branching networks of filaments. *Proceedings of the National Academy of Sciences of the United States of America,* 95(11), pp. 6181-6186

MUROHARA, T., WITZENBICHLER, B., SPYRIDOPOULOS, I., ASAHARA, T., DING, B., SULLIVAN, A., LOSORDO, D.W. and ISNER, J.M., 1999. Role of endothelial nitric oxide synthase in endothelial cell migration. *Arteriosclerosis, Thrombosis, and Vascular Biology,* 19(5), pp. 1156-1161

N
NAKAMURA, N., OBAYASHI, H., FUJII, M., FUKUI, M., YOSHIMORI, K., OGATA, M., HASEGAWA, G., SHIGETA, H., KITAGAWA, Y., YOSHIKAWA, T., KONDO, M., OHTA, M., NISHIMURA, M., NISHINAKA, T. and NISHIMURA, C.Y., 2000. Induction of aldose reductase in cultured human microvascular endothelial cells by advanced glycation end products. *Free radical biology & medicine,* 29(1), pp. 17-25

NAKAMURA, S., CHIKARAISHI, Y., TSURUMA, K., SHIMAZAWA, M. and HARA, H., 2010. Ruboxistaurin, a PKCbeta inhibitor, inhibits retinal neovascularization via suppression of phosphorylation of ERK1/2 and Akt. *Experimental eye research,* 90(1), pp. 137-145

NATARAJAN, R., FISHER, B.J. and FOWLER, I.,ALPHA A., 2003. Regulation of hypoxia inducible factor-1 by nitric oxide in contrast to hypoxia in microvascular endothelium. *FEBS Letters,* 549(1-3), pp. 99-104

NATIONAL INSTITUTE OF DIABETES AND DIGESTIVE AND KIDNEY DISEASES (NIDDK), 2008. *DCCT and EDIC: The diabetes control and complications trial and follow-*

up study. [online] Available from: http://diabetes.niddk.nih.gov/dm/pubs/control/index.htm [Accessed 07/14 2010]

NEUMANN, B., WALTER, T., HERICHE, J.K., BULKESCHER, J., ERFLE, H., CONRAD, C., ROGERS, P., POSER, I., HELD, M., LIEBEL, U., CETIN, C., SIECKMANN, F., PAU, G., KABBE, R., WUNSCHE, A., SATAGOPAM, V., SCHMITZ, M.H., CHAPUIS, C., GERLICH, D.W., SCHNEIDER, R., EILS, R., HUBER, W., PETERS, J.M., HYMAN, A.A., DURBIN, R., PEPPERKOK, R. and ELLENBERG, J., 2010. Phenotypic profiling of the human genome by time-lapse microscopy reveals cell division genes. *Nature,* 464(7289), pp. 721-727

NGUYEN, H., MORGAN, D.A. and FORWOOD, M.R., 2007. Sterilization of allograft bone: is 25 kGy the gold standard for gamma irradiation? *Cell and Tissue Banking,* 8(2), pp. 81-91

NISHIKAWA, T., EDELSTEIN, D., DU, X.L., YAMAGISHI, S., MATSUMURA, T., KANEDA, Y., YOREK, M.A., BEEBE, D., OATES, P.J., HAMMES, H.P., GIARDINO, I. and BROWNLEE, M., 2000. Normalizing mitochondrial superoxide production blocks three pathways of hyperglycaemic damage. *Nature,* 404(6779), pp. 787-790

NUSSENBAUM, F. and HERMAN, I.M., 2010. Tumor angiogenesis: insights and innovations. *Journal of oncology,* 2010, pp. 132641

O

OBARA, K., ISHIHARA, M., ISHIZUKA, T., FUJITA, M., OZEKI, Y., MAEHARA, T., SAITO, Y., YURA, H., MATSUI, T., HATTORI, H., KIKUCHI, M. and KURITA, A., 2003. Photocrosslinkable chitosan hydrogel containing fibroblast growth factor-2 stimulates wound healing in healing-impaired db/db mice. *Biomaterials,* 24(20), pp. 3437-3444

OBROSOVA, I.G., PACHER, P., SZABO, C., ZSENGELLER, Z., HIROOKA, H., STEVENS, M.J. and YOREK, M.A., 2005. Aldose reductase inhibition counteracts oxidative-nitrosative stress and poly(ADP-ribose) polymerase activation in tissue sites for diabetes complications. *Diabetes,* 54(1), pp. 234-242

OKOUCHI, M., OKAYAMA, N., IMAI, S., OMI, H., SHIMIZU, M., FUKUTOMI, T. and ITOH, M., 2002. High insulin enhances neutrophil transendothelial migration through increasing surface expression of platelet endothelial cell adhesion molecule-1 via activation of mitogen activated protein kinase. *Diabetologia,* 45(10), pp. 1449-1456

OUEDRAOGO, R., GONG, Y., BERZINS, B., WU, X., MAHADEV, K., HOUGH, K., CHAN, L., GOLDSTEIN, B.J. and SCALIA, R., 2007. Adiponectin deficiency increases leukocyte-endothelium interactions via upregulation of endothelial cell adhesion molecules in vivo. *The Journal of clinical investigation,* 117(6), pp. 1718-1726

P

PAGE, E.L., ROBITAILLE, G.A., POUYSSEGUR, J. and RICHARD, D.E., 2002. Induction of hypoxia-inducible factor-1alpha by transcriptional and translational mechanisms. *The Journal of biological chemistry,* 277(50), pp. 48403-48409

PALAZZO, A.F., JOSEPH, H.L., CHEN, Y.J., DUJARDIN, D.L., ALBERTS, A.S., PFISTER, K.K., VALLEE, R.B. and GUNDERSEN, G.G., 2001. Cdc42, dynein, and dynactin regulate MTOC reorientation independent of Rho-regulated microtubule stabilization. *Current biology : CB,* 11(19), pp. 1536-1541

PANDYA, N.M., DHALLA, N.S. and SANTANI, D.D., 2006. Angiogenesis--a new target for future therapy. *Vascular pharmacology,* 44(5), pp. 265-274

PARES, A., PLANAS, R., TORRES, M., CABALLERIA, J., VIVER, J.M., ACERO, D., PANES, J., RIGAU, J., SANTOS, J. and RODES, J., 1998. Effects of silymarin in alcoholic patients with cirrhosis of the liver: results of a controlled, double-blind, randomized and multicenter trial. *Journal of hepatology,* 28(4), pp. 615-621

PARK, J.Y., TAKAHARA, N., GABRIELE, A., CHOU, E., NARUSE, K., SUZUMA, K., YAMAUCHI, T., HA, S.W., MEIER, M., RHODES, C.J. and KING, G.L., 2000. Induction of endothelin-1 expression by glucose: an effect of protein kinase C activation. *Diabetes,* 49(7), pp. 1239-1248

PASCAL, M.M., FORRESTER, J.V. and KNOTT, R.M., 1999. Glucose-mediated regulation of transforming growth factor-beta (TGF-beta) and TGF-beta receptors in human retinal endothelial cells. *Current eye research,* 19(2), pp. 162-170

PASCERI, V., WU, H.D., WILLERSON, J.T. and YEH, E.T., 2000. Modulation of vascular inflammation in vitro and in vivo by peroxisome proliferator-activated receptor-gamma activators. *Circulation,* 101(3), pp. 235-238

PETRIE, R.J., DOYLE, A.D. and YAMADA, K.M., 2009. Random versus directionally persistent cell migration. *Nature reviews.Molecular cell biology,* 10(8), pp. 538-549

PINTER, E., MAHOOTI, S., WANG, Y., IMHOF, B.A. and MADRI, J.A., 1999. Hyperglycemia-induced vasculopathy in the murine vitelline vasculature: correlation with PECAM-1/CD31 tyrosine phosphorylation state. *The American journal of pathology,* 154(5), pp. 1367-1379

POIRIER, P. and DESPRES, J., 2003. Lipid disorders in diabetes. In: J.C. PICKUP and G. WILLIAMS, eds. *Textbook of Diabetes.* 3rd ed. Oxford, UK: Blackwell Science. pp. 54.1-54.21

POLLARD, T.D. and BORISY, G.G., 2003. Cellular Motility Driven by Assembly and Disassembly of Actin Filaments. *Cell,* 112(4), pp. 453-465

POLYAK, S.J., MORISHIMA, C., LOHMANN, V., PAL, S., LEE, D.Y., LIU, Y., GRAF, T.N. and OBERLIES, N.H., 2010. Identification of hepatoprotective flavonolignans from silymarin. *Proceedings of the National Academy of Sciences of the United States of America,* 107(13), pp. 5995-5999

PORTO DA ROCHA, R., LUCIO, D.P., SOUZA TDE, L., PEREIRA, S.T. and FERNANDES, G.J., 2002. Effects of a vitamin pool (vitamins A, E, and C) on the tissue necrosis process: experimental study on rats. *Aesthetic Plastic Surgery,* 26(3), pp. 197-202

POST-WHITE, J., LADAS, E.J. and KELLY, K.M., 2007. Advances in the use of milk thistle (Silybum marianum). *Integrative cancer therapies,* 6(2), pp. 104-109

POUYSSEGUR, J., DAYAN, F. and MAZURE, N.M., 2006. Hypoxia signalling in cancer and approaches to enforce tumour regression. *Nature,* 441(7092), pp. 437-443

PRADEEP, K., MOHAN, C.V.R., GOBIANAND, K. and KARTHIKEYAN, S., 2007. Silymarin modulates the oxidant–antioxidant imbalance during diethylnitrosamine induced oxidative stress in rats. *European journal of pharmacology,* 560(2-3), pp. 110-116

PRICCI, F., LETO, G., AMADIO, L., IACOBINI, C., CORDONE, S., CATALANO, S., ZICARI, A., SORCINI, M., DI MARIO, U. and PUGLIESE, G., 2003. Oxidative stress in diabetes-induced endothelial dysfunction involvement of nitric oxide and protein kinase C. *Free radical biology & medicine,* 35(6), pp. 683-694

PUENTE NAVAZO, M.D., CHETTAB, K., DUHAULT, J., KOENIG-BERARD, E. and MCGREGOR, J.L., 2001. Glucose and insulin modulate the capacity of endothelial cells (HUVEC) to express P-selectin and bind a monocytic cell line (U937). *Thrombosis and haemostasis,* 86(2), pp. 680-685

PUGH, C.W. and RATCLIFFE, P.J., 2003. Regulation of angiogenesis by hypoxia: role of the HIF system. *Nature medicine,* 9(6), pp. 677-684

PUOLAKKAINEN, P.A., TWARDZIK, D.R., RANCHALIS, J.E., PANKEY, S.C., REED, M.J. and GOMBOTZ, W.R., 1995. The Enhancement in Wound Healing by Transforming Growth Factor-[beta]1 (TGF-[beta]1) Depends on the Topical Delivery System. *Journal of Surgical Research,* 58(3), pp. 321-329

Q

QIU, Z., KWON, A.H. and KAMIYAMA, Y., 2007. Effects of plasma fibronectin on the healing of full-thickness skin wounds in streptozotocin-induced diabetic rats. *The Journal of surgical research,* 138(1), pp. 64-70

QUAGLIA, M.G., BOSSU, E., DONATI, E., MAZZANTI, G. and BRANDT, A., 1999. Determination of silymarine in the extract from the dried silybum marianum fruits by high performance liquid chromatography and capillary electrophoresis. *Journal of pharmaceutical and biomedical analysis,* 19(3-4), pp. 435-442

R

RAINA, K., RAJAMANICKAM, S., SINGH, R.P., DEEP, G., CHITTEZHATH, M. and AGARWAL, R., 2008. Stage-specific inhibitory effects and associated mechanisms of silibinin on tumor progression and metastasis in transgenic adenocarcinoma of the mouse prostate model. *Cancer research,* 68(16), pp. 6822-6830

RAMANA, K.V., FRIEDRICH, B., SRIVASTAVA, S., BHATNAGAR, A. and SRIVASTAVA, S.K., 2004. Activation of nuclear factor-kappaB by hyperglycemia in vascular smooth muscle cells is regulated by aldose reductase. *Diabetes,* 53(11), pp. 2910-2920

RAMASAMY, K. and AGARWAL, R., 2008. Multitargeted therapy of cancer by silymarin. *Cancer letters,* 269(2), pp. 352-362

RAMBALDI, A., JACOBS, B.P. and GLUUD, C., 2007. Milk thistle for alcoholic and/or hepatitis B or C virus liver diseases. *Cochrane database of systematic reviews (Online),* (4)(4), pp. CD003620

RASK-MADSEN, C. and KING, G.L., 2007. Mechanisms of Disease: endothelial dysfunction in insulin resistance and diabetes. *Nature clinical practice.Endocrinology & metabolism,* 3(1), pp. 46-56

RASK-MADSEN, C. and KING, G.L., 2008. Differential regulation of VEGF signaling by PKC-alpha and PKC-epsilon in endothelial cells. *Arteriosclerosis, Thrombosis, and Vascular Biology,* 28(5), pp. 919-924

RATTAN, V., SHEN, Y., SULTANA, C., KUMAR, D. and KALRA, V.K., 1997. Diabetic RBC-induced oxidant stress leads to transendothelial migration of monocyte-like HL-60 cells. *The American Journal of Physiology,* 273(2 Pt 1), pp. E369-75

RAVI, R., MOOKERJEE, B., BHUJWALLA, Z.M., SUTTER, C.H., ARTEMOV, D., ZENG, Q., DILLEHAY, L.E., MADAN, A., SEMENZA, G.L. and BEDI, A., 2000. Regulation of tumor angiogenesis by p53-induced degradation of hypoxia-inducible factor 1alpha. *Genes & development,* 14(1), pp. 34-44

RAYCHAUDHURY, A., ELKINS, M., KOZIEN, D. and NAKADA, M.T., 2001. Regulation of PECAM-1 in endothelial cells during cell growth and migration. *Experimental biology and medicine (Maywood, N.J.),* 226(7), pp. 686-691

RENARD, C.B., KRAMER, F., JOHANSSON, F., LAMHARZI, N., TANNOCK, L.R., VON HERRATH, M.G., CHAIT, A. and BORNFELDT, K.E., 2004. Diabetes and diabetes-associated lipid abnormalities have distinct effects on initiation and progression of atherosclerotic lesions. *The Journal of clinical investigation,* 114(5), pp. 659-668

REY, S. and SEMENZA, G.L., 2010. Hypoxia-inducible factor-1-dependent mechanisms of vascularization and vascular remodelling. *Cardiovascular research,* 86(2), pp. 236-242

RICHARD, D.E., BERRA, E., GOTHIE, E., ROUX, D. and POUYSSEGUR, J., 1999. p42/p44 mitogen-activated protein kinases phosphorylate hypoxia-inducible factor 1alpha (HIF-1alpha) and enhance the transcriptional activity of HIF-1. *The Journal of biological chemistry,* 274(46), pp. 32631-32637

RIDLEY, A.J., 2004. Pulling back to move forward. *Cell,* 116(3), pp. 357-358

ROHATGI, R., HO, H.Y. and KIRSCHNER, M.W., 2000. Mechanism of N-WASP activation by CDC42 and phosphatidylinositol 4, 5-bisphosphate. *The Journal of cell biology,* 150(6), pp. 1299-1310

ROHATGI, R., NOLLAU, P., HO, H.Y., KIRSCHNER, M.W. and MAYER, B.J., 2001. Nck and phosphatidylinositol 4,5-bisphosphate synergistically activate actin polymerization through the N-WASP-Arp2/3 pathway. *The Journal of biological chemistry,* 276(28), pp. 26448-26452

ROSSI, S., MARCIELLO, M., SANDRI, G., FERRARI, F., BONFERONI, M.C., PAPETTI, A., CARAMELLA, C., DACARRO, C. and GRISOLI, P., 2007. Wound dressings based on chitosans and hyaluronic acid for the release of chlorhexidine diacetate in skin ulcer therapy. *Pharmaceutical development and technology,* 12(4), pp. 415-422

ROUSSEAU, S., HOULE, F., LANDRY, J. and HUOT, J., 1997. p38 MAP kinase activation by vascular endothelial growth factor mediates actin reorganization and cell migration in human endothelial cells. *Oncogene,* 15(18), pp. 2169-2177

ROY, S., KAUR, M., AGARWAL, C., TECKLENBURG, M., SCLAFANI, R.A. and AGARWAL, R., 2007. P21 and P27 Induction by Silibinin is Essential for its Cell Cycle Arrest Effect in Prostate Carcinoma Cells. *Molecular cancer therapeutics,* 6(10), pp. 2696-2707

RUAS, J.L., POELLINGER, L. and PEREIRA, T., 2002. Functional analysis of hypoxia-inducible factor-1 alpha-mediated transactivation. Identification of amino acid residues critical for transcriptional activation and/or interaction with CREB-binding protein. *The Journal of biological chemistry,* 277(41), pp. 38723-38730

RUAS, J.L., POELLINGER, L. and PEREIRA, T., 2005. Role of CBP in regulating HIF-1-mediated activation of transcription. *Journal of cell science,* 118(Pt 2), pp. 301-311

RUSSO, A.A., JEFFREY, P.D., PATTEN, A.K., MASSAGUE, J. and PAVLETICH, N.P., 1996. Crystal structure of the p27Kip1 cyclin-dependent-kinase inhibitor bound to the cyclin A-Cdk2 complex. *Nature,* 382(6589), pp. 325-331

RYAN, J.A., 2010. *Use of corning cloning cylinders for harvesting cell colonies - protocol.* [online] Available from: http://catalog2.corning.com/Lifesciences/media/pdf/cc_cloning_protocol_1_03_cls_an_04 1w.pdf [Accessed 12/02 2010]

S

SALMI, H.A. and SARNA, S., 1982. Effect of silymarin on chemical, functional, and morphological alterations of the liver. A double-blind controlled study. *Scandinavian journal of gastroenterology,* 17(4), pp. 517-521

SCHALKWIJK, C.G. and STEHOUWER, C.D., 2005. Vascular complications in diabetes mellitus: the role of endothelial dysfunction. *Clinical science (London, England : 1979),* 109(2), pp. 143-159

SCHALKWIJK, C.G., STEHOUWER, C.D. and VAN HINSBERGH, V.W., 2004. Fructose-mediated non-enzymatic glycation: sweet coupling or bad modification. *Diabetes/metabolism research and reviews,* 20(5), pp. 369-382

SEMENZA, G.L., 2004. Hydroxylation of HIF-1: oxygen sensing at the molecular level. *Physiology (Bethesda, Md.),* 19, pp. 176-182

SEMENZA, G.L., 2000. Expression of hypoxia-inducible factor 1: mechanisms and consequences. *Biochemical Pharmacology,* 59(1), pp. 47-53

SEMENZA, G.L., 2002. Signal transduction to hypoxia-inducible factor 1. *Biochemical Pharmacology,* 64(5-6), pp. 993-998

SEMENZA, G.L., 2007. Evaluation of HIF-1 inhibitors as anticancer agents. *Drug discovery today,* 12(19-20), pp. 853-859

SENGOELGE, G., FODINGER, M., SKOUPY, S., FERRARA, I., ZANGERLE, C., ROGY, M., HORL, W.H., SUNDER-PLASSMANN, G. and MENZEL, J., 1998. Endothelial cell adhesion molecule and PMNL response to inflammatory stimuli and AGE-modified fibronectin. *Kidney international,* 54(5), pp. 1637-1651

SEPPA, H., GROTENDORST, G., SEPPA, S., SCHIFFMANN, E. and MARTIN, G.R., 1982. Platelet-derived growth factor in chemotactic for fibroblasts. *The Journal of cell biology,* 92(2), pp. 584-588

SERRANO, M., HANNON, G.J. and BEACH, D., 1993. A new regulatory motif in cell-cycle control causing specific inhibition of cyclin D/CDK4. *Nature,* 366(6456), pp. 704-707

SHAMLOO, A., MA, N., POO, M.M., SOHN, L.L. and HEILSHORN, S.C., 2008. Endothelial cell polarization and chemotaxis in a microfluidic device. *Lab on a chip,* 8(8), pp. 1292-1299

SHEN, C., LI, Q., ZHANG, Y.C., MA, G., FENG, Y., ZHU, Q., DAI, Q., CHEN, Z., YAO, Y., CHEN, L., JIANG, Y. and LIU, N., 2010. Advanced glycation endproducts increase EPC apoptosis and decrease nitric oxide release via MAPK pathways. *Biomedicine & Pharmacotherapy,* 64(1), pp. 35-43

SHERR, C.J., 1996. Cancer cell cycles. *Science (New York, N.Y.),* 274(5293), pp. 1672-1677

SHERR, C.J., 1994. G1 phase progression: Cycling on cue. *Cell,* 79(4), pp. 551-555

SHEU, M.L., HO, F.M., YANG, R.S., CHAO, K.F., LIN, W.W., LIN-SHIAU, S.Y. and LIU, S.H., 2005. High glucose induces human endothelial cell apoptosis through a phosphoinositide 3-kinase-regulated cyclooxygenase-2 pathway. *Arteriosclerosis, Thrombosis, and Vascular Biology,* 25(3), pp. 539-545

SIMON, M.C., 2006. Mitochondrial reactive oxygen species are required for hypoxic HIF alpha stabilization. *Advances in Experimental Medicine and Biology,* 588, pp. 165-170

SINGH, R.P., DHANALAKSHMI, S., AGARWAL, C. and AGARWAL, R., 2005. Silibinin strongly inhibits growth and survival of human endothelial cells via cell cycle arrest and downregulation of survivin, Akt and NF-kappaB: implications for angioprevention and antiangiogenic therapy. *Oncogene,* 24(7), pp. 1188-1202

SINGH, R.P., GU, M. and AGARWAL, R., 2008. Silibinin inhibits colorectal cancer growth by inhibiting tumor cell proliferation and angiogenesis. *Cancer research,* 68(6), pp. 2043-2050

SKIP BROWN, H., *Haematoxylin & Eosin.* [online] Available from: http://www.unc.edu/courses/2008fall/envr/431/001/Primer-H&Emay04.pdf [Accessed 06/15 2010]

SLAMA GERARD, 2003. Type 1 diabetes: an overview. In: J.C. PICKUP and WILLIAMS GARETH, eds. *Textbook of Diabetes.* 3rd ed. Oxford: Blackwell Science. pp. 3.1-3.17

SLIMAN, S.M., EUBANK, T.D., KOTHA, S.R., KUPPUSAMY, M.L., SHERWANI, S.I., BUTLER, E.S., KUPPUSAMY, P., ROY, S., MARSH, C.B., STERN, D.M. and PARINANDI, N.L., 2010. Hyperglycemic oxoaldehyde, glyoxal, causes barrier dysfunction, cytoskeletal alterations, and inhibition of angiogenesis in vascular endothelial cells: aminoguanidine protection. *Molecular and cellular biochemistry,* 333(1-2), pp. 9-26

SODHI, A., MONTANER, S., PATEL, V., ZOHAR, M., BAIS, C., MESRI, E.A. and GUTKIND, J.S., 2000. The Kaposi's sarcoma-associated herpes virus G protein-coupled receptor up-regulates vascular endothelial growth factor expression and secretion through mitogen-activated protein kinase and p38 pathways acting on hypoxia-inducible factor 1alpha. *Cancer research,* 60(17), pp. 4873-4880

SOLOWIEJ, A., BISWAS, P., GRAESSER, D. and MADRI, J.A., 2003. Lack of platelet endothelial cell adhesion molecule-1 attenuates foreign body inflammation because of decreased angiogenesis. *The American journal of pathology,* 162(3), pp. 953-962

SOTO, C., MENA, R., LUNA, J., CERBON, M., LARRIETA, E., VITAL, P., URIA, E., SANCHEZ, M., RECOBA, R., BARRON, H., FAVARI, L. and LARA, A., 2004. Silymarin induces recovery of pancreatic function after alloxan damage in rats. *Life Sciences,* 75(18), pp. 2167-2180

SOTO, C., PEREZ, J., GARCIA, V., URIA, E., VADILLO, M. and RAYA, L., 2010. Effect of silymarin on kidneys of rats suffering from alloxan-induced diabetes mellitus. *Phytomedicine : International Journal of Phytotherapy and Phytopharmacology,* 17(14), pp. 1090-1094

SOTO, C., RECOBA, R., BARRON, H., ALVAREZ, C. and FAVARI, L., 2003. Silymarin increases antioxidant enzymes in alloxan-induced diabetes in rat pancreas. *Comparative biochemistry and physiology.Toxicology & pharmacology : CBP,* 136(3), pp. 205-212

SRIVASTAVA, S.K., RAMANA, K.V. and BHATNAGAR, A., 2005. Role of aldose reductase and oxidative damage in diabetes and the consequent potential for therapeutic options. *Endocrine reviews,* 26(3), pp. 380-392

STEGENGA, M.E., VAN DER CRABBEN, S.N., BLUMER, R.M., LEVI, M., MEIJERS, J.C., SERLIE, M.J., TANCK, M.W., SAUERWEIN, H.P. and VAN DER POLL, T., 2008. Hyperglycemia enhances coagulation and reduces neutrophil degranulation, whereas hyperinsulinemia inhibits fibrinolysis during human endotoxemia. *Blood,* 112(1), pp. 82-89

STEGENGA, M.E., VAN DER CRABBEN, S.N., LEVI, M., DE VOS, A.F., TANCK, M.W., SAUERWEIN, H.P. and VAN DER POLL, T., 2006. Hyperglycemia stimulates coagulation, whereas hyperinsulinemia impairs fibrinolysis in healthy humans. *Diabetes,* 55(6), pp. 1807-1812

SUURNA, M.V., ASHWORTH, S.L., HOSFORD, M., SANDOVAL, R.M., WEAN, S.E., SHAH, B.M., BAMBURG, J.R. and MOLITORIS, B.A., 2006. Cofilin mediates ATP

depletion-induced endothelial cell actin alterations. *American journal of physiology.Renal physiology,* 290(6), pp. F1398-407

SUZUMA, K., NARUSE, K., SUZUMA, I., TAKAHARA, N., UEKI, K., AIELLO, L.P. and KING, G.L., 2000. Vascular endothelial growth factor induces expression of connective tissue growth factor via KDR, Flt1, and phosphatidylinositol 3-kinase-akt-dependent pathways in retinal vascular cells. *The Journal of biological chemistry,* 275(52), pp. 40725-40731

SVITKINA, T.M. and BORISY, G.G., 1999. Arp2/3 complex and actin depolymerizing factor/cofilin in dendritic organization and treadmilling of actin filament array in lamellipodia. *The Journal of cell biology,* 145(5), pp. 1009-1026

SZILAGI, I., TETENYI, P., ANTUS, S., SELIGMANN, O., CHARI, V.M., SEITZ, M. and WAGNER, H., 1981. Structure of silandrin and silymonin, two new flavanolignans from a white blooming Silybum marianum variety. *Planta Medica,* 43(10), pp. 121-127

T

TAGUCHI, T. and BROWNLEE, M., 2003. The biochemical mechanisms of diabetic tissue damage. In: J.C. PICKUP and WILLIAMS GARETH, eds. *Textbook of Diabetes.* 3rd ed. Oxford: Blackwell Science. pp. 47.1-47.15

TAKAMURA, Y., TOMOMATSU, T., KUBO, E., TSUZUKI, S. and AKAGI, Y., 2008. Role of the polyol pathway in high glucose-induced apoptosis of retinal pericytes and proliferation of endothelial cells. *Investigative ophthalmology & visual science,* 49(7), pp. 3216-3223

TAKATA, K., MORISHIGE, K., TAKAHASHI, T., HASHIMOTO, K., TSUTSUMI, S., YIN, L., OHTA, T., KAWAGOE, J., TAKAHASHI, K. and KURACHI, H., 2008. Fasudil-induced hypoxia-inducible factor-1alpha degradation disrupts a hypoxia-driven vascular endothelial growth factor autocrine mechanism in endothelial cells. *Molecular cancer therapeutics,* 7(6), pp. 1551-1561

TANG, N., WANG, L., ESKO, J., GIORDANO, F.J., HUANG, Y., GERBER, H., FERRARA, N. and JOHNSON, R.S., 2004. Loss of HIF-1α in endothelial cells disrupts a hypoxia-driven VEGF autocrine loop necessary for tumorigenesis. *Cancer Cell,* 6(5), pp. 485-495

TANG, T.T. and LASKY, L.A., 2003. The forkhead transcription factor FOXO4 induces the down-regulation of hypoxia-inducible factor 1 alpha by a von Hippel-Lindau protein-independent mechanism. *The Journal of biological chemistry,* 278(32), pp. 30125-30135

TANII, M., YONEMITSU, Y., FUJII, T., SHIKADA, Y., KOHNO, R., ONIMARU, M., OKANO, S., INOUE, M., HASEGAWA, M., ONOHARA, T., MAEHARA, Y. and SUEISHI, K., 2006. Diabetic microangiopathy in ischemic limb is a disease of disturbance of the platelet-derived growth factor-BB/protein kinase C axis but not of impaired expression of angiogenic factors. *Circulation research,* 98(1), pp. 55-62

TAYLOR, G.J., BANNISTER, G.C. and LEEMING, J.P., 1995. Wound disinfection with ultraviolet radiation. *The Journal of hospital infection,* 30(2), pp. 85-93

TEMES, E., MARTÍN-PUIG, S., ARAGONÉS, J., JONES, D.R., OLMOS, G., MÉRIDA, I. and LANDÁZURI, M.O., 2004. Role of diacylglycerol induced by hypoxia in the regulation of HIF-1α activity. *Biochemical and Biophysical Research Communications,* 315(1), pp. 44-50

TESFAMARIAM, B. and DEFELICE, A.F., 2007. Endothelial injury in the initiation and progression of vascular disorders. *Vascular Pharmacology,* 46(4), pp. 229-237

THANGARAJAH, H., VIAL, I.N., GROGAN, R.H., YAO, D., SHI, Y., JANUSZYK, M., GALIANO, R.D., CHANG, E.I., GALVEZ, M.G., GLOTZBACH, J.P., WONG, V.W., BROWNLEE, M. and GURTNER, G.C., 2010. HIF-1alpha dysfunction in diabetes. *Cell cycle (Georgetown, Tex.),* 9(1), pp. 75-79

THANGARAJAH, H., YAO, D., CHANG, E.I., SHI, Y., JAZAYERI, L., VIAL, I.N., GALIANO, R.D., DU, X.L., GROGAN, R., GALVEZ, M.G., JANUSZYK, M., BROWNLEE, M. and GURTNER, G.C., 2009. The molecular basis for impaired hypoxia-induced VEGF expression in diabetic tissues. *Proceedings of the National Academy of Sciences of the United States of America,* 106(32), pp. 13505-13510

THOMSON, S.E., MCLENNAN, S.V., HENNESSY, A., BOUGHTON, P., BONNER, J., ZOELLNER, H., YUE, D.K. and TWIGG, S.M., 2010. A novel primate model of delayed wound healing in diabetes: dysregulation of connective tissue growth factor. *Diabetologia,* 53(3), pp. 572-583

THORNALLEY, P.J., 2005. The potential role of thiamine (vitamin B1) in diabetic complications. *Current diabetes reviews,* 1(3), pp. 287-298

TOMLINSON, D.R., 2003. Pathogenesis of diabetic neuropathies. In: J.C. PICKUP and W. GARETH, eds. *Textbook of Diabetes 2.* 3rd ed. Oxford: Blackwell Science. pp. 50.1-50.12

TOYODA, M., SUZUKI, D., HONMA, M., UEHARA, G., SAKAI, T., UMEZONO, T. and SAKAI, H., 2004. High expression of PKC-MAPK pathway mRNAs correlates with glomerular lesions in human diabetic nephropathy. *Kidney international,* 66(3), pp. 1107-1114

TOYOSHIMA, H. and HUNTER, T., 1994. p27, a novel inhibitor of G1 cyclin-Cdk protein kinase activity, is related to p21. *Cell,* 78(1), pp. 67-74

TRAUB, W.H. and LEONHARD, B., 1995. Heat stability of the antimicrobial activity of sixty-two antibacterial agents. *The Journal of antimicrobial chemotherapy,* 35(1), pp. 149-154

TREINS, C., GIORGETTI-PERALDI, S., MURDACA, J. and VAN OBBERGHEN, E., 2001. Regulation of vascular endothelial growth factor expression by advanced glycation end products. *The Journal of biological chemistry,* 276(47), pp. 43836-43841

TRUDEAU, K., MOLINA, A.J., GUO, W. and ROY, S., 2010. High glucose disrupts mitochondrial morphology in retinal endothelial cells: implications for diabetic retinopathy. *The American journal of pathology,* 177(1), pp. 447-455

TSAI, M.J., LIAO, J.F., LIN, D.Y., HUANG, M.C., LIOU, D.Y., YANG, H.C., LEE, H.J., CHEN, Y.T., CHI, C.W., HUANG, W.C. and CHENG, H., 2010. Silymarin protects spinal cord and cortical cells against oxidative stress and lipopolysaccharide stimulation. *Neurochemistry international,* 57(8), pp. 867-875

TYAGI, A., SINGH, R.P., RAMASAMY, K., RAINA, K., REDENTE, E.F., DWYER-NIELD, L.D., RADCLIFFE, R.A., MALKINSON, A.M. and AGARWAL, R., 2009. Growth inhibition and regression of lung tumors by silibinin: modulation of angiogenesis by macrophage-associated cytokines and nuclear factor-kappaB and signal transducers and activators of transcription 3. *Cancer prevention research (Philadelphia, Pa.),* 2(1), pp. 74-83

TZIMA, E., KIOSSES, W.B., DEL POZO, M.A. and SCHWARTZ, M.A., 2003. Localized cdc42 activation, detected using a novel assay, mediates microtubule organizing center positioning in endothelial cells in response to fluid shear stress. *The Journal of biological chemistry,* 278(33), pp. 31020-31023

U

UKPDS GROUP, 1998. Intensive blood-glucose control with sulphonylureas or insulin compared with conventional treatment and risk of complications in patients with type 2 diabetes (UKPDS 33). *The Lancet,* 352(9131), pp. 837-853

ULBRICH, H., ERIKSSON, E.E. and LINDBOM, L., 2003. Leukocyte and endothelial cell adhesion molecules as targets for therapeutic interventions in inflammatory disease. *Trends in Pharmacological Sciences,* 24(12), pp. 640-647

V

VARGA, Z., UJHELYI, L., KISS, A., BALLA, J., CZOMPA, A. and ANTUS, S., 2004. Effect of silybin on phorbol myristate actetate-induced protein kinase C translocation, NADPH oxidase activity and apoptosis in human neutrophils. *Phytomedicine : International Journal of Phytotherapy and Phytopharmacology,* 11(2-3), pp. 206-212

VARMA, S., LAL, B.K., ZHENG, R., BRESLIN, J.W., SAITO, S., PAPPAS, P.J., HOBSON, R.W.,2ND and DURAN, W.N., 2005. Hyperglycemia alters PI3k and Akt signaling and leads to endothelial cell proliferative dysfunction. *American journal of physiology.Heart and circulatory physiology,* 289(4), pp. H1744-51

VELUSSI, M., CERNIGOI, A.M., DE MONTE, A., DAPAS, F., CAFFAU, C. and ZILLI, M., 1997. Long-term (12 months) treatment with an anti-oxidant drug (silymarin) is effective on hyperinsulinemia, exogenous insulin need and malondialdehyde levels in cirrhotic diabetic patients. *Journal of hepatology,* 26(4), pp. 871-879

VICENTE-MANZANARES, M., CHOI, C.K. and HORWITZ, A.R., 2009. Integrins in cell migration--the actin connection. *Journal of cell science,* 122(Pt 2), pp. 199-206

VICENTE-MANZANARES, M., MA, X., ADELSTEIN, R.S. and HORWITZ, A.R., 2009. Non-muscle myosin II takes centre stage in cell adhesion and migration. *Nature reviews.Molecular cell biology,* 10(11), pp. 778-790

VICENTE-MANZANARES, M., WEBB, D.J. and HORWITZ, A.R., 2005. Cell migration at a glance. *Journal of cell science,* 118(Pt 21), pp. 4917-4919

VICTOR, V.M., NUNEZ, C., D'OCON, P., TAYLOR, C.T., ESPLUGUES, J.V. and MONCADA, S., 2009. Regulation of oxygen distribution in tissues by endothelial nitric oxide. *Circulation research,* 104(10), pp. 1178-1183

W

WANG, G.L. and SEMENZA, G.L., 1993. General involvement of hypoxia-inducible factor 1 in transcriptional response to hypoxia. *Proceedings of the National Academy of Sciences of the United States of America,* 90(9), pp. 4304-4308

WANG, G.L., JIANG, B.H., RUE, E.A. and SEMENZA, G.L., 1995. Hypoxia-inducible factor 1 is a basic-helix-loop-helix-PAS heterodimer regulated by cellular O2 tension. *Proceedings of the National Academy of Sciences of the United States of America,* 92(12), pp. 5510-5514

WANG, G.L. and SEMENZA, G.L., 1995. Purification and characterization of hypoxia-inducible factor 1. *The Journal of biological chemistry,* 270(3), pp. 1230-1237

WANG, X.H., CHEN, S.F., JIN, H.M. and HU, R.M., 2009. Differential analyses of angiogenesis and expression of growth factors in micro- and macrovascular endothelial cells of type 2 diabetic rats. *Life Sciences,* 84(7-8), pp. 240-249

WATANABE, N. and HIGASHIDA, C., 2004. Formins: processive cappers of growing actin filaments. *Experimental cell research,* 301(1), pp. 16-22

WEBB, J.D., COLEMAN, M.L. and PUGH, C.W., 2009. Hypoxia, hypoxia-inducible factors (HIF), HIF hydroxylases and oxygen sensing. *Cellular and molecular life sciences : CMLS,* 66(22), pp. 3539-3554

WEIDMANN, A.E., 2008. *Investigation of hypoxia and hyperglycaemia mediated DNA damage in human umbilical vein endothelial cells.* [online] PhD thesis, Robert Gordon University.

WEIDMANN, A.E., STEWART, D., WAHLE, K. and KNOTT, R.M., 2005. Silymarin attenuates hypoxia and hyperglycemia induced DNA damage in a human umbilical vein endothelial cell line. *Diabetalogia,* 48(Suppl 1), pp. A 423

WEN, Z., DUMAS, T.E., SCHRIEBER, S.J., HAWKE, R.L., FRIED, M.W. and SMITH, P.C., 2008. Pharmacokinetics and metabolic profile of free, conjugated, and total silymarin flavonolignans in human plasma after oral administration of milk thistle extract. *Drug metabolism and disposition: the biological fate of chemicals,* 36(1), pp. 65-72

WERTH, S., URBAN-KLEIN, B., DAI, L., HÖBEL, S., GRZELINSKI, M., BAKOWSKY, U., CZUBAYKO, F. and AIGNER, A., 2006. A low molecular weight fraction of polyethylenimine (PEI) displays increased transfection efficiency of DNA and siRNA in fresh or lyophilized complexes. *Journal of Controlled Release,* 112(2), pp. 257-270

WOLF, G., 2002. Molecular mechanisms of diabetic mesangial cell hypertrophy: a proliferation of novel factors. *Journal of the American Society of Nephrology : JASN,* 13(10), pp. 2611-2613

WOLF, G., CHEN, S. and ZIYADEH, F.N., 2005. From the periphery of the glomerular capillary wall toward the center of disease: podocyte injury comes of age in diabetic nephropathy. *Diabetes,* 54(6), pp. 1626-1634

WOLF, G., REINKING, R., ZAHNER, G., STAHL, R.A. and SHANKLAND, S.J., 2003. Erk 1,2 phosphorylates p27(Kip1): Functional evidence for a role in high glucose-induced hypertrophy of mesangial cells. *Diabetologia,* 46(8), pp. 1090-1099

WOLF, G., SCHROEDER, R., THAISS, F., ZIYADEH, F.N., HELMCHEN, U. and STAHL, R.A., 1998. Glomerular expression of p27Kip1 in diabetic db/db mouse: role of hyperglycemia. *Kidney international,* 53(4), pp. 869-879

WOODFIN, A., VOISIN, M.B. and NOURSHARGH, S., 2007. PECAM-1: a multi-functional molecule in inflammation and vascular biology. *Arteriosclerosis, Thrombosis, and Vascular Biology,* 27(12), pp. 2514-2523

WOODLEY, D.T., FAN, J., CHENG, C.F., LI, Y., CHEN, M., BU, G. and LI, W., 2009. Participation of the lipoprotein receptor LRP1 in hypoxia-HSP90alpha autocrine signaling to promote keratinocyte migration. *Journal of cell science,* 122(Pt 10), pp. 1495-1498

WOODWARD, H.N., ANWAR, A., RIDDLE, S., TARASEVICIENE-STEWART, L., FRAGOSO, M., STENMARK, K.R. and GERASIMOVSKAYA, E.V., 2009. PI3K, Rho, and ROCK play a key role in hypoxia-induced ATP release and ATP-stimulated angiogenic responses in pulmonary artery vasa vasorum endothelial cells. *American journal of physiology.Lung cellular and molecular physiology,* 297(5), pp. L954-64

WORLD HEALTH ORGANISATION CONSULTATION, 2006. *Definition and diagnosis of diabetes mellitus and intermediate hyperglycemia : report of a WHO/IDF consultation.* Geneva, Switzerland: World Health Organisation.

WOTHERSPOON, F., BROWNE, D.L., MEEKING, D.R., ALLARD, S.E., MUNDAY, L.J., SHAW, K.M. and CUMMINGS, M.H., 2005. The contribution of nitric oxide and vasodilatory prostanoids to bradykinin-mediated vasodilation in Type 1 diabetes. *Diabetic medicine : a journal of the British Diabetic Association,* 22(6), pp. 697-702

X

XU, Y., WANG, S., FENG, L., ZHU, Q., XIANG, P. and HE, B., 2010a. Blockade of PKC-beta protects HUVEC from advanced glycation end products induced inflammation. *International immunopharmacology,* 10(12), pp. 1552-1559

XU, Y., ZUO, Y., ZHANG, H., KANG, X., YUE, F., YI, Z., LIU, M., YEH, E.T., CHEN, G. and CHENG, J., 2010b. Induction of SENP1 in endothelial cells contributes to hypoxia-driven VEGF expression and angiogenesis. *The Journal of biological chemistry,* 285(47), pp. 36682-36688

XUE, M., QIAN, Q., ADAIKALAKOTESWARI, A., RABBANI, N., BABAEI-JADIDI, R. and THORNALLEY, P.J., 2008. Activation of NF-E2-related factor-2 reverses biochemical dysfunction of endothelial cells induced by hyperglycemia linked to vascular disease. *Diabetes,* 57(10), pp. 2809-2817

Y

YAMADA, N., HORIKAWA, Y., ODA, N., IIZUKA, K., SHIHARA, N., KISHI, S. and TAKEDA, J., 2005. Genetic variation in the hypoxia-inducible factor-1alpha gene is associated with type 2 diabetes in Japanese. *The Journal of clinical endocrinology and metabolism,* 90(10), pp. 5841-5847

YAMAKAWA, M., LIU, L.X., DATE, T., BELANGER, A.J., VINCENT, K.A., AKITA, G.Y., KURIYAMA, T., CHENG, S.H., GREGORY, R.J. and JIANG, C., 2003. Hypoxia-inducible factor-1 mediates activation of cultured vascular endothelial cells by inducing multiple angiogenic factors. *Circulation research,* 93(7), pp. 664-673

YANG, X.M., WANG, Y.S., ZHANG, J., LI, Y., XU, J.F., ZHU, J., ZHAO, W., CHU, D.K. and WIEDEMANN, P., 2009. Role of PI3K/Akt and MEK/ERK in mediating hypoxia-induced expression of HIF-1alpha and VEGF in laser-induced rat choroidal neovascularization. *Investigative ophthalmology & visual science,* 50(4), pp. 1873-1879

YEE KOH, M., SPIVAK-KROIZMAN, T.R. and POWIS, G., 2008. HIF-1 regulation: not so easy come, easy go. *Trends in biochemical sciences,* 33(11), pp. 526-534

YOON, J.J., LEE, Y.J., KIM, J.S., KANG, D.G. and LEE, H.S., 2010. Betulinic acid inhibits high glucose-induced vascular smooth muscle cells proliferation and migration. *Journal of cellular biochemistry,* 111(6), pp. 1501-1511

YU, P., YU, D.M., QI, J.C., WANG, J., ZHANG, Q.M., ZHANG, J.Y., TANG, Y.Z., XING, Q.L. and LI, M.Z., 2006. *High D-glucose alters PI3K and Akt signaling and leads to endothelial cell migration, proliferation and angiogenesis dysfunction.* China:

YUN, S.P., LEE, M.Y., RYU, J.M., SONG, C.H. and HAN, H.J., 2009. Role of HIF-1alpha and VEGF in human mesenchymal stem cell proliferation by 17beta-estradiol: involvement of PKC, PI3K/Akt, and MAPKs. *American journal of physiology.Cell physiology,* 296(2), pp. C317-26

Z

ZBIKOWSKA, H.M., NOWAK, P. and WACHOWICZ, B., 2006. Protein modification caused by a high dose of gamma irradiation in cryo-sterilized plasma: protective effects of ascorbate. *Free radical biology & medicine,* 40(3), pp. 536-542

ZHANG, W., WANG, X., JIN, H., QIAN, R., ZHANG, G., CHEN, S. and HU, R., 2008. Effects of high glucose plus high insulin on proliferation and apoptosis of mouse endothelial progenitor cells. *Inflammation research : official journal of the European Histamine Research Society ...[et al.],* 57(12), pp. 571-576

ZHONG, H., CHILES, K., FELDSER, D., LAUGHNER, E., HANRAHAN, C., GEORGESCU, M.M., SIMONS, J.W. and SEMENZA, G.L., 2000. Modulation of hypoxia-inducible factor 1alpha expression by the epidermal growth factor/phosphatidylinositol 3-kinase/PTEN/AKT/FRAP pathway in human prostate cancer cells: implications for tumor angiogenesis and therapeutics. *Cancer Research,* 60(6), pp. 1541-1545

ZHONG, W., ZOU, G., GU, J. and ZHANG, J., 2010. L-arginine attenuates high glucose-accelerated senescence in human umbilical vein endothelial cells. *Diabetes research and clinical practice,* 89(1), pp. 38-45

ZHOU, B., WU, L.J., TASHIRO, S., ONODERA, S., UCHIUMI, F. and IKEJIMA, T., 2007. Activation of extracellular signal-regulated kinase during silibinin-protected, isoproterenol-induced apoptosis in rat cardiac myocytes is tyrosine kinase pathway-mediated and protein kinase C-dependent. *Acta Pharmacologica Sinica,* 28(6), pp. 803-810

ZI, X. and AGARWAL, R., 1999. Modulation of mitogen-activated protein kinase activation and cell cycle regulators by the potent skin cancer preventive agent silymarin. *Biochemical and biophysical research communications,* 263(2), pp. 528-536

ZIMMER, J.L. and SLAWSON, R.M., 2002. Potential repair of Escherichia coli DNA following exposure to UV radiation from both medium- and low-pressure UV sources used in drinking water treatment. *Applied and Environmental Microbiology,* 68(7), pp. 3293-3299

Appendix 1

Publications

GADAD, P.C., MOIR, D. and KNOTT, R.M., 2009. The effect of hypoxia and hyperglycemia on migration of microvascular endothelial cells. *45th EASD Meeting.* 29/09/2009 to 02/10/2009. European Association for the Study of Diabetes. *Diabetologia*, 52 Suppl 1, pp. S496

GADAD, P.C., MATTHEWS, K.H. and KNOTT, R.M., 2010. Effect of lyophilised wafer discs containing silymarin on the migration of microvascular endothelial cells. *UK-PharmSci 2010 - The Science of Medicine.* 1-3 September, 2010. *Journal of Pharmacy and Pharmacology*, 62 (10), Wiley Science. pp. 1264